

**Ecological Dynamics of Microbiomes in Food Processing Facilities:
Pathways to Improved Sanitation**

by

Zhaohui Xu

A thesis submitted in partial fulfillment of the requirements for the degree of

Doctor of Philosophy

in

Bioresource Technology

Department of Agricultural, Food and Nutritional Science

University of Alberta

©Zhaohui Xu, 2024

Abstract

Food processing environments serve as complex niches for bacterial colonization, adaption, persistence and dispersal, which subsequently shapes the microbial composition and diversity. This Ph.D. dissertation investigated the impact of biofilm formation, bacterial communication and cooperation on microbial community assembly, providing insights into the novel and specific intervention strategy.

The presence of microbes in food products depends on contamination from the raw materials or microbial communities in food processing facilities. By re-analysing data from 39 published studies, we found that while each food commodity possesses its own accessory microbiome, a core surface-associated microbiome exists across all commodities. Nutrient levels on food environment surfaces significantly impact biofilm community composition more than environmental processing surfaces. The longitudinal study in a pork processing facility revealed a high diversity of microbes, with addition of 74 novel species. Repeated isolation of the same meat-spoilage-associated strain across different sites and times displayed their transmission patterns and persistence over six months, pinpointing processing environments as the primary sources of microbes and identified specific sites for further interventions.

The presence of transmissible locus of stress tolerance (tLST) among gamma-proteobacteria enhances their microbial resistance to sanitation chemicals in planktonic state cells. Biofilms, the natural state of cells in food processing facilities, further reduce sanitation efficacy and facilitate microbial dispersal and persistence. Our investigations on the link of tLST to biofilm formation and disinfectant resistance showed that the presence of tLST in *E. coli* yielded higher biofilm biomass and enhanced their resistance to chlorine, hydrogen peroxide, and peroxyacetic acid in

biofilm-embedded cells. The phenotypic switch from floating biofilms (pellicle) to surface-associated biofilms is regulated more by bacterial communication and cooperation (quorum sensing) than unique gene presence/absence.

The application of ozone nanobubble on meat products *in situ* and *in vitro* showed that it displayed comparable bactericidal effect to peracetic acid and altered microbial composition, particularly eliminating the more undesirable microbes. Taking together, these findings contribute to a better understanding of the microbial ecology of food processing environments, facilitate the implementation of novel and site-specific interventions and potentially reduce food waste and outbreaks, promoting the development of a more sustainable food systems.

Preface

This thesis is an original work by Zhaohui Shaelyn Xu.

Chapter 2 of this thesis is a literature review that has been published as Zhaohui S. Xu, Tingting Ju, Xianqin Yang, Michael Gänzle (2023) "A Meta-Analysis of Bacterial Communities in Food Processing Facilities: Driving Forces for Assembly of Core and Accessory Microbiomes across Different Food Commodities". *Microorganisms*, 11(6), 1575. I was responsible for data curation, literature review and manuscript preparation. Dr. Tingting Ju provided help with statistical analysis. Dr. Xianqin Yang provided suggestions and manuscript revision. Dr. Michael Gänzle provided suggestions and contributed to concept formation and manuscript revision.

Chapter 3 of this thesis is an experimental work that has been published as Zhaohui S. Xu, Xianqin Yang, & Michael G. Gänzle (2021). "Resistance of biofilm-and pellicle-embedded strains of *Escherichia coli* encoding the transmissible locus of stress tolerance (tLST) to oxidative sanitation chemicals." *International Journal of Food Microbiology*, 359, 109425. I conducted the experiment and wrote the manuscript. Dr. Xianqin Yang and Dr. Michael Gänzle conceptualized the project and provided suggestions on the experiment design.

Chapter 4 of this thesis has been published as Zhaohui S. Xu, Tongbo Zhu, Zhiying Wang, Xianqin Yang & Michael G. Gänzle (2023). "Socializing at the Air-Liquid Interface: a Functional Genomic Analysis on Biofilm-Related Genes during Pellicle Formation by *Escherichia coli* and Its Interaction with *Aeromonas australiensis*." *Applied and Environmental Microbiology*, 89(7), e00456-23. I conducted the experiment and wrote the manuscript. Tongbo Zhu mentored and worked together with me to construct the mutants. Dr. Zhiying Wang helped with mutant primer design. Dr. Xianqin Yang provided suggestions on selection of biofilm-associated genes and

revised the manuscript. Dr. Michael Gänzle contributed to the hypothesis development and editing of manuscript.

Chapter 5 of this thesis is an experimental work that has been submitted as Zhaohui Xu, Vi Pham, Xianqin Yang, Michael Gänzle "High-Throughput Analysis of Microbiomes in a Meat Processing Facility: Dispersal, Persistence, and Biofilm Formation of Spoilage Bacteria" to *Microbiome*. My contribution to this study includes data analysis, data visualization and writing of manuscript. Dr. Dirk Thiele assisted with on-site sampling collection. Vi Pham contributed to the design of SNP calling workflow and manuscript revision. Dr. Xianqin Yang provided suggestions on on-site sampling strategies and reviewed the manuscript. Dr. Michael Gänzle conceptualized the project and contributed to manuscript editing.

Chapter 6 of this thesis is an experimental work by Zhaohui S. Xu, Janik Hettinger, Alex Athey, Xianqin Yang, Michael G. Gänzle, prepared for submission as "Ozone Nanobubble for Meat Spoilage Control". I conducted the *in-situ* experiments, sequenced the meat samples, and wrote the manuscript. Janik Hettinger worked together with me to conduct the tests of lab samples. Dr. Alex Athey installed ozone nanobubble machine both in lab and in the processing facility. Dr. Xianqin Yang provided suggestions on the selection of microbial community in meat samples. Dr. Michael Gänzle conceptualized the project and provided suggestions on experimental design.

Chapter 7 of this thesis is an experimental work outlines the diversity of 74 unknown species isolated from the pork processing facility. I conducted the experiment research on the phylogenetic and physiological characterization. Dr. Michael Gänzle provided suggestions on the experimental design. Dr. David Simpson suggested the use of Nanopore 96 WGS library preparation kit.

Dedication

This thesis is dedicated to my beloved parents, Quanfu Xu and Yuhuan Liu.

Thank you for the unwavering support and love. You always say that we work in the different fields and could not help me as much, but you have been always finding a way to help me solve the puzzles and enlighten my life ♡

Acknowledgements

Just as each research paper has its keywords, so does my Ph.D. life: 2019-2020: fresh and excitement; 2020-2021: COVID; 2021-2022: change; 2022-2023: struggle and gain; 2023-2024: determination. Throughout my five-year Ph.D. journey, I experienced moments of upset, laughter, doubt, and success. All these unforgettable experiences were made possible by my beloved family, friends, supervisors, and colleagues, to whom I am deeply grateful.

First and foremost, I extend my heartfelt thanks to my supervisor, Dr. Michael Gänzle. Thank you for giving me the opportunity to participate in the NUFS401 undergraduate project in 2018, where I discovered my passion for food microbiology and joined the wonderful 2-50 lab as a master student in 2019. Your constant encouragement and uplifting words helped me through the challenges and uncertainties. Thank you for always being there to help me interpret complex results and provide insightful feedback, shaping my research in ways I couldn't have achieved on my own. What matters more is that thank you for consistently treating me with understanding and compassion, giving me the freedom to explore new ideas, to try new things. Your kindness has left a lasting print on me, and it will continue to inspire me in the future. You have really raised my bar to look for the next supervisor.

I am also sincerely thankful to my committee member/co-supervisor, Dr. Xianqin Yang, for the prompt and valuable guidance on every project and for the encouragement and care when I worked at AAFC and attended the IAFP conference. I always feel inspired and uplifted after discussing my project with you, and I will carry this brightness into my next journey. I extend my gratitude to Dr. Lynn McMullen for every skeptical question during lab meetings and encouragement when I felt lost. Thank you for chairing my two most important exams, candidacy and defense; it was very reassuring to have you around. I also want to thank Dr. Roopesh Syamaladevi for supporting me as a supervisory committee member and every discussion on my project. A special thanks to Dr. Lisa Stein for serving as an examiner for both my candidacy and defense exams, to Dr. John Wolodko for participating in my candidacy exam, and to Dr. Danilo Ercolini for joining my defense exam oversea and providing incredible feedback.

The progress of my research would not have been possible without the collaboration and assistance of many individuals. I am grateful to Dr. Tingting Ju, Vi Pham, Tongbo Zhu, Janik Hettinger, Dr.

David Simpson, and Dr. Zhiying Wang for your invaluable contributions. Working with the teams from En Solucion, AAFC, Sunterra, and AFDP has been a privilege. I want to especially thank Dr. Alex Athey and Dr. Dirk Thiele for taking me as a research intern, teaching me every detail regarding ozone nanobubbles, and sharing your experiences of running a startup company. Thank you, Dr. Hui Wang, Dr. Peipei Zhang, Dr. Yuan Fang, Frances Tran, and Tinging Liu for the warm welcome and help during my short stay at AAFC. I also appreciate Karen, Lois, and the Sunterra team for accommodating my sampling plans and providing hands-on experience at Trochu Meat Plant. Thank you to Ross, Emma and Lauren for the help in AFDP. Teaching alongside Heather Vandertol-Vanier, Mandi Hoke, Dr. Danielle Balay, Pauline Chan, Abdelhamid Mohammed, and Dr. Chandre Van De Merwe has been a rewarding experience. I also thank the AFNS Graduate Student Association team for the joyful volunteering experiences.

I was fortunate to have joined Lab 2-50 and met so many kind, lovely, and amazing people. Special thanks to Luis Rojas Tovar, Maria Robles Hernandez, and Mégane Beauséjour for organizing gatherings and events that added fun to my research life. Thank you, Dr. Weilan Wang and Dr. Zhen Li, for welcoming me warmly to Lab 2-50. I am deeply grateful to Dr. Gautam Guar for being an excellent mentor during my NUFS401 project—without this experience, I wouldn't be where I am today. Thanks to all my colleagues: Dr. Nuanyi Liang, Dr. Justina Zhang, Savanna Wong, Dr. Denise Müller, Dr. Felicitas Psvaray, Dr. Qing Li, Dr. Rami Althnaibat, Dr. Justina Zhang, Mandy Sun, Anna Widenmann, Qin Li, Zoe Bumanis, Carris Jiang, Menglin Liu, Anying Nie, Morgan Gerlinsky, Robin Xiong, Clement Niyirora, Yuqi Shao, and Dr. Cisem Bulut Albayrak, Erica Li, Tienna Deitsch, Yuen Ying Chan for every chat, joke, and suggestion that enriched my research experience.

I am also grateful to my "foodie gang": Zheng Zhao, Tongbo Zhu, Jin Xie, and Vi Pham, for celebrating every birthday and holiday together. Though we are now spread across Denmark and Canada, I look forward to our next gathering. A special thanks to my labmate, collaborator, and friend, Vi Pham, for assisting with experiments, sharing my sorrows when I struggled with work or life, and cheering my successful moments.

Finally, heartfelt thanks to my friends Jingyi Hou, Anqi Jing, Summer Xi, Kitty Chen, and my dear family members in China for regularly checking on me and asking when I will graduate. Now you can go bragging that you have a doctoral friend/cousin/niece...

Table of Content

Abstract	II
Preface	IV
Dedication	VI
Acknowledgements	VII
Table of content	IX
List of tables	XIII
List of figures	XIV
List of abbreviations	XVIII
Chapter 1. General Introduction, Hypothesis and Objectives	1
1.1 Introduction.....	1
1.2 Hypothesis.....	6
1.3 Objectives	7
Chapter 2. A Meta-analysis of Bacterial Communities in Food Processing Facilities: Driving Forces for Assembly of Core and Accessory Microbiomes across Different Food Commodities	8
2.1 Introduction.....	8
2.2 Data collection	11
2.3 Impact of nutrient source and commodity on the composition of bacterial communities.....	14
2.4 Which bacteria are where?	18
2.5 Can a core microbiome of food processing facilities be identified?.....	24
2.6 The use of sanitizer and selective ecology:.....	33
2.7 Limitations	35
2.8 Conclusions and perspectives	36
Chapter 3. Resistance of Biofilm- and Pellicle-embedded Strains of <i>Escherichia coli</i> Encoding the Transmissible Locus of Stress Tolerance (tLST) to Oxidative Sanitation Chemicals	38
3.1 Introduction.....	38
3.2 Materials and methods	40
3.2.1 Strains and culture conditions.....	40
3.2.2 Mono- and dual-strain biofilm and pellicle formation	41
3.2.3 Sanitizers	42
3.2.4 Curli and cellulose expression.....	43

3.2.5 Effect of sodium hypochlorite on planktonic coculture	43
3.2.6 Effect of sodium hypochlorite on mono- and dual-cultures pellicle	44
3.2.7 Effect of sodium hypochlorite, hydrogen peroxide and peracetic acid on biofilms formed on stainless steel (SS) coupon	44
3.2.8 Quantification of the biomass in biofilms	44
3.2.9 Observation of biofilms with confocal laser scanning microscopy (CLSM)	45
3.2.10 Statistical analysis.....	45
3.3 Results.....	46
3.3.1 Chlorine resistance of planktonic cells.....	46
3.3.2 Pellicle formation, expression of curli, cellulose formation and chlorine resistance	48
3.3.3 Chlorine resistance of strains of <i>E. coli</i> in dual-strain biofilms	50
3.3.4 Disinfectant resistance of single-strain, dual-strain biofilms and pellicle embedded cells	53
3.3.5 Correlation of biofilm biomass and chlorine resistance	55
3.4 Discussion.....	57
Chapter 4. Socializing at the Air-Liquid Interface: A Functional Genomic Analysis on Biofilm-related Genes during Pellicle Formation by <i>Escherichia coli</i> and its Interaction with <i>Aeromonas australiensis</i>	64
4.1 Introduction.....	64
4.2 Materials and methods	66
4.2.1 Strains and culture conditions.....	66
4.2.2 Determination of pellicle formation	68
4.2.3 Genome sequencing and assessment of the presence and absence of operons in pellicle formation	68
4.2.4 Quantification of expression level of biofilm-related genes	69
4.2.5 Phylogenetic tree of the upstream region of the curli operon.....	71
4.2.6 Addition of N-acyl homoserine lactone to pellicle formation.....	71
4.2.7 Construction of <i>E. coli</i> FUA1882.....	72
4.2.8 Statistical analysis.....	78
4.3 Results.....	78
4.3.1 Comparative genomic analysis among pellicle forming strains and non-pellicle forming strains.....	78
4.3.2 Expression of genes related to pellicle formation	81
4.3.3 The addition of homoserine lactones interferes with pellicle formation	85

4.3.4 Deletion of <i>bcsG</i> , <i>curliU</i> and <i>sdiA</i> alters pellicle formation.....	86
4.3.5 Gene expression.....	89
4.4 Discussion.....	90
Chapter 5. High-Throughput Analysis of Microbiomes in a Meat Processing Facility: Are Food Processing Facilities an Establishment Niche for Persisting Bacterial Communities?	96
5.1 Introduction.....	96
5.2 Results.....	98
High throughput culture-dependent and culture-independent characterization of microbial communities in the meat processing facility.	98
Microbial diversity in the meat processing facility	105
Bacterial interactions on meat processing environmental and meat surfaces	107
Strain-level analysis of dispersal within the facility and persistence over time	112
5.3 Discussion.....	116
5.4 Materials and methods	121
Sampling strategy	121
Bacterial isolation and DNA extraction.....	122
Genome sequencing.....	123
Biofilm formation	125
Phylogenetic and single nucleotide polymorphism (SNP) analysis	126
Statistical analysis.....	128
Chapter 6. Ozone Nanobubble For Meat Spoilage Control.....	129
6.1 Introduction.....	129
6.2 Materials and methods	131
6.2.1 Strain and culture conditions	131
6.2.2 Sample preparation and inoculation	133
6.2.3 Sanitizer preparation.....	134
6.2.4 Efficacy of peracetic acid and ozone nanobubble solutions on inoculated meat samples and adipose tissues at various storage intervals.....	134
6.2.5 Impact of flow rate and solution volume on the efficacy of ozone nanobubble solutions	135
6.2.6 Determination of microbiota in treated meat under refrigerated vacuum-packaging storage.....	136
6.2.7 Microbial composition of meat samples collected <i>in situ</i>	136

6.2.8 Statistical analysis.....	137
6.3 Results.....	137
6.3.1 Ozone nanobubble solutions displayed comparable efficacy to peracetic acid on inoculated meat samples and adipose tissues at various storage intervals	137
6.3.2 Volume than flow rate impacted on the efficacy of ozone nanobubble solutions.....	141
6.3.3 Impact of storage temperature on disinfectant efficacy on meat microbiota	144
6.3.4 Microbial composition of meat samples collected <i>in situ</i>	146
6.4 Discussion.....	148
Chapter 7. Characterization and Diversity of 74 Novel Species Isolated from a Pork Processing Facility	153
7.1 Introduction.....	153
7.2 Materials and methods	153
7.2.1 Bacterial isolation, sequencing and download of type strain	153
7.2.2 Phylogenetic analysis and determination of pairwise average nucleotide identity	153
7.3 Results and discussion	154
Chapter 8. General Conclusion And Discussion	161
8.1 Translation of microbial ecology in food processing to practical sanitation protocols	161
8.2 Bacterial communication and cooperation on biofilm formation, resistance and persistence	163
8.3 Novel approaches for food safety and spoilage control.....	164
8.4 Limitations and future works	166
BIBLIOGRAPHY.....	167
APPENDIX.....	225

List of tables

Table 3.1. Strains used in this study.....	41
Table 3.2. Formation of floating biofilms (pellicles) by single and mixed cultures of three strains of <i>E. coli</i>	49
Table 3.3. Curli and/or cellulose expression of bacterial strains tested for biofilm formation... 50	
Table 4.1. Strains used in this study.	67
Table 4.2. Biofilm-related genes tested by RT-qPCR in this study.	71
Table 4.3. Primers used in this study.	74
Table 5.1. Bacterial isolates that represented less than 1% of the respective genera in Nanopore 16S rRNA gene sequencing or were not detected by sequencing.....	103
Table 5.2. Pairwise single nucleotide polymorphisms (SNPs) between genomes of isolates of <i>C. maltaromaticum</i> within the same phylogenetic cluster..	113
Table 6.1. Strains used in this study.....	132
Table 6.2. Bacterial cell counts of meat sample inoculated with 10^4 CFU/cm ² and stored vacuum-packaged for 7 d at 12 °C before and after treatment.	139
Table 6.3. Abundance of microbiota in vacuum-packaged pork samples after 3 month refrigerated storage. The microbial composition was compared among samples that were treated with/without ozone nanobubble solution <i>in situ</i>	147
Table 7.1. Summary of novel species isolated from the pork processing environments.....	154

List of figures

Figure 1.1. Determination of community assembly by selection, dispersal, drift, and diversification on the composition of environmental and product microbiota, and their effects on the quality and safety of food products.....	6
Figure 2.1. Principal coordinates analysis (PCoA) based on the Jaccard distance matrix for 96 surface-associated samples with different nutrient availabilities.....	15
Figure 2.2. Principal coordinates analysis (PCoA) based on the Jaccard distance matrix for 96 surface-associated samples from different food commodities.....	16
Figure 2.3. Principal coordinates analysis (PCoA) with Jaccard index for bacterial diversity based on 5 food processing facilities associated with different nutrients level. Points represent microbial communities collected from different processing facilities and are clusters based on same nutrient level: A, high; B, low; C, unknown.....	17
Figure 2.4. Principal Coordinate Analysis (PCoA) plot with Jaccard similarity for bacterial diversity among environmental biofilms formed under different nutrients level: red, high nutrient; blue, low nutrient.	18
Figure 2.5. Heatmap depicting the relative abundance of the occurrence of bacterial genera present in different food processing facilities.	19
Figure 2.6. Heatmap depicting the relative abundance of the occurrence of bacterial genera present in samples with different nutrient levels.	28
Figure 2.7. Venn Diagram presenting the genera shared among environmental surfaces with different nutrient level.....	29
Figure 2.8. The relative abundance of bacterial genera residing in biofilm consortia based on different food categories (A) and nutrient level (B).	33
Figure 3.1. Lethality of chlorine treatments to planktonic cells 12 strains of <i>E. coli</i> incubated with <i>Aeromonas australiensis</i> 03-09, <i>E. coli</i> O157:H7 1934 and <i>Carnobacterium maltaromaticum</i>	47
Figure 3.2. Pellicle formation and chlorine resistance of strains of <i>E. coli</i> . Panel A. Pellicle formed by <i>E. coli</i> FUA10043 after 6 days at ambient temperature in Luria broth. Panel B. Reduction of cell counts strains of <i>E. coli</i> in pellicles formed by single strain culture (black bars) or in multispecies pellicles formed in Luria broth at room temperature for 6 d, followed by treatment with 800 ppm NaClO.....	49

Figure 3.3. Reduction of cell counts of tLST-positive and tLST-negative strains of <i>E. coli</i> biofilms after treatment with NaClO.....	52
Figure 3.4. Reduction of cell counts of tLST-positive and tLST negative strains of <i>E. coli</i> after chlorine treatment of single species or multi-species biofilms. Biofilms were treated with 800ppm NaClO (Panel A), or 5% hydrogen peroxide (Panel B) or with 0.032% (v/v) peroxyacetic acid (Panel C).	54
Figure 3.5. Quantification of the biomass of biofilms formed by single species of multi-species biofilms using crystal violet staining..	56
Figure 3.6. Correlation of the reduction of cell counts after chlorine treatment and the biofilm biomass. Shown are single species biofilms of strains of <i>E. coli</i> (□) or multi-species biofilms with <i>E. coli</i> and <i>Aeromonas australiensis</i> 03-09 (▼), <i>E. coli</i> O157:H7 1934 (□) or <i>Carnobacterium maltaromaticum</i> 9-67 (□).....	59
Figure 4.1. The phylogenetic distance of the upstream region of curli (A) and cellulose (B) biosynthesis operon among 39 strains of <i>E. coli</i> with <i>Salmonella</i> Typhimurium CMCST_CEPR_1 as the reference (green).....	80
Figure 4.2. The expression level of biofilm-related genes in 8 strains of <i>E. coli</i> in pellicle-embedded cells (6d) relative to the expression in in planktonic cells (1d). Results are sub-grouped by genes associated with EPS biosynthesis (A) and regulatory system (B).	82
Figure 4.3. The expression level of biofilm-related genes in 8 strains of <i>E. coli</i> relative to that in <i>E. coli</i> incubated with biofilm producer <i>Aeromonas australiensis</i>	84
Figure 4.4. Pellicle formation by strains of <i>E. coli</i> at 25 °C in 24-well plate for 6 days.	86
Figure 4.5. Pellicle formation in wild type, mutant strains of <i>E. coli</i> FUA1882 and in after complementation of <i>bcsG</i> and <i>sdiA</i> in <i>E. coli</i> FUA1882 $\Delta bcsG::cam$ and $\Delta sdiA::cam$, respectively.	88
Figure 4.6. The expression level of curli and cellulose biosynthesis genes in <i>sdiA</i> -defected <i>E. coli</i> FUA1882 relative to wild type in planktonic cells (green bars) and pellicle-embedded cells (yellow bars).....	90
Figure 5.1. Heatmap of bacterial isolates collected from meat samples and environmental surface samples during the second time sampling, March 2023. Taxonomy classification was determined based on whole-genome pairwise alignment to Genome Taxonomy database.....	100

Figure 5.2. Relative abundance of uncultured genera identified in samples collected in March 2023 by sequencing of full length 16S rRNA genes.....	104
Figure 5.3. Principal coordinate analysis, using Bray-Curtis distance with isolates classified at species level for 70 sampling sites, collected in March 2023. The dissimilarity among collected samples were measured from four categories: A: type of surfaces, B: location, C: sanitation activity and D: zone classification.	106
Figure 5.4. Principal coordinate analysis (PCoA) plots of the Bray-Curtis distance matrix for bacteria community as determined by 16S rRNA amplicon sequencing of samples from March 2023. The samples were grouped based on surface type (A), location (B), sanitation activity (C) and zone classification (D).....	107
Figure 5.5. Bacterial coexistence network based on the microbial communities across 66 surface samples and 4 meat samples, comprising 1281 isolates classified by genome sequencing. Bacterial species with one-time occurrence among all sampling surfaces were not included.....	109
Figure 5.6. Quantification of the biomass (A) and composition of the microbial community (B) of biofilms that were reconstituted with isolates from 10 sampling sites..	110
Figure 5.7. Phylogenetic tree of strains of <i>C. maltaromaticum</i> based on core genome alignment, utilizing the GTR+I+G4 model with 1000 bootstrap replicates. The tree was rooted with the outgroup, <i>C. divergens</i> DSM20263..	114
Figure 5.8. Distribution of meat-spoilage associated isolates across various sampling sites from the meat processing facility. The symbols represent different bacterial species: <i>C. maltaromaticum</i> (◊), <i>C. divergens</i> (□), <i>S. proteamaculans</i> (◆), <i>R. rivi</i> (➤) and <i>R. inusitata</i> (■).....	115
Figure 5.9. Sampling strategy and experimental workflow.	122
Figure 6.1. Bacterial reduction of each inoculum strain after treatment.....	139
Figure 6.2. Bacterial cell counts of each inoculum strain after treatment. Cell counts were collected after treated samples stored at 8°C for 7 weeks.	141
Figure 6.3. Reduction of cell counts of in inoculum strains with treatment of 500ml solutions for 1min.	143
Figure 6.4. Reduction of cell counts of in inoculum strains after flow-system (30 ml/min) treatment..	144
Figure 6.5. Bacterial cell counts of inoculum strains in treated meat samples after vacuum-packaging storage.....	145

Figure 7.1. Phylogenetic distance (A) and Average Nucleotide Identity (ANI) (B) of the new species and their closely related type strains.159

List of abbreviations

CFU: colony forming units

SS: stainless steel

NFCS: non-food contact surface

FCS: food contact surface

PCA: plate count agar

APT: all-purpose tween

VRBG: violet red bile glucose

LBNS: Luria–Bertani without NaCl

GTDB: genome taxonomy database

SNP: single nucleotide polymorphism

ANOVA: analysis of variance

PCoA: principal coordinates analysis

PCR: polymerase chain reaction

PERMANOVA: permutational multivariate analysis of variance

WGS: whole genome sequencing

tLST: transmissible locus of stress tolerance

Chapter 1. General Introduction, Hypothesis and Objectives

1.1 Introduction

Foods are complex microbial ecosystems, and the presence of microbes play pivotal role in food safety and security as well as human health and nutrition. Food ecosystems are subject to large fluctuations in environmental conditions and are dynamic due to microbial composition, activities and interaction (Roy and Lapointe, 2016). With the development of Next Generation Sequencing (NGS) technologies and available bioinformatic tools (Kergourlay et al., 2015), growing efforts are documented to study the ecology, evolution and assembly of food microbial communities. The community assembly framework developed by Mark Vellend (Vellend, 2010), consisting of four main processes: dispersal, selection, diversification, and drift, has been interpreted in the production of a few fermented foods, including sourdough, cheese and fermented cabbages (Gänzle and Ripari, 2016; Louw et al., 2023), but not in other food commodities.

Dispersal. The movement of microorganisms across space influence the distribution and diversity of communities over time, and further shapes the microbial biogeographical patterns (Martiny et al., 2006). In food processing facilities, microbial dispersal involves the transmission of microbes from raw materials, human handling, surrounding environments (soil, water, and air), production and sanitation processes to food products (Fig 1.1). Examples of microbial transportation from raw materials include plant endophytes that colonize entire plant tissues (Kandel et al., 2017) and animal-associated microbiota carried during slaughtering processes (Quan et al., 2020). Microbes associated with improper human handling include *Salmonella*, Shiga toxin-producing *Escherichia coli* and *Staphylococcus aureus* (Augustin et al., 2020), which has been reported as the recurring culprit for foodborne outbreaks. Additionally, food processing facilities are open systems, which facilitate the dispersal of microbes from above sources to food products through plant design and

production processes (Yang et al., 2023a). Further, sanitation protocol, such as the use of high pressure hose spraying or cleaning by dry ice blasting generates splashes and aerosols, and further facilitate the translocation of microbes (Saini et al., 2012).

Selection. Selection is defined as "changes in community structure caused by differences in fitness" (Vellend, 2010). In food processing facilities, both abiotic and biotic factors shape the microbial assembly structure. Common abiotic factors include processing environments (temperature, humidity), habitat types (different nutrient levels in food products and processing commodities), hygienic design and the use of antimicrobials in sanitation plans. For instance, meat fabrication facilities typically operate at refrigerated temperatures, favoring the growth of psychrotrophic bacteria such as *Pseudomonas* and *Listeria monocytogenes* (Wei et al., 2019). Additionally, nutrient-rich environments such as direct food contact surfaces favor the growth of microbes with high *rrn* copy numbers, while microbes with low *rrn* copy numbers being preferred in nutrient-depleted environments (Dai et al., 2022). Bacterial cooperation is promoted in nutrient-scarce environments, while competition weighs more in nutrient-rich environments (Dai et al., 2022). Hygienic design determines the microbial assembly through i) creating inaccessible niches for disinfectants to reach, ii) types of cleaning and sanitation protocols, iii) dilution and biodegradation of applied sanitizers. For example, *Pseudomonas* are more tolerant to chemical sanitizers, while gram positive bacteria show improved survival in dry processing environments (Møretrø and Langsrud, 2017). The presence of genes mediating quaternary ammonium compounds (QAC) resistance among microorganisms including *L. monocytogenes*, *Pseudomonas* and *Staphylococcus* promote the development of persistent microbiota when biocides with suboptimal concentrations are applied in the food processing facility (Alvarez-Molina et al., 2023) or through the dilution in environments such as inaccessible niches with accumulated dirt and

grease (Martínez-Suárez et al., 2016). The use of antimicrobial compounds during sanitation protocols serves as another selection force for species richness and further impacted on the evolution of adaptive genetic and genomic traits (Wang et al., 2024). For example, General Stress Response regulon, stress survival Islet 1 and 2 (SSI-1, SSI-2) promotes the survival of *L. monocytogenes* under harsh environments (Harter et al., 2017).

Biotic factors include biofilm formation and interactions, development of persister cells, bacteriocin production, and horizontal gene transfer. Bacterial biofilms are a natural state of cells in environments. Formation of biofilms protects bacteria against harsh conditions e.g. shearing force, routine clean and sanitation (Bridier et al., 2011; Flemming and Wingender, 2010), while the synergistic or antagonistic interactions between microbes could outcompete the growth of specific organisms during biofilm formation. For example, the presence of *L. monocytogenes* on food processing surfaces is negatively correlated with the presence of *Janthinobacterium* (Fox et al., 2014). Persister cells, particular abundant in biofilms, display a substantial selective advantage in adapting to adverse conditions (Wood et al., 2013). The production of bacteriocins, on the other hand, can either promote the formation of biofilms (Bleich et al., 2015) or inhibit the growth of surrounding microorganisms (P. Zhang et al., 2019). The selection process for microbial community assembly may also depend on horizontal gene transfer, through the movement of mobile genetic elements and plasmids (Nemergut et al., 2013). A distinct example includes the presence of the mobile genomic island, transmissible locus of stress tolerance (tLST) (Kamal et al., 2021), which is commonly horizontally transferred among diverse members of beta- and gamma-Proteobacteria. The genotypic presence of this mobile element impedes the efficacy of heat treatment in planktonic cells of *Cronobacter sakazakii*, *Klebsiella pneumoniae*, *Pseudomonas aeruginosa*, and *E. coli* (Bojer et al., 2010; Gajdosova et al., 2011; Lee et al., 2015; Mercer et al.,

2015; Wang et al., 2020), as well as increase tolerance to oxidizing chemicals (chlorine, peracetic acid and hydrogen peroxide), and high hydrostatic pressure among food isolates of *E. coli* and *Salmonella* (Gayán et al., 2023; Li et al., 2020; Wang et al., 2021a, 2021b).

Diversification. The diversification process involves the generation of genetic variation or the creation of new species. Common evolutionary drivers such as horizontal gene transfer, and biofilm formation, positive selection, sanitation protocol with sublethal concentration accelerate diversification processes (Nemergut et al., 2013). The persistence of *L. monocytogenes* strains in seafood processing facilities over 17 years served as a compelling example of evolution through the acquisition of diverse prophages associated with sanitizer tolerance genes/operons (Harrand et al., 2020).

Drift. Drift is a stochastic process that alters the relative abundance of community members, which is the most complex process to understand and predict. In processing facilities, an accident plant fire - such as the fire tragedy at the Trochu meat plant in Alberta - can significantly impact the drift process by disrupting microbial communities and altering environmental conditions, leading to shifts in species composition and abundance (McLauchlan et al., 2020). Additionally, the impact of drift is magnified when populations are small, e.g. the establishment of a new food processing facility. It has been reported that strains of *Listeria* can colonize meat and seafood processing facilities within three months of the start of production and persist for years (Alvarez-Molina et al., 2021; Harrand et al., 2020). Thus, the cleaning of incoming raw materials, proper design of processing plants and sanitation protocols for equipment surface as well as incoming materials are crucial to diminish pathogenic populations at the beginning and prevent the establishment and colonization of foodborne pathogens in food processing environments in long term.

Efforts to comprehend microbial dynamics in food processing environments and devise economical sanitation protocols are expanding. However, our understanding of microbial dynamics, assembly processes, and their ecological and evolutionary drivers remains limited. Factors contributing to this limitation include the high diversity and rapid evolutionary rates of microorganisms, intricate microbial interactions, complex eco-evolutionary feedback loops, bias from culture-independent sequencing tools and a skewed emphasis in genomic data towards foodborne pathogens from outbreaks rather than encompassing environmental microbiota (including both spoilage and pathogenic organisms) in food processing plants and. Additionally, there is a deficiency in subtyping the environmental background microbiota and reassembling the bacterial communities to study their ecological and evolutionary processes, particularly in their dispersal and persistence patterns. By clarifying these research gaps may enhance biological control within food processing environments, advance sanitation strategies, ensure food safety and quality, and foster a more sustainable food system.

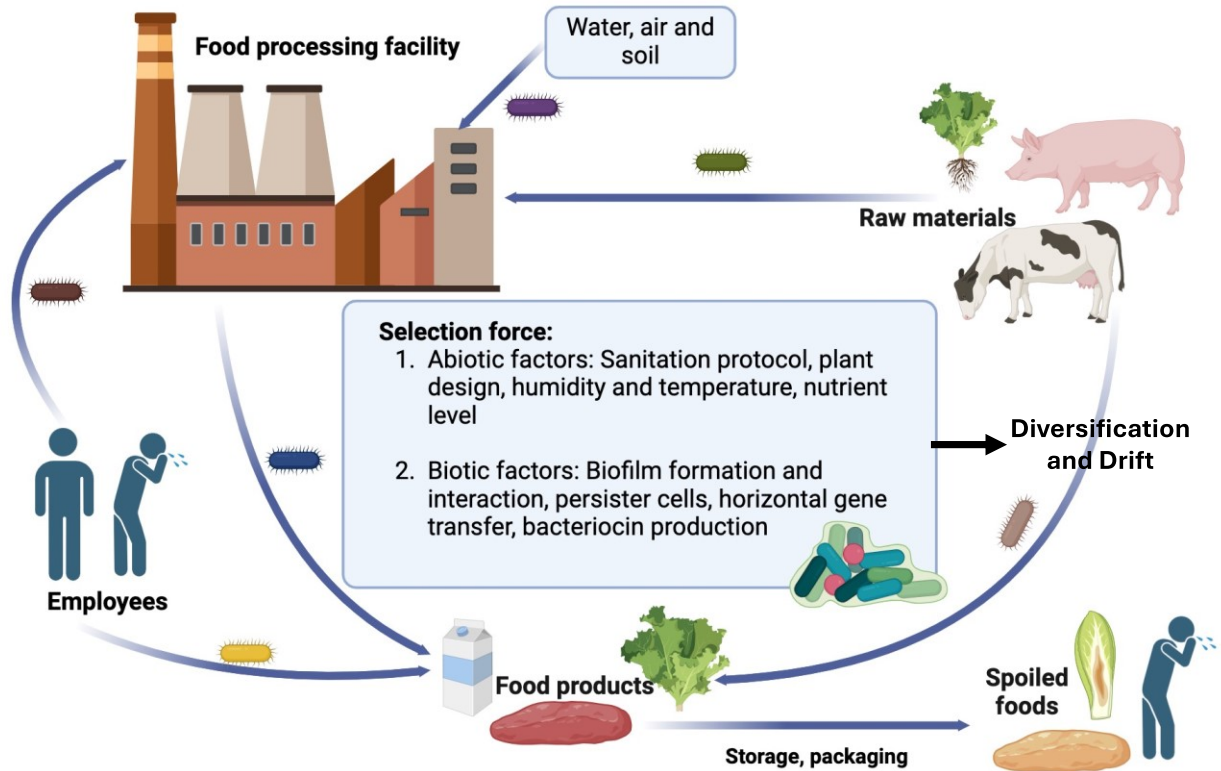


Figure 1.1. Determination of community assembly by selection, dispersal, drift, and diversification on the composition of environmental and product microbiota, and their effects on the quality and safety of food products.

1.2 Hypothesis

Microbial community assembly and biofilm formation in food processing environments are influenced by nutrient availability, specific genetic factors (such as tLST in *E. coli*), and intercellular communication. These factors, combined with environmental conditions and sanitation practices, shape the core microbiome and impact microbial diversity, persistence, and resistance. The application of ozone nanobubble solutions reduce meat spoilage and alter the microbial profiles in meat processing facilities.

1.3 Objectives

- 1) Discuss the impact of nutrient level on microbial community assembly in food processing environments and biofilm communities and identify the core microbiome among different food commodities (Chapter 2).
- 2) Evaluate the impact of tLST impact in strains of *E. coli* on biofilm formation and sanitizer resistance (Chapter 3).
- 3) Investigate the biofilm-associated genes on pellicle formation in strains of *E. coli* and role of intercell communication on the switch of surface-associated biofilms to floating pellicles (Chapter 4).
- 4) Characterize the microbial diversity, bacterial dispersal and persistence in a meat processing facility (Chapter 5).
- 5) Examine the application of ozone nanobubble solution on meat spoilage control and impact on meat microbiota profiles (Chapter 6).
- 6) Characterize 74 novel species isolated from the pork processing facility (Chapter 7)

Chapter 2. A Meta-Analysis of Bacterial Communities in Food Processing Facilities: Driving Forces for Assembly of Core and Accessory Microbiomes across Different Food Commodities

2.1 Introduction

According to the Food and Agricultural Organization, the demand for food is expected to increase by 56% to meet the needs of the growing global population (FAO, 2009). To address this challenge, several solutions have been proposed, with reducing food loss and waste being the most crucial one. Unfortunately, approximately 25% of food that is produced for human consumption is wasted, and this loss occurs at various stages of the food supply chain, from production to consumption (Janet et al., 2018). One of the significant contributors to food waste is microbial spoilage. This issue is of concern for food security, as food spoilage can lead to decreased food availability and increased prices, making it even more challenging for food-insecure populations to access sufficient nutritious food. Spoilage also is of concern for the sustainability of food production and emission of greenhouse gases, particularly for meat and meat products that have a high ecological footprint.

The microbial spoilage of food has been widely probed within food processing facilities across various food commodities. Processing facilities serve both as establishment niche, where it allows autochthonous microbes to colonize and persist over long periods of time, and as a persistent niche for microbes that are transmitted from raw materials or the environment (Holt, 2009). Researchers have approached microbial-mediated food spoilage from different angles, by examining the microbiome of raw materials and final products, the transmission from poor handling practices and the role of environmental surfaces during production. The assembly of bacterial communities in food processing facilities is influenced by four processes: selection, drift, speciation, and

dispersal (Vellend, 2010). More precisely, microbes coming into food processing facilities are limited by dispersal while persisting organisms are limited by selection due to routine sanitization. Species drift can be observed as bacteria population changes in conformity with changing processing environments. For example, psychrotrophic or psychrophilic organisms such as *Pseudomonas*, *Enterobacteriaceae*, and lactic acid bacteria can grow on fresh meat (Gill, 2014; Zhu et al., 2022), seafood (Zhu et al., 2022), fresh produce (Alegbeleye et al., 2022) during cold-temperature storage with different taxonomic abundance at the end of shelf life. The speciation process can occur more rapidly during biofilm formation in the processing environments, as biofilm provides an optimal environment for exchanges of genetic materials horizontally and for the evolution of vertically transmitted generic material (Bridier et al., 2011).

The ability of bacteria to form biofilms contributes to recurring contamination from environmental surfaces, both in food-contact and non-food-contact areas (Mertz et al., 2014; Wagner et al., 2020; Wang et al., 2018). In fact, the biofilm matrix serves as a physical shelter to bacterial cells, thus protecting them against antimicrobial interventions and serving as a reservoir for both spoilage and pathogenic microorganisms. Many food isolates from equipment surfaces have been shown to attach to different food materials and form biofilms *in vitro* (Abdallah et al., 2014; Liu et al., 2016). Recent studies have also identified residential bacterial communities embedded in biofilm matrix, as evidenced by quantifying biofilm biomass [8-10]. This poses a major challenge to conventional cleaning and sanitizing procedures in food processing facilities, raising concerns about cross-contamination from processing environments to products, and leading to food poisoning and deterioration issues.

The food industry, therefore, employs multiple measures to control the microorganism coming in with raw materials and those persisting in processing facilities. In general, Hazard Analysis Critical

Control Point (HACCP) has been well adopted worldwide, primarily focusing on enhancing food safety. Decontamination of the raw materials prior to production such as washing and sanitizing fresh produce with chlorine water (Mcglynn, 2004), washing of animal carcasses with hot water (Dickson and Anderson, 1992; Wheeler et al., 2014), and monitoring animal health and farm hygiene (United States of Food and Drug Administration, 2011) have been reported to reduce the population of bacteria on raw materials. The efficacy of cleaning and sanitation protocols, however, depends on the hygienic design of facilities and equipment, and on the training of personnel. In addition, plants are colonized by bacterial endophytes including *Bacillus*, *Burkholderia*, *Rahnella*, *Pseudomonas*, and *Klebsiella* (Kandel et al., 2017; Lodewyckx et al., 2002; Ryan et al., 2008) that cannot be removed without heating the entire plant tissue.

Although numerous studies have identified the composition of bacterial communities in facilities processing different food commodities and investigated the impact of processing environments on bacterial communities, little is known about how nutrient availability shapes their composition, or whether food processing facilities processing different food commodities harbor comparable bacterial communities. The composition of bacterial communities between environmental surfaces and food products has been compared for one minimally processed vegetable facility, one artisan cheese facility and two meat processing facilities by analyzing the relative abundance of taxa (De Filippis et al., 2013; Falardeau et al., 2019; Hultman et al., 2015; Valentino et al., 2022). These studies identified both the raw materials and the food processing environment as relevant sources of spoilage microbes. This review aimed to expand these analyses by providing a comprehensive summary of residential bacteria on environmental surfaces of processing facilities of multiple food commodities and by analysing whether the nutrient availability on specific surfaces impacts the composition of bacterial communities.

2.2 Data collection

Data collection was started by accessing references from four review papers (Alvarez-Ordóñez et al., 2019; De Filippis et al., 2021; Fagerlund et al., 2021; Yuan et al., 2019) on the bacterial ecology and communities involved in food spoilage as well as later publications that cited these reviews. Taken together, these four review papers provide a comprehensive summary of microbial communities found in different food processing facilities as a “beacon” for subsequent searches in citation databases. Additional studies were identified by using the keywords "food industry," "bacterial ecology," "bacterial communities", and "food spoilage" on Google Scholar. Priority was given to studies that sampled environmental surfaces and used 16S rRNA gene amplicon sequencing for analysis. Three studies using a culture-based approach to characterize bacterial communities in facilities producing meat and seafood were additionally included. The presence or absence of bacterial taxa in 96 samples collected from 39 processing facilities were compiled in Table S1. The 39 processing facilities included 16 facilities processing fresh meat (Brightwell et al., 2006; Cobo-Díaz et al., 2021; De Filippis et al., 2013; Ellerbroek, 1997; Fox et al., 2014; Hultman et al., 2015; Marouani-Gadri et al., 2009; Mettler and Carpentier, 1998; Møretrø et al., 2013; Røder et al., 2015; Stellato et al., 2016; Wagner et al., 2020; Wang et al., 2018; Yang et al., 2023b; Zwirzitz et al., 2021, 2020), 7 facilities processing seafood (Bjørge Thomassen et al., 2023; Guobjörnsdóttir et al., 2005; Langsrud et al., 2016; Maillet et al., 2021; Møretrø et al., 2016; Rodríguez-López et al., 2015), 3 facilities processing RTE foods (Fagerlund et al., 2017; Mertz et al., 2014; Pothakos et al., 2015), 5 facilities processing fresh produce (Gu et al., 2019; Liu et al., 2013; Tan et al., 2019; J. G. Xu et al., 2021; Xu et al., 2022), and 8 facilities processing cheese (Bokulich and Mills, 2013; Calasso et al., 2016; Dzieciol et al., 2016; Falardeau et al., 2019; Guzzon et al., 2017; Quijada et al., 2018; Schön et al., 2016; Stellato et al., 2015). In total, this

review summarised the microbial communities from 96 environmental surfaces. Three of the 39 facilities were characterized with respect to biofilm communities, these included two meat processing facilities and one cheese facility for a total of 13 surfaces that harbored biofilms.

Of the food processing facilities included in this study (Table S2.1), RTE and cheese processing facilities were located in North America and Europe; the meat processing facilities were located in North America, Oceania, and Europe. All of the seafood processing facilities sampled were located in Europe. The fresh produce processing facilities were located in North America and Asia. These geographical differences may reflect variations in processing methods, regional microbiota, cultural and environmental factors. For example, traditional and minimally processed food (raw milk cheese and fermented meats) are favored in the European Union, whereas Americans tend to be more open to the use of technologies during the production such as the use of the hormones/antibiotics for cattle, and irradiation treatment for food (Johnson, 2017; Marsha A. Echols, 1998). Additionally, grass-fed cattle with different breeds, shapes, and sizes, processed in smaller and artisan operations are used for consumptions in the EU. In contrast, in North America, feedlot-fed cattle are raised to a uniform size for large-scale industrial production (Beardsley, 2009), contributing to distinctive gut microbiota composition (Z. Zhang et al., 2021), which in turn potentially affects meat quality and the environmental microbiome in the processing facility. Processing facilities and meat animals in Oceania are more similar to those in the EU than to North America (Bell et al., 2011).

The condition and environment vary in different processing commodities. Seafood processing facilities typically maintain relatively high humidity and a temperature of 12°C (Langsrud et al., 2016), which can promote the proliferation of psychrotrophic microbes. Meat processing facilities generally maintain a temperature of less than 10°C to preserve meat products during the most of

processing stages (Canadian Food Inspection Agency, 2018), but temperatures differ between plants and even within different rooms of the same plant. In a meat abattoir, the temperature of the production room ranged from 14°C to 25°C with relative humidity between 35% to 90% (Møretrø et al., 2013). In a beef processing facility, the temperature in slaughter hall, cutting room and boning room was 10-15°C, 4-5°C, and 11-15°C, respectively (Marouani-Gadri et al., 2009). Fresh produce processing rooms are maintained at a temperature below 8°C (Xu et al., 2022). The processing room temperature for the cheese industry can vary depending on the specific type of cheese being produced and the stage of the cheese-making process. In general, cheese processing facilities maintain a higher processing temperature of over 20°C to promote the growth of mesophilic and/or thermophilic starter cultures. A lower temperature (9°C) with high relative humidity (75%) is maintained during ripening stage (Calasso et al., 2016). Salt concentration may additionally shape the bacterial ecology in cheese processing facilities. For example, halotolerant *Halomonas* was only identified in cheese processing facilities, potentially resulted from the brining process. Cleaning and sanitization control bacterial contamination in food processing facilities but also contribute to high temperature and humidity (Møretrø et al., 2013), serving as a potential source for cross contamination and selective pressure for microbial communities.

The datasets were analysed using permutational multivariate analysis of variance (PERMANOVA, 999 permutations, adonis2 function, vegan package, R v4.1.0) based on Jaccard similarity of bacterial communities with an error probability of 5% ($P \leq 0.05$) to determine whether areas with different nutrient densities harbor different communities of microbes. The data were visualized by Principal Coordinate Analysis (PCoA). Pairwise comparisons between groups were tested by the 'pairwise.adonis' function (pairwise.Adonis package, v0.4.1) with Bonferroni adjustment for multiple comparisons. Data were additionally analysed with Multiple Correspondence Analysis

(MCA), which uses the presence of individual genus as input variables to visualize the dataset. Results of PCoA are shown in the manuscript and results obtained with MCA are provided as supplementary figures.

2.3 Impact of nutrient source and commodity on the composition of bacterial communities.

We classified direct food contact surfaces and floor drains as "high nutrient" areas as these areas are characterized by the presence of product residue during processing. Non-food contact surfaces, walls and water hoses were characterized as "low nutrient" areas because they are unlikely to provide organic matter to support bacterial growth. The nutrient level of floors was categorized as "unknown". This differentiation does not account for the type of substrate (lipids, carbohydrate / sugars or proteins / amino acids) and the type of nutrients can only partially be inferred from the type of product that is processed in the specific facilities. Overall, the composition of bacterial communities in sites with different nutrient availabilities differs ($P < 0.05$) (Fig. 2.1). The bacterial community in high-nutrient surfaces differs from unknown surfaces ($P = 0.036$). Plotting the data separately by commodity revealed a partial overlap in the composition of bacterial communities in sites with high, low, and unknown nutrient availability (Fig. S2.1), with the exception of cheese processing facilities, where high and low-nutrient surfaces differed significantly ($P < 0.05$). The similarity of bacterial composition between different nutrient levels within one food commodity may be attributed to the smaller sample size of sites with low or unknown nutrient availability. In contrast, MCA visualized a largely distinct composition of bacterial communities in sites with different nutrient availability with individual taxon as input (Fig. S2.2).

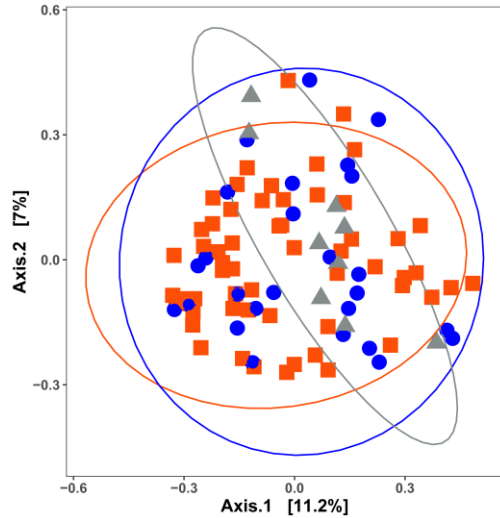


Figure 2.1. Principal coordinates analysis (PCoA) based on the Jaccard distance matrix for 96 surface-associated samples with different nutrient availabilities. Samples are coloured by nutrient availability: red, high nutrient; blue, low nutrient; grey, unknown surfaces. Permutational multivariate analysis of variance was used to statically differentiate the bacterial communities. Bacterial communities are significantly different ($P = 0.047$) among surfaces with different nutrient availability. Bacterial community on surfaces with unknown nutrient availability tend to differ from high nutrient surfaces (pairwise adjusted $P = 0.084$).

The PCoA plot of samples categorized by commodity also showed partial overlap of the bacterial communities in facilities producing different commodities (Fig. 2.2). Bacteria residing in RTE processing facilities shared a substantial number of bacterial taxa with other food processing facilities, while all other categories were significantly different from each other ($P < 0.05$) (Fig. 2). The size of the dataset allows further categorization by commodity and nutrient level (Fig. 2.3). With the exception of RTE processing facilities, high-nutrient level surfaces of processing facilities exhibited distinct bacterial communities (Fig. 2.3A). The overlap of bacteria was greater in low nutrient sites where only cheese plants had significantly distinct ecology compared to meat

and fresh produce processing facilities (Fig. 2.3B). Sites with unknown nutrient density, i.e., floors which were only sampled in fresh produce, cheese, and fresh meat facilities. The limited sample size perhaps largely resulted in the overlap, while MCA plot further reveals that different commodities clustered completely separately (Fig. S2.3C). The PCoA plot for those samples for which *in situ* biofilm formation was confirmed by quantification of the extracellular matrix was shown in Figure 2.4. The composition of bacterial biofilm communities in low-nutrient and high-nutrient samples was significantly different ($P < 0.05$) (Fig. 2.4).

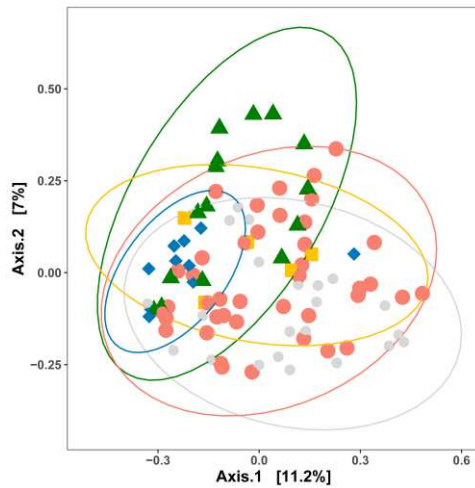


Figure 2.2. Principal coordinates analysis (PCoA) based on the Jaccard distance matrix for 96 surface-associated samples from different food commodities. Samples are coloured by food commodity: yellow, RTE processing facilities; red, meat processing facilities; blue, seafood processing facilities; green, fresh produce processing facilities; light grey, cheese processing facilities. Permutational multivariate analysis of variance was used to statically differentiate bacterial communities. The association of community variance with different food commodities are displayed in supplementary Table S2.2.

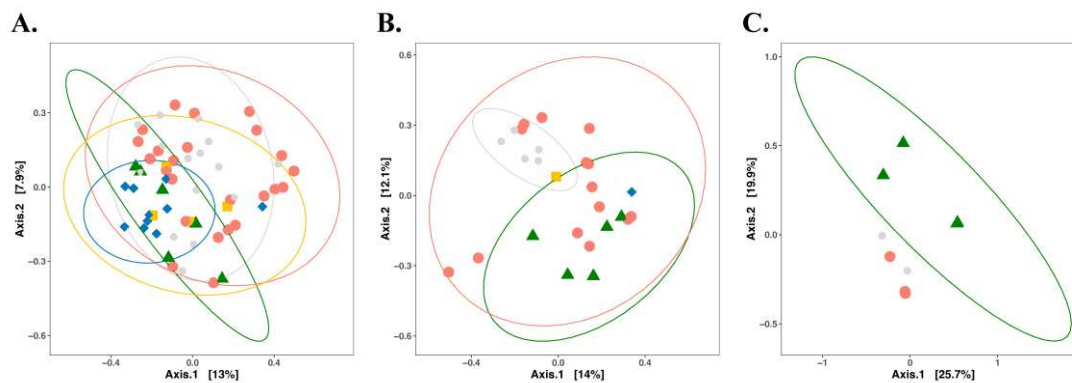


Figure 2.3. Principal coordinates analysis (PCoA) with Jaccard index for bacterial diversity based on 5 food processing facilities associated with different nutrients level. Points represent microbial communities collected from different processing facilities and are clusters based on same nutrient level: A, high; B, low; C, unknown. Light grey, cheese processing facilities; green, fresh produce processing facilities; red, meat processing facilities; yellow, RTE processing facilities; blue, seafood processing facilities. Permutational multivariate analysis of variance was used to statically differentiate bacterial communities. The association of community variance with different food commodities for high- and low-nutrient surfaces are displayed in supplementary Tables S2.3 and S2.4, respectively.

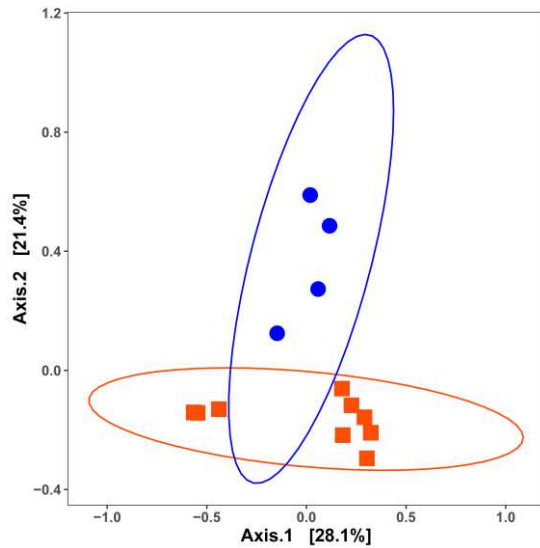


Figure 2.4. Principal Coordinate Analysis (PCoA) plot with Jaccard similarity for bacterial diversity among environmental biofilms formed under different nutrients level: red, high nutrient; blue, low nutrient. Data collected from two meat processing facilities and one cheese processing facility, contributing to 13 sampling surfaces in total. Permutational multivariate analysis of variance was used to statically differentiate bacterial communities.

2.4 Which bacteria are where?

Heatmaps depicting the percentage of samples in which specific taxa were present are shown in Figures 2.5, 2.6 and 2.8. The heatmaps were scaled to show the number of samples that tested positive for a specific taxon divided by the total number of samples. The majority of taxa depicted in the heatmaps were identified at the genus level, but some provided only family-level identification. The heatmaps shown in Figures 2.5, 2.6 and 2.8 differentiate samples by nutrient level, commodity and biofilm, respectively. Overall, *Pseudomonas*, *Stenotrophomonas*, *Acinetobacter*, *Serratia*, *Microbacterium*, *Psychrobacter*, and *Staphylococcus* were frequently present regardless of the food commodity with *Pseudomonas* species as the most prevalent taxa

(Fig. 2.5). Meanwhile, the composition of bacteria communities also differed among facilities processing different food commodities.

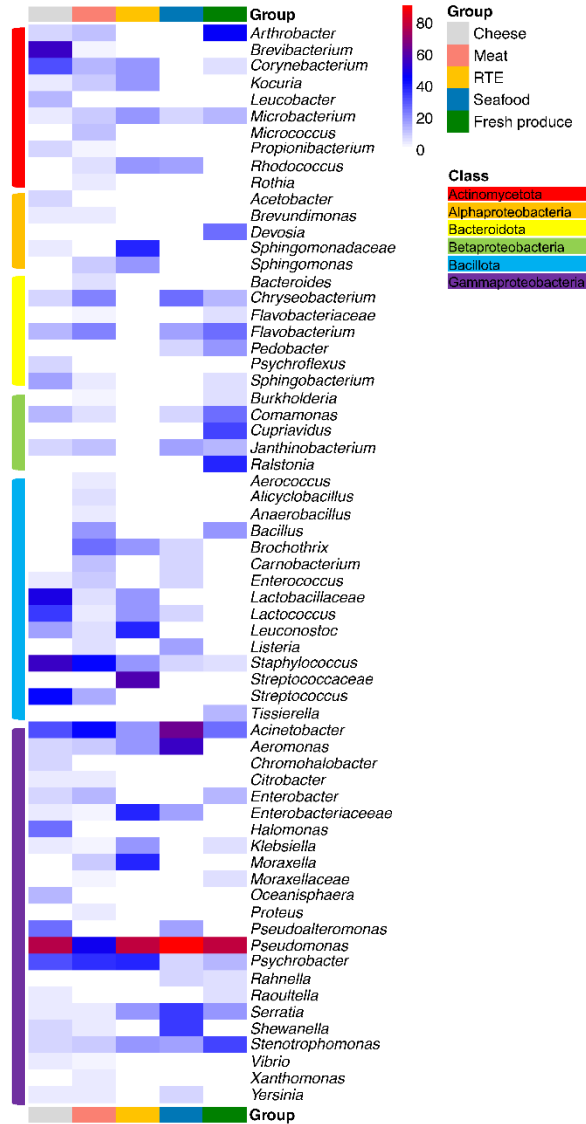


Figure 2.5. Heatmap depicting the relative abundance of the occurrence of bacterial genera present in different food processing facilities.

In cheese processing facilities, *Pseudomonas* was present in 17 out of 22 environmental surfaces, followed by *Brevibacterium*, and other *Bacillota* such as *Staphylococcus*, *Lactobacillus*,

Streptococcus, and *Lactococcus* (Fig. 2.5). Because most studies used in this meta-analysis identified bacteria at the genus level, and were completed before taxonomic re-organization of the genus *Lactobacillus* in 2020 (Zheng et al., 2020), *Lactobacillaceae* are often identified at the family level only (Fig. 2.5 and 2.6); this communication uses current taxonomy where this is supported by the data, or the terms “*Lactobacillaceae*” or “lactobacilli” where not. The processing steps in cheese production impact the composition of bacterial communities. For instance, brining and the use of surface-ripening provide favorable conditions for growth of acid-sensitive, salt-tolerant, and psychrotrophic bacteria which are abundant on smear-ripened cheeses but were also identified on environmental surfaces (Guzzon et al., 2017; Quijada et al., 2018). Coryneforms, such as *Brevibacterium*, *Corynebacterium*, as well as *Halomonas* and *Staphylococcus* are among the main microbial genera that were identified on the surface of smear-ripened cheeses (Wolfe et al., 2014). These organisms may cause defects in other types of cheeses (Hassan and Frank, 2011). The high prevalence of *Lactobacillus*, *Streptococcus*, and *Lactococcus* on surfaces is unsurprising given their role as starter cultures for cheese production (Falardeau et al., 2019; Guzzon et al., 2017). The *Lactobacillus* species detected were *L. delbrueckii* and *L. helveticus*, originating from thermophilic starter cultures used in cheese making. Equipment surfaces primarily harbored Gamma-proteobacteria such as *Psychrobacter*, *Acinetobacter*, and *Pseudoalteromonas*, which can cross-contaminate food samples (Falardeau et al., 2019; Guzzon et al., 2017; Quijada et al., 2018). The origin of the microbiome in on surfaces in cheese processing facilities varies among different plants and remains unclear. For example, *Corynebacterium*, *Staphylococcus*, and *Sphingobacterium* can be part of the raw milk or human skin microbiota (Kable et al., 2016) and subsequently spread to equipment surfaces. Lactose carry-over from vat milk or whey to non-food contact surfaces may contribute to the higher abundance of *Staphylococcus* spp. in cheeses

compared to other commodities, since lactose can stimulate the biofilm formation by *Staphylococcus* (Xue et al., 2014).

In meat processing facilities, common food spoilage bacteria including *Pseudomonas*, *Acinetobacter*, and *Psychrobacter* have been identified on over one third of the environmental surface samples (Fig. 2.5). The phylum of *Bacillota* also has a relatively high abundance with presence of *Staphylococcus*, *Brochothrix*, *Bacillus*, and *Streptococcus*. In addition to transmission from human and animal skin microbiota, high abundance of *Staphylococcus* and *Corynebacterium* has also been detected in air samples throughout a poultry slaughtering house (Ellerbroek, 1997). *Bacteroidota*, including *Chryseobacterium* and *Flavobacterium*, have the potential to cause spoilage of meat and have been isolated from both meat carcasses and environmental surfaces (Røder et al., 2015; Zwirzitz et al., 2021, 2020). *Brochothrix* is recognized as a spoiler of raw and packaged meat and has been identified on food processing surfaces (Ellerbroek, 1997; Wagner et al., 2020; Wang et al., 2018), which readily grows on meat and at low storage temperature (Illikoud et al., 2019), even if the contamination from equipment surfaces begins with a low cell population. *Enterobacteriaceae* and lactic acid bacteria including lactobacilli, *Leuconostoc*, and *Carnobacterium* also play important roles in meat spoilage either as spoilage organisms or as protective microbes that inhibit spoilage by others. Vacuum packaged fresh meat has a refrigerated shelf life of over 2 months, which of the microbes on meat grow during storage depends on the meat composition, the presence of competing microbes, storage conditions, packaging methods, and oxygen availability (Gill, 2014). In these products, *Enterobacteriaceae* are present in high abundance on the processing facilities surfaces but to a lesser extent in raw materials and products at the end of the shelf life, whereas lactic acid bacteria dominate meat microbiota at the end of the shelf life with low abundance in both processing surfaces and raw materials (Hultman et al., 2015).

Psychrotrophic clostridia, mainly *Clostridium estertheticum*, cause blown pack spoilage. While studies reviewed in this article did not identify the presence of psychrotrophic clostridia, these bacteria are known to be prevalent in the pelts and feces of slaughtered animals and have been detected in meat slaughtering facilities through PCR amplification of specific 16S rRNA regions (Brightwell et al., 2009). *Enterobacteriaceae* such as *Serratia*, *Enterobacter*, and *Hafnia* have also been linked to blown pack spoilage. In the 39 studies analysed in the current study, *Serratia* and *Enterobacter* were being more frequently identified than *Hafnia* (Fig. 2.5).

The bacterial communities in RTE processing facilities did not exhibit significant variations compared to other food commodities (Fig. 2.2), given the processing of diverse raw materials for the respective products. Despite variations in the bacterial community across three RTE processing facilities, members of the genus *Pseudomonas* have been consistently found on different environmental surfaces including slicers, walls, and other food contact surfaces (Fagerlund et al., 2017; Mertz et al., 2014; Pothakos et al., 2015). Their persistence even after regular sanitization protocols results from biofilm formation on abiotic surfaces, which may serve as an indicator of the efficacy of clean and sanitization practices to eradicate biofilms in the food processing facilities. Other spoilage-related taxa such as *Enterobacteriaceae*, *Streptococcaceae*, lactobacilli, *Brochothrix*, and *Leuconostoc* have been found to colonize on the equipment surfaces and to occur on RTE food products (Pothakos et al., 2015). Moreover, lactic acid bacteria especially *Leuconostoc* spp. grow at refrigeration temperature and typically dominate RTE meat microbiota at the end of the shelf life (Gill, 2014).

The food contact surfaces of seafood processing facilities were characterized by the unique presence of *Glutamicibacter*, *Aliivibrio*, *Escherichia*, *Morganella*. *Glutamicibacter*, and *Morganella*, which are associated with ocean fish (Bjørge Thomassen et al., 2023; Møretrø et al.,

2016). *Morganella* is a copious producer of histamine during storage of seafood, which can lead to intoxication after consumption of seafood, particularly scombroid fish (Canadian Food Inspection Agency, 2012). In addition, common seafood spoilers identified among diverse seafood products such as *Pseudomonas*, *Acinetobacter*, *Serratia*, *Psychrobacter*, and *Brochothrix* have also been isolated from environmental surfaces, suggesting the possibility of contamination from environmental surfaces. Marine spoilage bacteria including *Aeromonas*, *Pseudoalteromonas*, *Photobacterium*, and *Shewanella* are mostly found in the marine systems and seafood samples, contributing to seafood off-flavor and limited shelf-life. Analysis of a salmon processing facility revealed the presence of *Aeromonas* and *Shewanella* on environmental surfaces and in seawater, serving as a source of contamination of salmon fillet (Møretrø et al., 2016). On the other hand, *Pseudoalteromonas* and *Photobacterium* were absent on environmental surfaces but were found in raw fish and seawater (Mcglynn, 2004). Lactic acid bacteria, particularly *Carnobacterium* spp., have been isolated from fish gut and aquatic environments (Leisner et al., 2007). In both meat and seafood products, growth and metabolism of *Carnobacterium* spp. during refrigerated storage can have beneficial or detrimental effect on product quality; this depends on the strain- or species specific metabolic traits (Martin-Visscher et al., 2008; Visvalingam et al., 2019). Moreover, the nutrient availability also shapes the microbial composition in the seafood processing facilities. For example, the genera *Aeromonas*, *Acinetobacter*, *Pseudomonas*, *Shewanella*, *Chryseobacterium*, and *Flavobacterium* were present on both high and low nutrient surfaces, while *Comamonas* was exclusively found on low nutrient surfaces. Common ecological niches for *Comamonas* include freshwater, wastewater, fish gut, and plants (Chaillou et al., 2015; Wiernasz et al., 2021).

In fresh produce facilities, the most commonly identified genera were *Pseudomonas* and *Acinetobacter* from food contact surfaces, and *Comamonas*, *Chryseobacterium*, and

Janthinobacterium from non-food contact surfaces such as trolley and floor drains (Xu et al., 2022). *Janthinobacterium* was abundant in fresh water and fresh vegetables such as lettuce surface (Leff and Fierer, 2013), which could increase the risk of spoilage in fresh produce. In addition, it was also found that *Comamonas* and *Janthinobacterium* synergistically interact with other microorganisms like *Serratia* (Xu et al., 2022), contributing to the negative role in the shelf life of fresh-produce. Furthermore, fresh produce facilities uniquely harbored the plant-associated microbes *Rahnella* and *Ralstonia* (Liu et al., 2013). A strain of *Ralstonia* spp. was confirmed as a strong biofilm producer under low temperature condition (<10 °C), enhancing the mixed-species biofilm formation together with *E. coli* O157:H7, *Listeria monocytogenes*, and *Salmonella* (Liu et al., 2016). Taking into account the influence of nutrient levels on the composition of bacterial communities in the fresh produce production environment, a distinct presence of *Cellulosimicrobium*, *Corynebacterium*, *Sphingobacterium*, *Klebsiella*, *Microbacterium*, and *Rahnella* has been observed on nutrient-abundant surfaces across the five studies, while *Arthrobacter*, *Rhizobium*, *Rhodoferrax*, *Paenibacillus*, and *Staphylococcus* only presented on nutrient-deficient surfaces. Other common soil bacterial genera such as *Cupriavidus*, *Burkholderia*, and *Devosia* have been isolated from plant tissues (Lodewyckx et al., 2002; Verma et al., 2021; Xu et al., 2017) and uniquely presented in fresh produce processing facilities with relatively high occurrence (Fig. 2.5).

2.5 Can a core microbiome of food processing facilities be identified?

A core surface-associated microbiome of food processing facilities was identified from the 39 studies with the following order of taxa: *Pseudomonas*, *Acinetobacter*, *Staphylococcus*, *Psychrobacter*, *Stenotrophomonas*, *Serratia*, and *Microbacterium*. These 7 genera can be further characterized into two sub-groups: i) organisms that are commonly identified as food spoilage

organisms, including *Pseudomonas*, *Acinetobacter*, *Psychrobacter*, and *Serratia*, and ii) proximate microorganisms with spoilage potential. The spoilage potential of *Staphylococcus*, *Stenotrophomonas*, and *Microbacterium* has been confirmed in various studies through their ability to degrade lipid and protein *in vitro* (Maes et al., 2019a; Y. Zhang et al., 2019). In addition, *Staphylococcus aureus* causes food poisoning through the production of enterotoxins. Outbreaks associated with *S. aureus* have occurred in various types of food and are often linked to improper handling and poor personal hygiene. Food isolates of *S. aureus* may also pose a risk of transmitting multi-drug resistant *Staphylococcus* to humans through food consumption (Gutiérrez et al., 2012).

The core microbiome identified among different food commodities is not coincidental. Firstly, *Pseudomonas*, *Acinetobacter*, *Psychrobacter*, and *Serratia* are commonly found in natural environments such as soil and water and have a versatile lifestyle which allows them to utilize diverse energy sources and grow at chiller temperature (Dodd, 2014; García-López et al., 2014; Kämpfer, 2014; Rafii, 2014). Therefore, the commonly used method to extend shelf life, refrigeration, does not prevent their growth. Modified atmosphere packaging is currently in use to control the growth of *Pseudomonas*, *Acinetobacter*, and *Psychrobacter* based on their strictly aerobic features, while the facultative anaerobic *Serratia* spp. have been detected in the end products (Dodd, 2014; García-López et al., 2014; Kämpfer, 2014; Rafii, 2014). Secondly, growth of spoilage bacteria on food is often associated with production of volatile compounds, which is as a common cue for food deterioration. Given the involvement of bacterial volatile compounds in interkingdom interactions (Audrain et al., 2015; Schulz-Bohm et al., 2017), the volatiles may additionally act as signaling molecules that modulate the growth of other bacteria in food products and processing environments, and further impact the deterioration of food products, bacterial colonization, and biofilm formation on food equipment surfaces. This hypothesis, if confirmed,

can significantly broaden our understanding of dynamic interactions between bacterial volatile compounds, spoilage issues, and biofilm formation. Third, the core microbiome apparently resists cleaning and disinfection strategies in facilities processing different food commodities including seafood, fresh meat, RTE, and cheese (Langsrud et al., 2016; Maes et al., 2019a; Yang et al., 2023b). Even though cleaning and sanitization are not intended for achieving sterility in food processing facilities, the identification of core microbiome which has implications on shelf life of products would suggest that it may be necessary to implement more effective strategies to eradicate these microorganisms from food processing environments.

Differentiation of bacterial communities in processing facilities by nutrient availability (Fig. 2.6 and Fig. 2.7) revealed that 8 core taxa, *Arthrobacter*, *Brevibacterium*, *Flavobacterium*, *Staphylococcus*, *Pseudomonas*, *Psychrobacter*, *Stenotrophomonas*, and *Enterobacter*, were shared in all three different nutrient-variable niches. Nutrient-rich areas specifically harbored 16 bacterial genera, especially with relatively high presence of *Serratia*, while *Xanthomonas* was only present in nutrient-scarce environments (Fig. 2.7). The adaption of the oligotroph *Xanthomonas* to nutrient-deficient conditions has been linked to its low copy number of ribosomal RNA operons (Roller et al., 2016; Stoddard et al., 2015). *Arthrobacter* is a genus of mainly soil bacteria with nutritional versatility. For example, it can utilize diverse sources as carbon and energy sources such as carbohydrates, organic acids, amino acids, aromatic compounds, and nucleic acids (Gobbetti and Rizzello, 2014), leading to its presence on floors, surfaces as well as high and low nutrient surfaces. *Brevibacterium* spp., mainly present in meat and cheese processing facilities, can metabolize divergent carbon sources such as glucose and galactose, which are relatively abundant in the meat and cheese processing facilities. *Brevibacterium* also exhibits resistance to carbohydrate starvation (Forquin and Weimer, 2014), which perhaps explains its survival under

the conditions of nutrient deficient surfaces. The knowledge of nutrient adaptability among *Flavobacterium* species is limited. However, it displays physiological diversity and further results in its wide distribution in different food manufactures. Habitats include but not limited to cold freshwater and aquatic environments, soil, and food products such as fish, raw and processed meat, dairy products, and agricultural crops (Wańkiewicz and Irzykowska, 2014). The ability of *Staphylococcus*, *Pseudomonas*, *Psychrobacter*, and *Stenotrophomonas* to form biofilms (García et al., 2022; Wagner et al., 2021) allows them to reside and disperse on diverse surfaces with different nutrient levels, thus become frequent contaminants in food production areas. Microbial communities from high-nutrient surfaces tends to be different from that on floor surfaces. This difference can also be visualized by the Venn diagram as microorganisms do not overlap between high nutrient and unknown surfaces (Fig. 2.7), while floor samples did harbor some unique microorganisms with relatively low frequency of presence (data not shown).

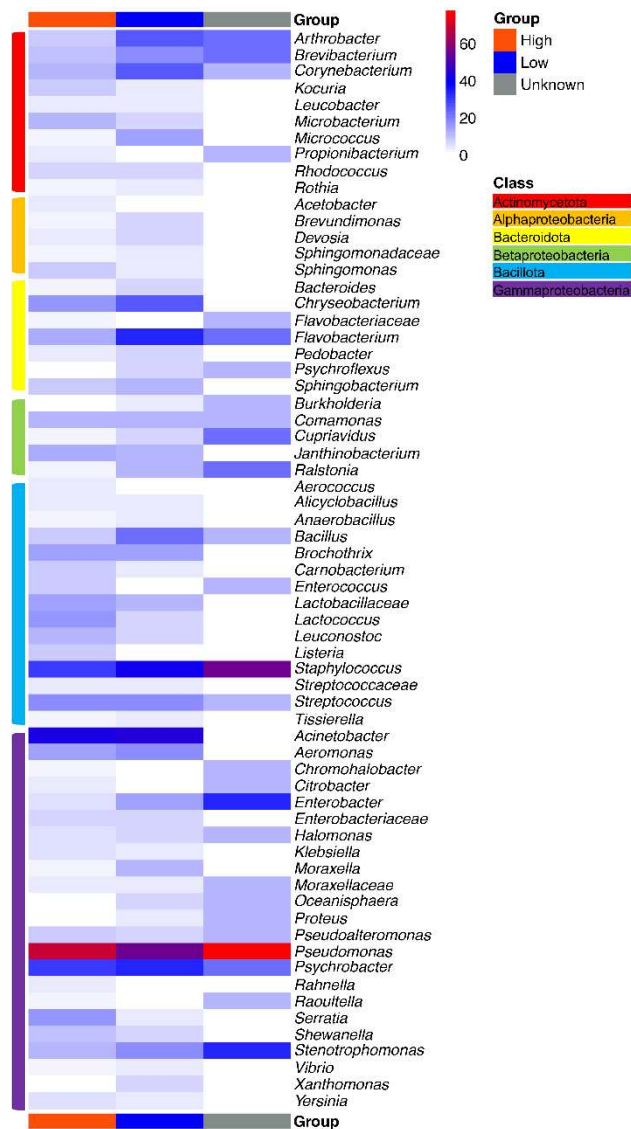


Figure 2.6. Heatmap depicting the relative abundance of the occurrence of bacterial genera present in samples with different nutrient levels.

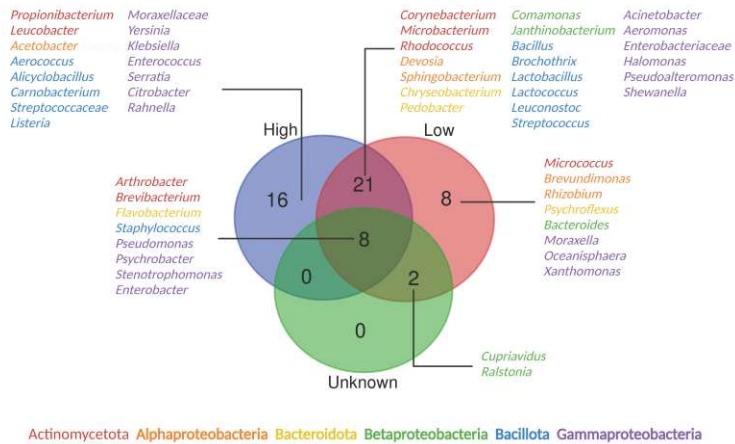


Figure 2.7. Venn Diagram presenting the genera shared among environmental surfaces with different nutrient level. Blue, high nutrient; Red, low nutrient; Green, unknown.

The persistence of diverse microbial communities among different processing facilities is likely related to the presence of these microbes in biofilm. Information on strain level (fewer than 20 SNPs) persistence of microbes in food processing facilities is available for *Listeria monocytogenes*, which is of particular concern for the food industry because it causes foodborne disease associated with consumption of cheeses, produce, and RTE meats (Daeschel et al., 2022). Sampling of a few meat processing facilities for about one year after the start of operation revealed that the facility was colonized by strains of *Listeria* within three months, and that some of these strains persisted as part of the microbiome in the facility (Alvarez-Molina et al., 2021). A seafood processing facility in the U.S. harbored the same strains of *Lm. monocytogenes* over a period of 17 years and the calibration of the mutation rate of these strains indicated that the strains likely colonized the facility after operations started in 1974, and remained in the facility since then (Harrand et al., 2020). Typing of *E. coli* O157:H7 by pulsed-field gel electrophoresis in 21 "high event periods" incidents across nine beef processing facilities throughout the United States

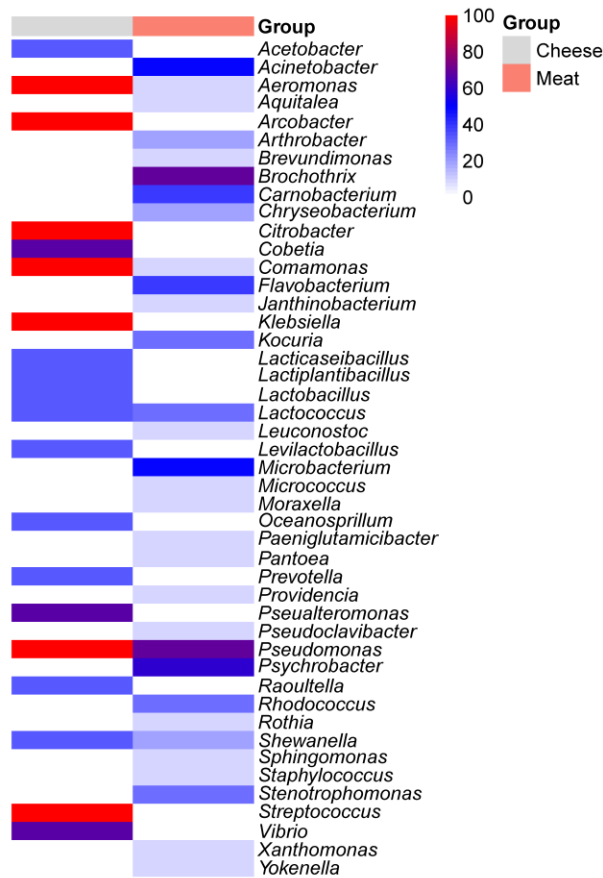
identified strains of *E. coli* O157:H7 with the same pulsed field gel electrophoresis patterns over extended periods of time in the same facility (two or more outbreaks in the same facility) and across facilities in the same geographical region (Arthur et al., 2014). Similar findings were noted for generic *E. coli* which had clonal strains persisting in the same facilities contaminating cuts and trimmings, as determined by multiple-locus variable-number tandem repeat analysis (Yang et al., 2017a, 2015). Some of those strains were obtained after post cleaning of the non-contact surfaces of conveyor belts (Yang et al., 2017b). The clonal relationship of post sanitation strains was further confirmed by whole genome analysis, with a cut-off for SNP at <20 (Yang et al., 2022). Persisting strains of *E. coli* were also observed for *E. coli* O157:H7 on pig farms, resulting in outbreaks (P. Zhang et al., 2021). In addition to biofilm formation, strains of *E. coli* strains may achieve persistence by their ability to utilize novel substrates (P. Zhang et al., 2021). Pathogenic bacteria, however, are not the primary biofilm forming organisms in food processing facilities but inhabit biofilms that are formed by other microbes (Fagerlund et al., 2021). Strain level identification of persistence of spoilage microbes is currently not available but the presence of a core microbiota that remained unchanged over 6 years in a meat processing facility implies strain-level persistence of spoilage microbes as well (Yang et al., 2023b).

Most common food spoilage microorganisms including *Pseudomonas* species exhibits strong biofilm formation ability across various food processing environments, regardless of the nutrient availability (Wagner et al., 2021, 2020). Despite the extensive data available on the microbial ecology of food processing facilities and the ability of isolates to form biofilms, only few studies analysed the microbial communities in biofilms samples in food processing facilities. Our study summarised 13 biofilm communities from one cheese processing industry and two meat processing facilities (Dzieciol et al., 2016; Maes et al., 2019b; Wagner et al., 2020). Three out of thirteen are

"low nutrient" spots collected from water hoses in meat processing facilities. Overall, nutrient availability significantly ($P < 0.01$) impacted biofilm bacterial communities (Fig. 2.4). *Rhodococcus*, *Stenotrophomonas*, *Microbacterium*, and *Flavobacterium* were frequently in samples from water hoses, a site with low-nutrient levels. The former two genera were absent in high nutrient level surfaces (Fig. 2.8B). *Rhodococcus* has been previously isolated from pink biofilms in bathrooms (Yano et al., 2013) and catabolizes a variety of substrates (Yam et al., 2011), which could explain its ability to thrive in an environment with low nutrient levels. Other genera such as *Brevundimonas*, *Janthinobacterium*, *Micrococcus*, *Paeniglutamicibacter*, *Pseudoclavibacter*, and *Sphingomonas* were only detected on low nutrient level surfaces. In contrast, high abundance (>50%) of *Pseudomonas*, *Psychrobacter*, *Brochothrix*, *Acinetobacter*, *Lactococcus*, and *Carnobacterium* was detected on nutrient-rich surfaces, and the latter two were absent on poor-nutrient surfaces (Fig. 2.8B). Of particular, *Pseudomonas* has been detected in all nine nutrient-rich biofilm samples. The nutrient availability is critical for *Pseudomonas fluorescens* to switch between free living cells and biofilm-embedded cells through regulating the production of a signaling molecule, cyclic-di-GMP. Briefly, bacterial cells tend to attach to surfaces and form biofilms under high nutrient conditions while nutrient-scarcity encourages cell dispersal with a lower level of cyclic-di-GMP (Chatterjee et al., 2014). In the food manufacturing settings, the nutrient availability on equipment surfaces fluctuates. On the one hand, this regulatory pattern can increase resistance to cleaning and sanitation by biofilm formation when nutrient levels are high but, on the other hand, favor cross contamination to other surfaces through dispersal when nutrients are scarce. Other common food spoilers such as *Shewanella*, *Staphylococcus*, *Streptococcus*, *Pseualteromonas*, *Leuconostoc*, and *Kocuria* are also part of the biofilm constitution isolated from nutrient-rich surfaces such as cutters and screw conveyor (Fig. 2.8B).

The diverse microbial communities in high-nutrient surfaces were largely attributed to floor drain biofilms as drainage provides a relatively stable niche. For instance, 15 different genera were present in floor drain biofilms from meat processing facilities while 20 different genera were isolated from floor drain biofilms from cheese processing facilities. Only *Lactococcus* and *Pseudomonas* overlapped in meat processing and cheese production manufactories (Fig. 2.8A) (Dzieciol et al., 2016; Maes et al., 2019b; Wagner et al., 2020).

(A)



(B)

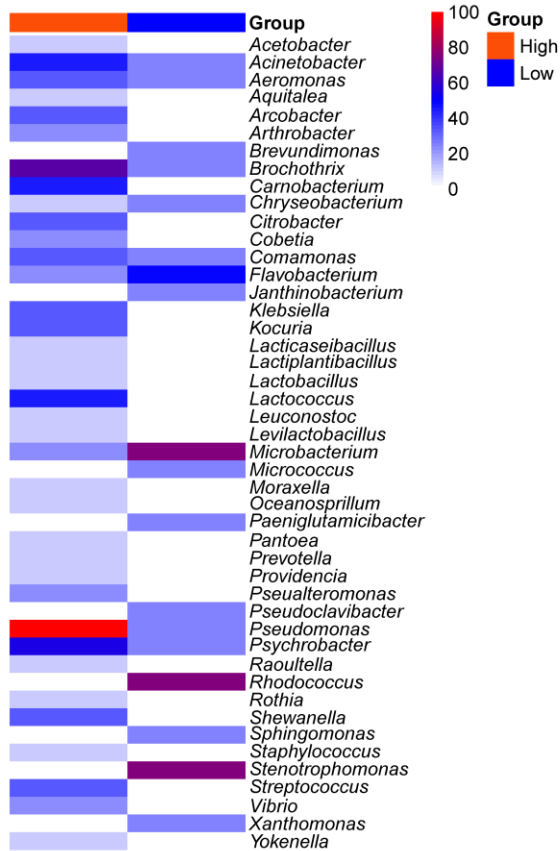


Figure 2.8. The relative abundance of bacterial genera residing in biofilm consortia based on different food categories (A) and nutrient level (B). Data collected from two meat processing facilities and one cheese processing facility, contributing to 13 sampling surfaces in total.

2.6 The use of sanitizer and selective ecology:

Appropriate hygienic design of equipment and facilities together with cleaning and sanitization procedures and training of personnel are the primary strategies to control resident microbes and to mitigate the risk of introducing microorganisms to food processing environments through raw materials, employees, water, soil and air. Improper hygienic design results in niches, or “dead areas” that are difficult to access during routine maintenance and inspections and are thus difficult to clean (Lelieveld et al., 2014). In addition, cleaning and sanitization procedures may only be

partially effective and further shape the bacterial ecology in food processing facilities via the following perspectives: first, some bacteria are eliminated while other bacteria are capable of surviving such efforts and persist within the facility. For example, the genera *Janthinobacterium* and *Aeromonas* were eliminated after cleaning and sanitization practices in a beef slaughtering plant, while *Pseudomonas*, *Comamonas*, *Acinetobacter*, and *Flavobacterium* were not (Wang et al., 2018). Cleaning and sanitation may thus inadvertently encourage the growth and spread of some undesirable, resistant microorganisms that persistently in the processing environment after more harmless competitors were eliminated. Second, bacteria may also acquire resistance to sanitizers due to repeated exposure to sublethal concentrations of biocides. For example, strains of *E. coli* isolated from chlorine-treated wastewater samples harbored the transmissible locus of stress tolerance genomic island, increasing its tolerance to common sanitizers in both planktonic and biofilm-embedded cells (Wang et al., 2020; Z. S. Xu et al., 2021). Achieving the desired concentration of sanitizers on equipment surfaces to effectively kill bacteria is also challenging, as the presence of water or debris on the surface can dilute the concentration of sanitizers while scratches and damages to equipment can serve as hidden habitats. For instance, the use of quaternary ammonium compounds, commonly used in food processing facilities to control *Listeria* spp., can promote the acquisition genes coding for resistance (Dutta et al., 2013; Møretrø et al., 2017). Third, the formation of biofilm on surfaces serves a physical barrier which limits the diffusion and results in low levels of exposure to sanitizers of bacteria in the interior of the biofilm (Bridier et al., 2011). A higher portion of biofilm-embedded cells survived after continuous exposure of benzalkonium chloride when compared to planktonic cells of *Salmonella* Enteritidis (Mangalappalli-Illathu et al., 2008). The formation of biofilm on surfaces in food processing facilities represents thus a survival strategy (Vestby et al., 2020) to adapt to the harsh conditions

including hot steam, wide temperature change and oxidative stress. Lastly, cleaning and sanitization contribute to high temperature and humidity, thus favoring bacterial growth, and may promote for cross contamination. For instance, the most abundant bacterial genera recovered from a seafood processing facility after cleaning and sanitization belong to *Aerococcus*, *Serratia*, *Enterobacter*, *Kocuria*, *Citrobacter*, *Pseudomonas*, and *Acinetobacter*, and the latter three were identified as strong biofilm producers at low temperatures (Langsrud et al., 2016). These findings thus further underscore the need for effective cleaning and sanitization in food processing facilities.

2.7 Limitations

This study highlights how nutrient availability and processing of different food commodities shape the composition of surface-associated microbial communities in common food processing facilities. Many bacterial activities and characteristics are strain-dependent and that compiling information mainly at the genus level may not fully capture the variations of each individual strain. A focus on strain-level characterization could provide a more comprehensive understanding of microbial communities in food processing environments. Additionally, the relative abundance of associated microorganisms was not considered, as most studies inform only on the presence of specific taxa while information on abundance is often missing.

More studies are focused on microbial communities in meat processing and cheese processing facilities, potentially leading to biases and confounding that may have impacted the conclusions on food commodities with fewer data points, such as seafood processing facilities. Microbial communities that are associated with low nutrient and unknown sites, such as non-food contact surfaces and floors, are also often sampled less frequently. However, the accumulation of physical,

chemical, and biological hazards on non-food contact surfaces and floors can cause cross contamination to food-contact surfaces. In addition, sanitation efforts typically focus less on non-food contact surfaces and floors compared to food contact surfaces. Therefore, future studies should consider sampling more areas, such as non-food contact surfaces and floors, to better understand microbial dispersal within facilities and ultimately help food processing facilities develop more comprehensive sanitation protocols. In addition, facilities processing other perishable products, such as eggs and milk, were not included.

2.8 Conclusions and perspectives

Our meta-analysis of microbial communities in food processing facilities indicates that the composition of bacterial community differs when exposed to different nutrient levels in the food manufacturing environments. The influence of nutrient availability on bacterial community is even more pronounced in biofilm-embedded cells. In addition, we identified a core community across food processing facilities irrespective of the commodity that is processed as well as accessory microbiomes associated with specific food commodities.

In ecological terms, processing facilities represent an establishment niche (Holt, 2009) for autochthonous microbes that colonize food processing facilities over evolutionary relevant timelines. The composition of these microbial communities is mainly shaped by selection and speciation. Processing facilities also represent a persistence niche (Holt, 2009) for allochthonous microbes which establish a temporary but not permanent presence. The composition of these microbial communities is shaped by selection and dispersal limitation (Vellend, 2010).

The control of allochthonous microbes relies on the control of dispersal by personnel, air and water, and by control of microbes that are associated with the raw materials. Animals and plants,

however, are invariably associated with commensal microbiota that will enter those facilities that process fresh meat or plants. Autochthonous microbes reside in non-food contact surfaces where they are not eliminated by routine sanitization measures. Dispersal from these non-foods contact surfaces to food is mediated by factors like condensation, airflow, and drain back-ups. Cleaning and sanitization can contribute to dispersal, e.g. by high pressure washing that generates aerosols (Saini et al., 2012; Wang et al., 2018). Both allochthones and autochthones are impacted by improvements in the hygienic design of processing facilities and equipment, improved cleaning and sanitization protocols, and improved training of personnel in food safety management. Our meta-analysis also underlines that more studies are required to explore the secret life of bacteria on non-food contact surfaces (hidden areas) and study biofilms as polymicrobial communities in food processing plants. The reconstitution of these polymicrobial biofilms *in vitro* allows to probe the distribution of each bacterium in this complex microbial system.

Indisputably, food waste due to microbial spoilage is closely connected to environment, animal feed, and human consumption. We thereby propose the concept of "one sustainability" to complement "one biofilm, one health" concept (Jacques and Malouin, 2022) to emphasize the importance of reducing food waste and promoting sustainability in the food industry, which could help to ensure that food resources are used more efficiently and that more people have access to safe and nutritious food.

Chapter 3. Resistance of biofilm-and pellicle-embedded strains of *Escherichia coli* encoding the transmissible locus of stress tolerance (tLST) to oxidative sanitation chemicals

3.1 Introduction

Biofilms are surface associated microbial communities where an extracellular matrix of polysaccharides, proteins, lipids, and water provides a three-dimensional structure. The formation of biofilms on surfaces is initiated by attachment, followed by formation of micro-colonies, biofilm maturation, and biofilm dispersion (O'Toole et al., 2000; Watnick and Kolter, 2000). Free-living cells bind to abiotic surfaces as the first stage of biofilm formation (Galié et al., 2018). Subsequently, surface structures including type 1 fimbriae, type 3 fimbriae, conjugative pili and curli mediate adhesion (Beloin et al., 2008). Maturation of biofilms is initiated by quorum sensing, which upregulates biosynthesis of the extracellular matrix and the formation of the three-dimensional architecture. Finally, biofilm-embedded cells detach and may colonize other areas (O'Toole et al., 2000). Biofilm formed at air-liquid interfaces are termed floating biofilms or pellicles. In Gram-negative bacteria, pellicle formation has been described for acetic acid bacteria, *Salmonella* spp., *Acinetobacter baumannii*, *Escherichia coli* (Golub and Overton, 2021; Marti et al., 2011; Møretrø et al., 2009; Scher et al., 2005). In *E. coli*, pellicle formation was attributed to the secretion and accumulation of diverse polysaccharides including polymeric β -(1 \rightarrow 6)-N-acetyl-D-glucosamine, colanic acid, and cellulose (Beloin et al., 2008).

The biofilm matrix maintains the microbial communities in place even at conditions of strong fluid flow, and thus impedes cleaning. In addition, the biofilm matrix protects biofilm-embedded cells against antimicrobial compounds, and thus impedes sanitation. Biofilms thus contribute to the persistence of bacteria in the food industry and in clinical settings despite regular cleaning and sanitation (Abdallah et al., 2014; Galié et al., 2018; Otter et al., 2015). Biofilm-forming bacteria

include pathogens that contribute to foodborne bacterial disease. Strains of *E. coli* O157:H7 isolated from a beef industry during “high event period” (HEP) share the same genotype (Arthur et al., 2014) and their persistence was linked to biofilm formation (Wang et al., 2014). Similarly, the survival in a meat processing plant of *E. coli* O157:H7 after sanitation increased when the organism was part a biofilm communities (Chitlapilly Dass et al., 2020). Strains of *Salmonella enterica* from beef trim also formed biofilms, which was related to enhanced sanitizer tolerance (Wang et al., 2017).

Research related to biofilm formation by foodborne bacterial pathogens was predominantly conducted with single-strain biofilms, however, biofilm communities generally involve multiple species in food processing facilities. Multi-species biofilms in a meat processing plant were composed of strains of the genera *Brochothrix*, *Pseudomonas* and *Psychrobacter*, which also commonly occur as meat spoilage organisms (Wagner et al., 2020). *Staphylococcus*, *Bacillus*, *Pseudomonas*, among others, also coexisted with *E. coli* O157:H7 in biofilms on the surface of stainless steel and polyvinyl chloride in a meat processing facility (Marouani-Gadri et al., 2009). *L. monocytogenes* also becomes established in multi-species biofilms, e.g. together with *E. coli* in the fish industry and with *Carnobacterium* spp. in meat plants (Rodríguez-López et al., 2015).

The food industry employs multiple measures, particularly hygienic design of equipment and facilities and appropriate cleaning and sanitation protocols with sodium hypochlorite, hydrogen peroxide, or peracetic acid to prevent biofilm formation or to eradicate existing biofilms. Novel or experimental tools include enzymatic disruption of biofilms, physical methods such as hot steam, ultrasound, or surface modification with nanocomposites (Galié et al., 2018; Yuan et al., 2019). Chlorine-based sanitizers are frequently used for sanitation of food processing plants, however,

foodborne pathogens including *E. coli* and *Salmonella* Enteritidis develop resistance against chlorine and related oxidizing chemicals when embedded in biofilms (Yang et al., 2016).

Chlorine resistance of *E. coli* and *Salmonella* is also mediated by the transmissible locus of stress tolerance (tLST) (Kamal et al., 2021), previously designated locus of heat resistance (LHR), a ~14kb genomic island (Mercer et al., 2015; Wang et al., 2020). tLST-positive and heat resistant strains of *E. coli* were isolated from meat processing plants (Dlusskaya et al., 2011; Guragain et al., 2021) but also from raw milk cheese, clinical setting, and wastewater samples (Peng et al., 2013; Zhi et al., 2016). Some tLST-positive strains of *E. coli* also form strong biofilms (Marti et al., 2017). Taken together, the presence of the tLST in biofilm-embedded cells of *E. coli* potentially further increases sanitation resistance, however, the resistance of biofilm embedded tLST-positive and tLST-negative cells has not been assessed experimentally. It was therefore the aim of the study to investigate whether the presence of tLST in strains of *E. coli* strains increases the tolerance of commonly used disinfectants in mono- or dual-strain biofilms formed on stainless steel and to determine whether pellicle formation by strains of *E. coli* also increases their chlorine resistance.

3.2 Materials and methods

3.2.1 Strains and culture conditions

Strains and their origin are shown in Table 3.1. Twelve tLST-negative strains of *E. coli*, thirteen tLST-positive strains of *E. coli*, *Aeromonas australiensis* 03-09, *Carnobacterium maltaromaticum* 9-67 and *E. coli* O157:H7 1934 were used in this study. Frozen (-80°C) stock cultures of Gram-negative bacteria were streaked on Luria–Bertani agar plates and incubated in 37°C incubator for 24h, followed by subculture in LB without NaCl (LBNS) broth overnight at 37°C with 200rpm agitation. *C. maltaromaticum* 9-67 was cultivated at 25°C. Selective MacConkey agar plates were used to distinguish non-lactose fermenters (*A. australiensis* 03-09 and *C. maltaromaticum* 9-67)

from twenty-five *E. coli* strains. Sorbitol MacConkey plates were used for enumeration of *E. coli* O157:H7 1934.

Table 3.1. Strains used in this study.

Group	Strain
<i>E. coli</i> tLST negative	FUA1838
	FUA1848
	FUA1860
	FUA1866
	FUA1869
	FUA1882
	FUA1888
	FUA10038
	FUA10043
	FUA10046
	AW1.7 Δ pHR1 (FUA1262)
	MG1655 (FUA1255)
	<i>E. coli</i> tLST positive
FUA10317	
FUA10318	
FUA10319	
FUA10320	
FUA10321	
FUA10322	
FUA10323	
FUA10324	
FUA10325	
AW1.7	
AW1.3	
Mixed-species biofilm provider	
	<i>Aeromonas australiensis</i> 03-09
	<i>E. coli</i> O157:H7 1934
	<i>Carnobacterium maltaromaticum</i> lab 9-67

3.2.2 Mono- and dual-strain biofilm and pellicle formation

The formation of mono-strain biofilms was observed only for strains of *E. coli*. Because food processing equipment is predominantly constructed with stainless steel (Simões et al., 2010), biofilm formation was observed on food-grade stainless steel coupons. Dual-strain biofilm were

formed by mixing one strain of *E. coli* with *A. australiensis* 03-09 or *C. maltaromaticum* 9-67 or *E. coli* O157:H7 1934. Aliquots of each overnight cultures (10 μ l) were inoculated into 2ml LBNS to achieve the 100-fold diluted bacterial suspension. Stainless steel (SS) coupons (grade 304, No.4 finish, 12mm diameter; Stanfos, Edmonton, AB, Canada) were placed into the bottom of a 24-well flat-bottom cell culture plate (Corning, Glendale, Arizona) and, the whole content of bacterial suspension described above was transferred into the plates and incubated at $23.5 \pm 0.3^{\circ}\text{C}$ for 6d. After 6d, biofilms grown on SS coupons and pellicles formed at the air-liquid interface were harvested with pipette tips and used for cell counts (control), disinfection treatment and biomass quantification. Cell counts were determined after gently washing the SS coupons to remove loosely attached planktonic cells, followed by addition of 2 mL of Dey-Engley (D/E) neutralizing broth to the SS coupons. Biofilm-embedded cells were detached by mixing with 1.64g glass beads and vortexing at maximum speed for 1min. Cell counts were expressed relative to the surface area of the SS coupons of 1.13cm². In dual-strain biofilms, differential cell counts were obtained with the selective media indicated above.

3.2.3 Sanitizers

Three different sanitizers were used in this study, which was diluted from the following stock solutions: 5% (w/v) sodium hypochlorite, 30% (v/v) hydrogen peroxide and 32% (v/v) peracetic acid in acetic acid (Sigma-Aldrich, St. Louis, MO). The final concentration of sanitizers was chosen to achieve a ~ reduction of cell counts by about 1 – 5 log (CFU/mL). Chlorine was diluted to a final concentration of 800ppm and 258ppm in PBS buffer (pH at 6.8) for the treatment of biofilm-embedded and planktonic cells, respectively. The treatment concentration of 5% (v/v) hydrogen peroxide and 0.032% (v/v) peracetic acid were prepared in sterile distilled water.

Chlorine test strips (MQuant, Billerica, MA) were used to determine the free chlorine concentration before treatment.

3.2.4 Curli and cellulose expression

Congo red indicator (CRI) plates were used to evaluate the expression of curli and cellulose production. The preparation of CRI plates was described previously (Wang et al., 2013) composed of 10g/L of Casamino Acids, 1g/L yeast extract, 20g/L Bacto agar, 40mg/L Congo Red and 20mg/L Coomassie brilliant Blue. The cellulose and curli production were determined by streaking overnight cultures on CRI plates and incubating at $23.5 \pm 0.3^{\circ}\text{C}$ for 6d. The colony morphology of red, brown, pink or white corresponded to both cellulose and curli production, to curli, to cellulose or to neither, respectively (Visvalingam et al., 2017).

3.2.5 Effect of sodium hypochlorite on planktonic coculture

For the planktonic dual-cultures, overnight cultures of strains of *E. coli* and *A. australiensis* 03-09, *C. maltaromaticum* 9-67 and *E. coli* O157:H7 1934 were equally aliquoted into 5 ml LBNS broth to achieve 100-fold dilution, then the suspension was incubated overnight prior to 25°C for chlorine treatment. The chlorine treatment on planktonic dual cultures with 258ppm sodium hypochlorite were performed as previously described (Visvalingam et al., 2018) with modification. In brief, 100 μl mixed-strain overnight cultures were added together with either 100 μl sterile water or sodium hypochlorite solution in a 1.5ml microcentrifuge tube. The tube was vortexed at maximum speed for 10s following with 50s incubation at $23.5 \pm 0.3^{\circ}\text{C}$. After 1min of treatment, the content of each tube was transferred into a 15ml conical tube containing 1.72ml of sterilized D/E neutralizing broth, followed by vortexing for 15s. Selective agar plates as described above were used after dilution for plating and incubated at 37°C for 18h.

For instance, white colonies were detected in Sorbitol MacConkey agar as *E. coli* O157:H7 1934 while other *E. coli* strains were presented with dark pink colonies. In MacConkey agar plate, white colonies were observed for *A. australiensis* 03-09 while strains of *E. coli* appeared with dark pink color. Growth of *C. maltaromaticum* 9-67 was inhibited on MacConkey agar plate. Each experiment was repeated three times with independent bacterial cultures (n=3).

3.2.6 Effect of sodium hypochlorite on mono- and dual-cultures pellicle

Air-liquid interface pellicles were lifted with a pipette tip and loosely attached cells were removed by rinsing three times in LBNS broth. Next, pellicles were treated with 1ml of 800ppm sodium hypochlorite solution or PBS buffer (control) for 1min in 24-well plates. Finally, treated pellicles were lifted and transferred into a 15ml centrifuge tube containing 2ml D/E neutralizing broth and 1.64g glass beads. The tube was vortexed vigorously for 1min to disrupt the pellicles. Samples were serially diluted with 0.1% peptone water and spread-plated on selective agar plates before incubation at 37°C for 18h.

3.2.7 Effect of sodium hypochlorite, hydrogen peroxide and peracetic acid on biofilms formed on stainless steel (SS) coupon

Mono- and dual-strain biofilms were formed on SS coupons as described before. At day 6, the coupon was taken out from 24-well plates and rinsed 3 times in LBNS broth to remove loosely attached cells. Then, each coupon was immersed into individual wells containing 1ml of 800ppm chlorine solution for 1min, 1ml of 5% hydrogen peroxide solution for 2min, 1mL of 0.032% (v/v) peracetic acid for 30s or PBS buffer (control) for 1min, respectively. Cell counts after treatments with sanitizing agents were determined as described in section 2.2.

3.2.8 Quantification of the biomass in biofilms

Biomass was quantified by following the modified crystal violet (CV) method. Briefly, biofilms on SS coupon were washed with sterile water for 3 times to remove loosely associated cells. After that, each coupon was air-dried completely before crystal violet staining. To stain the biofilms, 300µl of 1% (w/v) crystal violet in 95% (v/v) EtOH was added gently and incubated at $23.5 \pm 0.3^{\circ}\text{C}$ for 20min. Subsequently, stained coupons were rinsed 6 times with sterile water to remove excess stain. One ml 1% (w/v) sodium dodecyl sulfate (SDS) was added and incubated at $23.5 \pm 0.3^{\circ}\text{C}$ with shaking for 25min to release the dye. The absorbance of each sample was measured at 570nm using a plate reader (Varioskan Flash, Thermo Fisher Scientific). Three independent experiments with technical duplicates were conducted (n=6) for both mono- and dual-strain biofilms.

3.2.9 Observation of biofilms with confocal laser scanning microscopy (CLSM)

Biofilms formed on SS coupons and pellicles were stained with FilmTracer™ LIVE/DEAD® Biofilm viability kit (Invitrogen Ltd., Paisley, UK), which employs the cell permeant dye Syto9 and the cell impermeant dye propidium iodide, following the protocol provided by the manufacturer. Stained biofilms and pellicles were imaged by spinning disk confocal microscope, including motorised microscope base (IX-81, Olympus) and confocal scanning unit (CSU 10, Yokagawa). The excitation/emission fluorescence were 482/500nm for SYTO 9 and 490/635nm for PI. Microscopic images of the biofilms were acquired by Perkin Elmer's Volocity software. The mounted samples were observed using a 100X/1.49 oil objective.

3.2.10 Statistical analysis

Mean values for cell count reduction were collected by three biological replicates. Biomass was quantified by six independent experiments. All analyses were undertaken by two-way analysis of variance (ANOVA) using R statistical package (R Core Team, 2019). Tukey test was used to

determine the significant difference with an error probability of 5% ($P < 0.05$) as the threshold for significance.

3.3 Results

3.3.1 Chlorine resistance of planktonic cells

The tLST protects planktonic cultures of *E. coli* against chlorine (Wang et al., 2020). To determine the chlorine resistance of tLST-positive and tLST-negative biofilm-embedded cells of *E. coli*, an initial screening assessed the ability of 25 strains of *E. coli* to form single-species biofilms on stainless steel (Fig. S3.1). A majority of strains formed weak biofilms with the absence of visible exopolysaccharides and a cell count of about 10^7 cfu/cm² or less. Three tLST negative strains, *E. coli* FUA 1866, FUA 1882 and FUA 10043, produced robust pellicles with cell counts of more than 10^8 cfu/cm² (Fig. S3.1) and a biofilm structure that was visible without magnification (Fig. 3.2A). Subsequent experimentation focused on dual strain biofilms formed by strains of *E. coli* with *E. coli* O157:H5 1934, by strains of *E. coli* and the biofilm forming strains of *A. australiensis* 03-09 and *C. maltaromaticum* 9-67, and on pellicles.

To determine whether cultivation of tLST-positive and tLST-negative strains of *E. coli* in mixed culture with *E. coli* O157 1934, *A. australiensis* 03-09 or *C. maltaromaticum* 9-67 impacts chlorine resistance in planktonic cultures, the chlorine resistance of 6 tLST-positive and 6 tLST-negative *E. coli* strains grown in mixed culture with *A. australiensis* 03-09, *C. maltaromaticum* 9-67 or *E. coli* O157:H7 1934 was tested (Fig. 3.1). The reduction of viable cell counts of tLST-positive strains of *E. coli* strains ranged from about 1 to 2 log₁₀CFU/ml. In contrast, the lethality of chlorine treatment against of tLST-negative strains of *E. coli* was about 3 to 4log(N₀/N) higher than tLST positive strains (Fig. 3.1). Therefore, the presence of tLST in *E. coli* strains significantly ($P < 0.05$) increased the resistance of *E. coli* in mixed planktonic cultures to chlorine. The inactivation of *E.*

coli strains was not different if *E. coli* was incubated alone or together with *A. australiensis* 03-09, *C. maltaromaticum* 9-67 or *E. coli* O157:H7 1934.

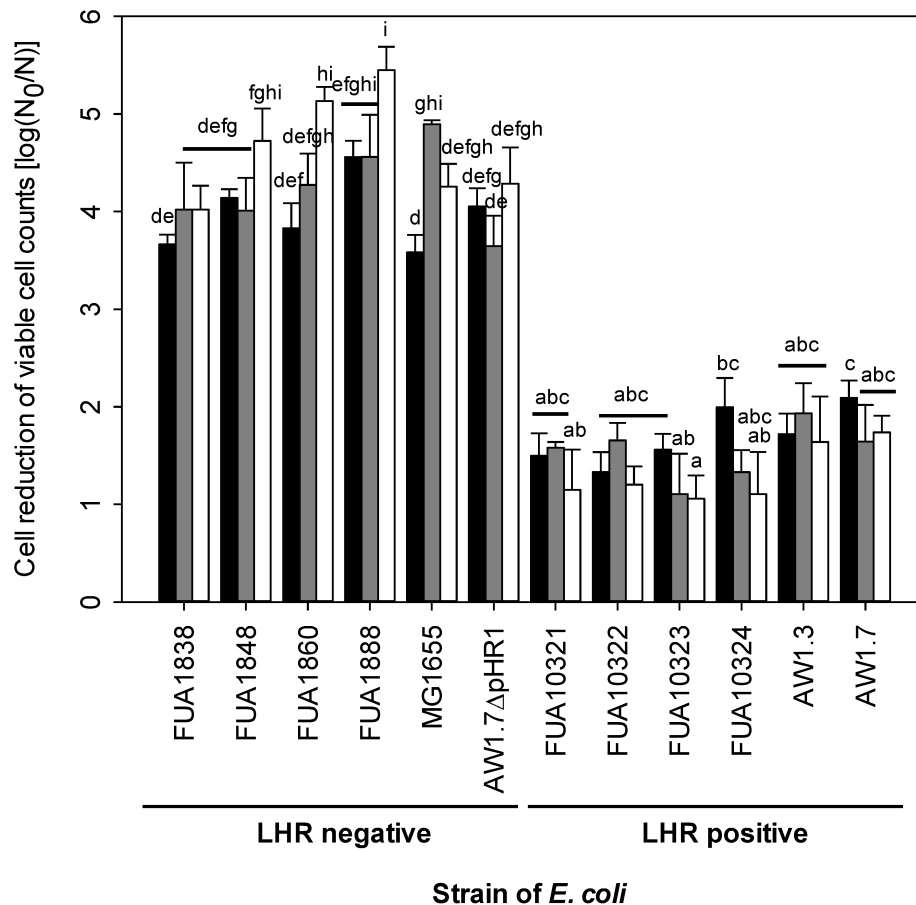


Figure 3.1. Lethality of chlorine treatments to planktonic cells 12 strains of *E. coli* incubated with *Aeromonas australiensis* 03-09 (black bars), *E. coli* O157:H7 1934 (gray bars) and *Carnobacterium maltaromaticum* 9-67 (white bars). Treatment lethality is expressed as the reduction of cell counts [$\log(N_0/N)$] after treatment with 258 ppm NaOCl for 1min. Data are shown as means \pm standard deviations for three independent experiments. Values differ significantly ($P < 0.05$) if the bars do not share a common superscript.

3.3.2 Pellicle formation, expression of curli, cellulose formation and chlorine resistance

The formation of pellicles at the air-liquid interface was previously observed for *E. coli* (Golub and Overton, 2021). Three of the strains of *E. coli* used in this study produced pellicles after 6d incubation at $23.5 \pm 0.3^\circ\text{C}$ in LBNS (Fig. 3.2A) and the structure of pellicles was evaluated by confocal laser scanning microscope (Fig. S3.2B). Pellicle formation was not detected when any of the three pellicle-forming strains of *E. coli* was co-cultured with *A. australiensis* 03-09, but strong pellicle formation was observed when pellicle forming strains of *E. coli* were co-cultured with *E. coli* MG1655 *lacZ*:tLST, *C. maltaromaticum* 9-67 or *E. coli* O157:H7 1934 (Table 3.2). To investigate whether pellicle embedded cells in mixed-cultures have higher resistance to chlorine compared to pellicle embedded cells in monocultures, we treated monoculture and mixed-culture pellicle embedded cells with 800ppm sodium hypochlorite solution (Fig. 3.2B). tLST-negative strains of *E. coli* survived in both single-strain and dual-strain pellicles after chlorine treatment with a reduction of viable cell counts of about $2\log(N_0/N)$, which was significantly less than the cell count reduction of tLST negative-strains embedded in biofilms on stainless steel. The resistance of pellicle-embedded strains of *E. coli* to chlorine was not different ($P > 0.05$) if cells were embedded in pellicles formed by single-strains or mixed-cultures. These data suggest that tLST-negative strains of *E. coli* embedded in pellicles are chlorine resistant.

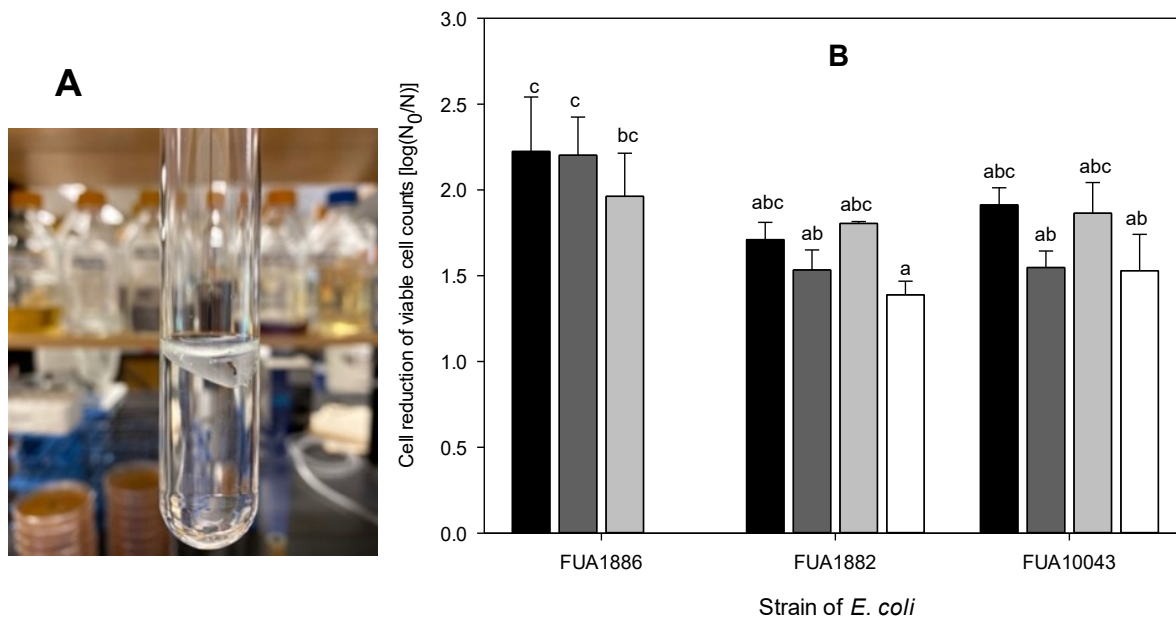


Figure 3.2. Pellicle formation and chlorine resistance of strains of *E. coli*. **Panel A.** Pellicle formed by *E. coli* FUA10043 after 6 days at ambient temperature in Luria broth. **Panel B.** Reduction of cell counts strains of *E. coli* in pellicles formed by single strain culture (black bars) or in multispecies pellicles formed in Luria broth at room temperature for 6 d, followed by treatment with 800 ppm NaClO. Multi-species pellicles were formed by incubation of pellicle forming *E. coli* strains with *E. coli lacZ:tLST* (dark gray), *E. coli* O157:H7 1934 (light gray) or *Carnobacterium maltaromaticum* 9-67 (white). Data are shown as means \pm standard deviations for three independent experiments. Values differ significantly ($P < 0.05$) if the bars do not share a common superscript.

Cellulose and curli contribute to the pellicle formation by *E. coli* (Golub and Overton, 2021; Hung et al., 2013). Therefore, curli and cellulose expression was assessed on Congo red indicator plates. Pellicle forming strains expressed curli and produced cellulose but not all curli and cellulose positive strains formed pellicles (Table 3.3). The production of cellulose was more common than expression of curli; with exception of *E. coli* FUA1848 all strains produced cellulose.

Table 3.2. Formation of floating biofilms (pellicles) by single and mixed cultures of three strains of *E. coli*.

	Strain of <i>E. coli</i>		
	FUA 1866	FUA 1882	FUA10043
Single	+	+	+
<i>E. coli</i> MG1655 <i>LacZ</i> :tLST	+	+	+
<i>Aeromonas</i> spp.	-	-	-
<i>E. coli</i> O157:H7	+	+	+
<i>Carnobacterium maltaromaticum</i>	+	+	+

+ pellicle formation; - no formation of pellicles.

Table 3.3. Curli and/or cellulose expression of bacterial strains tested for biofilm formation. Pellicle forming strains are printed in bold and underlined.

Strain of <i>E. coli</i>	Curli	Cellulose
FUA1838	+	+
FUA1848	-	-
FUA1860	-	+
<u>FUA1866</u>	+	+
FUA1869	-	+
<u>FUA1882</u>	+	+
FUA1888	-	+
FUA10038	+	+
<u>FUA10043</u>	+	+
FUA10046	-	+
MG1655 <i>LacZ</i> :tLST	-	+

Strains of *E. coli* examined for curli, and cellulose production are tLST negative

3.3.3 Chlorine resistance of strains of *E. coli* in dual-strain biofilms

The reduction of cell counts of tLST-positive and tLST-negative strains of *E. coli* in dual-strain biofilms after treatment with NaOCl is shown in Figure 3.3. The chlorine resistance of *E. coli* strains in dual-strain biofilms with *E. coli* O157:H7 1934 was assayed with 800ppm chlorine;

biofilms with *A. australiensis* 03-09 and *C. maltaromaticum* 9-67 were treated with 1200ppm chlorine concentration (Fig. 3.3). The 6 tLST-positive strains of *E. coli* embedded in dual-strain biofilms were more resistant ($P<0.001$) to chlorine when compared to the 6 tLST-negative strains of *E. coli*. In the dual-strain biofilms formed on stainless steel, the biofilm embedded cells of tLST negative strains of *E. coli* were reduced by 3 to 5log CFU/cm². In contrast, the reduction of viable cell counts of biofilm-embedded cells of tLST positive strains ranged from 1 to 2.5log CFU/cm². The lethality of 800 or 1200ppm chlorine against biofilm embedded dual-strain cultures (Fig. 3.3) was roughly comparable to the lethality of 258ppm chlorine against dual-strain planktonic cultures with the same strains (Fig. 3.1).

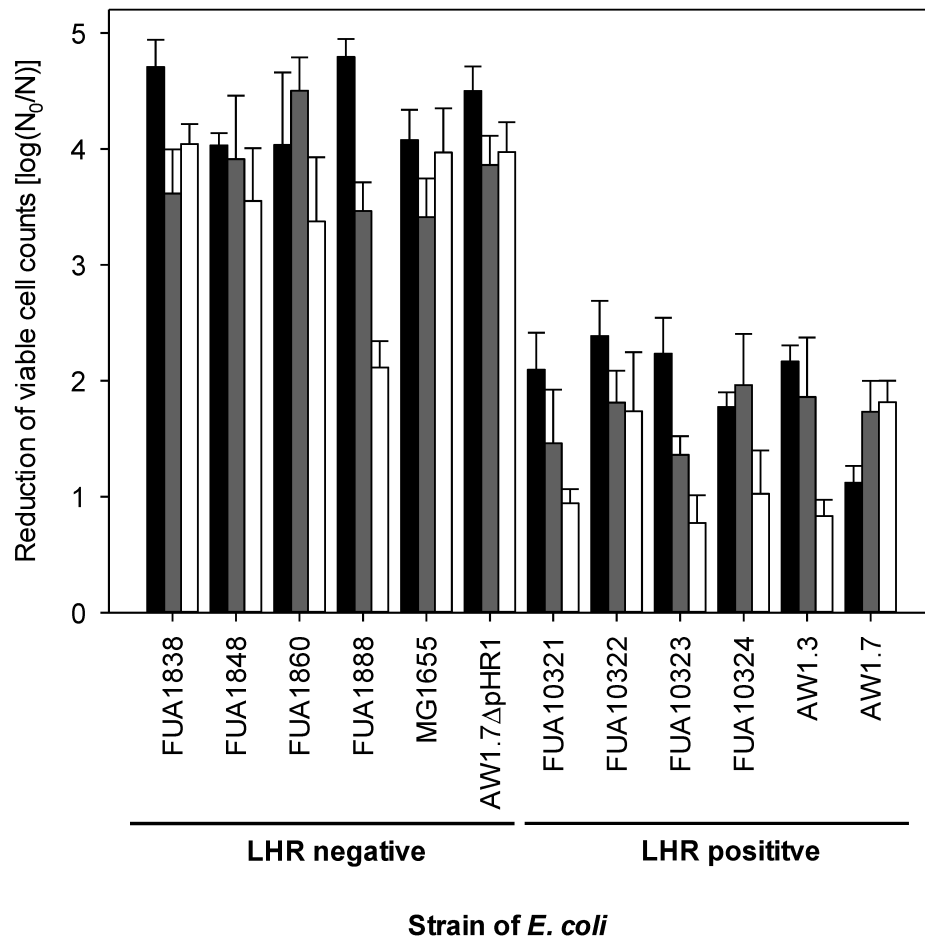


Figure 3.3. Reduction of cell counts of tLST-positive and tLST-negative strains of *E. coli* biofilms after treatment with NaOCl. *E. coli* strains were incorporated in biofilm produced by *Aeromonas australiensis* 03-09 (black bars), *E. coli* O157:H7 1934 (gray bars) and *Carnobacterium maltaromaticum* 9-67 (white bars). Biofilms were formed at room temperature for 6 d on stainless steel coupons. Biofilms formed by *Carnobacterium maltaromaticum* 9-67 and *Aeromonas australiensis* 03-09 were treated with 1200 ppm of NaOCl, biofilms formed by *E. coli* O157:H7 1934 were treated with 800 ppm NaOCl; Data are shown as means \pm standard deviations for three independent experiments.

3.3.4 Disinfectant resistance of single-strain, dual-strain biofilms and pellicle embedded cells

Peracetic acid and hydrogen peroxide are alternative sanitation agents in the food industry. To assess the resistance of biofilm-embedded cells to these sanitizing agents and to directly compare the resistance of strains of *E. coli* in different biofilm matrices, the resistance of *E. coli* in single-strain or dual-strain biofilms or pellicles was assessed (Fig. 3.4). In general, tLST-positive strains of *E. coli* were more resistant than tLST-negative strains to all three sanitizing agents irrespective of whether they were embedded in single- or dual strain biofilms (Fig. 3.4). For tLST-positive strains of *E. coli*, resistance to sanitizers was not strongly impacted by the different biofilm matrices. For tLST-negative strains of *E. coli*, the reduction of cell counts of the same strain in different biofilm matrices differed by up to 2log (CFU/cm²) but there was no consistent trend as to the biofilm matrix that generated the most resistant cells. The single species biofilm formed by tLST-negative strain of *E. coli* FUA 1838 on stainless steel coupon was significantly more sensitive to sodium hypochlorite and hydrogen peroxide than its dual-strain biofilms (P < 0.001) (Fig. 3.4). The pellicle forming tLST-negative strain *E. coli* FUA10043 was equally resistant as tLST-positive strains of *E. coli* embedded in biofilms attached to stainless steel.

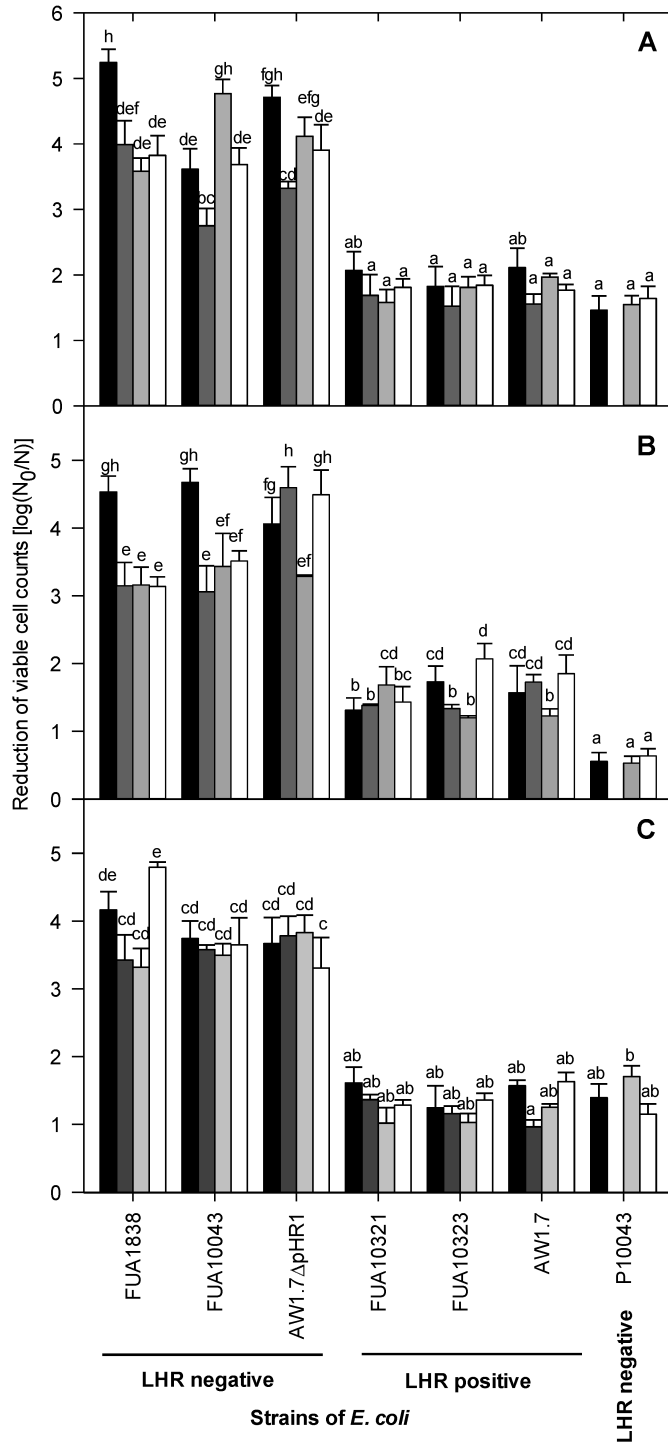


Figure 3.4. Reduction of cell counts of tLST-positive and tLST negative strains of *E. coli* after chlorine treatment of single species or multi-species biofilms. Bars represent single-species biofilms (black bars) or multi-species biofilms formed with *Aeromonas australiensis* 03-09 (dark

gray), *E. coli* O157:H7 1934 (light gray) or *C. maltaromaticum* 9-67 (white). Biofilms were formed on stainless steel coupon with Luria broth at room temperature for 6 d; P10043 represents pellicles formed by *E. coli* FUA10043. Biofilms were treated with 800ppm NaClO (**Panel A**), or 5% hydrogen peroxide (**Panel B**) or with 0.032% (v/v) peroxyacetic acid (**Panel C**). Data are shown as means \pm standard deviations for three independent experiments. Values differ significantly ($P < 0.05$) if the bars do not share a common superscript.

3.3.5 Correlation of biofilm biomass and chlorine resistance

Biomass was quantified with crystal violet staining (Fig. 3.5). Overall, tLST-positive strains of *E. coli* produced mono- and dual strains biofilms with higher biomass when compared to tLST-negative strains of *E. coli* ($P < 0.01$). Among tLST negative strains, the biomass of single-strain biofilms was less than the biomass of dual-strain biofilms ($P < 0.05$) except for the pellicle forming *E. coli* FUA10043. Figure 3.6 indicates a strong correlation between the biofilm biomass and the chlorine resistance of biofilm-embedded cells of *E. coli* ($R=0.903$, $P < 0.001$). tLST-positive strains of *E. coli* all clustered at the bottom right of the graph, indicating both a higher biofilm mass and a higher chlorine resistance in all tLST-positive strains. Therefore, biofilm biomass and chlorine resistance are positively associated.

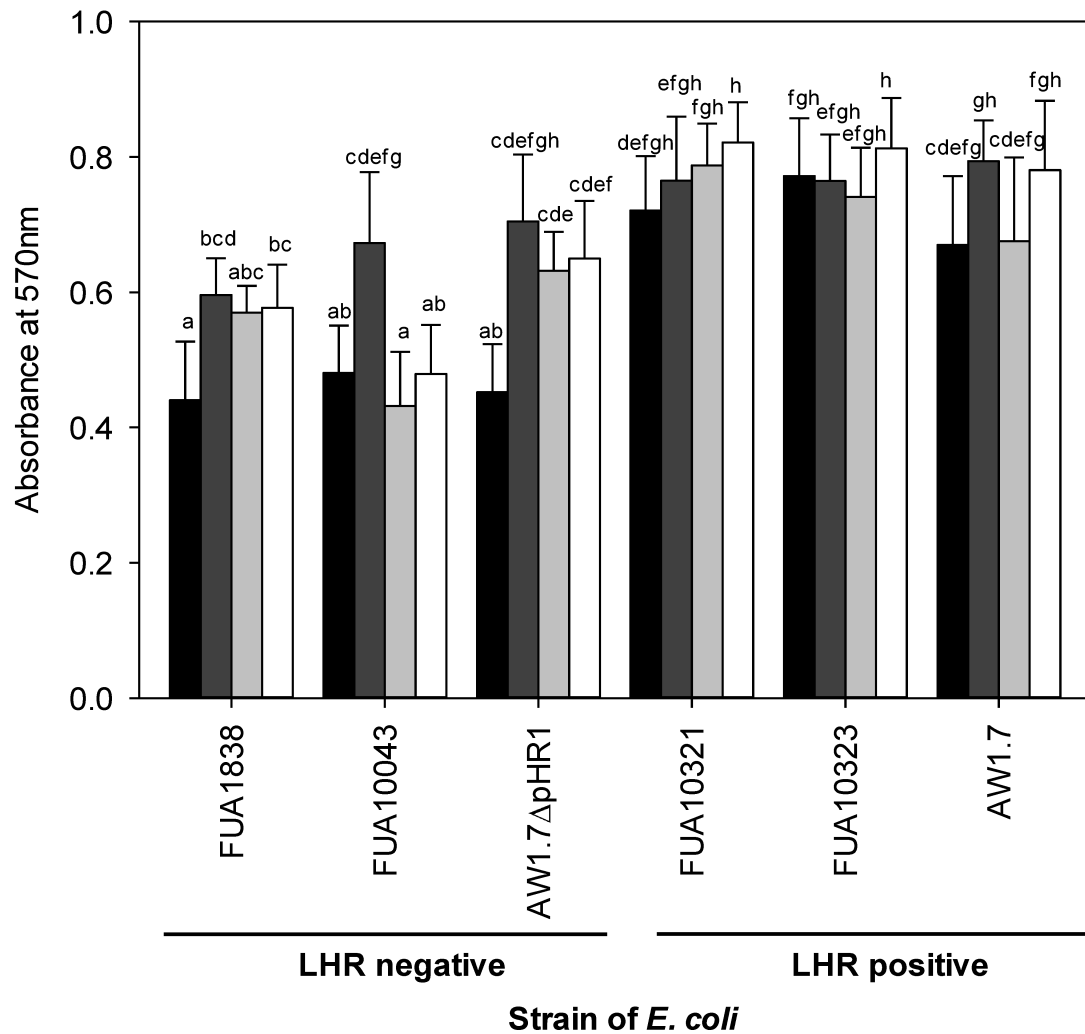


Figure 3.5. Quantification of the biomass of biofilms formed by single species of multi-species biofilms using crystal violet staining. Mono- and dual- species biofilms were formed on stainless steel coupon in Luria broth for 6 d at room temperature. Shown are data for mono-species biofilms (black bars) and multi-species biofilms formed by the strains of *E. coli* indicated and *Aeromonas australiensis* 03-09 (dark gray), *E. coli* O157:H7 1934 (light gray) and *Carnobacterium maltaromaticum* 9-67 (white). Data are shown as means \pm standard deviations for three

independent experiments. Values differ significantly ($P < 0.05$) if the bars do not share a common superscript.

3.4 Discussion

Experimentation described in this study analysed the biofilm forming ability of *E. coli* in mono- and dual-strain biofilms, and the effect of the presence of the tLST in strains of *E. coli* on resistance to sanitizing agents in biofilm-embedded cells. In planktonic state, proteins encoded by tLST play a protective role on oxidative stress by protein disaggregation and folding (Wang et al., 2020). tLST positive strain of *E. coli* also contain the biofilm-related operons accountable for curli, cellulose and synthesis of polymeric β -(1 \rightarrow 6)-N-acetyl-D-glucosamine (Marti et al., 2017) although it remains to be determined whether genes coding for biofilm formation are differentially distributed between tLST-positive and tLST-negative strains. We generally observed a higher biofilm density in tLST positive strains of *E. coli* in comparison to tLST-negative strains, which highly correlates to the enhanced sanitation resistance of biofilm-embedded cells in addition to the tLST-mediated resistance to chlorine and hydrogen peroxide (Fig. 6 and Wang et al., 2020). The association between the presence of tLST and higher biofilm density remains unclear. Multiple tLST variants are currently recognized; several of which also carry *ftsH* (Boll et al., 2017; Kamal et al., 2021; Marti et al., 2017). FtsH contributes to biofilm formation in *P. aeruginosa* (Kamal et al., 2019). Of the strains used in the present study, the tLST in *E. coli* FUA10321 and *E. coli* FUA10323 but not the tLST in *E. coli* AW1.7 include FtsH but formation of biofilms by these strains was roughly equivalent. An alternative explanation for the correlation of biofilm formation ability and the presence of the tLST may relate to the ecological adaptation of these strains. Potentially the selective pressure that maintains the tLST also selects for biofilm formation (Kamal et al., 2021). A high frequency of tLST-positive strains of *E. coli* was isolated from meat and dairy

products after thermal treatment (Boll et al., 2017; Marti et al., 2016; Zhang et al., 2020) as well as from chlorinated wastewater (Zhi et al., 2016). Moreover, oxidative stress agent such as hydrogen peroxide and hypochlorite stimulates biofilm formation in *Acinetobacter oleivorans* and *P. aeruginosa*, respectively (Jang et al., 2016; Stempel et al., 2017). Thus, the role of tLST in the biofilm phenotype that was observed in this study remains subject to future investigations. Irrespective of the mechanisms underlying the increase of biofilm density in tLST positive strains, the presence of tLST enhanced resistance against oxidative stress not only in planktonic cells (Wang et al., 2020) but also biofilm-embedded cells, as indicated by the higher chlorine concentration that was required to reduce viable cell counts. Therefore, biofilm growth of tLST-positive *E. coli* further enhances the chlorine resistance.

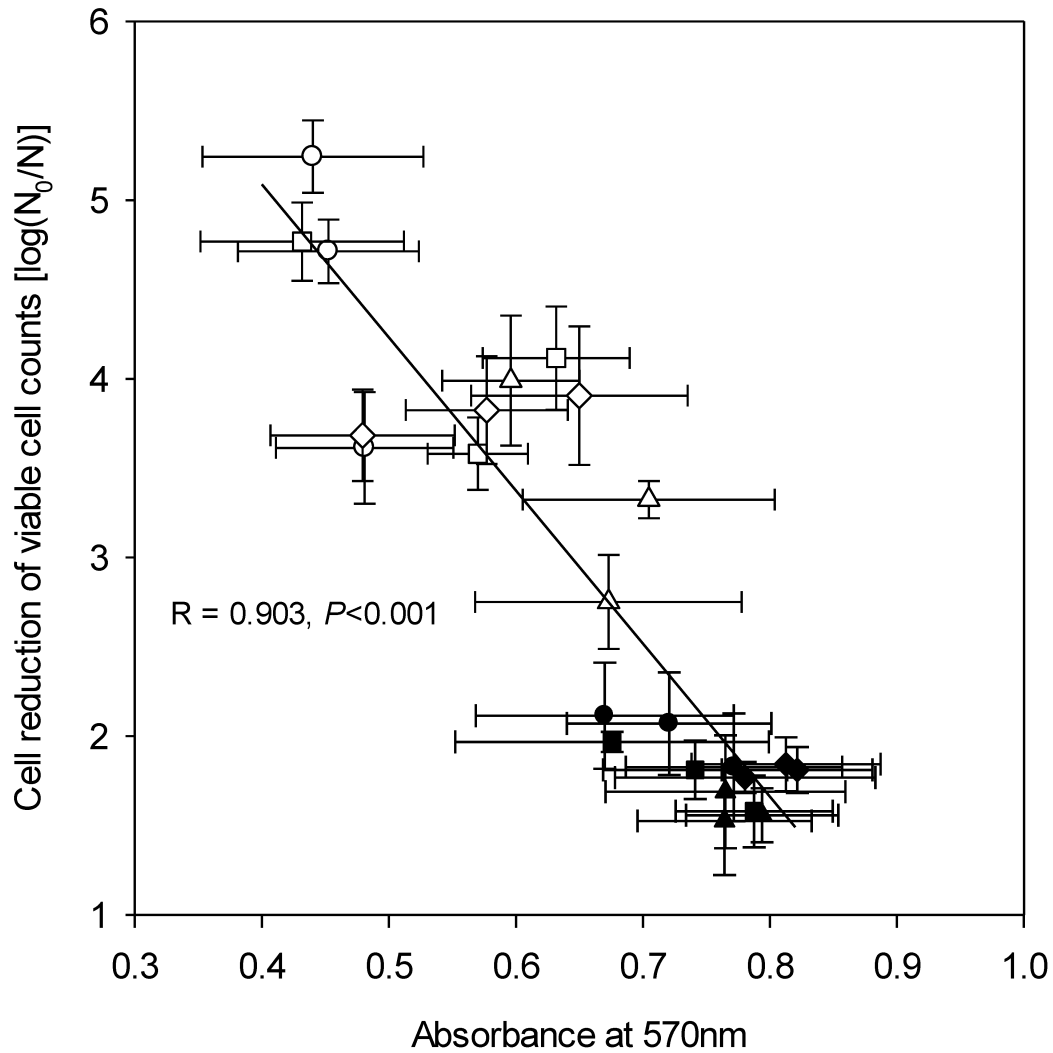


Figure 3.6. Correlation of the reduction of cell counts after chlorine treatment and the biofilm biomass. Shown are single species biofilms of strains of *E. coli* (□) or multi-species biofilms with *E. coli* and *Aeromonas australiensis* 03-09 (▼), *E. coli* O157:H7 1934 (□) or *Carnobacterium maltaromaticum* 9-67 (□). Data are shown as means ± standard deviation of three independent experiments. The line shows the linear regression of all data on the plot; the R-value of the linear regression is also indicated.

The transition of free-living microorganism to a biofilm lifestyle benefits its growth in a hostile condition with limited nutrients. Biofilms form on biotic or abiotic surfaces and also as floating

biofilms at the air-liquid interface. The potential mechanisms behind pellicle formation have been explained with regards to buoyancy, the secretion of surface-active agents like surfactants and pellicle attachment to edge of container close to the interface (Armitano et al., 2014). Comparable to biofilms formed on solid surfaces, pellicles are established in several stages. Initially, cells localise at the air-liquid interface by developing floating aggregates. Then cell replication results in the expansion of pellicle at the entire air-liquid interface, followed by EPS secretion and pellicle maturation (Armitano et al., 2014). The formation of pellicles by *E. coli* strains was initially described in uropathogenic *E. coli* (UPEC), enteropathogenic *E. coli* (EPEC) and *E. coli* K-12 (Golub and Overton, 2021; Hung et al., 2013; Wu et al., 2012). Major matrix components of pellicles include curli, cellulose, flagella and type 1 pili (Hung et al., 2013; Weiss-Muszkat et al., 2010). However, the role of pellicles in resistance of *E. coli* to disinfectants has not been studied. Our study demonstrated that pellicle-embedded tLST negative strains of *E. coli* were equally or more resistant than tLST positive strain of *E. coli* in surface attached biofilms. Whether the formation of pellicles in strains of *E. coli* impacts their virulence remains unknown. However, membrane proteins are overexpressed in another Gram-negative pellicle cells, *A. baumannii*, which potentially influence its virulence and persistence (Marti et al., 2011). Hence, this unique phenotype in *E. coli* strains deserves more investigation.

Biofilm communities in natural environments commonly include multiple species. Interspecific interactions in microbial consortia affect its development, composition, and antimicrobial resistance (Burmølle et al., 2014; Elias and Banin, 2012). In monocultures, *E. coli* O157:H7 1934 did not form biofilms at 15°C after 6d. However, this strain established biofilms when co-cultured with other species at the same incubation condition (Visvalingam et al., 2019). *A. australiensis* 3-09 and *C. maltaromaticum* 9-67, isolated from conveyor belts in a beef facility (Wang et al.,

2018), dominated multi-species biofilms (Visvalingam et al., 2019) and showed synergistic effects on biofilm formation when cultivated together with *Salmonella* Typhimurium (Visvalingam et al., 2018). The synergistic interspecific interactions also promote biomass production and thus significantly increase bacterial resistance to disinfectants when compared to single strain biofilms (Burmølle et al., 2006; Van der Veen and Abee, 2011). Biofilms in meat processing plants were reported to include strains of up to 22 genera, indicating that the cleaning and sanitation regime was not efficiently eliminating spoilage and pathogenic bacteria (Fagerlund et al., 2017).

Compared to planktonic state cells, bacterial biofilm cells exhibit higher resistance to sanitizers. One of the most distinctive features that distinguishes biofilm from planktonic cells is the complex structure of the EPS matrix, which represents around 90% of the total biofilm biomass and protects bacterial cells from harsh environment (Pinto et al., 2020). The role of biofilm formation on the resistance to antimicrobial agents has been extensively studied (Abdallah et al., 2014; Donlan, 2000; Flemming et al., 2016; Kostaki et al., 2012; O'Toole et al., 2000). First, the complex architecture of EPS acts as a physical barrier that limits biocide diffusion to the interior of the biofilm (Bridier et al., 2011). Second, the biofilm matrix reacts with antimicrobial agents, thereby compromising their efficacy (Flemming et al., 2016). Third, the exposure of biofilm-embedded cells to low concentrations of sanitizers supports adaptation and selects for biofilms-embedded cells with enhanced resistance (Bridier et al., 2011; Flemming et al., 2016). Fourth, bacterial cells enclosed in the matrix have a different lifestyle than planktonic cells owing to its low accessibility to nutrients and oxygen (Flemming et al., 2016), which also decreases its sensitivity to biocide reagents (Bridier et al., 2011). The present study demonstrated that the resistance of *E. coli* to sanitation chemicals was highly correlated to biofilm mass or density, which further highlights the role of the biofilm matrix in establishing a diffusion barrier. Moreover, chlorine is inactivated by

organic matter (Lambert and Johnston, 2001) and thus likely inactivated before it reaches the interior of the biofilm. The densest biofilm matrices were observed with pellicle-forming and tLST negative strain of *E. coli* (Fig. S2); these strains exhibited resistance to chlorine that was comparable to the resistance of tLST-positive cells embedded in less dense biofilms on stainless steel surface.

Pathogenic microorganisms are a main concern in food industry and their occurrence in biofilm-embedded cells increases their persistence and the risk of food contaminations. In food processing plants, biofilm form on both biotic surfaces and abiotic surfaces like conveyor belts, drying area and floor drain with abundance of moisture and nutrients (Srey et al., 2013), but also on employee gloves, packing materials and animal carcasses (Galié et al., 2018). Microbes that persist in biofilms on food-contact surfaces can consistently contaminate the food products. For example, biofilms that include Shiga toxin-producing *E. coli* are often found in meat plant associated with equipment surfaces and biofilm dispersal may lead to contamination of beef (Wang et al., 2012). Biofilm formation is also relevant for persistence and dispersal of *L. monocytogenes* onto ready-to-eat meat (Maury et al., 2019). Analysis of an outbreak of listeriosis that was linked to a single meat processing facility documented that isolates that were obtained over a period of 5 year differed in fewer than 11 SNP's (Lachmann et al., 2021), which implies that a single strain persisted in the same facility for 5 years. Hence, the formation of biofilms in food processing increases the risk of foodborne illness.

In conclusion, in this study, we demonstrated that the combination of the presence of tLST and biofilm formation encountered inside single- and dual-strain biofilms profoundly escalate disinfectant resistance. However, the complexity of multi-species biofilms is increased with the additional presence of many other microbial species in a real food processing facility. Thus, further

research on biofilms by using a more diverse community of strains and species is necessary, which would benefit the development of methods for controlling bacterial biofilms in food processing ecosystems.

Chapter 4. Socializing at the Air-Liquid Interface: A Functional Genomic Analysis on Biofilm-Related Genes during Pellicle Formation by *Escherichia coli* and Its Interaction with *Aeromonas australiensis*

4.1 Introduction

Bacterial biofilms are formed on solid surfaces by one or more species and represent a complex ecosystem, encased in a highly organized extracellular matrix (ECM) composed of extracellular polymeric substances including proteins, polysaccharides and DNA (Flemming et al., 2016). The biogenesis of surface-associated biofilm development involves biosynthesis of ECM, intracellular and intercellular signaling systems (Khambhati et al., 2021). Biofilms can also form at the air-liquid interface, these are termed floating biofilms or pellicles. This phenotype has been discovered in Gram-positive bacteria including *Bacillus subtilis* and *Bacillus cereus* (Armitano et al., 2014; Wijman et al., 2007) and in Gram-negative bacteria including *Pseudomonas aeruginosa* (Ude et al., 2006), *Vibrio parahaemolyticus* (Enos-Berlage et al., 2005), *E. coli* (Golub and Overton, 2021), *Shewanella oneidensis* (Liang et al., 2010), *Acinetobacter baumannii* (Chabane et al., 2014; Marti et al., 2011). Several food fermentations also depend on pellicle formation, e.g. fermentation of sour beer and kombucha by lactic acid bacteria and yeasts (Bouchez and De Vuyst, 2022; Umbard, 2015), and fermentation of vinegar by acetic acid bacteria (Bimmer et al., 2022; Yun et al., 2019). Comparable to surface-associated biofilms, pellicle formation is proposed to form in three steps: i) cell localization at the air-liquid interface by either cell aggregation or attachment to a solid surface, ii) replication of cells to cover the entire layer of the air-liquid interface, iii) maturation and development of the three-dimensional structures (Armitano et al., 2014; Liang et al., 2010).

Many factors contribute to bacterial pellicle formation. Flagellum-based motility was involved in pellicle formation in *B. subtilis* as well as *P. aeruginosa* (Hölscher et al., 2015). In *Salmonella*, pellicle formation was regulated by the metabolic sensor cAMP, which modulates the expression of transcriptional regulator *csgD* which, in turn, regulates the biosynthesis of curli and cellulose (Paytubi et al., 2017). In addition, quorum sensing played a role in pellicle formation of *A. baumannii* (Oh and Han, 2020). Pellicle formation in strains of *E. coli* has been reported in uropathogenic *E. coli* (UPEC), enteropathogenic *E. coli* (EPEC) as well as *E. coli* K-12. Specifically, the role of cellulose, curli, flagella, type 11 pili has been confirmed in *E. coli* UTI89 for pellicle integrity by mutational and biochemical analysis (Hadjifrangiskou et al., 2012; Hung et al., 2013; Weiss-Muszkat et al., 2010). The addition of transthyretin, which inhibits amyloid formation by the major curli subunit CsgA, also abolished pellicle formation in UTI89 (Jain et al., 2017) In *E. coli* K-12, the ECM of pellicles includes curli, cellulose, poly-N-acetyl glucosamine (PNAG) and colanic acid (Golub and Overton, 2021; Jeffries et al., 2021). A modified form of cellulose, phosphoethanolamine (pEtN) cellulose, is the second most abundant ECM component in wild-type strains of *E. coli* (Jeffries et al., 2021). A higher abundance of pEtN cellulose in *E. coli* AR3110 accounted for the formation of intact and cohesive pellicles, while *E. coli* UTI89 produced less pEtN cellulose and formed more brittle but adhesive pellicles (Jeffries et al., 2021). Deletion of genes coding for synthesis of cellulose or pEtN modification of cellulose did not substantially alter the architecture of biofilms but pellicle formation was dependent on pEtN cellulose as major component of the ECM (Jeffries et al., 2021).

We have previously observed that strains of *E. coli* formed pellicles in single cultures or in co-cultures with *Carnobacterium maltaromaticum* and *E. coli* O157:H7. However, they formed only a surface associated biofilm, which are subsequently referred to simply as biofilms, in co-cultures

with *Aeromonas australiensis* (Z. S. Xu et al., 2021). Few studies documented the regulation of genes contributing to pellicle formation in strains of *E. coli* growing alone or in co-cultures with other bacterial species. Therefore, the aim of this study was to identify whether the presence/absence of unique genes was responsible for pellicle formation, and to investigate the impact of cell-cell communication on dual-species pellicle formation.

4.2 Materials and methods

4.2.1 Strains and culture conditions

The present study employed all strains of *E. coli* in the FUA strain collection for which genome sequences were available at the time the experiments were conceptualized (n=39) and *A. australiensis*. The origin of the strains and genome accession numbers are shown in Table 4.1. Frozen (-80°C) stock cultures were streaked on Luria-Bertani agar plates (10 g/L tryptone, 5 g/L yeast extract, 10 g/L NaCl) and incubated in 37°C incubator for 24 h, followed by subculture in Luria-Bertani broth without salt (10 g/L tryptone, 5 g/L yeast extract) (LBNS) overnight at 37°C with shaking at 200 rpm. Strains of *E. coli* FUA1882 carrying plasmid pRK767 were grown in LBNS broth supplemented with tetracycline at a concentration of 15 mg/L. *E. coli* FUA1882 $\Delta bcsG::cam$ pRK767 and *E. coli* FUA1882 $\Delta bcsG::cam$ pRK767-*bcsG* were also supplemented with 1 mM isopropyl β -D-1-thiogalactopyranoside (IPTG) to induce the expression of the lac promoter.

Table 4.1. Strains used in this study.

Accession number	Strain	Phylogroup	Reference
JARJIP000000000	<i>E. coli</i> FUA1838	B1	
JARJIQ000000000	<i>E. coli</i> FUA1848	B2	
JARJIR000000000	<i>E. coli</i> FUA1860	F	
JARJIS000000000	<i>E. coli</i> FUA1866	B1	(Wang et al., 2020;
JARJIT000000000	<i>E. coli</i> FUA1869	D	Z. S. Xu et al., 2021)
JARJIU000000000	<i>E. coli</i> FUA1882	E	
JARJIV000000000	<i>E. coli</i> FUA1888	B2	
JARJIW000000000	<i>E. coli</i> FUA10038	D	
JARJIX000000000	<i>E. coli</i> FUA10043	F	
JARJIY000000000	<i>E. coli</i> FUA10046	B2	
LDYM000000000	<i>E. coli</i> GM16-6	A	
LDYL000000000	<i>E. coli</i> DM18-3	A	
LECH000000000	<i>E. coli</i> O104:H4 11-3088	B1	
LEAD000000000	<i>E. coli</i> O157:H7 1934	D	
LEAK000000000	<i>E. coli</i> O157:H7 LCDC7236	D	
LEAI000000000	<i>E. coli</i> O157:H7 CO283	D	
LEAJ000000000	<i>E. coli</i> O157:H7 E0122	D	
LEAB000000000	<i>E. coli</i> O145:NM 03-6430	D	
LDYN000000000	<i>E. coli</i> O26:H11 05-6544	A	
LECK000000000	<i>E. coli</i> O113:H4 09-0525	A	
LECN000000000	<i>E. coli</i> O76:H19 09-0523	B1	
LECM000000000	<i>E. coli</i> O45:H2 05-6545	B1	
LDZZ000000000	<i>E. coli</i> O121:H19 03-2832	B1	
LEAA000000000	<i>E. coli</i> O121:NM 03-4064	B1	
LECO000000000	<i>E. coli</i> O103:H2 PARC444 (FUA1314)	B1	(Mercer et al., 2015)
LECG000000000	<i>E. coli</i> O103:H2 PARC445 (FUA1315)	B1	
LECJ000000000	<i>E. coli</i> O111:NM PARC447	B1	
LDYO000000000	<i>E. coli</i> O26:H11 PARC448	B1	
LEAC000000000	<i>E. coli</i> O145:NM PARC449	D	
LECL000000000	<i>E. coli</i> O44:H18 PARC450	E	
LEAG000000000	<i>E. coli</i> O157:H7 CO6CE1943	D	
LEAE000000000	<i>E. coli</i> O157:H7 CO6CE900	D	
LEAH000000000	<i>E. coli</i> O157:H7 CO6CE2940	D	
LEAF000000000	<i>E. coli</i> O157:H7 CO6CE1353	D	
LECF000000000	<i>E. coli</i> O103:H25 338	B1	
LECI000000000	<i>E. coli</i> O111:NM 583	B1	
LDYI000000000	<i>E. coli</i> AW1.3	A	
LDYJ000000000	<i>E. coli</i> AW1.7	A	
LDYK000000000	<i>E. coli</i> AW1.7 ΔpHR1	A	
	<i>E. coli</i> FUA1882 Δ <i>besG</i> ::cam		This study
	<i>E. coli</i> FUA1882 Δ <i>curlU</i> ::cam		
	<i>E. coli</i> FUA1882 Δ <i>sdiA</i> ::cam		
	<i>E. coli</i> FUA1882 Δ <i>sdiA</i> ::cam pRK767		
	<i>E. coli</i> FUA1882 Δ <i>sdiA</i> ::cam pRK767- P _{sdiA} -sdiA		
	<i>E. coli</i> FUA1882 Δ <i>besG</i> ::cam pRK767		
	<i>E. coli</i> FUA1882 Δ <i>besG</i> ::cam pRK767 - <i>bcsG</i>		
	<i>Aeromonas australiensis</i> 0309		(Z. S. Xu et al., 2021)

4.2.2 Determination of pellicle formation

Pellicle formation of the 39 strains of *E. coli* was examined as described (Z. S. Xu et al., 2021). In brief, overnight cultures were diluted 100-fold in 2 ml LBNS, transferred into 24-well-flat-bottom cell culture plates and incubated at 25°C for 6d to visualize pellicle formation at the air-liquid interface. Pellicle formation was scored visually as strong, moderate, weak, and no pellicle (Hadjifrangiskou et al., 2012). Tetracycline and IPTG were supplemented accordingly as described above to evaluate the pellicle formation after complementation of *sdiA* and *bcsG* gene. Dual strain biofilms were formed after inoculation of LBNS with equal volumes of overnight cultures of *E. coli* and *A. australiensis* as described (Z. S. Xu et al., 2021).

4.2.3 Genome sequencing and assessment of the presence and absence of operons in pellicle formation

The genomes of 10 wild type strains of *E. coli* from this study were sequenced by Illumina MiSeq system as described previously (Wang et al., 2021b). Genomic DNA was extracted and purified using a Wizard® Genomic DNA Purification Kit following manufacturer's protocol (Promega, Madison, WI, USA). Genomic DNA was prepared as the input for DNA libraries using the Nextera XT DNA library preparation kit (Illumina Inc., San Diego, CA, USA). Libraries were sequenced with an MiSeq reagent kit v3 (600- cycles) (Illumina Inc.) using a 2 x 300-bp paired-end protocol. Raw reads were trimmed by Trimmomatic 0.36.4 with a sliding window quality cut-off at 20. De novo assembly was performed using SPAdes 3.12.0, with k-mer sizes of 21 and 33, and annotated with Prokka (Seemann, 2014) and Roary (Page et al., 2015). The phylogroups were predicted with the Clermont Phylotyper (Waters et al., 2020). Scoary (Brynildsrud et al., 2016) was used to identify genes that are unique in pellicle forming or non-pellicle forming strains. The nucleotide sequences of biofilm-related operons in *E. coli* MG1655 were downloaded from NCBI as a query

to blast against 39 strains of *E. coli* with cut-off parameters of 90% or 70% nucleotide identity and more than 80% coverage.

4.2.4 Quantification of expression level of biofilm-related genes

The expression of genes associated with biofilm formation was quantified with reverse transcriptase quantitative PCR (RT-qPCR) with RNA isolated from 3 non-pellicle forming strains and 5 pellicle forming strains. Biofilm formation on the solid surfaces rather than air-liquid was previously observed when pellicle forming strains of *E. coli* were co-cultured with *A. australiensis* as previously described (Z. S. Xu et al., 2021). To allow comparison of pellicle-forming and non-pellicle forming strains, overnight cultures that entered the stationary phase of growth about 8 h prior to RNA isolation but did not yet form biofilms or pellicle were used as reference conditions. Test conditions included planktonic cells after 6 d of incubation (non-pellicle forming strains of *E. coli* in single culture), pellicle-embedded cells after 6 d of incubation (pellicle forming strains of *E. coli* in single culture) and biofilm embedded strains (co-culture of strains of *E. coli* with *A. australiensis* 0309). Prior to RNA isolation, planktonic cells were diluted with LBNS broth to an OD_{600nm} of 0.3-0.4. One ml of culture was taken from dual-strain biofilm-embedded cultures. In single-strain pellicle forming strains, the pellicle was lifted with a pipette tip and washed with LBNS broth three times to remove loosely attached cells. Next, the pellicle layer was transferred to a 15 ml tube containing 2 ml LBNS broth and 1.64 g glass beads. The content in the tube was homogenized for 45 min to shear the pellicles. The upper part of the bacterial suspension (1 mL) was taken for RNA isolation. All samples of pellicle-embedded cells were adjusted to achieve OD_{600nm} of 0.3-0.4. RNeasy Protect and RNeasy Mini kit (Qiagen, Hilden, Germany) were used for RNA isolation and purification, followed by gDNA removal by RQ1 RNase-Free DNase (Promega, Madison, WI, USA). QuantiTect® reverse transcription kit (Qiagen) was used for

reverse transcription of RNA to cDNA. The expression level of targeted genes (Table 4.2) was measured by QuantiFast SYBR® Green PCR Kits (Qiagen) and the 7500 fast real-time PCR system (Applied Biosystems, Waltham, MS, USA). The glyceraldehyde-3-phosphate dehydrogenase gene (*gapA*) was used as the house-keeping gene to relate the expression of genes for biofilm / pellicle formation to the expression of genes coding for a key enzyme in the Embden-Meyerhof-Parnas pathway. DNase-digested RNA and water served as negative controls. The log₂-normalized relative gene expression level was calculated by the $\Delta\Delta$ CT method by calculating gene expression in single-strain pellicle-embedded cells of each strain of *E. coli* relative to the expression of the same gene in single-strain planktonic cells and dual-strain biofilm-embedded cells, respectively. Data shown are from three independent experiments with technical repeats.

Table 4.2. Biofilm-related genes tested by RT-qPCR in this study.

	Name	Function of gene product	Reference
EPS biosynthesis	<i>csgA</i>	Curli major subunit	(Lim et al., 2012; Wu et al., 2012)
	<i>csgD</i>	Transcription activation, curli	(Paytubi et al., 2017)
	<i>bcsA</i>	Cellulose biosynthesis	(Kwak et al., 2020)
	<i>fimA</i>	Type 1 fimbriae major subunit	(Hung et al., 2013)
	<i>wcaF</i>	Colanic acid synthesis	(Lavery et al., 2014)
Regulatory system	<i>cyaA</i>	Adenylate cyclase	(Paytubi et al., 2017)
	<i>rpoS</i>	RNA polymerase, sigma S (sigma 38) factor	(Liu et al., 2020; Schellhorn, 2020; Weber et al., 2006)
	<i>rfaH</i>	Transcription antiterminator	(Beloin et al., 2006)
Quorum sensing	<i>sdiA</i>	Homologs of LuxR, detect AHLs	
	<i>luxS</i>	AI-2 synthase	
	<i>lsrk</i>	autoinducer-2 kinase	(Kostakioti et al., 2013, 2009)
	<i>lsrR</i>	DNA-binding transcriptional repressor LsrR	
	<i>qseB</i>	Response regulator of the QseB/C two-component system	
	<i>qseC</i>	Sensor kinase component	

4.2.5 Phylogenetic tree of the upstream region of the curli operon

The nucleotide sequences of the upstream region of the curli biosynthesis and cellulose biosynthesis of *E. coli* MG1655 were retrieved from the NCBI database and used as query sequences for BLASTn against the genomes of the 39 strains of *E. coli* and the reference strain *Salmonella* Typhimurium CMCST_CEPR_1. Multiple-sequence alignment was performed by MUSCLE. The aligned sequences were further processed by MEGAX (Kumar et al., 2018) using the maximum likelihood method with 1000 bootstrap replicates. The tree was displayed in iTol (Letunic and Bork, 2021).

4.2.6 Addition of N-acyl homoserine lactone to pellicle formation

To evaluate the impact of N-acyl homoserine lactones (HSLs) on pellicle formation, N-butanoyl-L-homoserine lactone (C₄-HSL) and N-hexanoyl-L-homoserine lactone (C₆-HSL) (Sigma Aldrich, St. Louis, MO, USA), most commonly synthesized by *Aeromonas* species (Talagrand-Reboul et al., 2017), were incubated together with pellicle forming strains of *E. coli*. The two quorum sensing molecules were dissolved and diluted in dimethyl sulfoxide (DMSO) to 0.1 mM before use. Pellicle forming strains of *E. coli* were incubated with DMSO as the negative control. To prepare the dual-strain cultures, an equal volume of the 1:100 diluted overnight cultures of each strain was mixed together. Dual-strain and single-strain cultures with the addition of signalling molecules were incubated in a 24-well plate at 25°C for 6d. Two technical replicates for each sample were conducted in three independent assays.

4.2.7 Construction of *E. coli* FUA1882

The pellicle-forming strain of *E. coli* FUA1882 was used to assess the role of genes associated with the upstream region of curli biosynthesis (CurliU), modified cellulose biosynthesis (*bcsG*) and QS receptor (*sdiA*) on pellicle formation. The mutant strains were obtained by homologous recombination replacing the targeted gene of the wild type *E. coli* FUA1882 by a chloramphenicol cassette through the λ Red system (Mercer et al., 2012). Oligonucleotides' primers were purchased from Integrated DNA Technologies (Coralville, IA, USA) and are listed in Table 4.3. The mutant strain was complemented with the low copy number plasmid, pRK767. The complementing fragments were amplified by the primers listed in Table 2, using *E. coli* FUA1882 chromosomal DNA as the template. Plasmid pRK767- P_{sdiA}-sdiA contains *sdiA* with its native promoter region while pRK767 –bcsG only contains *bcsG* itself. The amplified fragments were each digested with HindIII and DpnI and ligated to pRK767 that had been pre-cut with the two enzymes. The recombinant plasmid was firstly introduced into competent *E. coli* Top10 by chemical

transformation. These plasmids and the empty pRK767 were transferred back to the mutant strains through electroporation. Mutation and complementation were confirmed by PCR and subsequent Sanger sequencing.

Table 4.3. Primers used in this study.

Primer	Sequence (5' - 3')	Description
gapA	GTTGACCTGACCGTTCGTCT ACGTCATCTTCGGTGTAGCC	RT-qPCR primer for <i>gapA</i>
csgA	CGGTGGTGGTGGTAATAACAG CAGAGTTACGGGCATCAGTTT	RT-qPCR primer for <i>csgA</i>
csgB	GCGCAAGAAGGTAGTAGCA TACCATAAGCACCTTGCG	RT-qPCR primer for <i>csgB</i>
csgD	GCTTGCCAGCTACCTGATTA TTATTAGACGCGCCGATACG	RT-qPCR primer for <i>csgD</i>
bcsA	TCACCACCCAGCAACATATC AGACTTTCCAGCGGCTTATC	RT-qPCR primer for <i>bcsA</i>
bcsG	CCTGTCACAATGGATTTCGC TTACAGTGGTCGTCGGTTG	RT-qPCR primer for <i>bcsG</i>
fimA	GTTGTTCTGTCGGCTCTGT CAAGCGGCGTTAACAACCTC	RT-qPCR primer for <i>fimA</i>
wcaF	TCGGCGATGACGTCAATTT GTGGCTACCGGTGCATAAA	RT-qPCR primer for <i>wcaF</i>
cyaA	AGATTGATCAGGTGCGTGAG GCGGAGACGCTAAGGTTATT	RT-qPCR primer for <i>cyaA</i>
rfaH	CCAGGAACACCTCGAAAGAG GGAACAATGGCTCACTGACT	RT-qPCR primer for <i>rfaH</i>
rpoS	CAGCCGTATGCTTCGTCTTA CGTCATCTTGCGTGGTATCT	RT-qPCR primer for <i>rpoS</i>
sdiA	CTGAGGCGTGGGTTAGTTATT CACATTAATGGCCCTGACTAAAG	RT-qPCR primer for <i>sdiA</i>
luxS	GTTGCTGATGCCTGGAAAG GTAAGTGCCACACTGGTAGA	RT-qPCR primer for <i>luxS</i>
qseB	TTTGCCCTGCTGGAATTA GGCATTACTGGTGACCTCTTC	RT-qPCR primer for <i>qseB</i>
qseC	CTGGACTCACTGGATAACCTTC TGCGCCGTGTGGTAAATA	RT-qPCR primer for <i>qseC</i>

lsrK	CTATACGCTGCTGGAAGAGATG CCGGGTCAATGGACAAGTTA	RT-qPCR primer for <i>lsrK</i>
lskR	AGCAAATTCGCCTGGTCA GCAACGGAGCCGGAATAATA	RT-qPCR primer for <i>lsrR</i>
pSIM19 check 1	GCGTAACTTCCGGAGCCACAC ACTGCATACTGCAGAACGTC	confirmation of pSIM19
pSIM19 check 2	CGTCGGCTTGAACGAATTGTTAG CGTCAATGCGCTGATGACAATCAGC	confirmation of pSIM19
pSIM19 check 3	CTTGCCGCATTTGGCATTCTGC ACCGTGGAACGGATGAAGGC	confirmation of pSIM19
pSIM19 check 4	GATCAGAAATGAGCGCCAGTCG TGAACCAGATCGCGCAGGAG	confirmation of pSIM19
pSIM19 check 5	GATTGCGCCTACCCGGATATTATCG CCGTAAGTGCATTCCGGATTAC	confirmation of pSIM19
pSIM19 check 6	GGCCTCGCTTATCAACCACC GTGGCACTACTCAACCCAC	confirmation of pSIM19
Cam-BcsG F	GGACGTTACGCCGACGGAAAAAGCCAGGGCAA CCAAAAAGTGTAGGCTGGAGCTGCTTC	Amplification of chloramphenicol cassette for <i>bcsG</i> mutant
1882-Cam-BcsG R	GCCGCAGAGGTTAACTCTGCGGCCTTTTTTCGTG CATGGGAATTAGCCATGGTCCATATG	
1882-BcsG down D F	ACTAAGGAGGATATTCATATGGACCATGGCTAAT TCCCATGCACGAAAAAGGCCGCAGAG	Amplification of <i>bcsG</i> downstream
1882-BcsG D R	CATGATTTAGCGGCTCCGGT	
BcsG Upstream F	CTGGCCCGCAGCATTTCATAC	Amplification of <i>bcsG</i> upstream
BcsG Upstream R	AAAGTATAGGAACTTCGAAGCAGCTCCAGCCTAC ACTTTTTGGTTGCCCTGGCTTTTTCC	
1882-BcsG-pUC19 Upstream	TTCACACAGGAAACAGCTATGACCATGATTACGC CAAGCTCTGGCCCGCAGCATTTCATAC	Overlapping primers for upstream of <i>bcsG</i> and empty vector (pUC19)
1882-BcsG-pUC19 Downstream	ACGTTGTAACACGACGGCCAGTGAATTCGAGCTC GGTACCATGATTTAGCGGCTCCGGTC	Overlapping primers for downstream of <i>bcsG</i> and empty vector (pUC19)
1882-CurliU F	CCAACCTGAGTCACGTTGACG	Amplification of <i>curliU</i> upstream
1882-CurliU-Cam R	GAAGCAGCTCCAGCCTACACATGAAAAACAAATT GTTATTTATGATGTTAACAATACTGG	
1882-Cam-CurliU F	CAGTATTGTTAACATCATAAATAACAATTTGTTTT TCATGTGTAGGCTGGAGCTGCTTC	Amplification of chloramphenicol cassette for <i>curliU</i> mutant

Cam-CurliU R	AATAATGTATGACCATGAATACTATGGACTTCAT TAAACAATGGGAATTAGCCATGGTCC	
CurliU-Cam F	GGACCATGGCTAATTCCTATTGTTTAATGAAGTC CATAGTATTCATGGTCATACATTATT	Amplification of <i>curliU</i> downstream
1882-CurliU R	CAGCTTCCCCATCGTGAC	
1882-CurliU-pUC19 Upstream	TCACACAGGAAACAGCTATGACCATGATTACGCC AAGCTCCAACCTGAGTCACGTTGACG	Overlapping primers for upstream of <i>curliU</i> and empty vector (pUC19)
1882-CurliU-pUC19 Downstream	CGACGTTGTAACGACGGCCAGTGAATTCGAGC TCGGTACCAGCTTCCCCATCGTGAC	Overlapping primers for downstream of <i>curliU</i> and empty vector (pUC19)
1882-SdiA F	GACCTCGAGGTAAAGCCTGG	Amplification of <i>sdiA</i> upstream
SdiA-Cam R	CTAGAAAGTATAGGAACTTCGAAGCAGCTCCAGC CTACACAGTAAACCGCAACGCCCTG	
Cam-SdiA F	TTATAAATGATACTCACTCTCAGGGGCGTTGCGG TTTACTGTGTAGGCTGGAGCTGCTTC	Amplification of chloramphenicol cassette for <i>sdiA</i> mutant
1882-Cam-SdiA R	TCAGCCGTTTTTGCATCTGGCACGCAGAAAGAA AAGCGCATGGGAATTAGCCATGGTCC	
1882-SdiA-Cam F	CTAAGGAGGATATTCATATGGACCATGGCTAATT CCCATGCGCTTTTCTTTCTGCGTGCC	Amplification of <i>sdiA</i> downstream
sdiA R	GCCTCAAGACCGCCAATGC	
1882-SdiA-pUC19 Upstream	TCACACAGGAAACAGCTATGACCATGATTACGCC AAGCTGACCTCGAGGTAAAGCCTGGC	Overlapping primers for upstream of <i>sdiA</i> and empty vector (pUC19)
1882-SdiA-pUC19 Downstream	TCACACAGGAAACAGCTATGACCATGATTACGCC AAGCTGACCTCGAGGTAAAGCCTGGC	Overlapping primers for downstream of <i>sdiA</i> and empty vector (pUC19)
bcsG::cam check 1	GCTTGAGGAATACCGTTCAC ATCCCTGGGTGAGTTTCACCAG	sequencing primers
curliU::cam check 1	CTGAAGAGGACCGCCATTG ATCCCTGGGTGAGTTTCACCAG	sequencing primers
curliU::cam check 2	GCAACTGACTGAAATGCCTC GACTGGATGGCCTGAGATA	sequencing primers
sdiA::cam check 1	GAAGCGGCAGCCAGTATTG ATCCCTGGGTGAGTTTCACCAG	sequencing primers
sdiA::cam check 1	GCAACTGACTGAAATGCCTC CGGACTGAGATTGAGCTGTTC	sequencing primers

curli U absent check	CTGGACCTGGTCGTACATTT CGGTGTAGTCCTTTCGTCAT	confirmation the deletion of <i>curliU</i> in wildtype chromosome
bcsG absent check	TCGCCGGTTTATGACGATAC CCACGACCACCATCACTTTA	confirmation the deletion of <i>bcsG</i> in wildtype chromosome
sdiA absent check	GCAGAAGAGGTCTACCATGAAA CACATTAATGGCCCTGACTAAAG	confirmation the deletion of <i>sdiA</i> in wildtype chromosome
lac-bcsG-pRK767	AGGAAACAGCTATGACCATGATTACGCCAAGCTT ATGACTCAATTTACGAAAATACCGC ACGTTGTAAAACGACGGCCAGTGAATTCGAGCTC GGTACCTTACTGCGGGTAAGGCACCC	overlapping primers for <i>bcsG</i> and empty vector
native-sdiA-pRK767	CGGCCAGTGAATTCGAGCTCGGTACCACTCATTA ATAACATAAGAGAATGTGATGGCTTG ACACAGGAAACAGCTATGACCATGATTACGCCAA GCTTTCAAATTAAGCCAGTAGCGGCC	overlapping primers for <i>sdiA</i> and empty vector
m13	CCCAGTCACGACGTTGTAAAACG AGCGGATAACAATTTACACACAGG	confirmation of complementing fragment in pRK767
Lac-bcsG check 1	CACTTTAGTCTTCCGGCTCG CCACGACCACCATCACTTTA	confirmation of <i>bcsG</i> insertion in pRK-767
Lac-bcsG check 2	CCCAGTCACGACGTTGTAAAACG TCGCCGGTTTATGACGATAC	confirmation of <i>bcsG</i> insertion in pRK-767
Native-sdiA check 1	CCCAGTCACGACGTTGTAAAACG CACATTAATGGCCCTGACTAAAG	confirmation of <i>sdiA</i> insertion in pRK-767
Native-sdiA check 2	AGCGGATAACAATTTACACACAGG GCAGAAGAGGTCTACCATGAAA	confirmation of <i>sdiA</i> insertion in pRK-767

4.2.8 Statistical analysis

Mean values of gene expression were collected by three independent experiments with technical replicates. The comparison of expression level of each gene between group of pellicles forming strains and non-pellicle forming strains was conducted by nested t-test (also known as two-level nested ANOVA) using GraphPad Prism 9.4.1. (San Diego, CA, USA). Statistically significant differences of gene expression levels in experimental groups relative to reference groups were determined by a t-test in R (R Core Team, 2015). The threshold of significance was an error probability of less than 5% ($P < 0.05$).

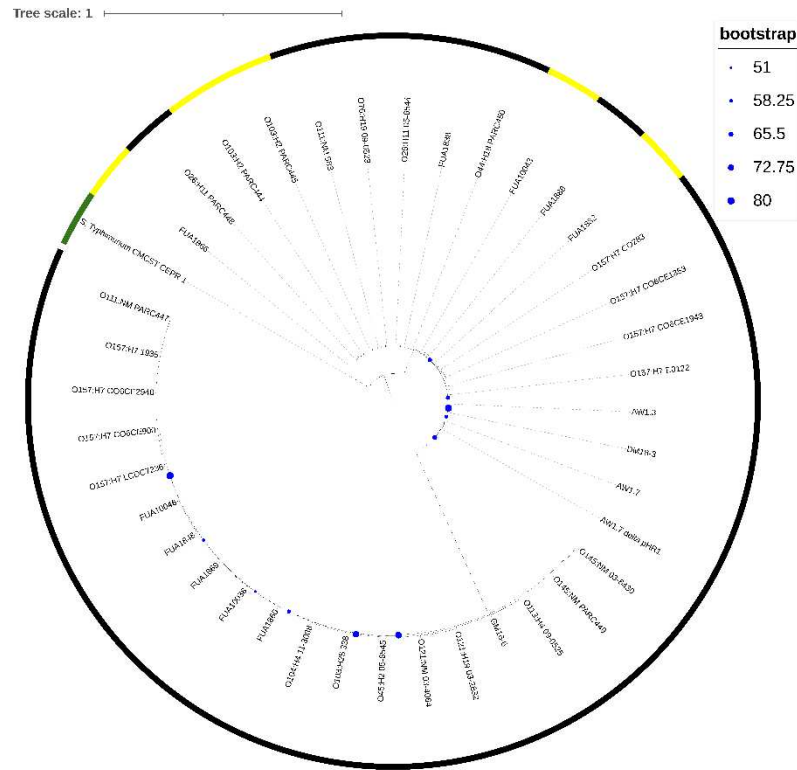
4.3 Results

4.3.1 Comparative genomic analysis among pellicle forming strains and non-pellicle forming strains

Pellicle formation was examined in 39 strains of *E. coli*. These strains represent the phylogroups A, B1, B2, D, E and F (Mercer et al., 2015) (Table 4.1). Of these, five formed pellicles. Scoary analysis did not identify any genes that were present in all five pellicle forming strains but were absent in all 34 strains that did not form pellicles. A heat map depicting the presence or absence of 27 biofilm-associated operons that encode for ECM biosynthesis, putative chaperone usher fimbriae, flagellar motility and regulatory systems is shown in Fig. S1. None of these operons was distributed differently between the pellicle forming and non-pellicle forming strains (Fig. S4.1). Because curli and pEtN modified cellulose differentially contribute to ECM formation in biofilms and pellicles, phylogenetic trees of the regulatory regions of curli and cellulose biosynthesis were constructed (Fig. 4.1). In the phylogenetic tree of the regulatory region for curli synthesis, ranging from 754 to 756 bp in the 39 strains, all pellicle forming strains clustered in three closely related clades that also included non-pellicle forming strains (Fig. 4.1A). Clustering of all pellicle-forming

strains was not observed for the regulatory region of cellulose synthesis (Fig. 4.1B). Taken together, the analysis of the presence / absence of biofilm-related genes and the phylogenetic analysis of regulatory regions of curli and cellulose synthesis suggest that gene regulation rather than the presence or absence of genes mediates pellicle formation by *E. coli*.

A



B

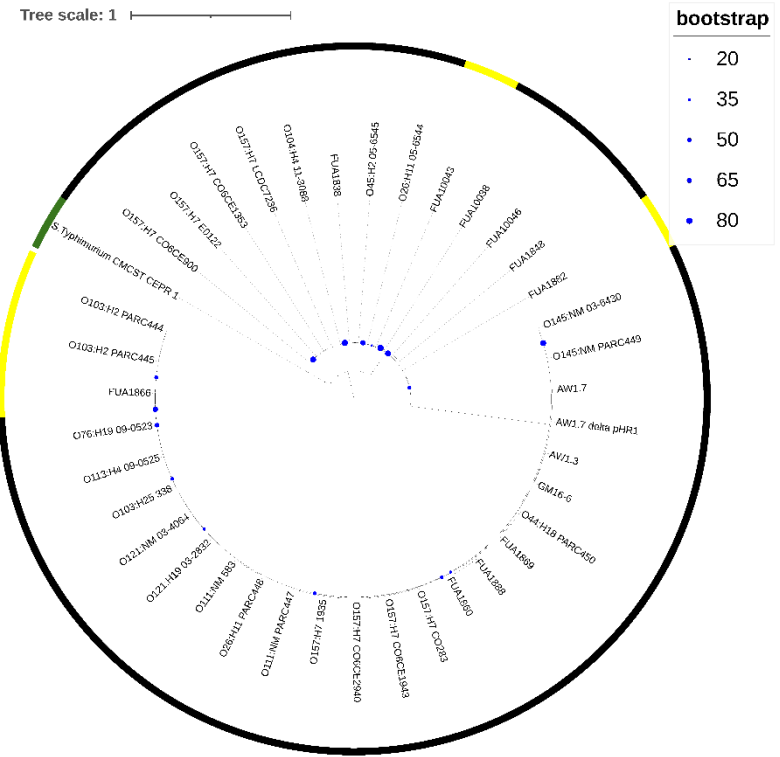


Figure 4.1. The phylogenetic distance of the upstream region of curli (A) and cellulose (B) biosynthesis operon among 39 strains of *E. coli* with *Salmonella* Typhimurium CMCST_CEPR_1 as the reference (green). Pellicle forming strains are colored with yellow while non-pellicle formers are colored with black. Bootstrap values below 80% are indicated by symbol size.

4.3.2 Expression of genes related to pellicle formation

To further study the role of gene regulation on pellicle formation, relative expression of genes associated with biofilm formation was quantified in eight strains of *E. coli*. The gene expression of single-culture pellicle-embedded or planktonic cells after 6d incubation was compared to gene expression in stationary phase and planktonic cells of the same strain after overnight culture (reference conditions). All of the nine genes were differentially expressed in pellicle-embedded cells in one or more of the pellicle-forming strains (Fig. 4.2). When comparing expression levels in the five pellicle forming strains relative to the 3 non-pellicle forming strains, the expression level of the cellulose major subunit (*bcsA*), the curli transcriptional regulator (*csgD*), the adenylate cyclase (*cyaA*) and the RNA polymerase sigma factor (*rpoS*) was downregulated ($P < 0.05$) in all 5 pellicle forming strains.

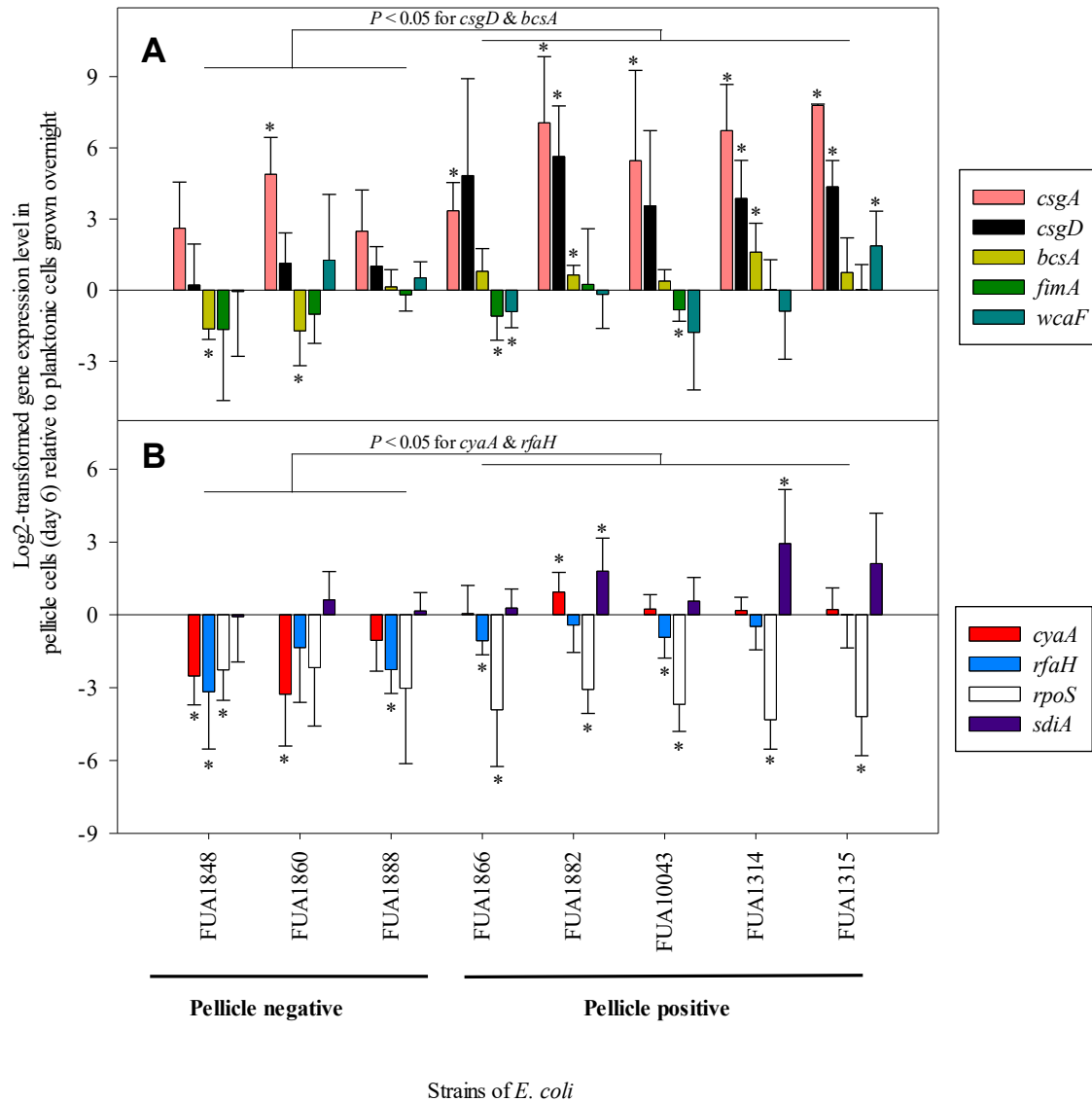


Figure 4.2. The expression level of biofilm-related genes in 8 strains of *E. coli* in pellicle-embedded cells (6d) relative to the expression in planktonic cells (1d). Results are sub-grouped by genes associated with EPS biosynthesis (A) and regulatory system (B). The bars represent the mean values with standard deviation as the error bars for three independent experiments. The gene expression level differs at a significant level ($P < 0.05$) between group of pellicle and non-pellicle strains as indicated. Asterisks (*) indicates the significant different expression level of the gene compared to the control condition.

Gene expression was also quantified in biofilm-embedded co-cultures of the same strains with *A. australiensis* after 6d incubation. In co-cultures, quantification of gene expression additionally included genes related to quorum sensing systems in *E. coli*. The genes *bcsA*, *csgD*, *cyaA* and *rfaH* genes were over-expressed in pellicle forming strains relative to biofilm-embedded strains in co-culture with *A. australiensis* (Figure 4.3A and 4.3B) and expression of these genes was higher in pellicle-forming strains of *E. coli* when compared to non-pellicle forming strains (Fig. 4.3A and 4.3B). In contrast, the expression of *csgA* and *wcaF* encoding for colanic acid biosynthesis was lower in pellicle-forming strains growing in single culture relative to coculture conditions (Fig. 4.3A). In addition, expression of *rpoS* differed significantly in single-culture pellicle-forming embedded cells relative to co-cultures with *A. australiensis* ($P < 0.05$) and this difference was higher in pellicle forming strains when compared to non-pellicle forming strains (Fig. 4.3B). The expression of genes involved in AI-2-mediated signalling (*luxS*, *lsrK*, *lsrR*) was down-regulated ($P < 0.05$) in all non-pellicle forming strains when single cultures were compared to co-cultures with *A. australiensis* (Fig. 4.3C). Expression of *sdiA* in strains growing in single cultures was lower when compared to co-cultures, and down-regulation of *sdiA* was more pronounced ($P < 0.05$) in non-pellicle forming strains when compared to pellicle forming strains (Fig. 4.3C). In contrast, the genes *qseB* and *qseC* were overexpressed in all pellicle forming strains but not in non-pellicle forming strains when single cultures were compared to co-cultures with *A. australiensis* (Fig. 4.3C). Only overexpression of type 1 fimbriae major subunit (*fimA*) was observed in both pellicle and non-pellicle strains of *E. coli* (Fig. 4.3A).

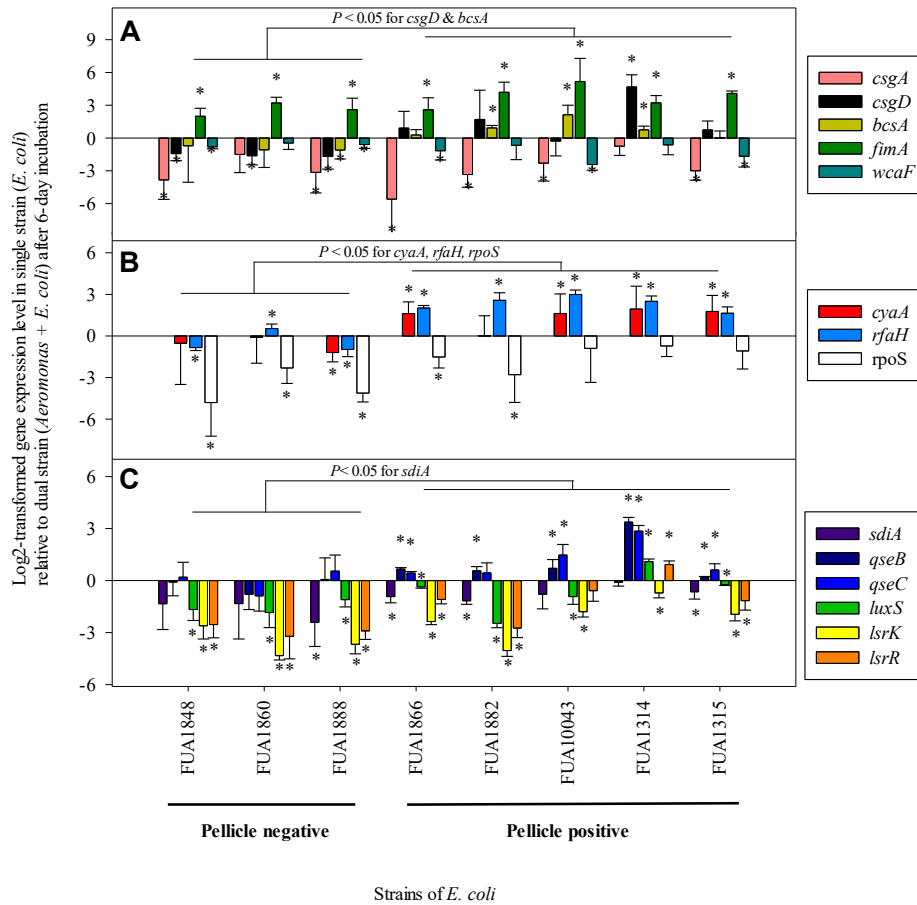


Figure 4.3. The expression level of biofilm-related genes in 8 strains of *E. coli* relative to that in *E. coli* incubated with biofilm producer *Aeromonas australiensis*. Strains of *E. coli* and *A. australiensis* formed solid-surface biofilms after 6d incubation while single strains of non-pellicle forming *E. coli* remained planktonic state cells. Results are subgrouped by genes associated with EPS biosynthesis (A), regulatory system (B) and quorum sensing (C). The bars represent the mean values with standard deviation as the error bars for three independent experiments. The gene expression level differs at a significant level ($P < 0.05$) between group of pellicle and non-pellicle strains as presented. The gene expression level significantly differs compared to control condition if asterisk (*) presents.

4.3.3 The addition of homoserine lactones interferes with pellicle formation

The analysis of gene expression indicated that inter-species quorum sensing is involved in the regulatory switch that determines whether strains of *E. coli* form pellicles or integrate into biofilms. To further elucidate the role of quorum sensing, pellicle formation in the 5 strains was determined in presence or absence of the quorum sensing molecules C₄-HSL and C₆-HSL (Fig. 4.4), which are produced by strains of *Aeromonas* (Talagrand-Reboul et al., 2017). Addition of DMSO as control did not interfere with pellicle formation (Fig. 4.4). Pellicle formation by *E. coli* was abolished by the addition of C₄-HSL but not C₆-HSL (Fig. 4.4).

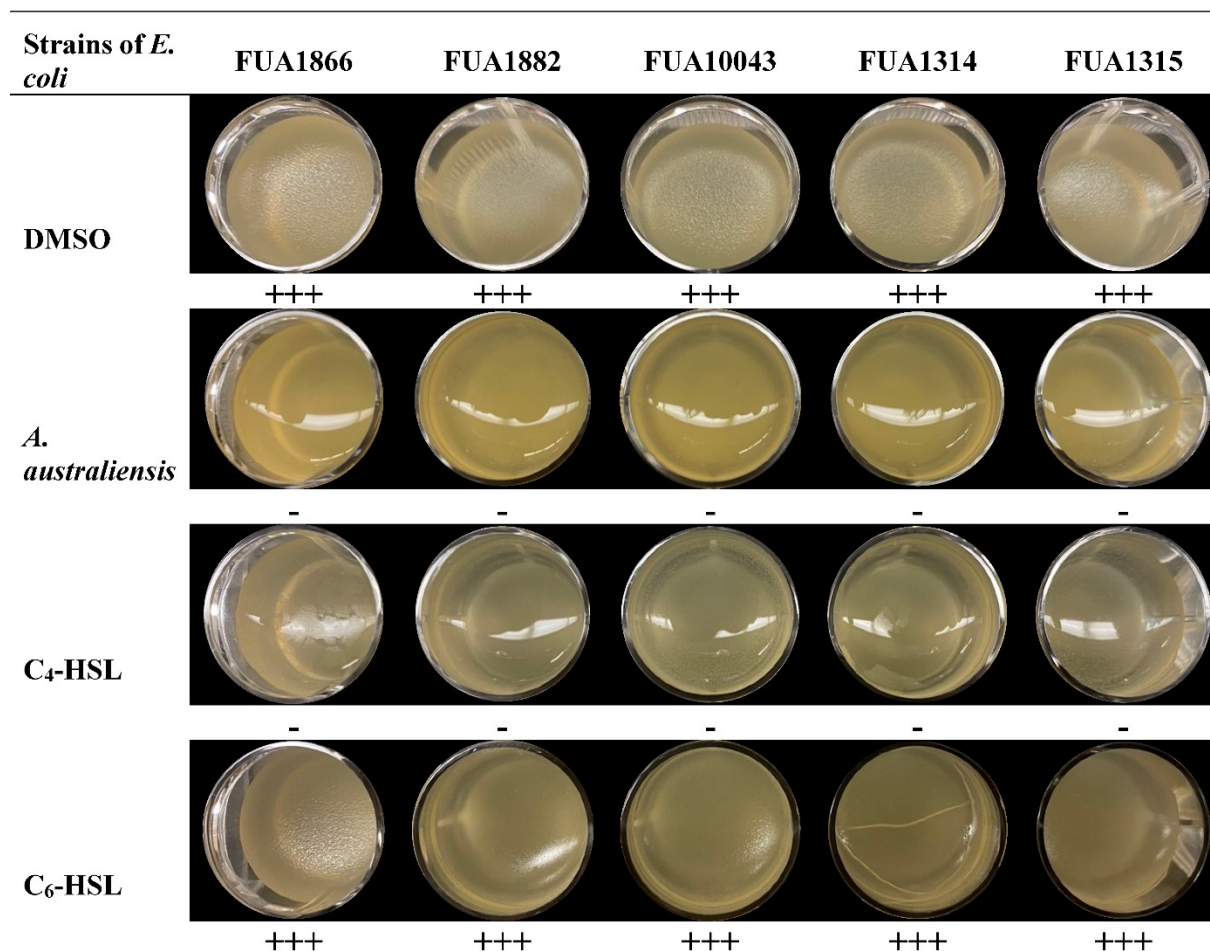


Figure 4.4. Pellicle formation by strains of *E. coli* at 25 °C in 24-well plate for 6 days. Pellicle formation of strains of *E. coli* with DMSO, *Aeromonas australiensis*, 0.1mM C₄-HSL or 0.1mM C₆-HSL, respectively. Pellicle formation was observed with the presence of DMSO and C₆-HSL, while aborted together with *Aeromonas australiensis* or C₄-HSL. Experiments were repeated independently three times.

4.3.4 Deletion of *bcsG*, *curliU* and *sdiA* alters pellicle formation

To further determine the role of modified cellulose, curli and quorum sensing in pellicle formation, *bcsG*, the regulatory region upstream of *curliU*, and *sdiA* was deleted in *E. coli* FUA1882. In *E. coli*, SdiA is the receptor protein for HSL signaling molecules (Talagrand-Reboul et al., 2017).

The deletion of either *bcsG*, responsible for phosphoethanolamine (pEtN) cellulose production, or the region upstream of the curli operon abolished pellicle formation (Fig. 4.5). The deletion of the autoinducer receptor *sdiA* in *E. coli* resulted in a thinner pellicle when the strain grew in single cultures (Fig. 4.5) but did not restore the pellicle formation when cocultured with *A. australiensis* (data not shown). Complementation of *sdiA* under control of its native promoter on the low-copy number plasmid pRK767 complemented the *sdiA* deletion and restored pellicle formation; likewise, complementation of *bcsG* restored pellicle formation in the corresponding mutant (Fig. 4.5). Interestingly, deletion of *sdiA* in *E. coli* also reduced the biomass of biofilms in co-cultures with *A. australiensis* from 1.64 ± 0.26 for the wild type to 0.76 ± 0.09 for *E. coli* $\Delta sdiA::cam$ ($P < 0.001$) (Fig. S4.2).

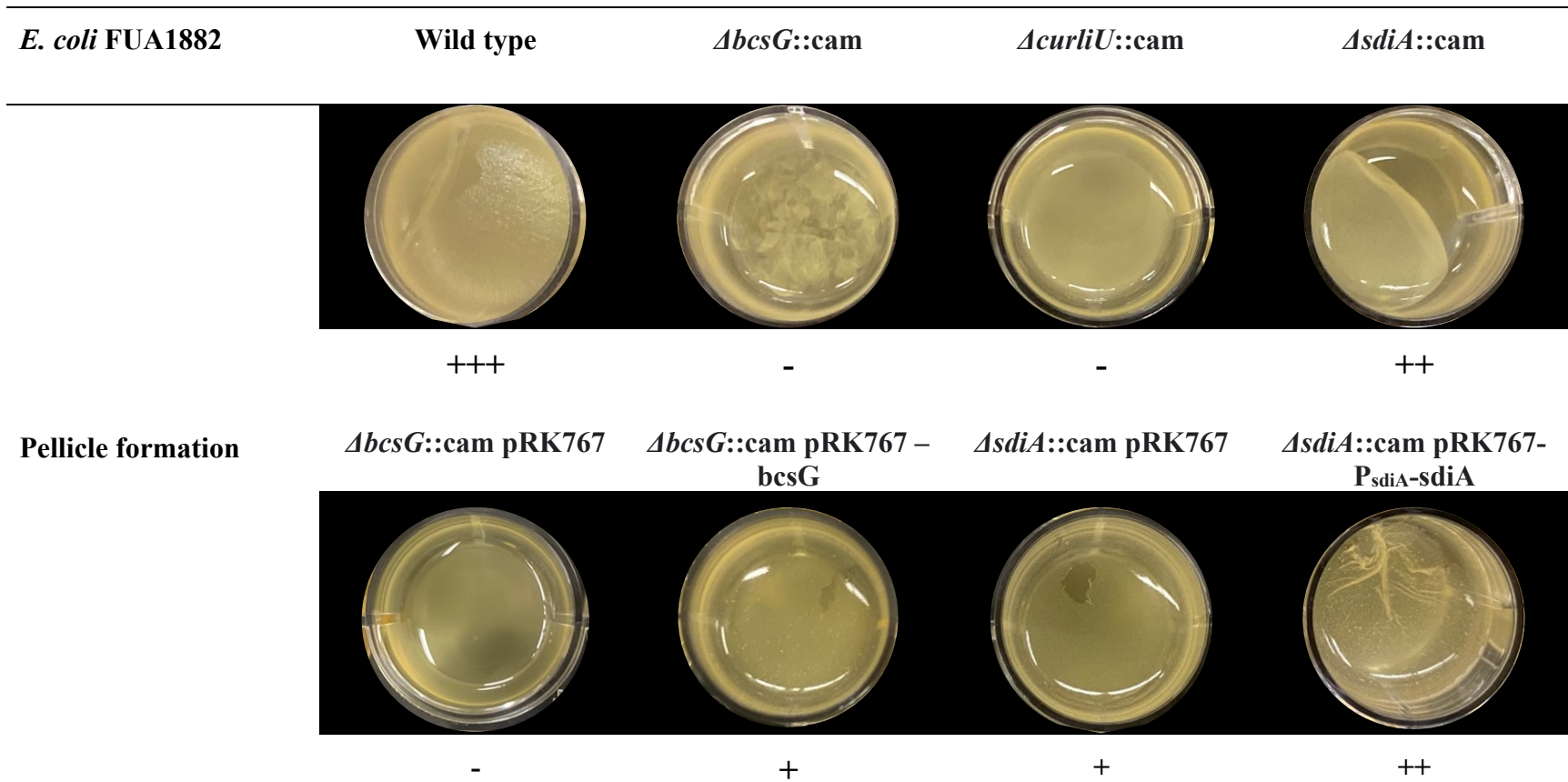


Figure 4.5. Pellicle formation in wild type, mutant strains of *E. coli* FUA1882 and in after complementation of *bcsG* and *sdiA* in *E. coli* FUA1882 $\Delta bcsG::cam$ and $\Delta sdiA::cam$, respectively. Shown is the pellicle formation as observed in three independent replicates and the picture representative for the replicate cultures. Pellicle formation: +++ Strong; ++ moderate, +Weak; - No

4.3.5 Gene expression

To determine the impact of quorum sensing on pellicle formation, the expression of biofilm related genes relative to the wild type strain was quantified in *E. coli* FUA1882 Δ *sdiA*::cam. Expression was quantified in planktonic cells and in pellicle-embedded cells (Figure 6). The deletion of *sdiA* increased ($P < 0.05$) the expression of *bcsG* and *csgD* in planktonic cells but the difference was less than two-fold (Fig. 4.6). In pellicle-embedded cells, the expression of *bcsA*, *csgA* and *csgB* was downregulated ($P < 0.05$) in *sdiA*-deficient *E. coli* FUA1882 Δ *sdiA*::cam compared to the wild type strain (Fig. 4.6).

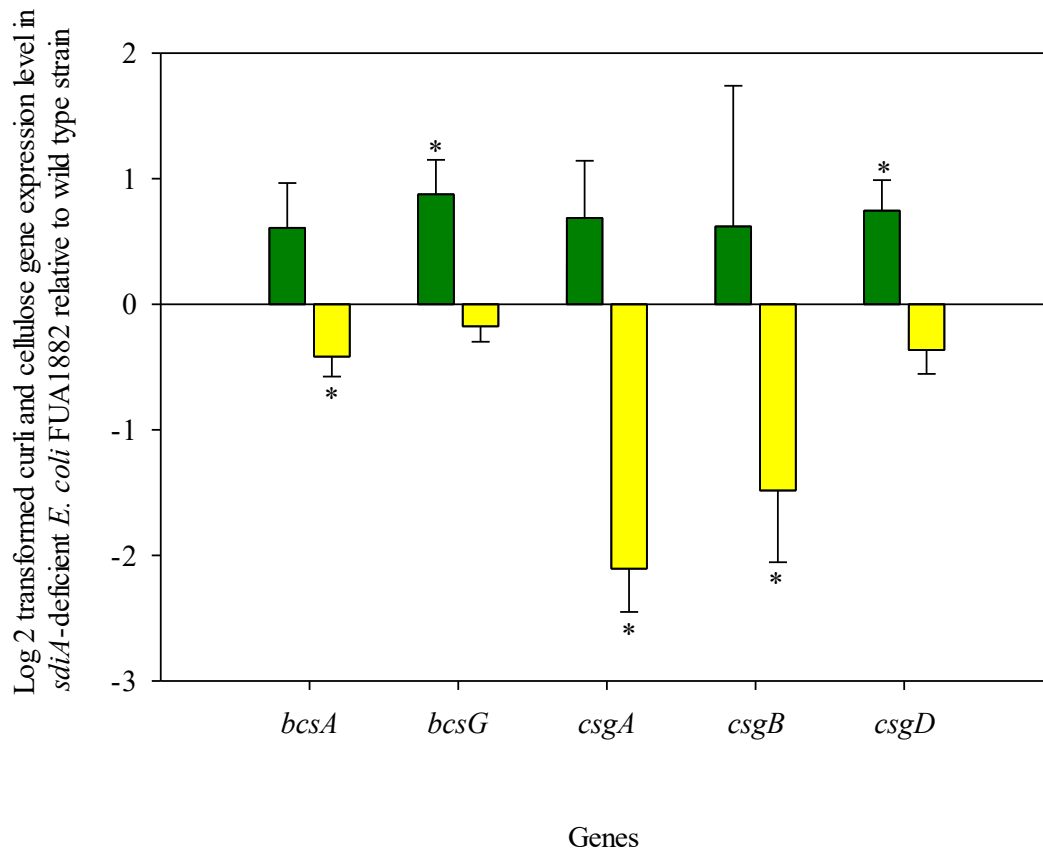


Figure 4.6. The expression level of curli and cellulose biosynthesis genes in *sdiA*-defected *E. coli* FUA1882 relative to wild type in planktonic cells (green bars) and pellicle-embedded cells (yellow bars). The bars represent the mean values with standard deviation as the error bars for three independent experiments. Asterisk (*) indicates $P < 0.05$ according to unpaired t-test.

4.4 Discussion

The wastewater isolate *E. coli* FUA10043 forms a pellicle when grown in single culture, with *C. maltaromaticum* and *E. coli* O157:H7 but only forms surface-associated biofilm (biofilms) when co-cultured with *A. australiensis* (Z. S. Xu et al., 2021). This phenomenon was also observed

in additional four strains of *E. coli* in the present study. We demonstrated by functional genomic analyses that pellicle formation by strains of *E. coli* itself or in co-cultures with *A. australiensis* was modulated by inter-species communication. Comparative genomic analyses indicated that pellicle-forming strains did not harbor any unique genes that were absent in non-pellicle formations strains.

Both curli and cellulose amyloid fibers are major components of extracellular matrices in pellicles and biofilms (Hung et al., 2013; Paytubi et al., 2017). Cellulose is not essential for pellicle formation by uropathogenic *E. coli* (Paytubi et al., 2017) as pellicle formation was weakened but not abolished in a cellulose-deficient mutant, *E. coli* UTI89 $\Delta yhjO$ ($=bcsA$). In contrast, deletion of *bcsG*, which converts cellulose to phosphoethanolamine-cellulose, abolished pellicle formation (Anderson et al., 2020; Hung et al., 2013). The formation of pellicles versus biofilms is regulated by the ratio of curli and modified cellulose (Jeffries et al., 2021) as demonstrated by deleting the genes coding for curli (Jeffries et al., 2021) or the regulatory region mediating expression of genes coding for curli (this study). Colanic acid and type 1 fimbriae are also part of the ECM in both pellicles and biofilms (Golub and Overton, 2021; Hung et al., 2013) but only gene related to type 1 fimbriae biosynthesis was distinctly overexpressed in pellicle-embedded relative to biofilm-embedded cells (this study), indicating that the abundance of fimbriae but not colanic acid is involved in the switch from biofilm to pellicle formation.

The regulation of pellicle versus biofilm formation in *E. coli* is poorly understood. Formation of pellicles in *E. coli* strains is mediated by multiple transcriptional factors that respond to environmental conditions. The production of secondary signalling molecule cyclic AMP (cAMP) is linked to the biosynthesis of curli and cellulose through the master the regulator protein CsgD. cAMP is produced by adenylate cyclase (CyaA) and activates the catabolite repressor protein

(CRP) (Fic et al., 2009), which alters the transcription of *csgD*. The production of curli and cellulose and hence pellicle formation was abolished in *cyaA*-deficient strain in UPEC isolates, while the addition of cAMP restored pellicle formation (Hufnagel et al., 2016). Our study demonstrated that *cyaA* was overexpressed in pellicle forming strains when compared to non-pellicle forming strains, and in the pellicle forming strains when compared to cells of the same strains embedded in biofilms (Fig. 4.2 & 4.3), suggesting that CyaA also is part of the regulatory network that regulates the pellicle-versus-biofilm decision.

Different from biofilm formation, which is mostly induced by environmental stress, the formation of pellicle at the air-liquid interface serves to access a favorable habitat for aerobic bacteria since it may provide higher concentration oxygen from air and nutrients from the medium (Armitano et al., 2014; Hölscher et al., 2015). In standing bodies of water, oxygen diffusion to the bottom occurs only by diffusion and the sediment is often anaerobic while in flowing bodies of water, fluid motion facilitates oxygen transport (Dugan et al., 2016; Koschorreck et al., 2017). In *Pseudomonas* and *Shewanella* species, pellicles were not formed at the air-liquid interface under anaerobic condition and pellicle formation was reduced at low-oxygen conditions (Scher et al., 2005; Yamamoto et al., 2011), indicating a decisive role of oxygen availability on pellicle formation. In *Shewanella*, oxygen also promoted cell aggregation (McLean et al., 2008). *A. australiensis* is a facultative anaerobe which was first isolated from an irrigation water system (Aravena-Román et al., 2013); *A. australiensis* 0309 is an isolate from a meat processing plant that forms biofilms but not pellicles (Visvalingam et al., 2019; Wang et al., 2018). Under aerobic conditions, co-cultures of *E. coli* and *A. australiensis* prevented the pellicle formation by *E. coli*, which integrated into biofilms instead (Z. S. Xu et al., 2021). This switch is likely beneficial for both organisms. Pellicle formation by *E. coli* may impede the growth and biofilm formation by *A. australiensis* in the same

culture vessel while integration of *E. coli* into a dual-species biofilm likely reduces the resource allocation for synthesis of the ECM. Our study provided several indications on how this switch from pellicle formation to biofilm formation is regulated. The expression of the transcriptional anti-terminator RfaH was lower in biofilm-embedded cells relative to pellicle-embedded cells (this study). Mutants of *E. coli* K-12 and UPEC that were deficient in RfaH over-expressed genes coding for antigen 43 (*ag43*), promoting cell aggregation and formation of microcolonies on abiotic surfaces (Beloin et al., 2006; Klemm and Schembri, 2004).

The interactions between strains of *E. coli* and *A. australiensis* during biofilm formation was related to quorum sensing (QS) through N-acyl homoserine lactones (AHLs) (Escobar-Muciño et al., 2022; Pappenfort and Bassler, 2016b). In Gram-negative bacteria, AHLs are synthesized and detected by LuxRI-type proteins and serve as the most common autoinducers (Pappenfort and Bassler, 2016b). Some bacteria including *E. coli* contain incomplete LuxI-LuxR QS circuits which do not produce AHLs but sense AHLs produced by other bacteria via the receptor SdiA (Case et al., 2008). The following evidence supports that conclusion that inter-species communication via AHLs regulates pellicle formation in the presence of *A. australiensis*: (i) Expression level of genes associated with quorum sensing was different in co-cultures compared to single culture (Fig. 4.3B); (ii) The addition of AHL molecules reduced pellicle formation (Fig. 4.4); (iii) The deletion of cell signaling sensor (SdiA) also reduced pellicle formation (Fig. 4.5); and (iv) The *sdiA*-mutant downregulated the biosynthesis of curli and cellulose in pellicle-embedded cells and produced thinner pellicles (Fig. 6). SdiA suppresses biofilm formation through downregulating the expression of motility, fimbriae and curli production in strains of atypical enteropathogenic *E. coli* and *K. pneumoniae* (Culler et al., 2018; Pacheco et al., 2021). Our results expand the knowledge on its role through the comparison of pellicles and biofilms. The *sdiA*-negative strain upregulated

bcsA, *bcsG*, *csgA*, *csgB* and *csgD* in planktonic cells when compared to the parent strain but downregulated the same genes in the pellicle-embedded cells (Fig. 4.6). These results indicate that SdiA has different roles for cells in planktonic versus pellicle embedded cells. Also, the deletion of *sdiA* in *E. coli* FUA1882 distinctly altered ($P < 0.05$) the expression level of the curli major and minor subunits in single-culture pellicle-embedded cells, hence potentially resulting in impaired biofilm formation on solid surfaces when co-cultured with *A. australiensis*. This hypothesis was further confirmed by the biofilm biomass data (Fig. S4.2).

A threshold of QS molecules prompts changes in cell regulation. For instance, the bioluminescence system in *V. fischeri* is tightly related to the concentration of signaling molecules. The exponential increase in signaling molecules results in light emission in *V. fischeri* (Miller and Bassler, 2001). A recent study additionally outlined that *P. aeruginosa* delivered a linear response to population densities (Rattray et al., 2022). In this study, however, the addition of *A. australiensis* or C₄-HSL (more signaling molecules) to pellicle forming strains of *E. coli* or deletion of *sdiA* (no signaling molecules) both negatively impacted pellicle formation. This unexpected finding indicates that in *E. coli*, which does not produce HSL but senses HSLs produced by others, quorum sensing may be involved in decisions on whether to form surface associated biofilms or pellicles by graded responses, opposite to the dichotomy of the quorum sensing ON/OFF state in those organisms that produce and sense HSL to generate a positive feedback loop. This observation, if confirmed, could significantly advance our knowledge on pellicle formation in single strains of *E. coli* mediated by complex regulatory circuits and expanded the current view of QS-dependent uniformity on dual-species pellicle formation.

In the natural environment, the presence of this polymeric multicellular assemblages (pellicle) at the air-liquid interface serves as an important survival strategy relative to planktonic cells. For

example, pellicle-forming strains of *Salmonella* established higher desiccation and chlorination tolerance under the sheltering of ECM component (Ramachandran et al., 2016; Scher et al., 2005). Wild type strains of *B. subtilis* produce robust and strong pellicles with a distinct architecture - "fruiting body formation" - serving as a preferential site for sporulation (Branda et al., 2004, 2001). Pellicle-embedded cells of *E. coli* exhibited a higher resistance to sodium chlorite, hydrogen peroxide and peracetic acid (Z. S. Xu et al., 2021). In the context of aquatic environments, growth at the air-liquid interface likely expose microorganisms to high levels of ultraviolet radiation (UV) (Cunliffe et al., 2013; Fiebig, 2019). Therefore, it is pivotal to gain deeper understanding of multicellular behaviors during pellicle formation, which may contribute to the development of novel methods to remove the pellicle matrix and combat the resistant microorganisms in these ecological niches, thus enhancing the safety and security of food product as well as the health of human, animals, and environment.

Chapter 5. High-throughput Analysis of Microbiomes in a Meat Processing Facility: Are Food Processing Facilities an Establishment Niche for Persisting Bacterial Communities?

5.1 Introduction

Global food systems are challenged to meet the rising demand for food while ensuring environmental sustainability in the face of climate change, population growth, and malnutrition (Klaura et al., 2023). Food waste due to microbial spoilage exacerbates these challenges. In 2019, approximately 77.4 million tonnes of pork, poultry, beef, or mutton were discarded, from which 20% was occurring during processing and packaging stages (Klaura et al., 2023). The food industry is thus prioritizing efforts to combat spoilage microbes and mitigate their adverse impacts on products' shelf life and quality.

The introduction of spoilage microbes onto meat products can occur from bacteria carried by the animals at slaughter, from the environment, or from microbes residing in the processing facility environment (Yang et al., 2023a). Muscle tissue is generally considered sterile, but the environment during slaughtering and fabrication are not, leading to microbial contamination with air, water, workers, and processing environment as vectors (Gill, 2005). Subsequently, these microbes can become established through biofilm formation (Snyder et al., 2024). Biofilm-embedded bacteria attach to the surface of equipment or the processing rooms. The protective barrier of the biofilm matrix and the development of persister cells under nutrient-deficient conditions increases bacterial resistance to sanitizers (Alvarez-Ordóñez et al., 2019; Flemming et al., 2016). The food industry controls biofilm formation by hygienic design of processing equipment and facilities; however, these efforts fail to fully control the problem and some microbes persist in food processing facilities. This is best documented for pathogenic bacteria. For example, a Canadian listeriosis outbreak in 2008 was attributed to *Listeria monocytogenes* persisting inside

of a slicing machine (Jespersen and Huffman, 2014) where they were not eradicated by routine sanitization measures.

Current studies on the composition of microbial communities in food processing facilities are predominantly based on high throughput sequencing of 16S rRNA gene amplicons (Fagerlund et al., 2021; Xu et al., 2023a). This approach identifies microbial taxa at the species- or genus level; however, many bacterial activities and characteristics are strain-dependent. For example, different strains of *Carnobacterium maltaromaticum* exhibited different spoilage-related activities and were affected differently by storage conditions (Casaburi et al., 2011). While metagenomic sequencing can provide strain level information (Podlesny et al., 2022; Van Rossum et al., 2020), SNP calling of high quality genome sequences of isolates remains the gold standard of strain-level identification. This approach is routinely used in outbreak investigations to identify the transmission paths of bacterial pathogens (Pightling et al., 2018).

Long-term persistence of microbes in food processing facilities implies that these facilities constitute an establishment niche rather than a persistence niche to which they recurrently transmit from other sources (Holt, 2009). Current data on strain-level bacterial persistence on farms or in food processing plants is limited to foodborne pathogens such as *L. monocytogenes* (Alvarez-Molina et al., 2021; Daeschel et al., 2022; Harrant et al., 2020), *Salmonella* (Tassinari et al., 2019) and *Escherichia coli* O157:H7 (Arthur et al., 2014). Spoilage microbes do not only contribute to food deterioration but the biofilms formed by these microbes also enable the persistence of microbes that do not form biofilms and may shelter foodborne pathogens (Fagerlund et al., 2021; Zwirzitz et al., 2021). The strain-level persistence of spoilage microbes, however, has not yet been described. Therefore, this study aims to use high-throughput cultivation to characterize the microbial community in a meat processing facility at the strain-level, and to determine the overlap

between isolates from different sites and meat products at two sampling times over a 6-month period. Isolates were also used to reconstitute multi-species biofilms to assess their biofilm formation and composition.

5.2 Results

High throughput culture-dependent and culture-independent characterization of microbial communities in the meat processing facility.

We used culture-dependent and culture-independent methodologies to characterize the microbial communities in the processing facility. The culture-dependent approach used PCA, APT and VRBG agars to enumerate total aerobic bacteria, lactic acid bacteria and *Enterobacteriaceae*. A total of 739 and 1435 isolates were obtained in the first (Sept 2022) and the second sampling (March 2023), respectively. Of these, 605 non-redundant isolates from the first sampling and 1281 non-redundant isolates from the second sampling were characterized at the species level by Sanger sequencing of the full-length 16S rRNA gene and Nanopore whole genome sequencing, respectively (Fig. 5.1 and Fig. S5.1). *Pseudomonas* species were the most prevalent, regardless of whether the sample was from meat or from surfaces before or after sanitation (Fig. 5.1 and Fig. S5.1). Other frequent isolates include *Enterobacteriaceae*, *Janthinobacterium*, *Psychrobacter*, *Acinetobacter* and *Flavobacterium*. Gram-positive organisms including lactic acid bacteria, staphylococci and *Brochothrix* only accounted for a small fraction of the total number of isolates (Fig. 5.1 and Fig. S5.1). The microbial diversity in meat samples at the time of packaging were similar for both sampling times. The microbial composition in the drain (cooler) after cleaning and sanitation, trolley (cooler) and tray (fabrication room) during production overlapped with that of meat collar samples. Microbial communities on surfaces obtained during production and after sanitation were generally similar (Fig. 5.1 and Fig. S5.1). Several genera including *Acinetobacter*,

Psychrobacter and *Serratia*, however, were not recovered from sanitized surfaces although these were highly prevalent during operation. After 90 days of vacuum-packaged refrigerated storage, meat microbiota changed and facultative anaerobes including *Carnobacterium*, *Lactococcus*, *Leuconostoc* and *Latilactobacillus* species and *Enterobacterales* of the genera *Rahnella*, *Hafnia*, *Serratia*, *Yersinia* and *Rouxiella* dominated. Pathogens were not detected but the non-pathogenic *Listeria welshimeri* was found on the inner surface of connection joints of a conveyor belt (D-BT3 CD).

Frigoribacterium sp001421165 and *Psychrobacter maritimus* in D-Wall in cooler, *Pseudochrobactrum* sp in D-Apron, *Janthinobacterium* sp002878455 in D-Wizard knife, *Pseudomonas extremaustralis* in D-Shrink tunnel, *Pseudomonas* sp002874965 in D-pipes 1, *Bacillus altitudinis*, *Priestia megaterium*, *Enterococcus viikkiensis*, *Pigmentiphaga litoralis* in D-Wall in shipping truck, *Yersinia intermedia* in D-Bloody drain, *Pseudoclavibacter* sp and *Variovorax* sp in D-Plastic curtain, *Specibacter* sp. and *Shewanella glacialis* in D-drain in cooler 2, *Serratia* sp in D-Side cutting board, *Aeromonas salmonicida* and *Pseudomonas mohnii* in D-ES1, *Stenotrophomonas* sp in D-Knife sharpener (plastic), *Sphingobacterium* sp000938735, *Microbacterium* sp002979655 and *Pseudomonas* sp010095445 in D-Drain in cooler 1, *Polaromonas* sp in Water sample, *Janthinobacterium* sp009923995 in D-Break table, *Pseudomonas taetrolens* in D-Door, *Pseudomonas cremoris* in D-T5, *Janthinobacterium* sp in D-Drain in cutting room, *Paeniglutamicibacter antarcticus*, *Flavobacterium frigidimaris*, *Acinetobacter albensis* and *Pseudomonas tritici* in D-Drain in bagging station, *Pseudomonas koreensis* in D-BT3 (AP), *Listeria welshimeri*, *Morganella* sp, and *Buttiauxella massiliensis* in D-BT3 CI, *Serratia fonticola* in D-BT1 CI. Isolates are designated with sp# if a matching sequence is available in the GTDB but the species has not been formally described; taxa are designated with sp. if no sequence with ANI > 95% was available on the GTDB.

Each sample was additionally characterized by sequencing of full length 16S rRNA gene amplicons to identify uncultured organisms (Fig. 5.2 and Fig. S5.2). Of 4 out of 70 samples collected in March 2023, the biomass was too low to obtain PCR amplicons. In 54 of the remaining 66 samples, more than 75% of the bacterial diversity at genus level was cultured, while in 6 samples, culture-based methodology accounted for less than 25% (Fig. 5.2). The proportion of uncultured organisms was particularly high on sanitized surfaces where dead microbial cells are

present. Additionally, our culture-based approach did not recover strict anaerobes. Low abundance taxa in nutrient-deficient surfaces such as pipes, curtain and walls were also identified with sequencing but not with culturing. The higher proportion of uncultured genera among samples collected in September 2022 (Fig. S5.2) may relate to the smaller number of isolates collected. The genera *Janthinobacterium*, *Paraburkholderia*, *Brevundimonas*, *Devosia* and *Dellaglioia* were underrepresented or not recovered by culture but accounted for a substantial proportion of sequences in several samples (Fig. 5.2 and Fig. S5.2).

Conversely, multiple taxa were frequently cultured but represented less than 1% of the 16S rRNA gene sequences or were not represented (Table 5.1). Only one sequencing read (out of 15,122 reads) was classified as *Listeria* but *L. welshimeri* was isolated from a conveyor-related surface.

Table 5.1. Bacterial isolates that represented less than 1% of the respective genera in Nanopore 16S rRNA gene sequencing or were not detected by sequencing.

Isolates at genus level	# of species	Sampling sites
<i>Acinetobacter</i>	1	D-knife sharpener steel.
<i>Aerococcus</i>	1	C-Wizard knife
<i>Bacillus</i>	2	C-retail, D-QC1
<i>Brevundimonas</i>	1	C-work table
<i>Brochothrix</i>	1	D-apron, D-Trolley, D-BT2(AP), Loin D0
<i>Carnobacterium</i>	2	C-Retail, D-cutting board W (AP), D-QC1, D-retail saw, D-shrink tunnel C-CB2, D-wizard knife, D-break table, D-BT1, D-BT2(AP), D-cutting board W (AP), D-drain in cooler 1, D-Little hole (Floor trap), Loin D0, Picnic D0
<i>Chryseobacterium</i>	2	BT1-CI, D-Trim 1, D-knife sharpener steel, D-Pipes 2
<i>Enterococcus</i>	1	D-wall in shipping truck
<i>Epilithonimonas</i>	1	D-drain in bagging station, D-knife sharpener steel
<i>Erwinia</i>	1	D-pipes 1
<i>Flavobacterium</i>	3	BT3-CI, D-break saw, D-break table, D-ES1, D-bloody drain
<i>Frigoribacterium</i>	1	D-Wall in cooler
<i>Janthinobacterium</i>	2	D-ss on top of CB BT1, D-wizard knife
<i>Kocuria</i>	1	C-Wizard knife, D-cutting board East
<i>Latilactobacillus</i>	1	D-BT3, Loin D0, Picnic.3.mon
<i>Listeria</i>	1	BT3-CI
<i>Macrococcus</i>	1	C-retail
<i>Microbacterium</i>	3	D-wall in shipping truck, D-BT3, D-Pipes 2, plastic-curtain, D-drain in cooler 1
<i>Moellerella</i>	1	Loin 3mon
<i>Morganella</i>	1	BT3-CI
<i>Neobacillus</i>	1	C-CB3
<i>Ochrobactrum</i>	1	C-drain
<i>Paeniglutamicibacter</i>	1	D-drain in bagging station
<i>Pantoea</i>	2	D-shrink tunnel, D-side cutting board, C-work table
<i>Pedobacter</i>	2	D-Wall in cooler, D-ss on top of CB BT1
<i>Pigmentiphaga</i>	1	D-wall in shipping truck
<i>Plantibacter</i>	1	C-break table, D-air blower, D-drain in bagging station
<i>Polaromonas</i>	1	water sample
<i>Priestia</i>	1	D-wall in shipping truck
<i>Providencia</i>	1	D-BT1
<i>Pseudoclavibacter</i>	1	plastic curtain
<i>Pseudomonas</i>	1	C-retail
<i>Psychrobacter</i>	2	D-apron, D-QC1
<i>Rahnella</i>	1	D-break table
<i>Renibacterium</i>	1	C-worktable
<i>Serratia</i>	4	BT1-CI, D-gloves, D-drain in cutting room AP, D-knife slicing plastic, D-Little hole (Floor trap), D-ss on top of CB BT1, BT3-CI, D-BT3, D-BT3(AP), D-QC2, D-ss holder under cutting board
<i>Specibacter</i>	1	Drain in cooler 2
<i>Sphingobacterium</i>	3	BT3-CI, D-BT1(AP), D-BT2(AP), C-work table, D-drain in cooler 1
<i>Staphylococcus</i>	3	C-retail, C-Wizard knife, D-side cutting board, D-ss on top of CB BT1
<i>Stenotrophomonas</i>	3	D-gloves, BT3-CI, D-BT3, Picnic D0, D-knife sharpener steel
<i>Yersinia</i>	1	D-bloody drain

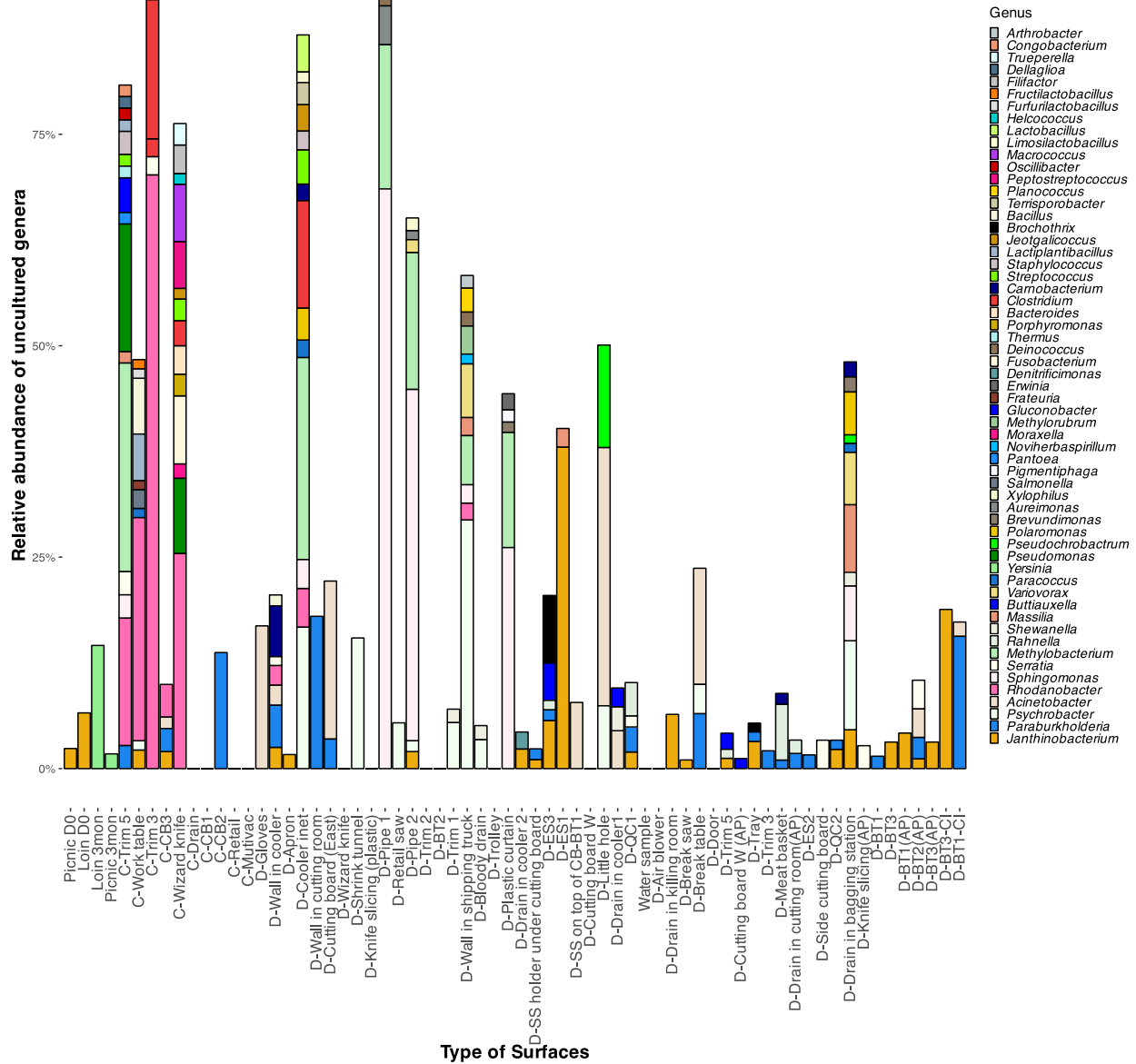


Figure 5.2. Relative abundance of uncultured genera identified in samples collected in March 2023 by sequencing of full length 16S rRNA genes. Genera with a relative abundance less than 1% are not shown. Sampling sites without a stacked bar indicates all genera was recovered by surface plating.

Microbial diversity in the meat processing facility

Both culture-dependent and culture-independent approaches revealed diverse microbial communities in the meat processing facility. A collection of 1,885 isolates from two sampling periods represented 4 phyla: *Pseudomonadota*, *Bacillota*, *Bacteroidota* and *Actinomycetota*. During the first sampling, 28 genera and 76 species were cultured; during the second sampling, 47 genera and 137 species were identified. (Fig. 5.1 & Fig. S5.1). Multiple isolates from the second sampling could not be assigned to known species in the GTDB, indicating isolation of 71 novel taxa (Fig. 5.1). These isolates are designated as "sp." or "sp" followed by numbers. The culture-independent approach identified 67 and 68 genera with a relative abundance of 1% or higher in September 2022 and March 2023, respectively. Among these, 23 genera were identified in both sampling times.

The composition of microbial communities on meat and environmental samples were analysed with the Bray-Curtis distance across four classifications: (i) type of surfaces, (ii) location, (iii) zone concept based on the proximity to food products (FDA, 2017), and (iv) pre- and post-sanitation. Analyses, conducted based on both culture-dependent and culture-independent approaches, showed significant differences in the surface microbiome before and after sanitation but differentiation based on surface type, location, or classified zone at either sampling time did not reveal differences (Fig. 5.3, Fig. 5.4, and Fig. S5.3).

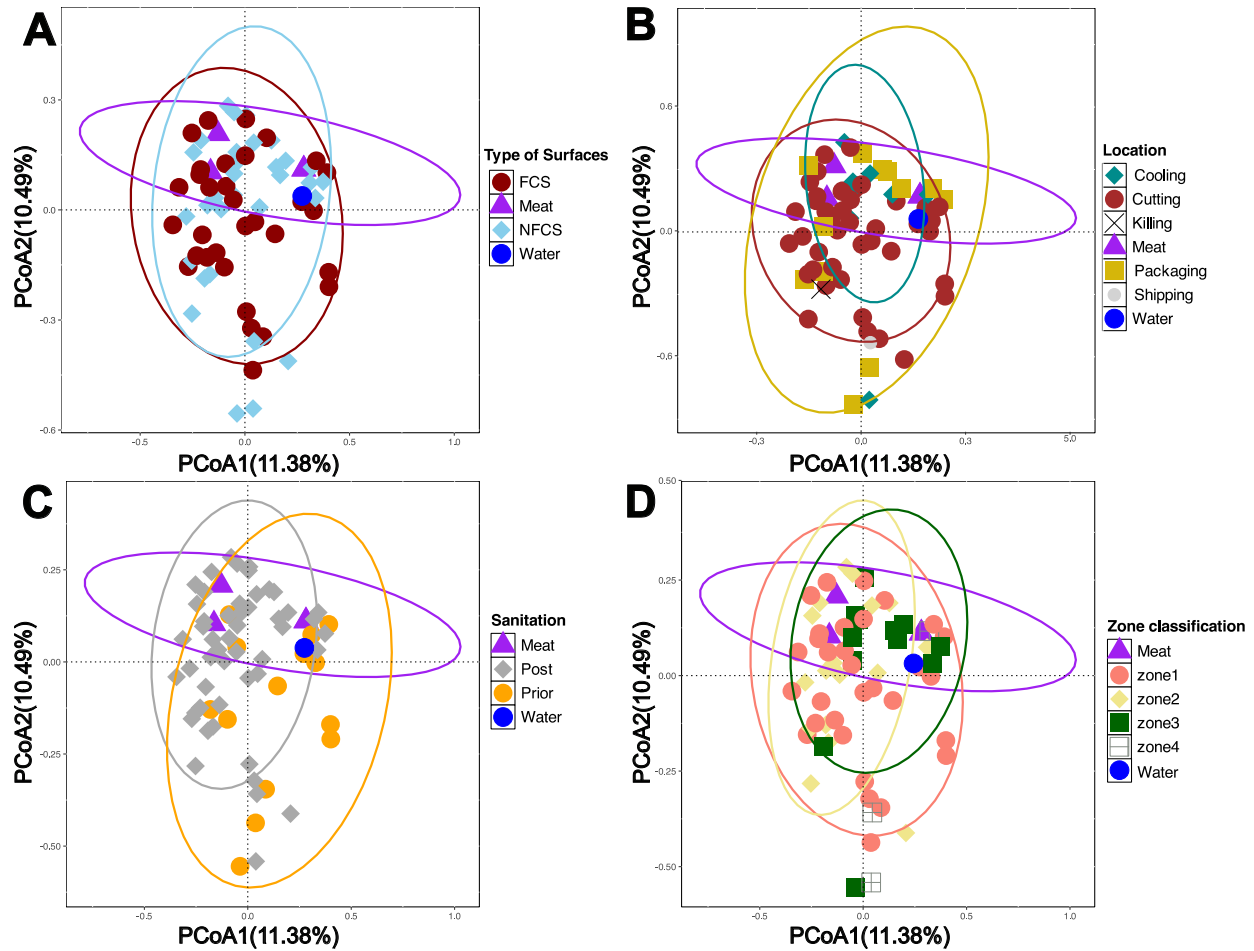


Figure 5.3. Principal coordinate analysis, using Bray-Curtis distance with isolates classified at species level for 70 sampling sites, collected in March 2023. The dissimilarity among collected samples were measured from four categories: A: type of surfaces, B: location, C: sanitation activity and D: zone classification. Permutational multivariate analysis of variance was used to statistically differentiate among the bacterial communities. The associations of community variance with different categories are displayed in Supplementary Table S2.

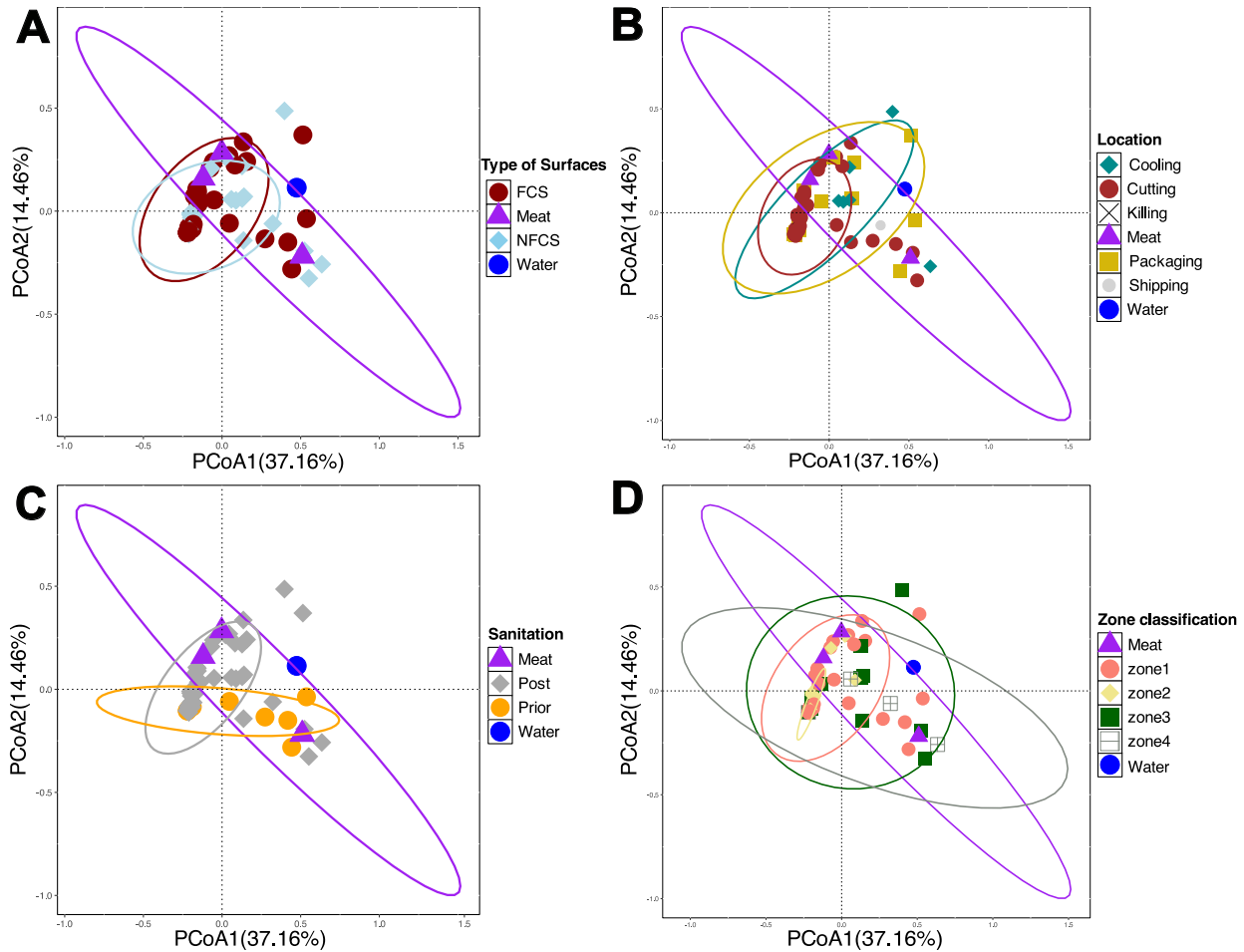


Figure 5.4. Principal coordinate analysis (PCoA) plots of the Bray-Curtis distance matrix for bacteria community as determined by 16S rRNA amplicon sequencing of samples from March 2023. The samples were grouped based on surface type (A), location (B), sanitation activity (C) and zone classification (D). Permutational multivariate analysis of variance was used to statistically differentiate among the bacterial communities. The associations of community variance with different surface groups are displayed in Supplementary Table S2.

Bacterial interactions on meat processing environmental and meat surfaces

Bacterial correlation networks of isolates and 16S rRNA gene amplicons obtained in March 2023 were constructed to explore patterns of bacterial co-occurrence (Fig. 5.5 and Fig. S5.4). The

positive correlations between species suggest synergistic relationships and possibly preferences for similar growth conditions, contamination patterns, or surrounding environments (Yang et al., 2023a). The analysis based on culture-independent approach identified multiple clusters with species of the genera *Psychrobacter*, *Janthinobacterium*, *Pseudomonas*, *Acinetobacter* and *Pantoea* at the centre (Fig. 5.5). Spoilage-associated microorganisms such as *Carnobacterium* and *Lactilactobacillus* co-occurred with Gram-negative organisms (Fig. 5.5 and Fig. S5.4). Most *Pseudomonas* species correlated with others, implying the synergistic inter-species interactions in the meat processing environment. *Janthinobacterium* displayed positive correlations with *Serratia liquefaciens*, *Pseudomonas* and *Pedobacter* species (Fig. 5.5). Co-occurrence patterns among several novel species imply their unique ecological roles. The network analysis based on 16S rRNA genes identified three clusters: one large cluster and two smaller ones (Fig. S5.4), and only partially overlapped with the species level interactions (Fig. 5.5).

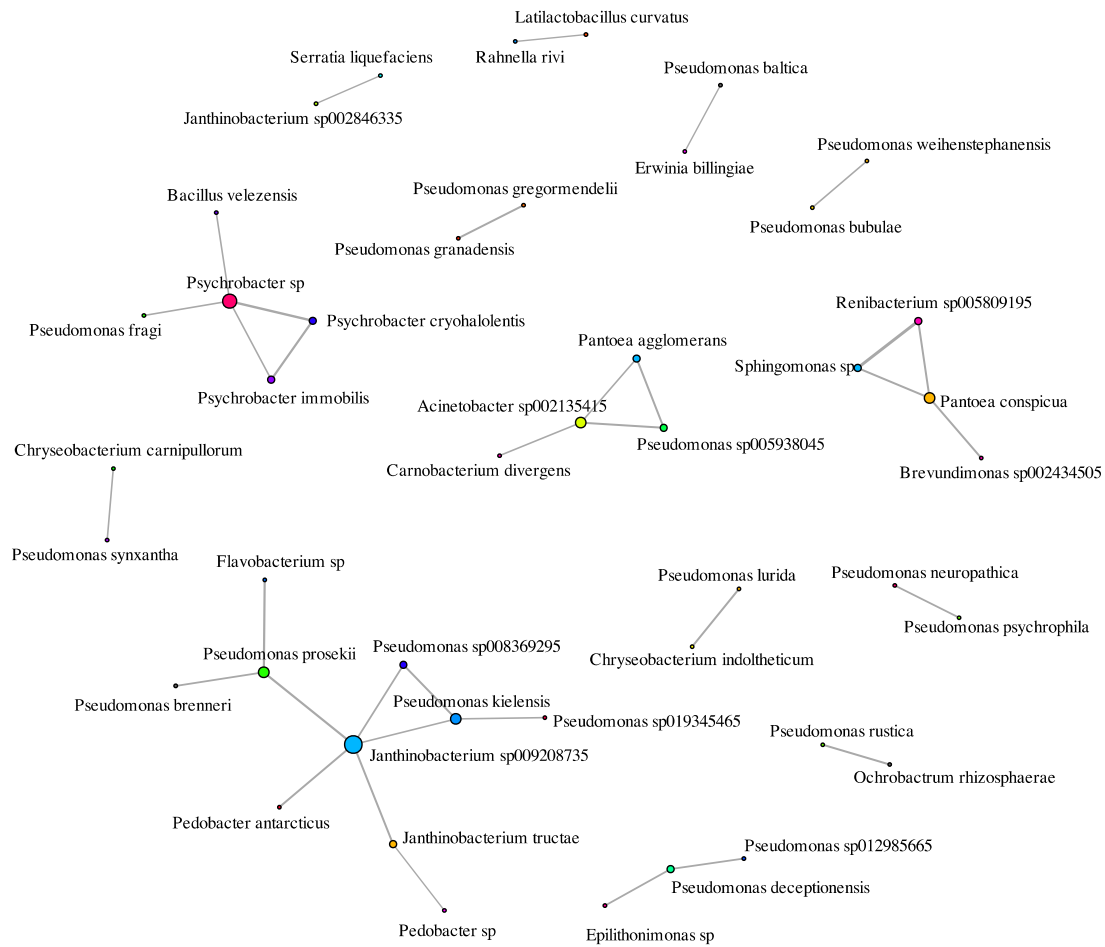


Figure 5.5. Bacterial coexistence network based on the microbial communities across 66 surface samples and 4 meat samples, comprising 1281 isolates classified by genome sequencing. Bacterial species with one-time occurrence among all sampling surfaces were not included. Nodes are colored at species level. The network connections are determined using Spearman correlation test. Only correlations with a significance level of $P < 0.0001$ and a coefficient of ≥ 0.5 are included.

Biofilm formation

To determine the ability of the microbial communities to form biofilms, we reconstituted isolates of 10 sampling sites to obtain communities with 5 – 15 species. All microbial communities formed

biofilms with a crystal violet absorption ranging from 0.4 to 2.4 after 6 d incubation. Microbial communities from stored meat showed weakest biofilm formation (Fig. 5.6A). Multi-species biofilms had a significantly higher biomass at 4°C than at 25°C, except for mixed cultures from the clean drain (Fig. 5.6E). The highest biomass (2.40 ± 0.29) occurred in a sample grown at 4°C (Fig. 5.6K).

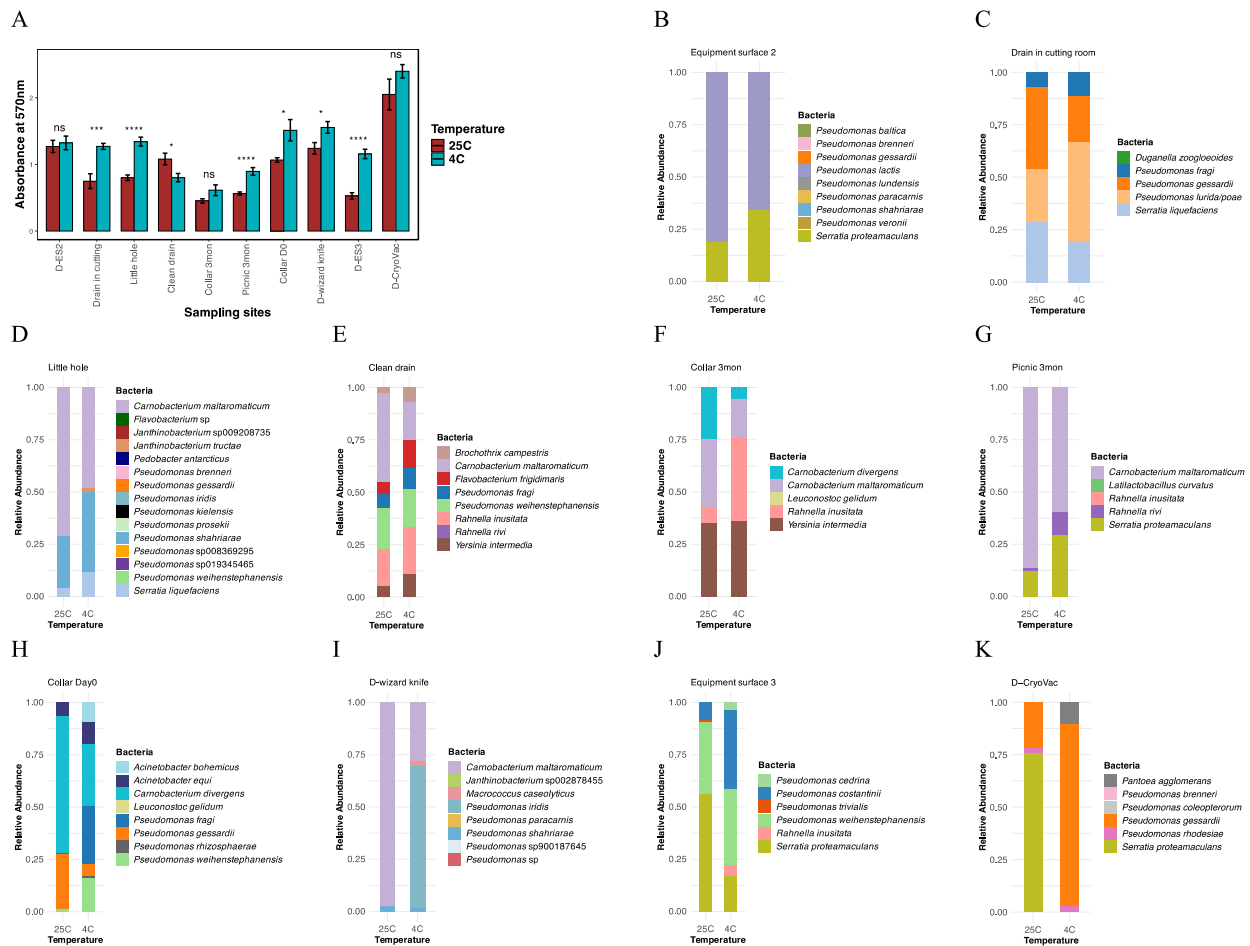


Figure 5.6. Quantification of the biomass (A) and composition of the microbial community (B) of biofilms that were reconstituted with isolates from 10 sampling sites. Multi-species biofilms were grown at 4°C and 25°C in LBNS broth for 6d before staining with crystal violet and accessing growth. Bacterial composition of biofilms from four non-food-contact surfaces (B: D-ES2, C:

Drain in cutting room, D: Little hole (Floor trap), E: Clean drain), three meat samples (F: Collar 3mon, G: Picnic 3mon, H: Collar Day0) and three food-contact surfaces (I: D-wizard knife, J: D-ES3, K: D-CryoVac) were evaluated. The experiment was repeated with three biological replicates and mean value of cell counts was used to determine the relative abundance of each taxon. T test was used to determine the biomass difference within each sampling site. Significance levels are indicated as follows: ns ($p > 0.05$), * ($p < 0.05$), *** ($p < 0.001$), **** ($p < 0.0001$).

Temperature altered the biofilm community composition and the type of biofilms. Overall, a high temperature (25°C) favored the growth of *Carnobacterium* species (Fig. 5.6). In contrast, the abundance of *Serratia* species was independent of incubation temperature (Fig. 5.6). *Leuconostoc gelidum* (Fig. 5.6F and Fig. 5.6H), *Lt. curvatus* (Fig. 5.6G), *Duganella zoogloeoidea* (Fig. 5.6C) and *Pedobacter antarcticus* (Fig. 5.6D) were not detected in multi-species biofilms regardless of incubation temperature. Pellicles were formed by the microbial community isolated from fresh meat at 4°C but not at 25°C.

The microbial composition of biofilm examined by culturing and 16S rRNA sequencing revealed agreement on the diversity and abundance. Prevalent genera included *Carnobacterium*, *Pseudomonas*, *Macrococcus*, *Brochothrix*, and *Enterobacteriaceae*, while *Leuconostoc*, *Lactilactobacillus* and *Duganella* was detected with less than 1% abundance (Table S5.4). Of note, *Janthinobacterium* spp. had low abundance in culturing but were the second most abundant genus in a floor trap sample incubated at 4°C. This finding and the high frequency of uncultured *Janthinobacterium* isolates (Fig. 5.2) emphasize the necessity of using different culture conditions to recover this organism.

Strain-level analysis of dispersal within the facility and persistence over time

To identify strain-level dispersal within the facility and persistence over time, we generated core genome phylogenetic trees of all species that were isolated from stored meat samples, i.e. *Carnobacterium*, *Rahnella* and *Serratia* (Fig. 5.7 and Fig. S5.5). Pairwise SNP analysis was then used to identify closely related isolates at the strain level (Tables 5.2 and S5.3). The high relatedness of isolates from fresh and stored meats: 0 – 2 SNPs (Table 5.2), is expected as sampling likely isolated the same strain and thus validates the workflow for genome sequencing and SNP calling.

Table 5.2. Pairwise single nucleotide polymorphisms (SNPs) between genomes of isolates of *C. maltaromaticum* within the same phylogenetic cluster. Strain IDs are color-coded vertically by isolates collected in the first sampling (light blue) and the second sampling (pink), or horizontally based on isolates from meat samples (purple), FCS (red), and NFCS (sky blue).

	SX455	MC12	L6	TC1285	TC1253	P4	P18	P15
SX455*	-							
MC12	38	-						
L6	34	25	-					
TC1285	35	33	34	-				
TC1253	35	1	1	28	-			
P4	35	28	28	33	1	-		
P18	35	<1	<1	<1	1	<1	-	
P15	33	1	1	1	2	1	<1	-
	L3	P16	P1			MC11	TC650	TC966
L3*	-				MC11*	-		
P16	<1	-			TC650	10	-	
P1	<1	<1	-		TC966	8	2	-
	TC922	TC807				TC1275	TC219	
TC922	-				TC1275	-		
TC807	2	-			TC219	<1	-	

* Indicates the reference genome for pairwise SNP comparison among isolates in the same cluster

Figure 5.8 depicts the isolates from various sampling sites that differ in fewer than 10 SNPs on a schematic map of the processing facility. These isolates were considered to represent the same strain. Strains of all of species of interest were isolated at both sampling points (Table 5.2 and Table S5.3). Figure 5.8 thus indicates how spoilage-associated microbes dispersed across environmental surfaces and meat samples at a strain-level. Notably, none of the strains was detected in the killing room, which was sampled only at one site. Isolates of *C. maltaromaticum* from fresh and stored meat samples were closely related to isolates from drain samples in the cooler room, a sanitized conveyor belt, the working table or the vacuum packaging machine (Fig. 5.7 and Fig. 5.8).

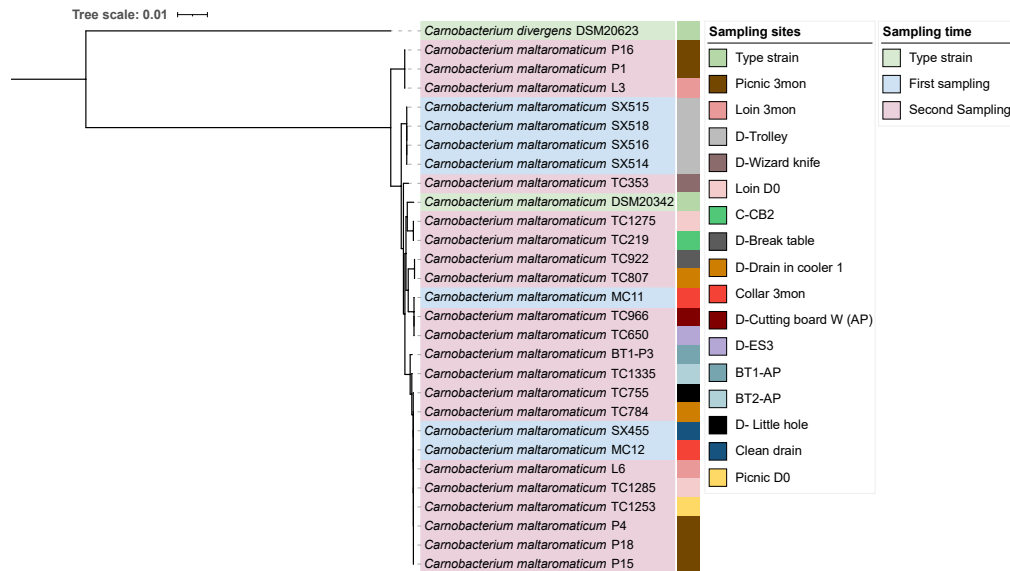


Figure 5.7. Phylogenetic tree of strains of *C. maltaromaticum* based on core genome alignment, utilizing the GTR+I+G4 model with 1000 bootstrap replicates. The tree was rooted with the outgroup, *C. divergens* DSM20263. Strains are color-coded based on sampling time or type strain (clades) and 16 sampling sites (color legend). The type strain *C. maltaromaticum* DSM 20342 was utilized for tree visualization.

Isolates of *C. divergens* from the same meat sample pre- and post-storage were identical (0 SNP) and matched other environmental isolates, which has persisted over 6 months regardless of sanitation measures (Fig. S5.5A and Table S5.3). Different strains of *C. divergens* dispersed across various environmental surfaces in the packaging area. For example, isolates from the conveyor belt (D-T5) differed by fewer than 4 SNPs from those on the equipment surface (ES3), quality control table, shrink tunnel, and working table (Fig. 5.8).

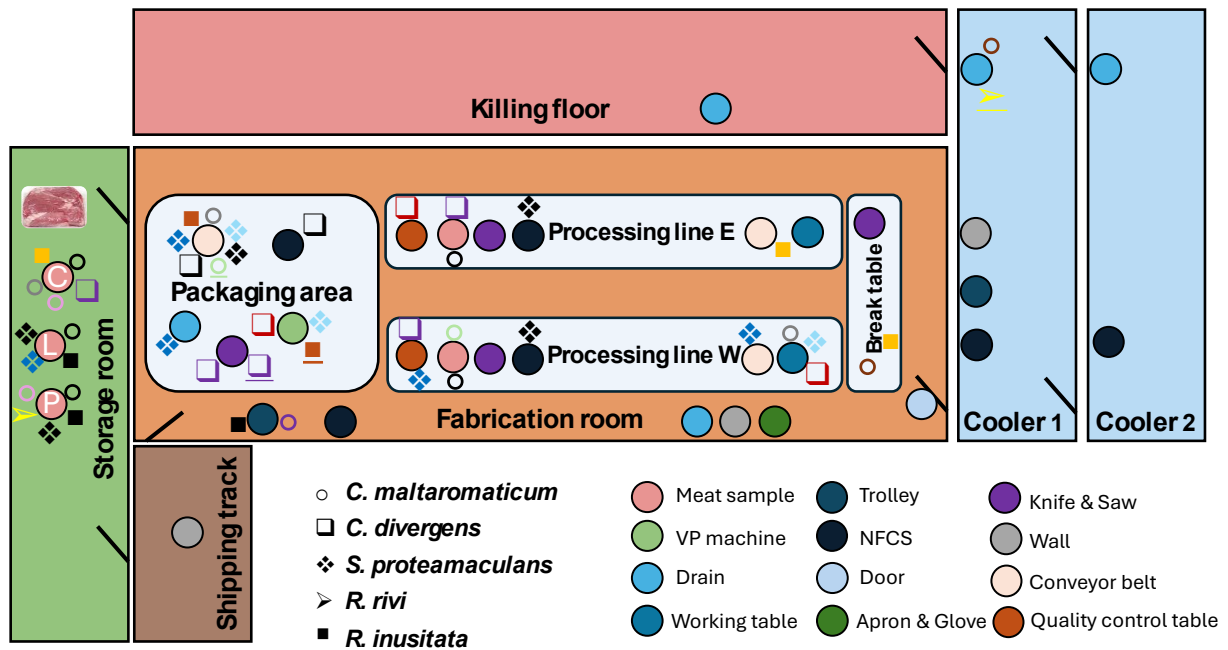


Figure 5.8. Distribution of meat-spoilage associated isolates across various sampling sites from the meat processing facility. The symbols represent different bacterial species: *C. maltaromaticum* (○), *C. divergens* (□), *S. proteamaculans* (◇), *R. rivi* (➤) and *R. inusitata* (■). Underlined symbols denote isolates collected after cleaning and sanitation. Only isolates with fewer than 10 SNPs are shown. Isolates of the same strain dispersed across the facility are labeled with the same color symbols.

One drain isolate of *Rahnella rivi* collected post sanitation during the first time sampling differed by 3 SNPs from isolates identified in the stored picnic sample from the second sampling. Meat isolate, *Rahnella inusitata* MC41 from the first sampling differed by 3 or fewer SNPs from isolates collected from the conveyor belt and the break table in the second sampling. One isolate of *R. inusitata* from D-tray (TC1041) transmitted to other stored meat samples (<2 SNPs).

Isolates of *Serratia proteamaculans*, differed by 2 SNPs, were found among meat isolates, NFCSS like quality control tables and drains, and FCSs such as conveyor belts (D-CB#2) over a period of six months (Table S5.3). Two isolates that were collected from the same sampling site (D-ES3) over a period of six months differed by 2 SNPs. These isolates also differed by fewer than 5 SNPs from an environmental isolate from D-ES2 (NFCSS of the CryoVac machine) and the CryoVac machine (D-T5). Taken together, meat isolates of *C. maltaromaticum* and *R. rivi* mainly originated from the drain area in cooler room while meat isolates of *C. divergens* and *S. proteamaculans* dispersed and persisted both food contact and non-food contact surfaces in the packaging area.

5.3 Discussion

High-throughput culture-dependent and culture-independent analysis of microbiome dynamics in the meat processing facility. Sequence-based approaches are fast, affordable and also accounted for microbes that occur in low abundance or are difficult to cultivate. However, 16S rRNA amplicon sequencing typically characterizes bacterial communities at the genus level and is subject to biases introduced by DNA extraction and PCR amplification (Laursen et al., 2017). In addition, DNA based analyses do not differentiate between viable and dead cells (Ruan et al., 2024; Wuyts et al., 2018), which is particularly relevant for post-sanitation surfaces. Metagenomic sequencing, on the other hand, is constrained by the limitation of current reference databases, and by contamination in low-biomass samples (Kennedy et al., 2023). Culture-based methods used to

identify bacteria in food processing facilities focused on foodborne pathogens and employed selective media to enumerate or isolate *Listeria monocytogenes*, *E. coli* O157:H7, and *Salmonella* (Arthur et al., 2014; Ferreira et al., 2011).

We employed a high-throughput culture-based approach in combination with sequencing of full length 16S rRNA gene amplicons. Complementing this high-throughput culture-based approach with genome sequencing enabled us to characterize isolates at the strain level and thus to identify their persistence and dispersal in the facility. The culture-independent approach identified significantly more bacterial taxa, with the exception of *Janthinobacterium* and *Dellaglioia*; however, dominant taxa identified by sequencing were also detected by the culture-dependent methods. *Janthinobacterium* species was isolated from the drains of a food processing facility (Fox et al., 2014) and spoiled MAP-packaged broiler meat (Lauritsen et al., 2019). *Dellaglioia* species have been identified in various meat samples (Cauchie et al., 2020; Hultman et al., 2020; Jääskeläinen et al., 2016; Pothakos et al., 2014) but their role in spoilage is unclear. Knowledge on this organism is limited because culture media for cultivation of *Dellaglioia* spp. were published only in 2024 (Werum and Ehrmann, 2024). Conversely, 41 genera that were identified by culture represented fewer than 1% of the total sequencing reads. Therefore, obtaining cultured isolates is essential to expand the database of reference genomes and for subsequent physiological characterization as documented by high-throughput culture-based analyses of the gut microbiome (Forster et al., 2019; Zou et al., 2019), plant roots (J. Zhang et al., 2021) and marine samples (Joint et al., 2010). Taken together, the combination of both sequence-based and culture-based method is necessary to accurately represent the structure of the microbial communities in food processing facilities.

Microbial diversity in the meat processing facility. The meat processing facility harbored diverse microbial communities which includes 71 bacterial taxa that were not previously cultured or characterized. Isolates with high abundance and occurrence include representatives of genera that were frequently found within the meat processing environment such as *Pseudomonas*, *Acinetobacter*, *Psychrobacter*, and *Flavobacterium* which are also considered to spoil fresh meat (Xu et al., 2023a). Common representatives on vacuum-packaged meat, such as lactic acid bacteria (*Carnobacterium*, *Leuconostoc* and *Lactilactobacillus*), *Brochothrix* and *Enterobacteriaceae* (*Serratia*, *Rahnella*, and *Hafnia*), were also found on environmental surfaces in the meat processing facility. Animal-associated microbes such as *Clostridium*, *Clostridioides*, *Escherichia*, *Prevotella*, *Bacteroides*, and *Treponema* (Quan et al., 2020), were absent in both meat and environmental surface samples, supporting the prior conclusions that core microbiome across different food communities primarily originates from the processing facilities rather than the respective raw materials (Xu et al., 2023a).

Meat spoilage-associated microbes are prevalent in the reconstituted biofilm communities. Reconstruction of model communities allows for a deeper understanding of microbial interactions in biofilm consortia (O'Toole, 2024; Shayanthan et al., 2022). Biofilms provide an ecological niche for bacterial co-existence and co-operation and protect microbes against routine cleaning and sanitation, thus supporting persistence (Alvarez-Ordóñez et al., 2019; Sadiq et al., 2023). Past studies have predominantly focused on biofilm formation in single- and dual-species, with only a few recent studies investigating bacterial interactions and composition in the reconstituted multi-species biofilms of environmental isolates, typically within an incubation temperature range of 7°C to 15°C (Fagerlund et al., 2017; Langsrud et al., 2016; Rolon et al., 2024; Sadiq et al., 2023; Wang et al., 2024). We documented the ability of environmental isolates to form biofilm at

refrigerated temperature (4°C). The ability of forming biofilms at refrigerated temperature increases risks associated with psychrotrophic pathogens, such as *L. monocytogenes*. We also observed that one microbial community formed surface-attached biofilms at ambient temperature but floating pellicles at refrigeration temperature. Pellicle formation in *Acinetobacter baumannii* and *Pseudomonas aeruginosa* is associated with cyclic diguanylate (c-di-GMP) (Ahmad et al., 2020; Li et al., 2012), whose signal transduction is temperature-dependent (Almblad et al., 2021). The switch of biofilm phenotypes also depends in inter-species communication (Xu et al., 2023b). Thus, the collection of isolates also allows further comprehensive research on microbial interactions and resistance to sanitation of biofilm-embedded microbes.

Strain-level characterization of dispersal within the facility and persistence over time. Past studies on strain-level bacterial persistence in food processing facilities focused on pathogens (Arthur et al., 2014; Estrada and Harris, 2024; Yang et al., 2017a), documenting strain-level persistence over a period of 17 years (Harrand et al., 2020). In investigations of foodborne outbreaks, a threshold of 21 SNPs is widely used for strain-level identification (Pightling et al., 2018). Most studies on persistence of *Listeria* in food processing facilities used the same SNP threshold [40–44]. However, *L. monocytogenes* evolved in a cold-smoked salmon processing facility with a mutation rate of only 0.35 SNPs per genome per year (Harrand et al., 2020). In addition to the environmental conditions including nutrient availability or environmental stress, the bacterial mutation rate depends on the bacterial species and the time of observation (Kuo and Ochman, 2009). The SNP threshold for strain-level identification thus depends on the context. The cut-off of 21 SNPs is supported by tens of thousands of sequenced genomes in outbreak investigations (Pightling et al., 2018) but such calibration data is unavailable for persisting spoilage

microbes. We thus used a conservative SNP threshold of 10 SNPs, three times higher than the number of false positives of the SNP calling workflow, to achieve strain-level identification.

Meat processing facilities are exposed to a constant influx of bacteria from animals, water, air, and workers. Colonization by external microbes and persistence are determined by dispersal and selection, respectively (Vellend, 2010). Bacterial dispersal can be limited by control of incoming bacteria from animals, air, water and employees while the persistence of bacteria is determined by nutrient availability, resistance to cleaning and sanitation as well as biofilm formation (Xu et al., 2023a). Our study indicates that microbes dispersed spatially across surfaces and meat samples within the facility and persisted over 6 months. Our data together with literature data on persistence of *L. monocytogenes* indicates that microbial persistence in food processing facilities is the rule rather than an exception. The packaging area and floor drains in the cooler emerged as "hotspots" for bacterial persistence and subsequent transmission to meat samples. Common hypotheses to explain persistence includes biofilm formation, stress resistance and inappropriate design of facilities and equipment (Ferreira et al., 2014). The product flow, movement of air and workers, and cleaning and sanitation measures, e.g. high-pressure cleaning of floor drains which creates aerosols (Saini et al., 2012), constitute mechanisms of bacterial dispersal in food processing facilities.

In conclusion, despite the development and feasibility of culture-independent sequencing approaches in studying microbial ecology and diversity, Robert Koch's assertion that "a pure culture is the foundation of all research" remains relevant (Thomas D. Brock, 1999) when appropriately complemented with sequenced-based tools. The combination of high-throughput culture-dependent and culture-independent methods captured the diversity of microbes and demonstrated bacterial persistence in the processing facility. This finding provides evidence that

food processing facilities are an establishment niche for spoilage bacteria, and food-borne pathogens. The prevalence of spoilage-associated isolates in synthetic biofilm communities suggests that biofilm formation contributes to persistence within the facility. These findings enhance our knowledge on source tracking of microbial food spoilage and promote the development of improved intervention strategies in food processing facilities.

5.4 Materials and methods

Sampling strategy

The sampling plan was conducted in an Alberta pork processing facility producing packed fresh pork with a shelf life of three months for overseas shipment. Sampling activities were carried out in September 2022 and March 2023 (Fig 5.9), in various rooms such as kill floor (15°C), cooler (-3°C to -1°C), fabrication room (1°C to 4°C), storage room (1°C), shipping truck (1°C) and packaging area (1°C). To investigate as many different sites as possible at different conditions and how the microbial composition overlaps with meat productions, sampling was performed on both non-food-contact surfaces (NFCS) and food-contact surfaces (FCS) during operation hours, after cleaning and disinfection, and after production. Meat samples were obtained directly from the production line and swabbed. Subsequently, meat samples were vacuum-packed and stored at 1°C for a duration of three months, reflecting the anticipated shelf life, prior to sample collection. In total, 14 NFCS, 30 FCS and 2 meat samples were collected during the first sampling, while 32 NFCS, 37 FCS and 4 meat samples were collected during the second sampling. A standardized surface area of approximately 600 cm² was swabbed using pre-moistened Whirl-Pak® Speci-Sponge® Environmental Surface Sampling Bag (Sigma Aldrich, St. Louis, USA). All sponge samples were kept in a bag at 4°C for further processing within 24 h.

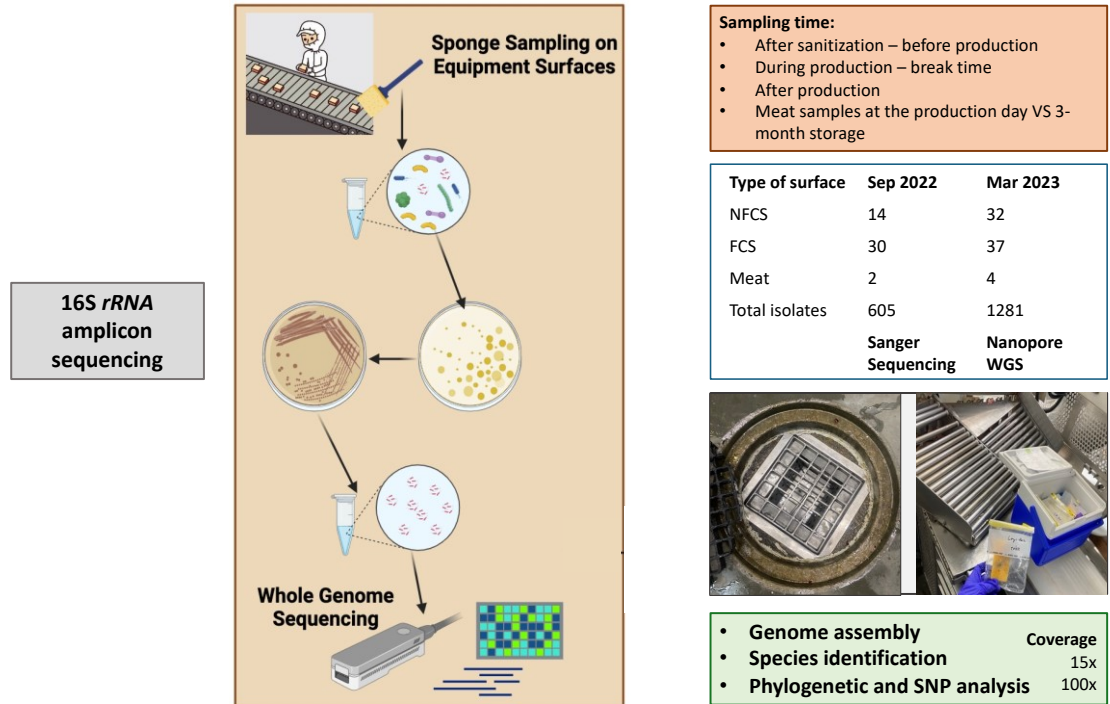


Figure 5.9. Sampling strategy and experimental workflow.

Bacterial isolation and DNA extraction

To each sponge sample, 10 ml of 0.1% peptone water was added. The sponge sample was massaged from outside the bag for 2 min to homogenize (Yang et al., 2021) . The swab fluid was diluted and plated on Plate Count agar, All Purpose Tween agar and VRBG agar to enumerate total aerobic bacteria, lactic acid bacteria and coliforms, respectively. Plates were incubated at 25°C for 72 hours for cell counts determination and colony isolation. A total of 9 sponge samples were not detected with any bacteria (6 samples from first time sampling and 3 samples from second time sampling), and thus only 40 samples from the first time sampling and 70 samples from second time sampling were included for both culture-based and culture-independent analysis.

To characterize the isolates, 2-5 representative colonies for each distinct morphology was streaked on corresponding plates. The number of colonies streaked was equal to or exceeded the square

root of the total number of colonies on the plate. Repeated streak was performed until a uniform colony morphology was achieved. The number of isolates for each sample ranged from 6 to 35. Isolates were subcultured into liquid medium to prepare for DNA extraction and frozen culture stocks of 30% glycerol and stored at -80°C. Five and three low-biomass surfaces did not yield any culturable isolates during the first and second sampling, respectively (Table S1). Genomic DNA of each isolate was extracted using the Qiagen Blood & Tissue Kit (Qiagen, Hilden, Germany) following the manufacturer's protocol for Gram-positive bacteria. DNA concentration and purity were assessed using the NanoDrop spectrophotometer (Thermo Fisher Scientific). Clonal isolates within each sponge sample were determined by Random Amplified Polymorphic DNA PCR using Rep5 primer (GTG GTG GTG GTG GTG). PCR was performed with genomic DNA as the template in a reaction volume of 25 ul containing 1 ul genomic DNA, 12.5 ul DreamTaq Master Mix, 1ul 50 mM MgCl₂, 1ul 100 nmol Rep5 primer. Thermocycler conditions were set to: 1 min of incubation at 96°C; 3 cycles of 3 min at 96°C, 5 min at 35°C, and 5 min at 75°C; and 32 cycles of 1 min at 96°C, 2 min at 55°C, 3 min at 75°C, and 2 min at 75°C. RAPD PCR products were separated on 1% agarose gel (60V, 2.5h) and were visualized by UV transillumination after staining with SYBR Safe.

Genome sequencing

To achieve the species identification, isolates from the first sampling were identified based on the 16S rRNA gene by Sanger sequencing. The 16S rRNA gene region was amplified using primers 27F (5'-AGA GTT TGA TCM TGG CTC AG-3') and 1492R (5'- GGY TAC CTT GTT ACG ACT T-3') with the following thermocycler condition: initial denaturation at 95°C for 5 minutes, followed by 30 cycles of denaturation at 95°C for 30 seconds, annealing at 60°C for 10 seconds, and elongation at 72°C for 90 seconds, with a final extension step at 72°C for 10 minutes. PCR

products underwent gel electrophoresis (1.5%) for quality control and were subsequently purified using the Qiagen QIAquick PCR Purification Kit (Qiagen, Hilden, Germany) before Sanger sequencing. Forward and reverse nucleotide sequences were manually inspected and corrected using SnapGene viewer, followed by alignment using EMBOSS prior to blasting against the NCBI database and RDP classifier training set No. 19 to achieve species-level taxonomic assignment (Wang and Cole, 2024).

For isolates obtained in the second sampling, the protocol for sequence-based identification was modified owing to advances in the Oxford Nanopore Whole Genome sequencing platform. DNA concentration was re-assessed using the dsDNA broad-range assay kits for the Qubit 4 fluorometer (Thermo Fisher Scientific, Schwerte, Germany). The protocol started with 450 ng input DNA per isolate. DNA library was prepared following the protocol of Native Barcoding Kit 96 V14 (SQK-NBD114.96) and loaded onto R10.4.1 MinION flow cell. Raw data were basecalled by Guppy basecaller and genome was assembled by following the nextflow epi2me/wf-bacterial-genome workflow. The genome coverage ranges from 5 - 70, with a mean coverage of 18 among 1052 sequenced genomes. Taxonomy classification was determined by Genome Taxonomy Database Toolkit (GTDB-Tk v2.4.0) based on Genome Taxonomy Database (Chaumeil et al., 2022).

Additionally, microbial composition and diversity of each meat and environmental sample were analysed by Nanopore full length 16S rRNA gene sequencing. One ml of sponge swab fluid was used to extract the community DNA using the DNeasy Blood & Tissue kit, following the manufacturer's instructions for extracting DNA from Gram-positive bacteria. Three negative extraction controls without any bacterial pellets were also included. The quality and quantity of the extracted DNA was determined using a Nanodrop spectrophotometer. In total, 42 out of 46 sponge samples collected in September 2022 were sequenced targeting at full-length 16S rRNA

gene, while 66 out of 70 collected in March 2023 were processing. Low biomass samples, collected after cleaning and sanitation, resulted in unprocessed samples for 16S rRNA sequencing. DNA libraries were prepared using the 16S Barcoding Kit 1-24 (SQK-16S024) protocol and sequenced on R 9.4.1 Flongle flow cells. Raw data were basecalled by Guppy basecaller, with the use of model "dna_r9.4.1_450bps_hac". Subsequently, epi2me-labs/wf-16Ss workflow was used to blast against "ncbi_16s_18s" database and only read length between 1200 - 1800 bp were kept for taxonomy classification.

Biofilm formation

Ten sites which includes *Carnobacterium* and *Serratia* species were chosen to reconstitute multiple-species biofilms and assess their microbial community composition and biofilm formation. Frozen (-80°C) stock cultures of bacterial isolates were streaked onto Luria–Bertani agar plates and incubated in a 25°C incubator for 48 hours, followed by subculture in Luria–Bertani without NaCl (LBNS) broth at 25°C for an additional 48 hours without agitation. A preliminary assessment was conducted to optimize biofilm formation over 2, 4, and 6 days, with the most robust biofilm formation observed after 6 days of incubation. To simulate the meat processing environment, multispecies biofilms were cultivated on food-grade stainless steel coupons (grade 304, No.4 finish, 12 mm diameter; Stanfos, Edmonton, AB, Canada) at both 4 and 25 degrees, following the established protocol (Z. S. Xu et al., 2021). Briefly, overnight cultures of each isolate were standardized to ensure equal bacterial populations. One ml each standardized overnight culture was then combined together and mixed by vortexing to create an overnight culture cocktail. This cocktail was then diluted 100-fold in 2 mL of LBNS suspension. Stainless steel (SS) coupons were placed into the bottom of a 24-well flat-bottom cell culture plate (Corning, Glendale, Arizona) and the 2ml diluted bacterial suspension was transferred into each well. The

plate was incubated at 4°C and 25°C for 6 days. After 6 days of incubation, biofilms grown on SS coupons were harvested and used for cell counts determination and biomass quantification. Cell counts were determined after gently washing of the coupons to remove loosely attached planktonic cells. Biofilm-embedded cells were detached by vortexing with glass beads at maximum speed for 1 min. One ml of detached-biofilm suspension was used for differential cells counts of each isolate based on their bacterial morphology on LB agar, APT agar and *Yersinia* selective agar, and the other aliquot (1 ml) was used for DNA extraction and Nanopore 16S full length sequencing, as described above. Biofilm biomass was quantified with crystal violet staining by following the established protocol (Z. S. Xu et al., 2021) and measured as absorbance at 570 nm using plate reader (Varioskan Flash, Thermo Fisher Scientific). Three independent experiments with technical duplicates were conducted (n = 3) for microbial composition determination and biofilm biomass quantification.

Phylogenetic and single nucleotide polymorphism (SNP) analysis

Phylogenetic analysis was conducted on all isolates of species that were isolated from meat after 3-month of refrigerated storage, including *Carnobacterium maltaromaticum*, *Carnobacterium divergens*, *Rahnella rivi*, *Rahnella inusitata* and *Serratia proteamaculans*. Sequencing libraries with the Nanopore Native Barcoding Kit V14 on the Nanopore MinION R10.4.1 flow cell aimed to achieve a 100-fold to 200-fold higher coverage. Raw data in pod5 format were subset to extract information on read ID and channel using the Pod5 package v0.3.10 (available at <https://github.com/nanoporetech/pod5-file-format>). Subsequently, data were basecalled by Dorado basecaller (available at <https://github.com/nanoporetech/dorado>) with the basecalling model of dna_r10.4.1_e8.2_400bps_sup@v4.3.0 and demultiplexed by dorado demux to achieve per barcoded groups. The barcoded sample was basecalled using Dorado duplex. Basecalled reads

were filtered by Chopper (Nanopack) (De Coster and Rademakers, 2023) to retain those with a quality score of at least 20 and a read length of at least 500bp. Porechop_ABI v0.5.0 (Bonenfant et al., 2023) was employed to trim adapter sequences and enhance quality. Read quality was assessed after filtering and adapter trimming using the FastQC program (available at <https://www.bioinformatics.babraham.ac.uk/projects/fastqc/>). Post-QC reads were *De novo* assembled using Flye v2.9.3 (Kolmogorov et al., 2019) with 0.03 read error rate and polished with Medaka v1.11.3 (available at <https://github.com/nanoporetech/medaka>). Prokka v1.14.5 (Seemann, 2014) was used for genome annotation and core genome was aligned by Roary (Page et al., 2015), with the minimum percentage identity for Blastp set at 90%. The aligned sequences were further filtered through TrimAL v1.2 (Capella-Gutiérrez et al., 2009). A Maximum likelihood (ML) phylogenetic tree was constructed based on the core gene alignment using RAxML-NG v1.12.1 (Kozlov et al., 2019). ModelTest-NG v0.1.7 (Darriba et al., 2020) was employed to predict the best nucleotide substitution model and bootstrap replicate values. The resulting phylogenetic tree was visualized using iTOL (Letunic and Bork, 2021) and refined by Inkscape.

FastANI (v1.34) was used for whole-genome pairwise alignment (Jain et al., 2018) and only isolates with over 99.90% ANI value were taken for SNP analysis (Rodriguez-R et al., 2024). Firstly, post-QC reads underwent mapping against assembled reference genome with Minimap2 via the `epi2me-labs /wf-alignment` workflow. Subsequently, SNPs were called using variant caller Clair3 v1.0.7 (Zheng et al., 2022). Additional parameters were configured to tailor the SNP calling process: All contigs were considered in the analysis. Phasing by Whatsp was omitted during full alignment calling. Haploid mode was enabled, wherein only the presence of 1/1 was regarded as indicative of a variant. Lastly, only candidates passing SNP minimum allele frequency (AF) threshold were considered, while indel candidates were ignored. Output results were visualized on

Integrative Genomic Viewer (IGV 2.17.2) and manually checked to eliminate false positive variants. The criteria for elimination were as follows: i) indels are eliminated, ii) a quality score of at least 2, iii) a variant distance bias of at least 0.00001 (Hall et al., 2023). Pairwise SNP matrix table was generated using the CFSAN SNP pipeline (Davis et al., 2015).

Statistical analysis

Data visualization and statistical analysis were performed in R environment (version 4.3.1). Bacterial diversity was assessed using permutational multivariate analysis of variance (PERMANOVA, 999 permutations, *adonis2* function, *vegan* package, R v4.3.0) based on the Bray-Curtis dis-similarity of bacterial communities with an error probability of 5% ($p \leq 0.05$) to determine whether sampling areas from different type of surfaces, location, sanitation activity and zones harbored different communities of microbes. The data were visualized by principal coordinate analysis (PCoA). Pairwise comparisons between groups were tested by the ‘pairwise.adonis’ function (*pairwiseAdonis* package, v0.4.1) with Bonferroni adjustment for multiple comparisons. Prior to spearman's rank analysis, samples with significantly fewer reads than the average were excluded. Data were then rarefied into the minimum total reads using *vegan* package. Spearman's rank correlation was performed to infer the co-occurrence of bacterial isolates with the use of *psych* package. The correlation with p value less than 0.01 and absolute value coefficient > 0.5 was considered as significant. The microbial network analysis was then created and visualized using *igraph* package. T test was used to determine the significant difference in biomass of each sampling site between growth condition at 25°C and 4°C.

Chapter 6. Ozone Nanobubble for Meat Spoilage Control

6.1 Introduction

Food waste represents a considerable global challenge. The United Nations estimates that 17% of global food production is wasted, with meat accounting for over 20% of this loss (FAO, 2015; United Nations, 2023). Microbial meat spoilage can occur during transportation, processing, or storage, often resulting in the product reaching its expiry date before sale or consumption. Extending the shelf life of meat products is therefore a critical objective.

To control food pathogens and spoilers on meat surfaces after slaughtering, antimicrobial spraying is approved by Canada and US (Hauge et al., 2023) and widely used in meat processing plants. Commonly used antimicrobial solutions include organic acids such as lactic, acetic, citric, peracetic acid, as well as chlorine-based compounds such as sodium hypochlorite (Government of Alberta, 2013). Peracetic acid and chlorine products are especially common due to their high efficacy and low cost (Freitas et al., 2021). However, peracetic acid poses significant risks due to its corrosive nature, potential to cause chemical burns, and fire-promoting properties (National Center for Biotechnology Information, 2024). Moreover, the effectiveness of these traditional methods is often limited by high organic load in meat matrices and therefore rapid development of microbial resistance (Martínez-Suárez et al., 2016; Mercer et al., 2015).

In recent decades, there has been growing interest in using ozone in the food industry, driven by consumer demand for more environmentally friendly food additives. Ozone is acknowledged as Generally Recognized As Safe (GRAS) in 1995 in the United States for the purpose of disinfecting bottled water. By June 2001, the US Food and Drug Administration (FDA) had approved ozone, in both its gaseous and aqueous forms, as an antimicrobial agent for direct application on foods,

including meat products (Rice et al., 2002; Xue et al., 2023). Its antimicrobial effectiveness is due to its strong oxidizing capacity, which inactivates microorganisms by progressively oxidizing cell components (Korany et al., 2018). Ozone's high instability and reactivity, which cause it to rapidly degrade back to molecular oxygen without leaving toxic by-products, also limit its residual action against bacteria due to its instability and short lifespan in water. This limitation can be mitigated by combining ozone with nanobubble technology.

Nanobubbles are nanometer-sized gaseous cavities in a liquid solution (Seridou and Kalogerakis, 2021). Unlike ordinary macro and micro-sized bubbles, which have larger diameters and rise quickly to the surface of an aqueous solution, nanobubbles remain in liquids for an extended period (Thi Phan et al., 2020). Fine and ultrafine bubbles can be generated through various methods, with hydrodynamic cavitation being the most frequently used (Javed et al., 2023). Factors such as temperature, applied pressure, and the type of dissolved gas influence both the stability and generation of nanobubbles (Soyluoglu et al., 2023). Traditional aqueous ozone consists of macro and micro-sized bubbles that are irregularly shaped and uniform in size, leading to quick breakdown and ineffective cleaning (Sarron et al., 2021). In contrast, ozone nanobubble technology provides a stable solution with a high concentration of dissolved ozone in the form of nanobubbles, ensuring uniform surface coverage and improved antimicrobial efficacy.

Several studies have explored the effects of ozone nanobubble solutions on food products. For example, ozone nanobubble treatment resulted in a 1-log reduction of *Listeria monocytogenes* on the surfaces of apples, celery, and lettuce, without affecting the color of the fresh produce (Upadhyay, 2021). Additionally, parsley washed with ozone nanobubble solutions exhibited increased firmness and reduced weight loss (Shi et al., 2023). In freshwater applications, ozone nanobubbles significantly lowered the bacterial load of the fish pathogen *Aeromonas veronii* while

maintaining the safety of Nile tilapia (Dien et al., 2021). The current study aims to fill gaps in the literature by further exploring the application of ozone nanobubble technology in controlling microbial spoilage in meat products. By addressing the limitations of traditional disinfection methods and leveraging the benefits of nanobubbles, this research seeks to enhance meat safety and extend shelf life, ultimately contributing to a reduction in food waste and improved food safety.

6.2 Materials and methods

6.2.1 Strain and culture conditions

Strains, their origin and growth conditions are shown in Table 6.1. Seven meat-spoilage-associated strains were used in this study. Frozen ($-80\text{ }^{\circ}\text{C}$) stock cultures of each microorganism were streaked on All Purpose Tween (APT) agar plates and incubated at corresponding conditions for their optimal growth (Table 6.1). APT agar supplemented with streptomycin was used to selectively culture *Brochothrix thermosphacta* A401. *Carnobacterium maltaromaticum* A404 was cultured on mCTAS agar. Both *Lactobacillus sakei* and *Leuconostoc gelidum* were grown on MRS agar (Sigma-Aldrich, St. Louis, MO, USA) supplemented with vancomycin, with different incubation temperatures to differentiate their growth. *Yersinia* selective agar was employed to distinguish Gram-negative bacteria based on cell morphology.

Table 6.1. Strains used in this study.

FUA number	Strain name	Resources	Growth condition	Selective media
3558	<i>Brochothrix thermosphacta</i> A401	Retail meat isolate	APT broth, 25 °C, aerobic	APT agar supplemented with streptomycin
3559	<i>Carnobacterium maltaromaticum</i> A404	Retail meat isolate	APT broth, 30 °C, aerobic	mCTAS agar
3560	<i>Leuconostoc gelidum</i> C202	Retail meat isolate	APT broth, 25 °C, anaerobic	MRS agar supplemented with vancomycin
3561	<i>Leuconostoc gelidum</i> ssp. <i>gasicomitatum</i> A209	Retail meat isolate	APT broth, 25 °C, anaerobic	MRS agar supplemented with vancomycin
3562	<i>Latilactobacillus sakei</i> B310	Retail meat isolate	APT broth, 30 °C, anaerobic	MRS agar supplemented with vancomycin
1497	<i>Yersinia rohdei</i> 47	Ground beef	APT broth, 37 °C, aerobic	<i>Yersinia</i> selective agar
1451	<i>Hafnia paralvei</i> 1	Ground beef	APT broth, 37 °C, aerobic	<i>Yersinia</i> selective agar

6.2.2 Sample preparation and inoculation

Fresh vacuum-packaged pork meat was purchased from a local grocery store. Upon unpacking, the meat was dried, and superficial excess fat and tendons were removed. The meat was then stored in a freezer until it was semi-frozen to facilitate the cutting process. Once frozen, samples with a diameter of 2 cm were cut using a circular cutter and trimmed to a height of 1.5 cm, resulting in a surface area of 15.7 cm². Given the natural variability in meat consistency, efforts were made to ensure uniformity in sample texture and structure. For adipose tissue samples, the skin was removed, and square samples with a side length of 2 cm and a thickness of 0.5 cm were prepared, yielding a surface area of 12 cm². All samples were stored at -20°C until further use.

Overnight cultures of each of the seven validated bacterial strains were prepared. From these cultures, a mixture cocktail was created to achieve final concentrations of 10² CFU/mL and 10⁴ CFU/mL. To verify the concentration of each strain in the overnight cultures, an OD600 measurement was performed using a Vis/UV-Vis Spectrophotometer (GENESYS™). Prior to inoculation, the pre-prepared meat samples were defrosted, sterilized by spraying with 100% ethanol, and flamed multiple times to ensure sterility. It was experimentally determined that each sample absorbs approximately 0.5 mL of liquid. The culture mix was prepared and appropriately diluted to achieve the desired bacterial concentrations. Samples were then submerged in the culture mix for 1 minute to achieve inoculations of 10² and 10⁴ CFU/cm². To determine the desired sample concentration, the following formula was used:

$$\begin{aligned} \text{Surface area} \times \text{desired sample concentration} \\ = \text{Volume absorbance} \times \text{concentration culture mix} \end{aligned}$$

Example calculation for 10² CFU/cm²:

$$15.7 \times 10^2 \text{ CFU/cm}^2 = 0.5 \text{ mL} \times 10^7 \text{ CFU/mL}$$

$$\rightarrow \quad ? = 3.49$$

Therefore, the inoculation was carried out with a diluted culture mix at a concentration of $10^{3.49}$ CFU/ml to achieve a final concentration of 10^2 CFU/cm² on the sample. After inoculation, the samples were air-dried for 30 minutes in a sterile environment and subsequently handled for further testing.

6.2.3 Sanitizer preparation

Ozone nanobubble solutions were generated using commercial equipment (En solución, Austin, Texas). An ozone concentration of 7 ppm was used for meat treatment and monitored through the dashboard. An ozone colorimeter (MQuant, Billerica, MA) was used to determine the absolute ozone concentration before treatment. To compare the efficacy of the ozone nanobubble solution, two commercial sanitizers were used in this study. These sanitizers were diluted from the following stock: 32% (v/v) peracetic acid in acetic acid (Sigma-Aldrich, St. Louis, MO) and lactic acid (Sigma-Aldrich, St. Louis, MO). The final concentration of the sanitizers was chosen according to their application in the local meat industry. Peracetic acid was diluted to a final concentration of 400 ppm in sterile distilled water, while a final concentration of 4% lactic acid was achieved for treatment.

6.2.4 Efficacy of peracetic acid and ozone nanobubble solutions on inoculated meat samples and adipose tissues at various storage intervals

To evaluate the efficacy of ozone nanobubble solution in comparison to the current application of peracetic acid solution in pork carcass washing, inoculated meat samples (muscle and adipose tissues) were prepared and tested in the following approaches: i) Meat samples were directly

vacuum packaged after inoculation and will be treated after seven days of storage at 12°C; ii) Meat muscle and adipose tissues were treated without packaging and storage to check the efficacy of the treatment; iii) Meat muscle and adipose tissues were treated right after inoculation, vacuum-packaged, and stored at 8°C for 7 weeks. Meat samples were subsequently transferred into sterile 50 mL tubes containing 30 mL of sterile water as control, 30 mL of 400 ppm peracetic acid, or 30 mL of 7 ppm ozone nanobubble solution. The meat sample was then vortexed at the maximum speed for 10s and sit for 50s to achieve 1 minute treatment. Subsequently, meat samples were transferred to a 50ml tube with 2g sterile glass beads and 10 mL of D/E neutralizing broth. The whole content was then vortexed for 1 minute to detach bacteria from meat surfaces. Bacterial suspension was serially diluted, plated on different selective media and incubated accordingly (see Table 6.1). Overall, *Brochothrix*, *Latilactobacillus*, *Hafnia*, and *Yersinia* were incubated for 24h before counting, while *Carnobacterium* and *Leuconostoc* were cultivated for 48 hours.

6.2.5 Impact of flow rate and solution volume on the efficacy of ozone nanobubble solutions

To evaluate the impact of flow rate and volume on the efficacy of ozone nanobubble solutions, meat samples were additionally treated with 500 ml desired solutions at 20 rpm or in a flow pumping system. Briefly, three sterile beakers were filled with 500 mL of sterile water, 400 ppm peracetic acid and 7 ppm ozone nanobubble, respectively. The liquid in beakers were continuously stirred at 20 rpm. Then, samples were held in the beakers with tweezers and kept in for 1 minute, followed by cell count determination, as described above.

In meat processing plants, meat is typically sprayed or rinsed with disinfectants rather than being immersed in them. To simulate a gentle rinsing process, a 'flow system' approach was adopted. A hose pump, calibrated to deliver a constant flow rate of 30 mL/min, was employed to minimize mechanical stress. Prior to treating the meat samples, the hose was flushed with 100% ethanol

followed by sterile water. Each meat sample underwent a 1-minute rinse with sterile water, or solutions containing either 400 ppm peracetic acid, 7 ppm ozone nanobubble solution, or 4% lactic acid. After each treatment, hose was rinsed with sterile water to remove residues from the previously used disinfectant. Care was taken to ensure complete drainage of water from the hose between treatments to not falsify the results. Cell count was determined by following the steps described above.

6.2.6 Determination of microbiota in treated meat under refrigerated vacuum-packaging storage

To evaluate the impact of storage temperature on the efficacy of the different disinfectants, the Day 0 treatment with 30 mL solution was repeated, with additional lactic acid treatment with untreated samples. The samples are then vacuum packaged by Multivac c200 (MULTIVAC, Brampton, Canada) and stored at -1°C for 8 weeks. At 1, 2, 4, and 8 weeks, the samples were collected for cell count determination (described above). Used bags for meat sample are at oxygen transmission rate (OTR) of $52 \frac{cm^3}{m^2 \times 24 h}$ at 0 % relative humidity.

6.2.7 Microbial composition of meat samples collected *in situ*

To evaluate the effect of ozone nanobubble solution on meat sample *in situ*, 4 vacuum packaged primal cuts, 2 pork legs and 2 tenderloins, that were stored at 0 ± 1 °C for shelf-life testing were rinsed with water or ozone nanobubble solution for 2 minutes. After treatment, meat samples were vacuum packaged again and stored at 0 ± 1 °C for 30 d before determination of cell counts and DNA extraction and sequencing.

Upon the end of storage, the entire surface of each meat sample was swabbed using Pre-moistened Whirl-Pak® Speci-Sponge® Environmental Surface Sampling Bag (Sigma Aldrich, St. Louis,

USA). To each sponge sample, 10 ml of 0.1% peptone water was added and massaged from outside the bag for 2 min to homogenize. Microbial composition and diversity of each meat sample was analysed by Nanopore full length 16S gene sequencing. One ml of sponge swab fluid was used to extract community DNA by DNeasy Blood & Tissue kit, following the manufacturer's instructions for extracting DNA from Gram-positive bacteria. One negative extraction control without any bacterial pellets were also included. The quality and quantity of the extracted DNA was determined using a Nanodrop spectrophotometer. DNA libraries were prepared using the 16S Barcoding Kit 1-24 (SQK-16S024) protocol and sequenced on R 9.10.1 Flongle flow cells. Raw data were basecalled by Guppy basecaller, with the use of model "dna_r9.4.1_450bps_hac". Subsequently, the epi2me-labs/wf-16Ss workflow was employed for taxonomic classification, using the "ncbi_16s_18s" database. Only reads with lengths between 800 and 2000 bp were retained, classified to the genus level with at least 95% identity.

6.2.8 Statistical analysis

Mean values for cell count reduction were collected by three biological replicates. T test or one way analysis of variance (ANOVA) was performed to determine the significant difference of various treatment on bacterial cell reduction, with an error probability of 5% ($P < 0.05$) as the threshold for significance.

6.3 Results

6.3.1 Ozone nanobubble solutions displayed comparable efficacy to peracetic acid on inoculated meat samples and adipose tissues at various storage intervals

To compare the efficacy of ozone nanobubble solution in stored meat, fresh meat, and fresh meat after storage with peracetic acid, meat samples including both muscle and adipose tissues were

inoculated with common meat-spoilage microorganisms at 10^2 and 10^4 CFU/cm² to simulate the cell population in real processing environments. Subsequently, cell reduction after ozone or peracetic acid treatment (30ml, 1min) was determined. In one-week stored meat samples, *L. gelidum* and *H. parvalvei* dominated the growth irrespective before and after treatment (Table 6.2). Neither peracetic acid nor ozone nanobubble achieved more than 2 logs cell reduction, while peracetic acid are slightly more bactericidal than ozone nanobubble in stored meat samples. Among meat samples at Day 0, lethal activity was only significantly higher in peracetic acid than that of ozone-treated samples, despite of muscle or adipose tissues (Fig 6.1). However, the difference tended to decrease by increasing the inoculum to 10^4 CFU/cm². Overall, ozone nanobubble tended to be more effective on *B. thermosphacta*, *Leuconostoc* and *Y. rohdei*, while difference at significant level was not observed. Further, we investigated whether the treatment impact the cell population after long term storage at low temperature. Results implied no difference between the two disinfectants and the control group after seven weeks, neither for the 10^2 inoculation nor the 10^4 inoculations (Fig 6.2). *Brochothrix* was more affected by the treatment with peracetic acid and ozone than the other species. The 10^4 inoculations also implies that peracetic acid has a stronger impact on *Carnobacterium*, but this was not confirmed in the 10^2 inoculations. Cell population of *Yersinia* among muscle samples was less than 100 CFU/cm². In contrast, adipose samples presented challenges for interpretation due to suboptimal growth conditions for *Carnobacterium*, *Leuconostoc* and *Yersinia* (Fig 6.2C and 6.2D). No difference in cell counts of *Brochothrix* between control, peracetic acid, and ozone-treated samples was observed, all reaching around 5.8 log CFU/cm² despite the initial inoculation density. Cell counts for *Latilactobacillus* and *Hafnia* reach up to 7-8 log CFU/cm². There is no difference between the different treatment groups.

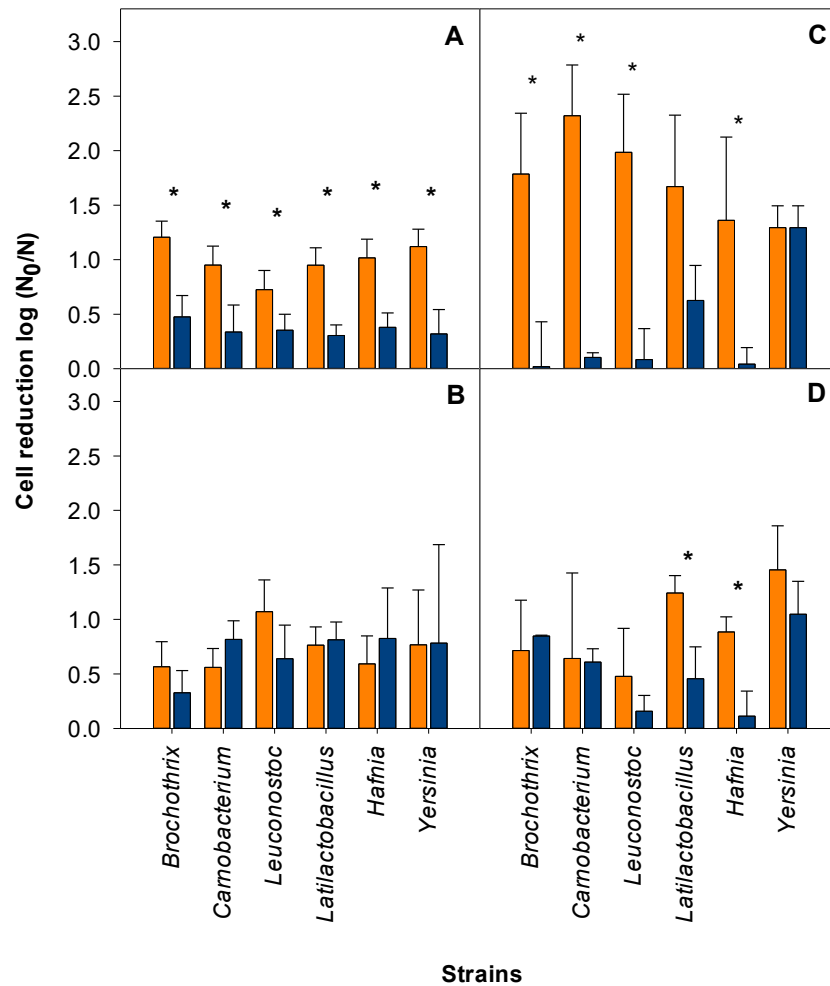


Figure 6.1. Bacterial reduction of each inoculum strain after treatment. Samples of pork muscle (A and B) and adipose tissue (C and D) were inoculated with 10^2 CFU/cm² (upper panels) or 10^4 CFU/cm² (lower panels). Samples were treated with 30 ml of water (gray), 400 ppm peracetic acid solution (orange), or 7 ppm ozone nanobubble (dark blue) for 1 minute. Cell counts were collected right **after treatment**. Data are shown as means \pm standard deviations for three independent experiments. An asterisk indicates values differ significantly ($P < 0.05$).

Table 6.2. Bacterial cell counts of meat sample inoculated with 10^4 CFU/cm² and stored vacuum-packaged for 7 d at 12 °C before and after treatment.

Inoculum strains	Bacterial cell counts (Log CFU/cm ²)		
	Control	PAA	O ₃ nanobubble
<i>Brochothrix thermosphacta</i> A401	6.36 ± 0.25	5.73 ± 0.33	6.14 ± 0.12
<i>Carnobacterium maltaromaticum</i> A404	5.47 ± 0.35	4.09 ± 0.95	5.34 ± 0.80
<i>Leuconostoc gelidum</i> *	8.08 ± 0.30	7.41 ± 0.64	7.73 ± 0.51
<i>Latilactobacillus sakei</i> B310	5.47 ± 1.54	5.03 ± 1.28	5.23 ± 1.12
<i>Hafnia paralvei</i> 1	7.30 ± 0.30	6.78 ± 0.12	7.02 ± 0.27
<i>Yersinia rohdei</i> 47	5.60 ± 0.31	5.20 ± 0.49	5.48 ± 0.58

*Mix strains of *L. gelidum* C202 and *Leuconostoc gelidum* ssp. *gasicomitatum* A209

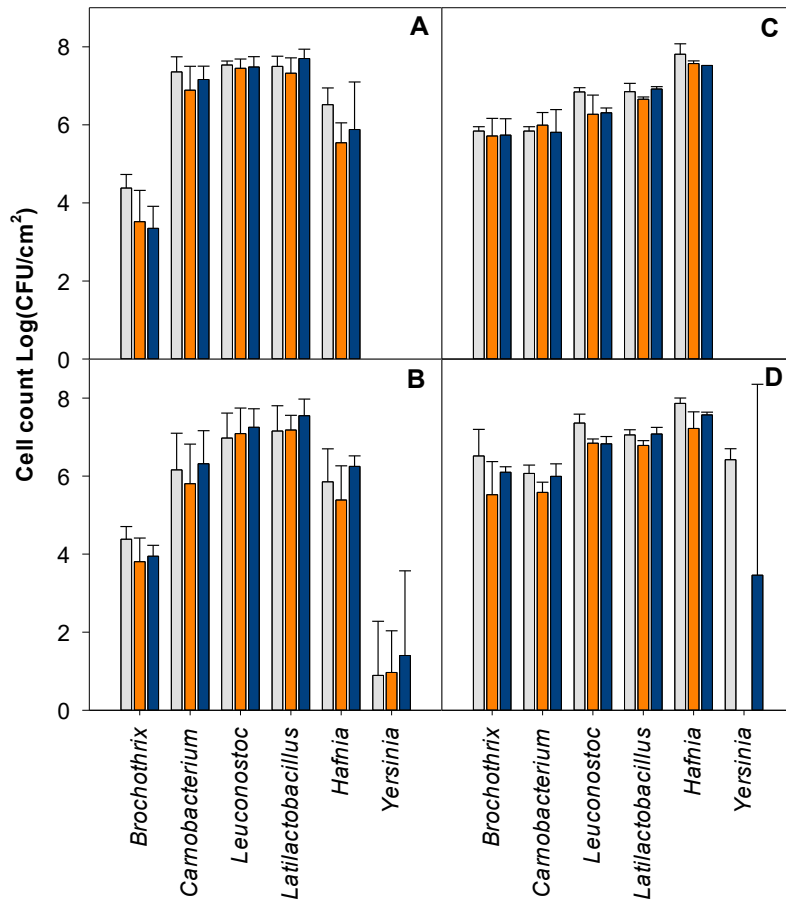


Figure 6.2. Bacterial cell counts of each inoculum strain after treatment. Samples of pork muscle (A and B) and adipose tissue (C and D) were inoculated with 10^2 CFU/cm² (upper panels) or 10^4 CFU/cm² (lower panels). Samples were treated with 30 ml of water (gray), 400 ppm peracetic acid solution (orange), or 7 ppm ozone nanobubble (dark blue) for 1 minute. **Cell counts were collected after treated samples stored at 8°C for 7 weeks.** Data are shown as means \pm standard deviations for three independent experiments.

6.3.2 Volume than flow rate impacted on the efficacy of ozone nanobubble solutions

Given the minimal effect of ozone nanobubble on meat bacterial load removal, we evaluated the influence of solution volume and flow on ozone efficacy. Although significant difference was not

observed among peracetic acid and ozone nanobubble treatment, increasing the treatment volume from 30ml to 500ml increased the bactericidal effect of ozone nanobubble in muscle samples (Fig 6.3). For instance, there was 1 log cell reduction on *Brochothrix*, *Latilactobacillus* and *Yersinia* for meat inoculated with 10^2 CFU/cm². The high variation of cell reduction was attributed to the level of *Brochothrix* in a few samples were below detection limit (6.36 CFU/cm²). The cleaning efficacy of both treatments was not correlated with the concentration of initial inoculate. The flow system results indicate no significant difference in cell reduction between treatments with ozone, peracetic acid, and lactic acid among Gram-positives (Fig 6.4). Ozone nanobubble solution displayed minimal effect on eliminating Gram negative bacteria in flow system, indicating that volume rather than flow rate impacts the efficacy of ozone nanobubble treatment on meat samples. In contrast, ozone nanobubble exhibited 1-2.5 log cell reduction with the following order *Latilactobacillus*, *Brochothrix* and *Carnobacterium*. The reduction efficacy is comparable to peracetic acid and lactic acid ($P > 0.05$).

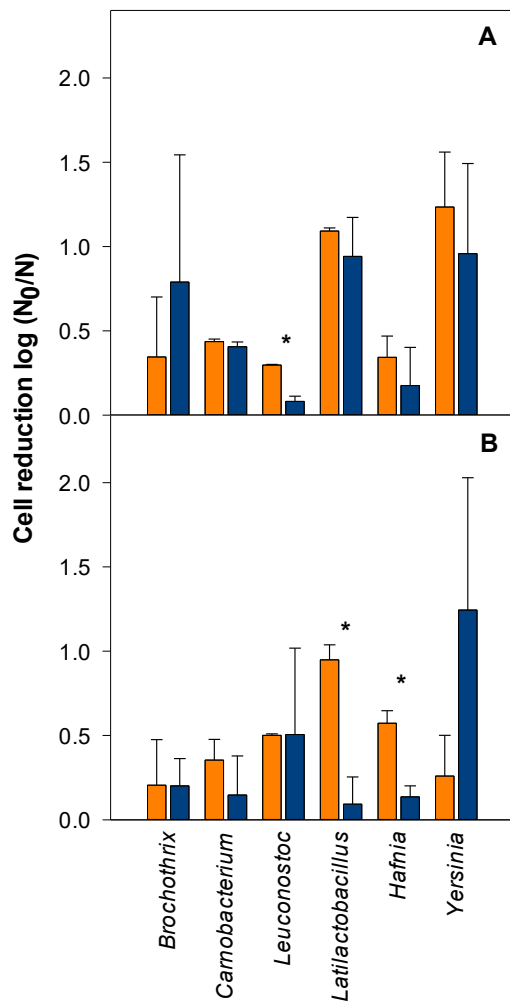


Figure 6.3. Reduction of cell counts of in inoculum strains with treatment of 500ml solutions for 1min. Inoculated pork muscle samples were treated with 400 ppm peracetic acid (orange bars) or 7 ppm ozone nanobubble (dark blue bars). Meat samples were inoculated with 10² CFU/cm² (A) or 10⁴ CFU/cm² (B). Data are shown as means ± standard deviations for three independent experiments. An asterisk indicates values differ significantly ($P < 0.05$).

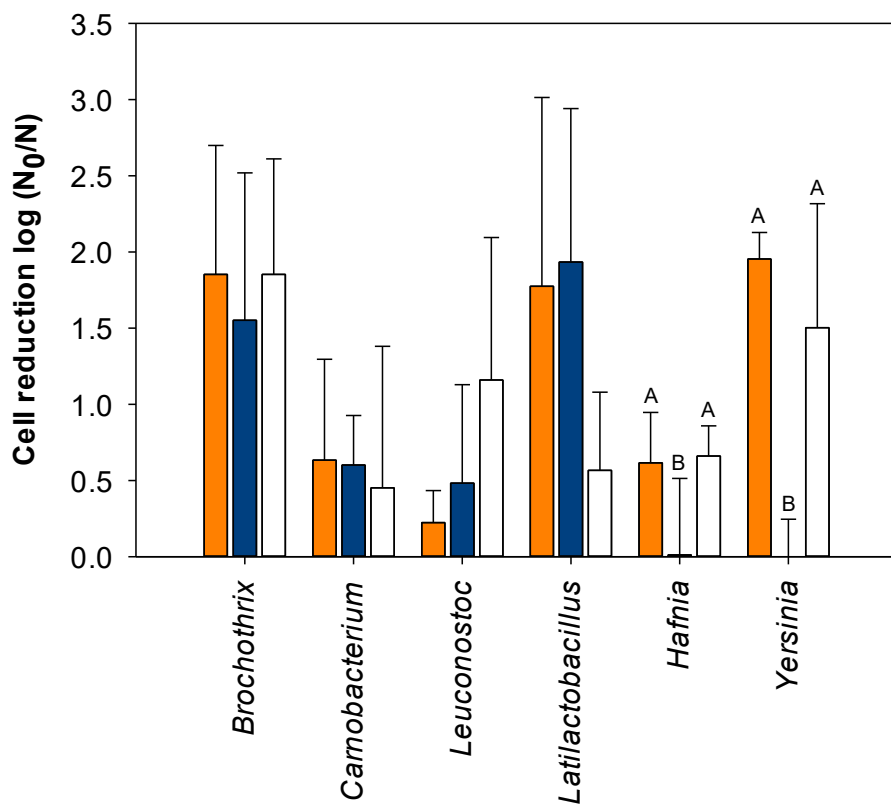


Figure 6.4. Reduction of cell counts of in inoculum strains after flow-system (30 ml/min) treatment. Inoculated pork muscle samples were treated with 400 ppm peracetic acid (orange bars), 7 ppm ozone nanobubble (dark blue bars), 2% lactic acid (white bars). Data are shown as means \pm standard deviations for three independent experiments. Values differ significantly ($P < 0.05$) if the bars do not share a common superscript.

6.3.3 Impact of storage temperature on disinfectant efficacy on meat microbiota

To assess the influence of storage temperature on efficacy of the different disinfectants, the Day 0 treatment with 30 mL was repeated. After storage for 8 weeks at -1°C , cell population of each species increased, ranging from 2 log to 6 log CFU/cm² (Fig 6.5). Specifically, *Leuconostoc* and *Latilactobacillus* dominated the growth with 5-6 log increases, while *Carnobacterium*,

Brochothrix, *Hafnia* and *Yersinia* grew by 2-3 logs. Bacterial populations surged upon week 6 and stabilized or decreased by week 8.

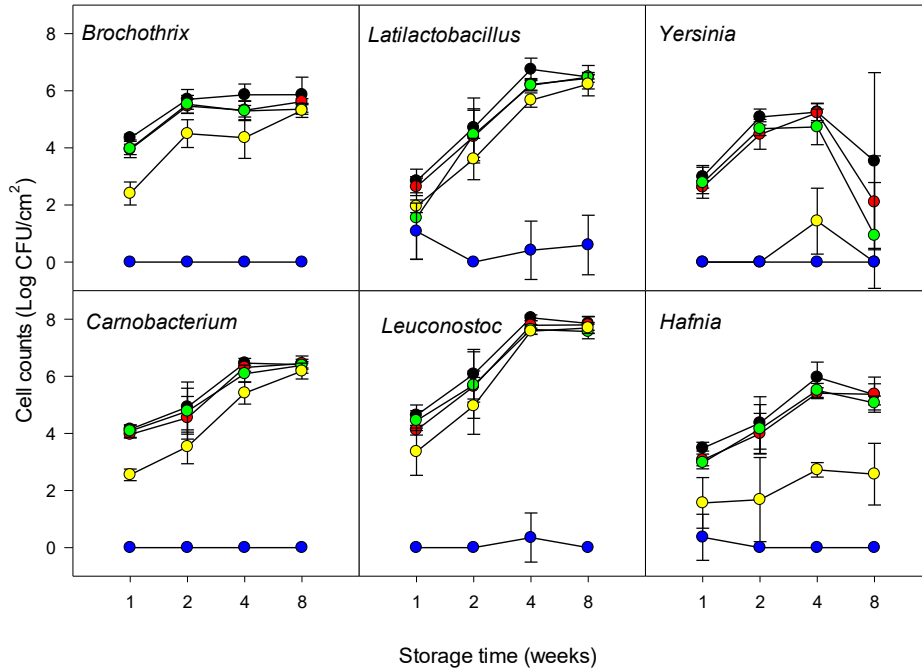


Figure 6.5. Bacterial cell counts of inoculum strains in treated meat samples after vacuum-packaging storage. Each meat sample were inoculated with 10^2 CFU/cm² (black) and treated with water (red), ozone nanobubble (green), peracetic acid (yellow) or lactic acid (blue). Cell counts were determined after 1 week, 2 weeks, 4 weeks, and 8 weeks of storage at -1°C . Results are reported as means \pm standard deviations (n=3).

Compared to untreated samples, sterile water treatment showed no difference in cell counts. Ozone nanobubble treatment slightly decreased cell populations by 0.5 log. Peracetic acid (PAA) demonstrated enhanced bactericidal effects, especially against *Brochothrix*, *Carnobacterium*, *Hafnia*, and *Yersinia*. Lactic acid solution was the most effective, reducing counts of all species to below detectable levels except for *Leuconostoc* and *Latilactobacillus*, which remained under 0.5 log CFU/cm² throughout storage. *Yersinia* showed the most striking difference; after an initial

increase in cell counts across all groups by week 6, counts decreased, with peracetic acid and ozone nanobubble achieving complete inhibition. These results align with those after seven weeks of storage at 8°C, which also showed low *Yersinia* counts (Fig 6.2).

6.3.4 Microbial composition of meat samples collected *in situ*

To examine the application of ozone nanobubbles on the microbial composition of meat samples *in situ*, two pork leg and two tenderloin samples from the production lines were rinsed with ozone nanobubble solution or water as control for 1 min. The meat samples then were stored for 3 months before sampling and sequencing. Microbial diversity varied among the samples. For example, *Morganella*, *Janthinobacterium*, *Rahnella*, *Leuconostoc*, and *Clostridium* only presented in leg samples, while *Providencia* and *Buttiauxella* were only found in tenderloin samples (Table 6.3). *Serratia*, *Yersinia*, *Carnobacterium*, and *Dellaglioia* were present in all samples, and their populations were not associated with ozone treatment. *Serratia* displayed highest abundance irrespective treatment and type of pork samples. The application of ozone nanobubbles decreased microbial diversity compared to control samples (Table 6.3), including absence of sequencing reads of *Clostridium* species in leg samples and a significant decrease (25%) or below detection limit of *Vagococcus* in leg and tenderloin samples, respectively.

Table 6.3. Abundance of microbiota in vacuum-packaged pork samples after 3 month refrigerated storage. The microbial composition was compared among samples that were treated with/without ozone nanobubble solution *in situ*.

Genus	Bacterial Relative abundance (%) in pork samples			
	Leg Control	Leg Ozone	Tenderloin Control	Tenderloin Ozone
<i>Serratia</i>	37.57	56.72	68.03	88.74
<i>Pseudomonas</i>	0.09	0.06	0.31	0.20
<i>Yersinia</i>	2.79	10.46	1.90	0.96
<i>Vagococcus</i>	34.97	9.12	10.45	-
<i>Carnobacterium</i>	5.88	8.31	13.86	8.29
<i>Morganella</i>	3.78	7.91	-	-
<i>Janthinobacterium</i>	-	3.26	-	-
<i>Dellagليا</i>	1.52	1.94	2.92	0.88
<i>Rahnella</i>	0.62	1.57	0.03	0.15
<i>Hafnia</i>	0.19	0.32	0.50	-
<i>Leuconostoc</i>	1.80	0.19	0.03	-
<i>Latilactobacillus</i>	0.04	0.05	0.04	0.20
<i>Budvicia</i>	-	0.03	-	-
<i>Obesumbacterium</i>	-	0.03	0.07	-
<i>Rouxiella</i>	-	0.03	-	-
<i>Clostridium</i>	10.38	-	-	-
<i>Lactococcus</i>	0.24	-	-	-
<i>Dysgonomonas</i>	0.04	-	-	-
<i>Enterococcus</i>	0.04	-	-	-
<i>Lactiplantibacillus</i>	0.04	-	-	-
<i>Buttiauxella</i>	-	-	-	0.60
<i>Providencia</i>	-	-	1.87	-

6.4 Discussion

To combat the food spoilage crisis and achieve a "greener" production process for improved food sustainability, this study evaluated the suitability and effectiveness of ozone nanobubble on meat spoilage control. Ozone has been widely used in various industries and there has been renewed interest in ozone treatment (aqueous and gaseous) in the food processing industry for eliminating food pathogens in fresh produce, raw meat and fish products, and fermented sausages for mold control (Dubey et al., 2022; Giménez et al., 2024; Xue et al., 2023; Ziyaina and Rasco, 2021). For example, low dose gaseous ozone is effective against *Listeria monocytogenes* on beef surfaces to a level below the detection limit (Giménez et al., 2021). The application of aqueous ozone on different offal (head, heart and liver) achieved a reduction 0.6-1.25 Log CFU/sample (Vargas et al., 2021). Aqueous ozone demonstrated significant inactivation of *Clostridium perfringens*, when in combined with heat treatment (Novak and Yuan, 2004). Despite ozone's potent antimicrobial properties, its effectiveness in the liquid phase is limited by its instability. Encapsulating ozone in nano-sized bubbles within water improves its stability. However, in alignment to the previous study on ozone nanobubble spray for the reduction of *Escherichia coli* O157:H7 on fresh beef surfaces (Kalchayanand et al., 2019), our study found that ozone nanobubble treatment demonstrated comparable microbial reduction loads to aqueous ozone on pork samples. The limited efficacy of ozone nanobubbles on meat samples may be attributed to the high level of organic matter in the meat matrix, which can rapidly neutralize the strong oxidative properties of ozone (Korany et al., 2018). For example, organic matter present in diluted milk or apple juice dramatically impacted the antimicrobial efficacy of ozonated water (Korany et al., 2018). Our observation that increasing the solution volume enhanced microbial inactivation further supports this hypothesis. Additionally, recent research demonstrated that increasing the volume of ozone nanobubbles during treatment

significantly improved its efficacy against *L. monocytogenes* biofilms on stainless steel surfaces (IAFP abstract).

Meat muscle after slaughtering is generally considered as sterile. A one-log cell count reduction during carcass washing with ozone nanobubble, therefore, is substantial in reducing the microbial loads prior to the fabrication and delaying spoilage process. Moreover, the application of different disinfectants together with packaging methods, and storage conditions such as humidity and temperature further alter the composition of meat microbiota (Hultman et al., 2015) and subsequently determine the organoleptic properties of meat products. Common meat-spoiling microbes include psychrotrophic *Pseudomonas*, *Acinetobacter*, *Staphylococcus*, *Psychrobacter*, lactic acid bacteria, *Enterobacteriaceae*, and clostridia (Xu et al., 2023a). Depending on the storage conditions, these microorganisms produce enzymes that break down carbohydrates, proteins, and lipids, resulting in off-odors, slime production, and discoloration (Iulietto et al., 2015). In vacuum-packaged meat products, strict aerobes are completely inhibited, while lactic acid bacteria (*Carnobacterium*, *Lactilactobacillus*, *Leuconostoc*) and *Enterobacteriales* (*Serratia*, *Rahnella*, *Hafnia*, and *Yersinia*) dominate the microbial growth. Additionally, the microbial interactions within the meat microbiome also impact meat quality. For example, *Carnobacterium* can spoil meat through acid production or eliminate other microorganisms via bacteriocin production (P. Zhang et al., 2019), which might explain the inconsistent population of *Yersinia* observed during the experiment. Our study found that the application of 4% lactic acid solution effectively eliminated throughout spoilage microorganisms under chilling storage (-1°C). However, its use remains challenging due to restrictions by the European Food Safety Authority (EFSA) (Hugas and Tsigarida, 2008). Although the latest tests by EFSA concluded that lactic acid solutions (2%-5%) pose no safety or environmental concerns, their efficacy on wild pigs remains inconclusive

(Lambré et al., 2022). The use of peracetic acid, on the other hand, displayed strong inhibitory effects on *Brochothrix*, *Hafnia*, and *Yersinia*, which are generally more problematic than lactic acid bacteria due to their proteolytic and lipolytic activities at low dosage. Populations as low as 10^4 CFU/cm² of these bacteria can lead to meat spoilage, whereas spoilage signs are not visible until the population of lactic acid bacteria reaches $10^7 - 10^8$ CFU/cm² (Yang, 2016). Our metagenomic data illustrated that the application of ozone nanobubble significantly decreased *Vagococcus* population below the detection limit. The identification of *Vagococcus* in spoiled meat is less common compared to other lactic acid bacteria such as *Leuconostoc*, *Carnobacterium*, and *Lactilactobacillus*. However, a few new species of *Vagococcus* have been isolated from modified atmosphere packaging (MAP) meat products (Johansson et al., 2023, 2020). In fact, *Vagococcus* outgrew the later shelf-life microbiota in fresh whole broiler meat packaged in 80%O₂/20%CO₂ modified atmosphere (Lauritsen et al., 2019). Although the bactericidal effect of ozone nanobubble on *Clostridium* microbial load was not directly examined in this study, *Clostridium* was detected in water-washed samples but absent in those treated with ozone nanobubbles. This observed shift in microbial composition can be attributed to the breakdown of ozone into oxygen during treatment, which might inhibit the growth of clostridia and thereby reduce the risks of blown pack spoilage in meat products.

The major sources of post-contamination on meat products include dirt, water, the animal itself, tools and equipment used during the operation processes (Clotey, 1985; Taylor and Aiyegoro, 2024). A recent review demonstrated that microbiota originating from food processing environments, rather than those associated with animals, are the primary source of microbial contamination (Xu et al., 2023a). For example, conveyor belt was identified as the primary vector for the transmission of *E. coli* after sanitation, while cutting tables and mesh gloves served as the

were critical sources of contamination for meat spoilers including *Pseudomonas*, *Carnobacterium*, and *Yersinia* between shifts (Wang et al., 2018; Yang et al., 2017a). Moreover, microbes survived even after deep sanitation program that includes dirt and soil removal, cleaning and degreasing, and sanitisation on conveyor belts (Wang et al., 2018). One plausible explanation is the ability of microbes to form biofilms on equipment surfaces, contributing to their persistence and further contamination of meat products. Shiga toxin-producing *Escherichia coli* O157:H7 and non-O157 strains, for instance, demonstrated biofilm formation on food-grade equipment surfaces and impedes the efficacy of chlorine and quaternary ammonium chloride-based sanitizers (Wang et al., 2012). Owing to the beneficial properties of nanobubbles e.g. larger specific surface area, higher mass transfer efficiency, higher interface absolute zeta potential, slower rising velocity, longer stability, and stronger oxidation ability (Akshith et al., 2024), nanobubble technology together with ozone treatment could be a promising disinfectant for surface cleaning and sanitizing. The use of 100 ppm chlorine solutions with air and CO₂ nanobubbles substantially reduced the cells of *L. monocytogenes* biofilms formed on stainless steel (Sekhon et al., 2022). Moreover, the incorporation of air, N₂, and CO₂ nanobubbles in chlorine (200 ppm) and peracetic acid (80 ppm) solutions resulted in higher log reductions of both fresh (3 days) and aged (30 days) *L. monocytogenes* biofilms on various surfaces, including stainless steel, polypropylene, and silicone, compared to antimicrobial solutions without nanobubbles (Unger et al., 2023). The incorporation of nanobubble and cold plasma activated water, on the other hand, reduced the dual-species biofilm to below detection limit. More specifically, increasing the flow regime from laminar circulation ($0.88 \pm 0.16 \log \text{CFU/cm}^2$) to turbulent circulation ($1.22 \pm 0.43 \log \text{CFU/cm}^2$) substantially increased the reduction of cells in dual-species biofilms (Dhaliwal et al., 2024). Taken together, the modest effect of ozone nanobubble solution on meat products, combined with its effective

performance on equipment surfaces and biofilm-embedded cells, suggests that ozone nanobubble solution is alternative disinfectant for microbial control during meat production, thereby improving the safety and quality of meat products.

Chapter 7. Characterization and Diversity of 74 Novel Species Isolated from a Pork Processing Facility

7.1 Introduction

The isolation of bacteria from food processing plants suggested that 219 isolates belong to undescribed bacteria taxa. This chapter aims to determine which of these isolates represent novel species when using the criteria less than 70% digital DNA–DNA hybridization (dDDH) and less than 95% average nucleotide identity (ANI) when compared to the most closely related type strain, i.e. the criteria that are most commonly used for the genome-based taxonomy of bacteria (Chun et al., 2018).

7.2 Materials and methods

7.2.1 Bacterial isolation, sequencing and download of type strain

Bacterial isolates were obtained, sequenced and aligned to Genomic Taxonomy Database (GTDB) as described before. Genomes with less than 95% average nucleotide identity (ANI) were considered as potential novel species. In addition, the assigned taxonomy with "genus name & 9-digit numbers" represents available genome in GTDB database (Parks et al., 2021), but their physiological characterization is missing, thus included in the analysis. To determine the phylogenetic distance of each isolate to its closely related to species, NCBI Datasets was used to retrieve type strain genomes from NCBI database (O’Leary et al., 2024). Type strain information was cross-checked with LPSN-DSMZ database (<https://lpsn.dsmz.de/>).

7.2.2 Phylogenetic analysis and determination of pairwise average nucleotide identity

To determine the closely related species to the potential novel species, FastANI was used to obtain the pairwise nucleotide average identity (Jain et al., 2018). Two to five type strains most closely

related to the novel species were selected for subsequent phylogenetic analysis. Genomes of type strains and isolates of novel species were annotated with Prokka (Seemann, 2014), and protein sequences were used to infer their phylogenetic distance through PhyloPhlan v3.1.1 (Asnicar et al., 2020) based on universal marker genes in phyloPhlan database. MAFFT was used for multiple sequence alignment (Kato and Standley, 2013), and the alignments were trimmed with TrimAl (Capella-Gutiérrez et al., 2009). The phylogenetic tree was inferred using IQ-TREE (Nguyen et al., 2015).

7.3 Results and discussion

Of the 1281 sequenced isolates, 219 were not assigned to known species according to the GTDB database (ANI <95%). Pairwise whole-genome alignment analysis indicated that these isolates belong to 74 distinct species, distributed across 26 genera and 4 phyla (Table 7.1). Their phylogenetic distance and ANI are illustrated in Figure 7.1. Particularly, 26 out of 74 the potential novel species belong to the *Pseudomonas* genus (Table 7.1). In fact, the genus *Pseudomonas* exhibits extensive genetic diversity, with 300 species identified, owing to their versatile lifestyle among diverse environments. The rapid identification of new *Pseudomonas* species and frequent misclassification in taxonomy (Girard et al., 2021; Passarelli-Araujo et al., 2022) underscore the necessity of further subdividing the genus *Pseudomonas*. Subsequent characterization, including growth conditions, biofilm formation, and lipolytic and proteolytic activities, will be conducted to evaluate their biofilm formation ability and spoilage potential for understanding their physiological features in food processing environments.

Table 7.1. Summary of novel species isolated from the pork processing environments.

Phylum	Strain ID	Isolation source	Taxon*
Actinomycetota	TC276	D-wall in cooler	<i>Frigoribacterium</i> sp nov. 001421165
	TC783	D- drain in cooler 1	<i>Microbacterium</i> sp nov. 002979655
	TC172	C- break table	<i>Microbacterium</i> sp nov. 015350795
	TC452	D- pipes2	<i>Microbacterium</i> sp nov.1
	TC129	C- QC2	<i>Microbacterium</i> sp nov.2
	TC136	C- QC2	<i>Microbacterium</i> sp nov.3
	TC857	D-air blower	<i>Plantibacter</i> sp nov.1
	TC168	C- break table	<i>Plantibacter</i> sp nov.2
	TC566	D- plastic curtain	<i>Pseudoclavibacter</i> sp nov.
	TC169	C- break table	<i>Renibacterium</i> sp nov. 005809195
	TC593	D- drain in cooler2	<i>Specibacter</i> sp nov.
Bacillota	TC223	C-retail	<i>Macrococcus</i> sp nov. 019357535
	TC104	C-CB3	<i>Neobacillus</i> sp nov. 002559145
Bacteroidota	TC732	D- knife sharpener (steel)	<i>Epilithonimonas</i> sp nov. 1
	TC1206	D- drain in bagging	<i>Epilithonimonas</i> sp nov. 2
	TC604	D- drain in cooler2	<i>Flavobacterium</i> sp nov. 003668995
	TC687	D-ES1	<i>Flavobacterium</i> sp nov. 2
	TC780	D - little hole	<i>Flavobacterium</i> sp nov. 3
	TC781	D - little hole	<i>Flavobacterium</i> sp nov. 4
	TC1208	D- drain in bagging	<i>Flavobacterium</i> sp nov. 5
	TC1211	D- drain in bagging	<i>Flavobacterium</i> sp nov. 6
	TC906	D-break saw	<i>Flavobacterium</i> sp nov.1
	TC837	Water sample	<i>Pedobacter</i> sp nov.1
	TC712	D- SS on top of CB-BT1	<i>Pedobacter</i> sp nov.2
	TC808	drain in cooler 1	<i>Sphingobacterium</i> sp nov. 000938735
	Pseudomonadota	TC683	D-ES1
T981		D-T5	<i>Acinetobacter</i> sp nov. 002135415
TC133		C- QC2	<i>Brevundimonas</i> sp nov. 002434505
SX535		CB3	<i>Ewingella</i> sp nov.
TC1122		D- drain in cutting room (AP)	<i>Janthinobacterium</i> sp nov.
TC711		D- SS on top of CB-BT1	<i>Janthinobacterium</i> sp nov. 002846335
TC350		D-wizard knife	<i>Janthinobacterium</i> sp nov. 002878455
TC779		D - little hole	<i>Janthinobacterium</i> sp nov. 009208735

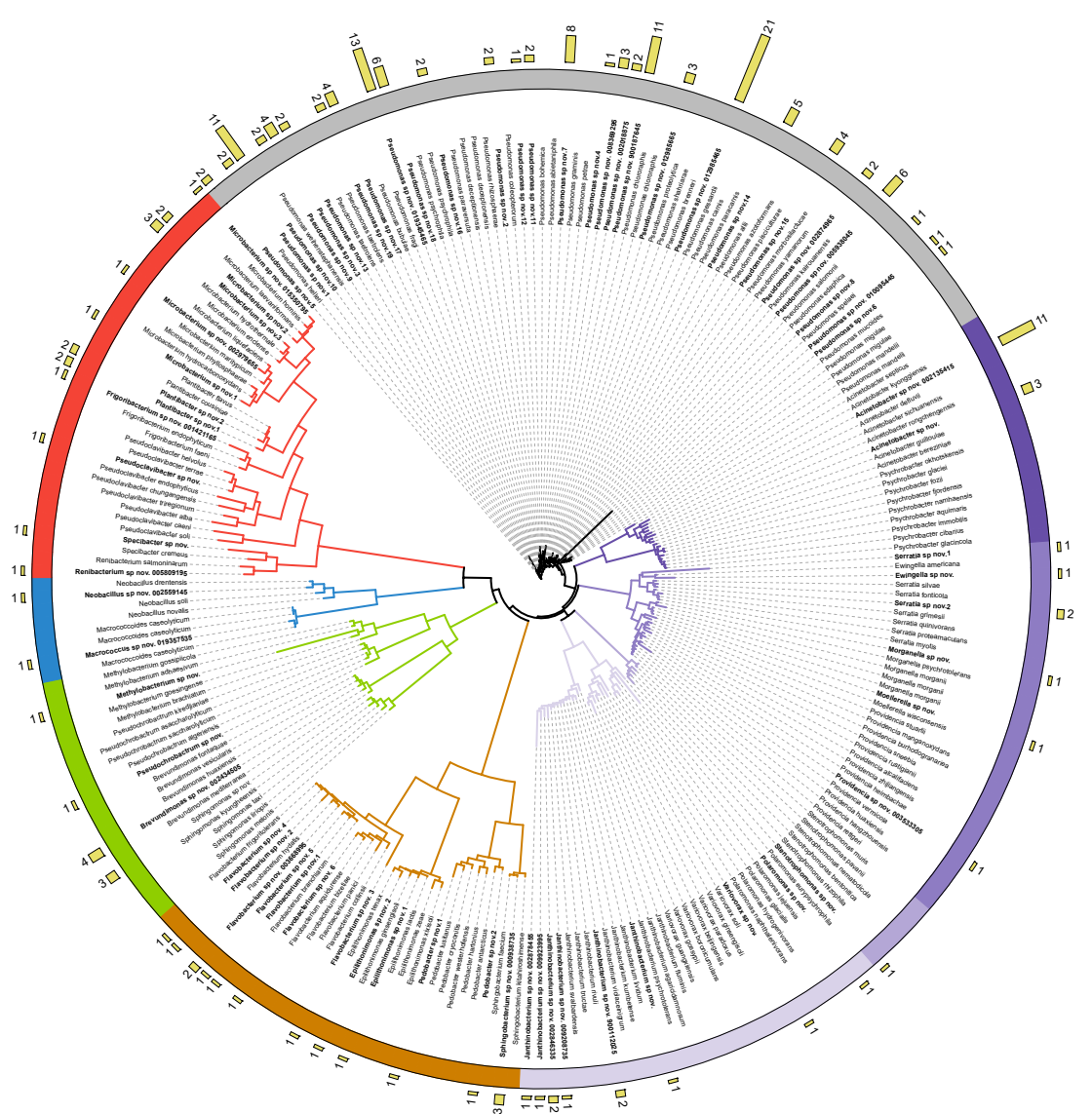
Phylum	Strain ID	Isolation source	Taxon*
Pseudomonadota	TC934	D-break table	<i>Janthinobacterium</i> sp nov. 009923995
	TC787	D- drain in cooler 1	<i>Janthinobacterium</i> sp nov. 900112025
	TC82	C-work table	<i>Methylobacterium</i> sp nov.
	L18	Loin 3 month	<i>Moellerella</i> sp nov.
	TC12	BT3-CI	<i>Morganella</i> sp nov.
	TC839	Water sample	<i>Polaromonas</i> sp nov.
	BT1-P2	BT1-2nd	<i>Providencia</i> sp nov. 003533305
	TC309	D- apron	<i>Pseudochrobactrum</i> sp nov.
	TC27	BT3-CI	<i>Pseudomonas</i> sp nov. 012985465
	TC793	D- drain in cooler 1	<i>Pseudomonas</i> sp nov. 012985665
	TC192	C-QC1	<i>Pseudomonas</i> sp nov. 900187645
	TC1046	D-T3	<i>Pseudomonas</i> sp nov. 002018875
	TC405	D-pipes1	<i>Pseudomonas</i> sp nov. 002874965
	T974	D-T5	<i>Pseudomonas</i> sp nov. 005938045
	T603	D- drain in cooler2	<i>Pseudomonas</i> sp nov. 008369295
	TC795	D- drain in cooler 1	<i>Pseudomonas</i> sp nov. 010095445
	TC1213	D- drain in bagging	<i>Pseudomonas</i> sp nov. 019345465
	T1031	D-T5	<i>Pseudomonas</i> sp nov.1
	TC1092	D- meat basket	<i>Pseudomonas</i> sp nov.10
	TC124	C- QC2	<i>Pseudomonas</i> sp nov.11
	TC131	C- QC2	<i>Pseudomonas</i> sp nov.12
	TC523	D-bloody drain	<i>Pseudomonas</i> sp nov.13
	TC1290	Meat - loin	<i>Pseudomonas</i> sp nov.14
	TC1184	D-QC2(Mar 7th)	<i>Pseudomonas</i> sp nov.15
	TC1195	D- drain in bagging	<i>Pseudomonas</i> sp nov.16
	TC1200	D- drain in bagging	<i>Pseudomonas</i> sp nov.17
	TC1056	D-T3	<i>Pseudomonas</i> sp nov.18
	TC1048	D-tray	<i>Pseudomonas</i> sp nov.19
	TC921	D-break table	<i>Pseudomonas</i> sp nov.2
	TC941	D-door	<i>Pseudomonas</i> sp nov.3
	TC943	D-door	<i>Pseudomonas</i> sp nov.4
	TC835	D-QC1	<i>Pseudomonas</i> sp nov.5
	TC1106	D- drain in cutting room (AP)	<i>Pseudomonas</i> sp nov.6
	TC447	D- pipes2	<i>Pseudomonas</i> sp nov.7
	TC465	D-trim 2 (T2)	<i>Pseudomonas</i> sp nov.8

Phylum	Strain ID	Isolation source	Taxon*
Pseudomonadota	TC1078	D- meat basket	<i>Pseudomonas</i> sp nov.9
	TC620	D-ss hold under cutting board	<i>Serratia</i> sp nov.1
	SX649	clean cb\$3	<i>Serratia</i> sp nov.2
	TC81	C-work table	<i>Sphingomonas</i> sp nov.
	TC717	D- knife sharpener (steel)	<i>Stenotrophomonas</i> sp nov.
	TC581	D- plastic curtain	<i>Variovorax</i> sp nov.

* Taxon followed by 9-digit number indicates the genomes available in GTDB database without physiological characterization.

A.

Tree scale: 0.1



Taxonomy

- Actinomycetota
- Bacillota
- Bacteroidota
- Alphaproteobacteria
- Burkholderiales
- Xanthomonadales
- Enterobacterales
- Moraxellaceae
- Pseudomonadaceae

Frequency

- Number of isolates

B.

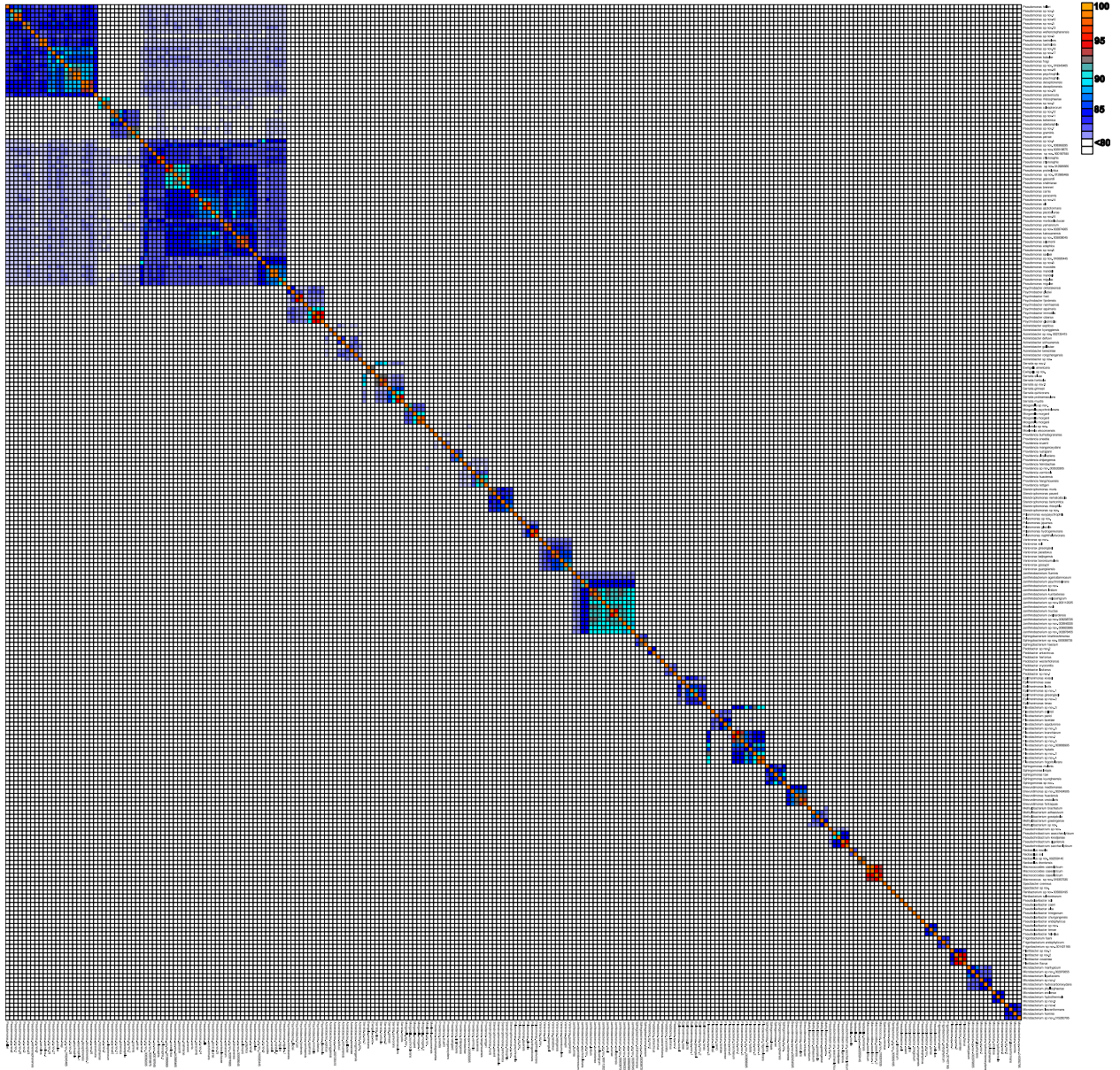


Figure 7.1. Phylogenetic distance (A) and Average Nucleotide Identity (ANI) (B) of the new species and their closely related type strains. **A.** Phylogenetic tree of 168 type strains and 74 potential new species reconstructed by PhyloPhlAn 3.1.1 based on 400 universal marker genes from phylophlan database, inferred by IQTree. Colors denote different taxa: red for Actinomycetota, blue for Bacillota, brown for Bacteroidota, green for Alphaproteobacteria, grey

and purple for Gammaproteobacteria. The bar plot indicates the number of isolates obtained for each potential new species. **B.** Heatmap of ANI values from whole-genome comparisons of 242 genomes, generated using FastANI.

Chapter 8. General Conclusion and Discussion

Food processing environments serve as complex niches for bacterial colonization, adaption, persistence and dispersal, which subsequently shapes the microbial composition and diversity. A core microbiome exists regardless of different commodities, while each food commodity possesses its own accessory microbiome (Chapter 2). The determination of core and accessory microbiomes is driven by various selection factors. My doctoral research project focused on the impact of biofilm formation, bacterial communication and cooperation on microbial community assembly, providing insights into the use of ozone nanobubble solutions as novel intervention strategies.

8.1 Translation of microbial ecology in food processing to practical sanitation protocols

Contamination of food products with food pathogens and spoilage microorganism may occur in various stages. From the farm level, microbes can be introduced from soil, water manure, compost, and scat (Bottichio et al., 2020). The Shiga toxin-producing *Escherichia coli* outbreaks in 2018 associated with romaine lettuce was considered airborne and linked to feedlot and irrigation water contamination (FDA, 2024). From the operation unit, microbes are introduced by the surrounding environment and their diversity and abundance are shaped by employees, hygienic design, sanitation strategies and packaging methods (Fig 1.1). From the fork level, how food is prepared and maintained in the retails or households also impact the composition of microbes and further determine food safety and quality. For example, *Salmonella* is the most frequent food pathogen that have been isolated in domestic kitchen and equipment surfaces including refrigerator door handles, tap handles and kitchen sinks (Borrusso and Quinlan, 2017; Evans and Redmond, 2019). It is thus critical to understand the microbial community dynamics at various stages to better support root cause analysis (The Pew Charitable Trusts, n.d.). The implementation of hazard analysis critical control point (HACCP) programs has improved the safety of food products, while

to some extent, it also shaped the microbial condition by critical control point and the use of prerequisite programs. More specifically, the letter of guarantee from suppliers can limited the dispersal of microbes from raw materials to food products. Other prerequisite programs such as hygienic design, sanitation programs and personnel training also serve as selection forces to determine the microbial conditions of food products. The common critical control points such as heating and pasteurization, could drive the diversification process and serve as biotic factors for selection. An expelling example is the occurrence of tLST operon among strains of *E. coli* that were isolated from meat processing facility that pasteurize carcasses with steam/hot water and and pasteurized milk (Guragain et al., 2023; Machado et al., 2023; Zhang and Yang, 2022). In chapter 3, I further investigated the role of tLST against oxidative stress in biofilm-embedded cells. The presence of tLST locus is positively correlated with biofilm biomass and enhance resistance to common sanitizers. The prevalence of this mobile genomic island is 2.7% among strains of *E. coli* and both intra and interspecies transmission were observed from chromosomal and plasmid-borne tLST (Zhang and Yang, 2022).

In chapter 2, I identified a core microbiome regardless of different commodities e.g. dairy, produce, or ready-to-eat products, suggesting that the (refrigerated) processing environment rather than the respective raw materials are a primary source of microbes. The high throughput analysis further proved this concept that common meat spoilers isolated from the meat samples are genetically identical to environmental isolates such as floor drains, equipment surfaces and conveyor belts, irrespective sanitation efforts (Chapter 5). Indeed, different food commodities harbor various microbes, however, the presence of core microbiome highlights the needs for a well-designed environmental sampling and testing programme to identify contamination sources, detect potentially persistent hazards together with implementation of adequate hygiene strategies to

control the bacterial persistence (Koutsoumanis et al., 2024). For example, the utilization of WGS captured the transmission patterns of *L. monocytogenes* from the dairy farm environments to dairy processing facility, and the implementation of interventions has intensively minimized *Listeria* spp. contamination in the processing environment (Bolten et al., 2024).

8.2 Bacterial communication and cooperation on biofilm formation, resistance and persistence

Bacteria communicate and cooperate by secreting molecules in response to changes in the surrounding environment and microbial community structures. Intercellular communication involves the production, release, detection, and response to signal molecules (autoinducers) through a process termed quorum sensing (QS) (Miller and Bassler, 2001; Waters and Bassler, 2005). The dynamic concentration of autoinducers further direct bacteria to track cell density and microbial composition and subsequently alter their gene expression levels accordingly (Papenfort and Bassler, 2016a). Both Gram-positive and Gram-negative bacteria use quorum sensing. Gram-positive systems typically use secreted autoinducing peptides while Gram-negative bacteria produce and use autoinducer N-acyl homoserine lactones (AHLs) (Verbeke et al., 2017). The cross-kingdom interactions between yeast/mold and bacteria are associated with volatile compounds (Tilocca et al., 2020). Additionally, other molecules such as indole and 2-heptyl-3-hydroxy-4-quinolone have been found to be involved in QS systems that enable inter- and intraspecies communications (Diggle et al., 2007; Lee and Lee, 2010). In food and food processing environments, QS is associated with microbial adaption to dynamic environments through biofilm formation, alternation to food quality by food spoilage or food fermentation (Falà et al., 2022). For instance, Quorum sensing (QS) promotes spoilage of carrot slices by *Serratia plymuthica* through enhanced colonization and mucoid growth while an AHL-deficient mutant displayed reduced

spoilage and spoilage phenotype was restored by adding synthetic signal (Wevers et al., 2009). All phases of biofilm formation are associated with quorum sensing including cell attachment, biofilm maturation and dispersal through regulating the secretion of extracellular polymeric substances. In Chapter 4, I found that that QS not only regulated biofilm formation through curli and cellulose biosynthesis but also determined the phenotypic change of surface-associated biofilms to floating biofilms. The compact structure of pellicles increased its resistance to common disinfectants and floor drains or other cervices area could be a niche for pellicle establishment, thus increasing the risk of bacterial persistence. The prevalence of common meat spoilers in reconstituted multi-species biofilms (up to 12 different species) further suggests that microbe-microbe communication and bacterial co-existence alter the composition of microbial diversity and contribute the persistence of certain microbes.

Genes associated with cooperation can spread among microbes through horizontal gene transfer (HGT). The cooperation between biofilm formation and tLST indicates that their co-occurrence further exacerbates the risk of bacterial persistence (Chapter 3). Intense sanitization (IS) procedure thus has been used to deeply clean the processing environments. Even though the application of IS procedure disrupted bacteria to a lower level with a reduced microbial diversity (Bosilevac et al., 2024), certain species survived IS procedure and microbial diversity surged after 4 weeks, which might unintentionally support the colonization of other microbes through biofilm formation due to a lack of competition within the multispecies mixture (Wang et al., 2024).

8.3 Novel approaches for food safety and spoilage control

Considering the complexity of microbial communities in food and food processing environment, emerging research thus aimed to i) effectively isolate and identify target microorganisms for food safety and spoilage control; ii) develop novel disinfectant reagents to eliminate spoilage and

pathogenic microbes; and iii) utilize AI-based tools to monitor the microbial conditions from a larger-scale database. For instance, the use of Highly Pathogenic *Salmonella* (HPS) multiplex PCR assay can differentiate the pathogenicity of the *Salmonella* (Harhay et al., 2024) and biosensor-based methods are used for rapid microbial assessment (Law et al., 2014; Pampoukis et al., 2022). The identification and characterization of over 70 novel species (Chapter 7) on the other hand, indicate that culture-dependent approaches are still fundamental for microbial research and should be complemented with culture-independent approaches (16S amplicon sequencing and metagenomic sequencing) to fully uncover the complexity of microbial dynamics and interactions. The combination of more than one preservation approach (hurdle technology) enhanced microbial control in the food and food processing environments. For example, refrigeration and modified atmosphere packaging have been used to eliminate undesirable microbes and heat-stable bacteriocin nisin are used to control spore-forming microorganisms in canning vegetable (Mukhopadhyay and Gorris, 2014). Novel sanitizers include electrolysed water and cold plasma water are environmental friendly and demonstrate efficacy on eliminating bacterial biofilms and disrupting bacterial transmission (Gao et al., 2022; Mai-Prochnow et al., 2021; Rahman et al., 2016; Ravash et al., 2023). In chapter 6, we examined another potential novel sanitizer, ozone nanobubble, for meat spoilage control. With the rapid development of artificial intelligence (AI) technologies, its potential in agriculture and food systems has drawn more attention. The use of AI-based tools for data collection and analysis has demonstrated potential inspection of food microbes from raw materials to distribution and retails (C. Qian et al., 2023; Chenhao Qian et al., 2023; Snyder et al., 2024). The use of digital tools, such as predictive models can translate bench-top data with simulated environments to estimate microbial behaviors, providing essential information for Quantitative Microbiological Risk Assessment (Koutsoumanis et al., 2021). The

use of predictive modeling and development of digital food systems, however, still face challenges due to the microbial complexity of food and food processing environments, and limited data availability from industries and consumers (Chenhao Qian et al., 2023).

8.4 Limitations and future works

Although this dissertation provide insights on microbial ecology in food systems, further research is required to fully grasp the complexity of eco-evolutionary dynamics (Pelletier et al., 2009). For instance, this study examined biofilm formation across single-, dual-, and multi-species, questions remain about which microbes act as pioneers in biofilm formation, how microbial dynamics progress through biofilm formation cycles (attachment, maturation, and dispersal), and how these dynamics affect the composition of extracellular polymeric substances (EPS). Additionally, despite we have grown biofilms and tested antimicrobial sprays in simulated processing environments, more sophisticated tools, such as the industrial surfaces biofilm reactor (BioSurface, Bozeman, Montana), are needed to accurately mimic the effects of flow and shear forces in real processing conditions. Investigating food-associated "model communities" (O'Toole, 2024) and understanding how pathogenic microbes such as *L. monocytogenes*, *Salmonella*, or *E. coli* O157:H7 interact with environmental microbiota and impact disinfectant efficacy should also be prioritized. Incoming bacteria from raw materials shapes the microbial composition and diversity in the food processing environment. Further sampling should be conducted to map these bacteria in relation to the plant's environmental microbiota and the microbiota of the final products. With the advent of next-generation sequencing, there is an urgent need to develop a comprehensive database of spoilage microbes to better depict microbial networks in food ecosystems. Focus of these research efforts will help address the food waste crisis and contribute to a safer and more sustainable food system.

Bibliography

- Abdallah, M., Benoliel, C., Drider, D., Dhulster, P., Chihib, N.E., 2014. Biofilm formation and persistence on abiotic surfaces in the context of food and medical environments. *Arch. Microbiol.* 196, 453–472. <https://doi.org/10.1007/s00203-014-0983-1>
- Ahmad, I., Nygren, E., Khalid, F., Myint, S.L., Uhlin, B.E., 2020. A Cyclic-di-GMP signalling network regulates biofilm formation and surface associated motility of *Acinetobacter baumannii* 17978. *Sci. Rep.* 10, 1–11. <https://doi.org/10.1038/s41598-020-58522-5>
- Akshit, F.N.U., Mao, T., Mohan, M.S., 2024. Future perspective of nanobubble technology in dairy processing applications. *Trends Food Sci. Technol.* 147, 104420. <https://doi.org/10.1016/J.TIFS.2024.104420>
- Alegbeleye, O., Odeyemi, O.A., Strateva, M., Stratev, D., 2022. Microbial spoilage of vegetables, fruits and cereals. *Appl. Food Res.* 2, 100122. <https://doi.org/10.1016/J.AFRES.2022.100122>
- Almblad, H., Randall, T.E., Liu, F., Leblanc, K., Groves, R.A., Kittichotirat, W., Winsor, G.L., Fournier, N., Au, E., Groizeleau, J., Rich, J.D., Lou, Y., Granton, E., Jennings, L.K., Singletary, L.A., Winstone, T.M.L., Good, N.M., Bumgarner, R.E., Hynes, M.F., Singh, M., Stietz, M.S., Brinkman, F.S.L., Kumar, A., Brassinga, A.K.C., Parsek, M.R., Tseng, B.S., Lewis, I.A., Yipp, B.G., MacCallum, J.L., Harrison, J.J., 2021. Bacterial cyclic diguanylate signaling networks sense temperature. *Nat. Commun.* 12, 1986. <https://doi.org/10.1038/s41467-021-22176-2>
- Alvarez-Molina, A., Cobo-Díaz, J.F., Alexa, E.A., Crispie, F., Prieto, M., López, M., Cotter, P.D., Alvarez-Ordóñez, A., 2023. Sequencing-based analysis of the microbiomes of Spanish food processing facilities reveals environment-specific variation in the dominant taxa and

antibiotic resistance genes. Food Res. Int. 173, 113442.
<https://doi.org/10.1016/J.FOODRES.2023.113442>

Alvarez-Molina, A., Cobo-Díaz, J.F., López, M., Prieto, M., de Toro, M., Alvarez-Ordóñez, A., 2021. Unraveling the emergence and population diversity of *Listeria monocytogenes* in a newly built meat facility through whole genome sequencing. Int. J. Food Microbiol. 340, 109043. <https://doi.org/10.1016/j.ijfoodmicro.2021.109043>

Alvarez-Ordóñez, A., Coughlan, L.M., Briandet, R., Cotter, P.D., 2019. Biofilms in food processing environments: challenges and opportunities. Annu. Rev. Food Sci. Technol. 10, 173–195. <https://doi.org/10.1146/annurev-food-032818-121805>

Anderson, A.C., Burnett, A.J.N., Hiscock, L., Maly, K.E., Weadge, J.T., 2020. The *Escherichia coli* cellulose synthase subunit G (BcsG) is a Zn²⁺-dependent phosphoethanolamine transferase. J. Biol. Chem. 295, 6225–6235. <https://doi.org/10.1074/JBC.RA119.011668>

Aravena-Román, M., Beaz-Hidalgo, R., Inglis, T.J.J., Riley, T. V., Martínez-Murcia, A.J., Chang, B.J., Figueras, M.J., 2013. *Aeromonas australiensis* sp. nov., isolated from irrigation water. Int. J. Syst. Evol. Microbiol. 63, 2270–2276. <https://doi.org/10.1099/IJS.0.040162-0/CITE/REFWORKS>

Armitano, J., Méjean, V., Jourlin-Castelli, C., 2014. Gram-negative bacteria can also form pellicles. Environ. Microbiol. Rep. 6, 534–544. <https://doi.org/10.1111/1758-2229.12171>

Arthur, T.M., Bono, J.L., Kalchayanand, N., 2014. Characterization of *Escherichia coli* O157: H7 strains from contaminated raw beef trim during " high event periods ". Appl. Environ. Microbiol. 80, 506–514. <https://doi.org/10.1128/AEM.03192-13>

Asnicar, F., Thomas, A.M., Beghini, F., Mengoni, C., Manara, S., Manghi, P., Zhu, Q., Bolzan,

- M., Cumbo, F., May, U., Sanders, J.G., Zolfo, M., Kopylova, E., Pasolli, E., Knight, R., Mirarab, S., Huttenhower, C., Segata, N., 2020. Precise phylogenetic analysis of microbial isolates and genomes from metagenomes using PhyloPhlAn 3.0. *Nat. Commun.* 11, 1–10. <https://doi.org/10.1038/s41467-020-16366-7>
- Audrain, B., Létoffé, S., Ghigo, J.M., 2015. Airborne bacterial interactions: Functions out of thin air? *Front. Microbiol.* 6, 1476. <https://doi.org/10.3389/FMICB.2015.01476>
- Augustin, J.C., Kooh, P., Bayeux, T., Guillier, L., Meyer, T., Jourdan-Da Silva, N., Villena, I., Sanaa, M., Cerf, O., 2020. Contribution of foods and poor food-handling practices to the burden of foodborne infectious diseases in france. *Foods* 9, 1644. <https://doi.org/10.3390/FOODS9111644>
- Beardsley, E., 2009. In Europe, A Cow Over Hormone-Treated U.S. Beef. [WWW Document]. NPR. URL <https://www.npr.org/templates/story/story.php?storyId=113314725> (accessed 3.30.23).
- Bell, A.W., Charmley, E., Hunter, R.A., Archer, J.A., 2011. The Australasian beef industries— Challenges and opportunities in the 21st century. *Anim. Front.* 1, 10–19. <https://doi.org/10.2527/AF.2011-0015>
- Beloin, C., Michaelis, K., Lindner, K., Landini, P., Hacker, J., Ghigo, J.M., Dobrindt, U., 2006. The transcriptional antiterminator RfaH represses biofilm formation in *Escherichia coli*. *J. Bacteriol.* 188, 1316–1331. <https://doi.org/10.1128/JB.188.4.1316-1331.2006>
- Beloin, C., Roux, A., Ghigo, J.M., 2008. *Escherichia coli* biofilms, in: Romeo, T. (Ed.), *Bacterial Biofilms. Current Topics in Microbiology and Immunology*. Springer, Berlin, Heidelberg., pp. 249–289. https://doi.org/10.1007/978-3-540-75418-3_12

- Bimmer, M., Mientus, M., Klingl, A., Ehrenreich, A., Liebl, W., 2022. The roles of the various cellulose biosynthesis operons in *Komagataeibacter hansenii* ATCC 23769. *Appl. Environ. Microbiol.* 88. <https://doi.org/10.1128/AEM.02460-21>
- Bjørge Thomassen, G.M., Krych, L., Knøchel, S., Mehli, L., 2023. Bacterial community development and diversity during the first year of production in a new salmon processing plant. *Food Microbiol.* 109, 104138. <https://doi.org/10.1016/J.FM.2022.104138>
- Bleich, R., Watrous, J.D., Dorrestein, P.C., Bowers, A.A., Shank, E.A., 2015. Thiopeptide antibiotics stimulate biofilm formation in *Bacillus subtilis*. *Proc. Natl. Acad. Sci. U. S. A.* 112, 3086–3091. https://doi.org/10.1073/PNAS.1414272112/SUPPL_FILE/PNAS.201414272SI.PDF
- Bojer, M.S., Struve, C., Ingmer, H., Hansen, D.S., Krogfelt, K.A., 2010. Heat resistance mediated by a new plasmid encoded Clp ATPase, ClpK, as a possible novel mechanism for nosocomial persistence of *Klebsiella pneumoniae*. *PLoS One* 5, e15467. <https://doi.org/10.1371/journal.pone.0015467>
- Bokulich, N.A., Mills, D.A., 2013. Facility-specific “house” microbiome drives microbial landscapes of artisan cheesemaking plants. *Appl. Environ. Microbiol.* 79, 5214–5223. <https://doi.org/10.1128/AEM.00934-13>
- Boll, E.J., Marti, R., Hasman, H., Overballe-Petersen, S., Stegger, M., Ng, K., Knøchel, S., Krogfelt, K.A., Hummerjohann, J., Struve, C., 2017. Turn up the heat - food and clinical *Escherichia coli* isolates feature two transferrable loci of heat resistance. *Front. Microbiol.* 8, 579. <https://doi.org/10.3389/fmicb.2017.00579>
- Bolten, S., Ralyea, R.D., Lott, T.T., Orsi, R.H., Martin, N.H., Wiedmann, M., Trmcic, A., 2024.

- Utilizing whole genome sequencing to characterize *Listeria* spp. persistence and transmission patterns in a farmstead dairy processing facility and its associated farm environment. *J. Dairy Sci.* in press. <https://doi.org/10.3168/JDS.2024-24789>
- Bonenfant, Q., Noe, L., Touzet, H., 2023. Porechop_ABI: discovering unknown adapters in Oxford Nanopore Technology sequencing reads for downstream trimming. *Bioinforma. Adv.* 3, vbac085. <https://doi.org/10.1093/BIOADV/VBAC085>
- Borrusso, P.A., Quinlan, J.J., 2017. Prevalence of pathogens and indicator organisms in home kitchens and correlation with unsafe food handling practices and conditions. *J. Food Prot.* 80, 590–597. <https://doi.org/10.4315/0362-028X.JFP-16-354>
- Bosilevac, J.M., Guragain, M., Barkhouse, D.A., Velez, S.E., Katz, T.S., Lu, G., Wang, R., 2024. Impact of intense sanitization procedures on bacterial communities recovered from floor drains in pork processing plants. *Front. Microbiol.* 15. <https://doi.org/10.3389/FMICB.2024.1379203/FULL>
- Bottichio, L., Keaton, A., Thomas, D., Fulton, T., Tiffany, A., Frick, A., Mattioli, M., Kahler, A., Murphy, J., Otto, M., Tesfai, A., Fields, A., Kline, K., Fiddner, J., Higa, J., Barnes, A., Arroyo, F., Salvatierra, A., Holland, A., Taylor, W., Nash, J., Morawski, B.M., Correll, S., Hinnenkamp, R., Havens, J., Patel, K., Schroeder, M.N., Gladney, L., Martin, H., Whitlock, L., Dowell, N., Newhart, C., Watkins, L.F., Hill, V., Lance, S., Harris, S., Wise, M., Williams, I., Basler, C., Gieraltowski, L., 2020. Shiga Toxin–Producing *Escherichia coli* Infections Associated With Romaine Lettuce—United States, 2018. *Clin. Infect. Dis.* 71, e323. <https://doi.org/10.1093/CID/CIZ1182>
- Bouchez, A., De Vuyst, L., 2022. Acetic acid bacteria in sour beer production: friend or foe? *Front.*

Microbiol. 0, 2490. <https://doi.org/10.3389/FMICB.2022.957167>

Branda, S.S., González-Pastor, J.E., Ben-Yehuda, S., Losick, R., Kolter, R., 2001. Fruiting body formation by *Bacillus subtilis*. Proc. Natl. Acad. Sci. U. S. A. 98, 11621–11626. <https://doi.org/10.1073/pnas.191384198>

Branda, S.S., González-Pastor, J.E., Dervyn, E., Dusko Ehrlich, S., Losick, R., Kolter, R., 2004. Genes involved in formation of structured multicellular communities by *Bacillus subtilis*. J. Bacteriol. 186, 3970–3979. <https://doi.org/10.1128/JB.186.12.3970-3979.2004>

Bridier, A., Briandet, R., Thomas, V., Dubois-Brissonnet, F., 2011. Resistance of bacterial biofilms to disinfectants: a review. Biofouling 27, 1017–1032. <https://doi.org/10.1080/08927014.2011.626899>

Brightwell, G., Boerema, J., Mills, J., Mowat, E., Pulford, D., 2006. Identifying the bacterial community on the surface of Intralox™ belting in a meat boning room by culture-dependent and culture-independent 16S rDNA sequence analysis. Int. J. Food Microbiol. 109, 47–53. <https://doi.org/10.1016/J.IJFOODMICRO.2006.01.008>

Brightwell, G., Broda, D.M., Boerema, J.A., 2009. Sources of psychrophilic and psychrotolerant clostridia causing spoilage of vacuum-packed chilled meats, as determined by PCR amplification procedure. J. Appl. Microbiol. 107, 178–186. <https://doi.org/10.1111/J.1365-2672.2009.04193.X>

Brynildsrud, O., Bohlin, J., Scheffer, L., Eldholm, V., 2016. Rapid scoring of genes in microbial pan-genome-wide association studies with Scoary. Genome Biol. 17, 1–9. <https://doi.org/10.1186/s13059-016-1108-8>

Burmølle, M., Ren, D., Bjarnsholt, T., Sørensen, S.J., 2014. Interactions in multispecies biofilms:

do they actually matter? *Trends Microbiol.* 22, 84–91.
<https://doi.org/10.1016/j.tim.2013.12.004>

Burmølle, M., Webb, J.S., Rao, D., Hansen, L.H., Sørensen, S.J., Kjelleberg, S., 2006. Enhanced biofilm formation and increased resistance to antimicrobial agents and bacterial invasion are caused by synergistic interactions in multispecies biofilms. *Appl. Environ. Microbiol.* 72, 3916–3923. <https://doi.org/10.1128/AEM.03022-05>

Calasso, M., Ercolini, D., Mancini, L., Stellato, G., Minervini, F., Di Cagno, R., De Angelis, M., Gobbetti, M., 2016. Relationships among house, rind and core microbiotas during manufacture of traditional Italian cheeses at the same dairy plant. *Food Microbiol.* 54, 115–126. <https://doi.org/10.1016/J.FM.2015.10.008>

Canadian Food Inspection Agency, 2018. Handling of Meat Products - Archived - Chapter 4 - Meat Processing Controls and Procedures - Food safety for industry - Canadian Food Inspection Agency [WWW Document]. URL <https://inspection.canada.ca/food-safety-for-industry/archived-food-guidance/meat-and-poultry-products/manual-of-procedures/chapter-4/eng/1367622697439/1367622787568?chap=4> (accessed 3.30.23).

Canadian Food Inspection Agency, 2012. Food Safety Facts on Scombroid Poisoning - Canadian Food Inspection Agency [WWW Document]. URL <http://www.inspection.gc.ca/food/information-for-consumers/fact-sheets-and-infographics/food-poisoning/scombroid/eng/1332280657698/1332280735024> (accessed 4.17.23).

Capella-Gutiérrez, S., Silla-Martínez, J.M., Gabaldón, T., 2009. TrimAl: a tool for automated alignment trimming in large-scale phylogenetic analyses. *Bioinformatics* 25, 1972–1973.

<https://doi.org/10.1093/bioinformatics/btp348>

- Casaburi, A., Nasi, A., Ferrocino, I., Di Monaco, R., Mauriello, G., Villani, F., Ercolini, D., 2011. Spoilage-related activity of *Carnobacterium maltaromaticum* strains in air-stored and vacuum-packed meat. *Appl. Environ. Microbiol.* 77, 7382–7393. <https://doi.org/10.1128/AEM.05304-11>
- Case, R.J., Labbate, M., Kjelleberg, S., 2008. AHL-driven quorum-sensing circuits: their frequency and function among the Proteobacteria. *ISME J.* 2008 24 2, 345–349. <https://doi.org/10.1038/ismej.2008.13>
- Cauchie, E., Delhalle, L., Taminiou, B., Tahiri, A., Korsak, N., Burteau, S., Fall, P.A., Farnir, F., Baré, G., Daube, G., 2020. Assessment of spoilage bacterial communities in food wrap and modified atmospheres-packed minced pork meat samples by 16S rDNA metagenetic analysis. *Front. Microbiol.* 10, 483567. <https://doi.org/10.3389/FMICB.2019.03074/BIBTEX>
- Chabane, Y.N., Marti, S., Rihouey, C., Alexandre, S., Hardouin, J., Lesouhaitier, O., Vila, J., Kaplan, J.B., Jouenne, T., Dé, E., 2014. Characterisation of pellicles formed by *Acinetobacter baumannii* at the air-liquid interface. *PLoS One* 9. <https://doi.org/10.1371/journal.pone.0111660>
- Chaillou, S., Chaulot-Talmon, A., Caekebeke, H., Cardinal, M., Christieans, S., Denis, C., Hélène Desmonts, M., Dousset, X., Feurer, C., Hamon, E., Joffraud, J.J., La Carbona, S., Leroi, F., Leroy, S., Lorre, S., Macé, S., Pilet, M.F., Prévost, H., Rivollier, M., Roux, D., Talon, R., Zagorec, M., Champomier-Vergès, M.C., 2015. Origin and ecological selection of core and food-specific bacterial communities associated with meat and seafood spoilage. *ISME J.* 9, 1105–1118. <https://doi.org/10.1038/ISMEJ.2014.202>

- Chatterjee, D., Cooley, R.B., Boyd, C.D., Mehl, R.A., O'Toole, G.A., Sondermann, H., 2014. Mechanistic insight into the conserved allosteric regulation of periplasmic proteolysis by the signaling molecule cyclic-di-GMP. *Elife* 3, 1–29. <https://doi.org/10.7554/ELIFE.03650>
- Chaumeil, P.A., Mussig, A.J., Hugenholtz, P., Parks, D.H., 2022. GTDB-Tk v2: memory friendly classification with the genome taxonomy database. *Bioinformatics* 38, 5315–5316. <https://doi.org/10.1093/BIOINFORMATICS/BTAC672>
- Chitlapilly Dass, S., Bosilevac, J.M., Weinroth, M., Elowsky, C.G., Zhou, Y., Anandappa, A., Wang, R., 2020. Impact of mixed biofilm formation with environmental microorganisms on *E. coli* O157:H7 survival against sanitization. *npj Sci. Food* 4, 1–9. <https://doi.org/10.1038/s41538-020-00076-x>
- Chun, J., Oren, A., Ventosa, A., Christensen, H., Arahal, D.R., da Costa, M.S., Rooney, A.P., Yi, H., Xu, X.W., De Meyer, S., Trujillo, M.E., 2018. Proposed minimal standards for the use of genome data for the taxonomy of prokaryotes. *Int. J. Syst. Evol. Microbiol.* 68, 461–466. <https://doi.org/10.1099/ijsem.0.002516>
- Clottey, S.J.A., 1985. Manual for the slaughter of small ruminants in developing countries. [WWW Document]. FAO Anim. Prod. Heal. Pap. URL <http://www.fao.org/3/x6552e/X6552E00.htm#TOC> (accessed 7.21.24).
- Cobo-Díaz, J.F., Alvarez-Molina, A., Alexa, E.A., Walsh, C.J., Mencía-Ares, O., Puente-Gómez, P., Likotrafiti, E., Fernández-Gómez, P., Prieto, B., Crispie, F., Ruiz, L., González-Raurich, M., López, M., Prieto, M., Cotter, P., Alvarez-Ordóñez, A., 2021. Microbial colonization and resistome dynamics in food processing environments of a newly opened pork cutting industry during 1.5 years of activity. *Microbiome* 9, 1–19. <https://doi.org/10.1186/S40168-021-01131->

- Culler, H.F., Couto, S.C.F., Higa, J.S., Ruiz, R.M., Yang, M.J., Bueris, V., Franzolin, M.R., Sircili, M.P., 2018. Role of SdiA on biofilm formation by atypical enteropathogenic *Escherichia coli*. *Genes (Basel)*. 9. <https://doi.org/10.3390/GENES9050253>
- Cunliffe, M., Engel, A., Frka, S., Gašparović, B.Ž., Guitart, C., Murrell, J.C., Salter, M., Stolle, C., Upstill-Goddard, R., Wurl, O., 2013. Sea surface microlayers: a unified physicochemical and biological perspective of the air–ocean interface. *Prog. Oceanogr.* 109, 104–116. <https://doi.org/10.1016/J.POCEAN.2012.08.004>
- Daeschel, D., Pettengill, J.B., Wang, Y., Chen, Y., Allard, M., Snyder, A.B., 2022. Genomic analysis of *Listeria monocytogenes* from US food processing environments reveals a high prevalence of QAC efflux genes but limited evidence of their contribution to environmental persistence. *BMC Genomics* 23, 488. <https://doi.org/10.1186/s12864-022-08695-2>
- Dai, T., Wen, D., Bates, C.T., Wu, L., Guo, X., Liu, S., Su, Y., Lei, J., Zhou, J., Yang, Y., 2022. Nutrient supply controls the linkage between species abundance and ecological interactions in marine bacterial communities. *Nat. Commun.* 2022 131 13, 1–9. <https://doi.org/10.1038/s41467-021-27857-6>
- Darriba, Di., Posada, D., Kozlov, A.M., Stamatakis, A., Morel, B., Flouri, T., 2020. ModelTest-NG: A new and scalable tool for the selection of DNA and protein evolutionary models. *Mol. Biol. Evol.* 37, 291–294. <https://doi.org/10.1093/MOLBEV/MSZ189>
- Davis, S., Pettengill, J.B., Luo, Y., Payne, J., Shpuntoff, A., Rand, H., Strain, E., 2015. CFSAN SNP pipeline: An automated method for constructing snp matrices from next-generation sequence data. *PeerJ Comput. Sci.* 2015, e20. <https://doi.org/10.7717/PEERJ-CS.20/SUPP-1>

- De Coster, W., Rademakers, R., 2023. NanoPack2: population-scale evaluation of long-read sequencing data. *Bioinformatics* 39, btad311. <https://doi.org/10.1093/BIOINFORMATICS/BTAD311>
- De Filippis, F., La Stora, A., Villani, F., Ercolini, D., 2013. Exploring the Sources of Bacterial Spoilers in Beefsteaks by Culture-Independent High-Throughput Sequencing. *PLoS One* 8, 70222. <https://doi.org/10.1371/journal.pone.0070222>
- De Filippis, F., Valentino, V., Alvarez-Ordóñez, A., Cotter, P.D., Ercolini, D., 2021. Environmental microbiome mapping as a strategy to improve quality and safety in the food industry. *Curr. Opin. Food Sci.* 38, 168–176. <https://doi.org/10.1016/J.COFS.2020.11.012>
- Dhaliwal, H.K., Yang, X., Roopesh, M.S., 2024. Continuous production and recirculation of plasma-activated water bubbles under different flow regimes for mixed-species bacterial biofilm inactivation inside pipelines. *J. Food Saf.* 44, e13128. <https://doi.org/10.1111/JFS.13128>
- Dickson, J.S., Anderson, M.E., 1992. Microbiological Decontamination of Food Animal Carcasses by Washing and Sanitizing Systems: A Review. *J. Food Prot.* 55, 360–366.
- Dien, L.T., Linh, N., Sangpo, P., Senapin, S., St-Hilaire, S., Rodkhum, C., Dong, H., 2021. Ozone nanobubble treatments improve survivability of Nile tilapia (*Oreochromis niloticus*) challenged with a pathogenic multi-drug-resistant *Aeromonas hydrophila*. *J. Fish Dis.* 44, 1435–1447. <https://doi.org/10.1111/JFD.13451>
- Diggle, S.P., Matthijs, S., Wright, V.J., Fletcher, M.P., Chhabra, S.R., Lamont, I.L., Kong, X., Hider, R.C., Cornelis, P., Cámara, M., Williams, P., 2007. The *Pseudomonas aeruginosa* 4-Quinolone Signal Molecules HHQ and PQS Play Multifunctional Roles in Quorum Sensing

and Iron Entrapment. Chem. Biol. 14, 87–96.
<https://doi.org/10.1016/J.CHEMBIOL.2006.11.014>

Dlusskaya, E.A., McMullen, L.M., Gänzle, M.G., 2011. Characterization of an extremely heat-resistant *Escherichia coli* obtained from a beef processing facility. J. Appl. Microbiol. 110, 840–849. <https://doi.org/10.1111/j.1365-2672.2011.04943.x>

Dodd, C.E.R., 2014. *Pseudomonas* | Introduction. Encycl. Food Microbiol. Second Ed. 244–247.
<https://doi.org/10.1016/B978-0-12-384730-0.00282-2>

Donlan, R.M., 2000. Role of biofilms in antimicrobial resistance. ASAIO J. 46, S47-52.

Dubey, P., Singh, A., Yousuf, O., 2022. Ozonation: an evolving disinfectant technology for the food industry. Food Bioprocess Technol. 15, 2102–2113. <https://doi.org/10.1007/S11947-022-02876-3/TABLES/2>

Dugan, H.A., Woolway, R.I., Santoso, A.B., Corman, J.R., Jaimes, A., Nodine, E.R., Patil, V.P., Zwart, J.A., Brentrup, J.A., Hetherington, A.L., Oliver, S.K., Read, J.S., Winters, K.M., Hanson, P.C., Read, E.K., Winslow, L.A., Weathers, K.C., 2016. Consequences of gas flux model choice on the interpretation of metabolic balance across 15 lakes. Inl. Waters 6, 581–592. <https://doi.org/10.1080/IW-6.4.836>

Dutta, V., Elhanafi, D., Kathariou, S., 2013. Conservation and Distribution of the Benzalkonium Chloride Resistance Cassette *bcrABC* in *Listeria monocytogenes*. Appl. Environ. Microbiol. <https://doi.org/10.1128/AEM.01751-13>

Dzieciol, M., Schornsteiner, E., Muhterem-Uyar, M., Stessl, B., Wagner, M., Schmitz-Esser, S., 2016. Bacterial diversity of floor drain biofilms and drain waters in a *Listeria monocytogenes* contaminated food processing environment. Int. J. Food Microbiol. 223, 33–40.

<https://doi.org/10.1016/J.IJFOODMICRO.2016.02.004>

Elias, S., Banin, E., 2012. Multi-species biofilms: living with friendly neighbors. *FEMS Microbiol.*

Rev. 36, 990–1004. <https://doi.org/10.1111/j.1574-6976.2012.00325.x>

Ellerbroek, L., 1997. Airborne microflora in poultry slaughtering establishments. *Food Microbiol.*

14, 527–531. <https://doi.org/10.1006/FMIC.1997.0119>

Enos-Berlage, J.L., Guvener, Z.T., Keenan, C.E., McCarter, L.L., 2005. Genetic determinants of

biofilm development of opaque and translucent *Vibrio parahaemolyticus*. *Mol. Microbiol.* 55,

1160–1182. <https://doi.org/10.1111/J.1365-2958.2004.04453.X>

Escobar-Muciño, E., Arenas-Hernández, M.M.P., Luna-Guevara, M.L., 2022. Mechanisms of inhibition of quorum sensing as an alternative for the control of *E. coli* and *Salmonella*.

Microorg. 2022, Vol. 10, Page 884 10, 884.

<https://doi.org/10.3390/MICROORGANISMS10050884>

Estrada, E.M., Harris, L.J., 2024. Phenotypic characteristics that may contribute to persistence of

Salmonella strains in the pistachio supply chain. *J. Food Prot.* 87, 100268.

<https://doi.org/10.1016/J.JFP.2024.100268>

Evans, E.W., Redmond, E.C., 2019. Domestic Kitchen Microbiological Contamination and Self-

Reported Food Hygiene Practices of Older Adult Consumers. *J. Food Prot.* 82, 1326–1335.

<https://doi.org/10.4315/0362-028X.JFP-18-533>

Fagerlund, A., Langsrud, S., Møretrø, T., 2021. Microbial diversity and ecology of biofilms in

food industry environments associated with *Listeria monocytogenes* persistence. *Curr. Opin.*

Food Sci. 37, 171–178. <https://doi.org/10.1016/J.COFS.2020.10.015>

Fagerlund, A., Møretrø, T., Heir, E., Briandet, R., Langsrud, S., 2017. Cleaning and disinfection

- of biofilms composed of *Listeria monocytogenes* and background microbiota from meat processing surfaces. *Appl. Environ. Microbiol.* 83, e01046-17. <https://doi.org/10.1128/AEM.01046-17>
- Falà, A.K., Álvarez-Ordóñez, A., Filloux, A., Gahan, C.G.M., Cotter, P.D., 2022. Quorum sensing in human gut and food microbiomes: Significance and potential for therapeutic targeting. *Front. Microbiol.* 13, 1002185. <https://doi.org/10.3389/FMICB.2022.1002185/BIBTEX>
- Falardeau, J., Keeney, K., Trmčić, A., Kitts, D., Wang, S., 2019. Farm-to-fork profiling of bacterial communities associated with an artisan cheese production facility. *Food Microbiol.* 83, 48–58. <https://doi.org/10.1016/J.FM.2019.04.002>
- FAO, 2015. Food loss and wastes facts.
- FAO, 2009. How to Feed the World in 2050 2050, 1–35.
- FDA, 2024. Southwest Agricultural Region Environmental Microbiology Study (2019 – 2024) [WWW Document]. URL <https://www.fda.gov/food/environmental-studies/southwest-agricultural-region-environmental-microbiology-study-2019-2024> (accessed 7.23.24).
- FDA, 2017. Control of *Listeria monocytogenes* in ready-to-eat foods: guidance for industry [WWW Document]. URL <https://www.fda.gov/regulatory-information/search-fda-guidance-documents/draft-guidance-industry-control-listeria-monocytogenes-ready-eat-foods> (accessed 5.16.24).
- Ferreira, V., Barbosa, J., Stasiewicz, M., Vongkamjan, K., Switt, A.M., Hogg, T., Gibbs, P., Teixeira, P., Wiedmann, M., 2011. Diverse geno- and phenotypes of persistent *Listeria monocytogenes* isolates from fermented meat sausage production facilities in Portugal. *Appl. Environ. Microbiol.* 77, 2701–2715. <https://doi.org/10.1128/AEM.02553-10>

- Ferreira, V., Wiedmann, M., Teixeira, P., Stasiewicz, M.J., 2014. *Listeria monocytogenes* persistence in food-associated environments: Epidemiology, strain characteristics, and implications for public health. *J. Food Prot.* 77, 150–170. <https://doi.org/10.4315/0362-028X.JFP-13-150>
- Fic, E., Bonarek, P., Gorecki, A., Kedracka-Krok, S., Mikolajczak, J., Polit, A., Tworzydło, M., Dziedzicka-Wasylewska, M., Wasylewski, Z., 2009. CAMP receptor protein from *Escherichia coli* as a model of signal transduction in proteins - A review. *J. Mol. Microbiol. Biotechnol.* 17, 1–11. <https://doi.org/10.1159/000178014>
- Fiebig, A., 2019. Role of *Caulobacter* cell surface structures in colonization of the air-liquid interface. *J. Bacteriol.* 201. <https://doi.org/10.1128/JB.00064-19>
- Flemming, H.-C., Wingender, J., 2010. The biofilm matrix. *Nat. Rev. Microbiol.* 2010 89 8, 623–633. <https://doi.org/10.1038/nrmicro2415>
- Flemming, H.-C., Wingender, J., Szewzyk, U., Steinberg, P., Rice, S.A., Kjelleberg, S., 2016. Biofilms: an emergent form of bacterial life. *Nat Rev Microbiol* 14, 563–575. <https://doi.org/10.1038/nrmicro.2016.94>
- Forquin, M.P., Weimer, B.C., 2014. *Brevibacterium*. *Encycl. Food Microbiol.* Second Ed. 324–330. <https://doi.org/10.1016/B978-0-12-384730-0.00047-1>
- Forster, S.C., Kumar, N., Anonye, B.O., Almeida, A., Viciani, E., Stares, M.D., Dunn, M., Mkandawire, T.T., Zhu, A., Shao, Y., Pike, L.J., Louie, T., Browne, H.P., Mitchell, A.L., Neville, B.A., Finn, R.D., Lawley, T.D., 2019. A human gut bacterial genome and culture collection for improved metagenomic analyses. *Nat. Biotechnol.* 37, 186–192. <https://doi.org/10.1038/s41587-018-0009-7>

- Fox, E.M., Solomon, K., Moore, J.E., Wall, P.G., Fanning, S., 2014. Phylogenetic profiles of in-house microflora in drains at a food production facility: Comparison and biocontrol implications of *Listeria*-positive and -negative bacterial populations. *Appl. Environ. Microbiol.* 80, 3369–3374. <https://doi.org/10.1128/AEM.00468-14>
- Freitas, B. de O., Leite, L. de S., Daniel, L.A., 2021. Chlorine and peracetic acid in decentralized wastewater treatment: Disinfection, oxidation and odor control [WWW Document]. *Process Saf. Environ. Prot.* <https://doi.org/10.1016/j.psep.2020.11.047>
- Gajdosova, J., Benedikovicova, K., Kamodyova, N., Tothova, L., Kaclikova, E., Stuchlik, S., Turna, J., Drahovska, H., 2011. Analysis of the DNA region mediating increased thermotolerance at 58 °C in *Cronobacter* sp. and other enterobacterial strains. *Antonie Van Leeuwenhoek* 100, 279–289.
- Galié, S., García-Gutiérrez, C., Miguélez, E.M., Villar, C.J., Lombó, F., 2018. Biofilms in the food industry: health aspects and control methods. *Front. Microbiol.* 9, 898-undefined. <https://doi.org/10.3389/fmicb.2018.00898>
- Gänzle, M., Ripari, V., 2016. Composition and function of sourdough microbiota: From ecological theory to bread quality. *Int. J. Food Microbiol.* 239, 19–25. <https://doi.org/10.1016/j.ijfoodmicro.2016.05.004>
- Gao, Y., Francis, K., Zhang, X., 2022. Review on formation of cold plasma activated water (PAW) and the applications in food and agriculture. *Food Res. Int.* 157, 111246. <https://doi.org/10.1016/J.FOODRES.2022.111246>
- García-López, M.L., Santos, J.A., Otero, A., Rodríguez-Calleja, J.M., 2014. *Psychrobacter*. *Encycl. Food Microbiol.* Second Ed. 261–268. <https://doi.org/10.1016/B978-0-12-384730->

0.00285-8

García, G., Girón, J.A., Yañez, J.A., Cedillo, M.L., 2022. *Stenotrophomonas maltophilia* and Its Ability to Form Biofilms. *Microbiol. Res. (Pavia)*. 14, 1–20. <https://doi.org/10.3390/MICROBIOLRES14010001>

Gayán, E., Wang, Z., Salvador, M., Gänzle, M.G., Aertsen, A., 2023. Dynamics of high hydrostatic pressure resistance development in RpoS-deficient *Escherichia coli*. *Food Res. Int.* 164, 112280. <https://doi.org/10.1016/J.FOODRES.2022.112280>

Gill, C.O., 2014. Spoilage Factors Affecting | Microbiological. *Encycl. Meat Sci.* 388–393. <https://doi.org/10.1016/B978-0-12-384731-7.00090-8>

Gill, C.O., 2005. Sources of microbial contamination at slaughtering plants. *Improv. Saf. Fresh Meat* 231–243. <https://doi.org/10.1533/9781845691028.2.231>

Giménez, B., Graiver, N., Giannuzzi, L., Zaritzky, N., 2021. Treatment of beef with gaseous ozone: Physicochemical aspects and antimicrobial effects on heterotrophic microflora and *Listeria monocytogenes*. *Food Control* 121, 107602. <https://doi.org/10.1016/J.FOODCONT.2020.107602>

Giménez, B., Zaritzky, N., Graiver, N., 2024. Ozone treatment of meat and meat products: a review. *Front. Food Sci. Technol.* 4, 1351801. <https://doi.org/10.3389/FRFST.2024.1351801>

Girard, L., Lood, C., Höfte, M., Vandamme, P., Rokni-Zadeh, H., van Noort, V., Lavigne, R., De Mot, R., 2021. The Ever-Expanding *Pseudomonas* Genus: Description of 43 New Species and Partition of the *Pseudomonas putida* Group. *Microorganisms* 9. <https://doi.org/10.3390/MICROORGANISMS9081766>

Gobbetti, M., Rizzello, C.G., 2014. *Arthrobacter*. *Encycl. Food Microbiol.* Second Ed. 69–76.

<https://doi.org/10.1016/B978-0-12-384730-0.00009-4>

Golub, S.R., Overton, T.W., 2021. Pellicle formation by *Escherichia coli* K-12: role of adhesins and motility. *J. Biosci. Bioeng.* 131, 381–389. <https://doi.org/10.1016/j.jbiosc.2020.12.002>

Government of Alberta, 2013. Antimicrobial spray treatment of red meat in small abattoirs.

Gu, G., Ottesen, A., Bolten, S., Wang, L., Luo, Y., Rideout, S., Lyu, S., Nou, X., 2019. Impact of routine sanitation on the microbiomes in a fresh produce processing facility. *Int. J. Food Microbiol.* 294, 31–41. <https://doi.org/10.1016/J.IJFOODMICRO.2019.02.002>

Guobjörnsdóttir, B., Einarsson, H., Thorkelsson, G., 2005. Microbial adhesion to processing lines for fish fillets and cooked shrimp: Influence of stainless steel surface finish and presence of gram-negative bacteria on the attachment of *listeria monocytogenes* [WWW Document]. *Food Technol. Biotechnol.* URL <https://www.semanticscholar.org/paper/Microbial-Adhesion-to-Processing-Lines-for-Fish-and-Guðbjörnsdóttir-Einarsson/fadff0fa2c1cb195e40460ce8176a7d6bc0d8a7c> (accessed 1.26.23).

Guragain, M., Brichta-Harhay, D.M., Bono, J.L., Bosilevac, J.M., 2021. Locus of heat resistance (LHR) in meat-borne *Escherichia coli*: screening and genetic characterization. *Appl. Environ. Microbiol.* 87, e02343-20-undefined. <https://doi.org/10.1128/AEM.02343-20>

Guragain, M., Schmidt, J.W., Dickey, A.M., Bosilevac, J.M., 2023. Distribution of Extremely Heat-Resistant *Escherichia coli* in the Beef Production and Processing Continuum. *J. Food Prot.* 86, 100031. <https://doi.org/10.1016/J.JFP.2022.100031>

Gutiérrez, D., Delgado, S., Vázquez-Sánchez, D., Martínez, B., Cabo, M.L., Rodríguez, A., Herrera, J.J., García, P., 2012. Incidence of *staphylococcus aureus* and analysis of associated bacterial communities on food industry surfaces. *Appl. Environ. Microbiol.* 78, 8547–8554.

<https://doi.org/10.1128/AEM.02045-12/ASSET/E7F95824-1A50-4098-9CF4-74052E0BE500/ASSETS/GRAPHIC/ZAM9991039070002.JPEG>

- Guzzon, R., Carafa, I., Tuohy, K., Cervantes, G., Verneti, L., Barmaz, A., Larcher, R., Franciosi, E., 2017. Exploring the microbiota of the red-brown defect in smear-ripened cheese by 454-pyrosequencing and its prevention using different cleaning systems. *Food Microbiol.* 62, 160–168. <https://doi.org/10.1016/J.FM.2016.10.018>
- Hadjifrangiskou, M., Gu, A.P., Pinkner, J.S., Kostakioti, M., Zhang, E.W., Greene, S.E., Hultgren, S.J., 2012. Transposon mutagenesis identifies uropathogenic *Escherichia coli* biofilm factors. *J. Bacteriol.* 194, 6195–6205. <https://doi.org/10.1128/JB.01012-12>
- Hall, M.B., Rabodoarivelo, M.S., Koch, A., Dippenaar, A., George, S., Grobbelaar, M., Warren, R., Walker, T.M., Cox, H., Gagneux, S., Crook, D., Peto, T., Rakotosamimanana, N., Grandjean Lapierre, S., Iqbal, Z., 2023. Evaluation of Nanopore sequencing for *Mycobacterium tuberculosis* drug susceptibility testing and outbreak investigation: A genomic analysis. *The Lancet Microbe* 4, e84–e92. [https://doi.org/10.1016/S2666-5247\(22\)00301-9](https://doi.org/10.1016/S2666-5247(22)00301-9)
- Harhay, D., Brader, K.D., Bono, J., Harhay, G.P., Bosilevac, M., Katz, T.S., 2024. Protocol for Identifying Highly Pathogenic *Salmonella* Using the HPS Multiplex PCR Assay [WWW Document]. *Protocols.io*. <https://doi.org/dx.doi.org/10.17504/protocols.io.6qpvr3on3vmk/v1>
- Harrand, A.S., Jagadeesan, B., Baert, L., Wiedmann, M., Orsi, R.H., Dudley, E.G., 2020. Evolution of *Listeria monocytogenes* in a food processing plant involves limited single-nucleotide substitutions but considerable diversification by gain and loss of prophages. *Appl. Environ. Microbiol.* 86, e02493-19.

- Harter, E., Wagner, E.M., Zaiser, A., Halecker, S., Wagner, M., Rychli, K., 2017. Stress survival islet 2, predominantly present in *Listeria monocytogenes* strains of sequence type 121, is involved in the alkaline and oxidative stress responses. *Appl. Environ. Microbiol.* 83. <https://doi.org/10.1128/AEM.00827-17>
- Hassan, A.N., Frank, J.F., 2011. Microorganisms Associated With Milk. *Encycl. Dairy Sci.* Second Ed. 447–457. <https://doi.org/10.1016/B978-0-12-374407-4.00309-5>
- Hauge, S.J., Bjørkøy, S., Holthe, J., Røtterud, O.J., Skjerve, E., Midtsian, M., Lian, I., Alvseike, O., Nagel-Alne, G.E., 2023. Assessment of in-plant decontamination of broiler carcasses by immersion in hot water and lactic acid in Norway. *Food Control* 152, 109873. <https://doi.org/10.1016/J.FOODCONT.2023.109873>
- Hölscher, T., Bartels, B., Lin, Y.-C., Gallegos-Monterrosa, R., Price-Whelan, A., Kolter, R., Dietrich, L.E.P., Kovács, Á.T., 2015. Motility, chemotaxis and aerotaxis contribute to competitiveness during bacterial pellicle biofilm development HHS Public Access. *J Mol Biol* 427, 3695–3708. <https://doi.org/10.1016/j.jmb.2015.06.014>
- Holt, R.D., 2009. Bringing the Hutchinsonian niche into the 21st century: ecological and evolutionary perspectives. *Proc. Natl. Acad. Sci.* 106, 19659–19665.
- Hufnagel, D.A., Evans, M.L., Greene, S.E., Pinkner, J.S., Hultgren, S.J., Chapman, M.R., 2016. The catabolite repressor protein-cyclic AMP complex regulates *csgD* and biofilm formation in uropathogenic *Escherichia coli*. *J. Bacteriol.* 198, 3329–3334. https://doi.org/10.1128/JB.00652-16/SUPPL_FILE/ZJB999094261SO5.PDF
- Hugas, M., Tsigarida, E., 2008. Pros and cons of carcass decontamination: The role of the European Food Safety Authority. *Meat Sci.* 78, 43–52.

<https://doi.org/10.1016/j.meatsci.2007.09.001>

- Hultman, J., Johansson, P., Björkroth, J., Drake, H.L., 2020. Longitudinal metatranscriptomic analysis of a meat spoilage microbiome detects abundant continued fermentation and environmental stress responses during shelf life and beyond. *Appl. Environ. Microbiol.* 86, e01575-20. <https://doi.org/10.1128/AEM.01575-20>
- Hultman, J., Rahkila, R., Ali, J., Rousu, J., Björkroth, K.J., 2015. Meat processing plant microbiome and contamination patterns of cold-tolerant bacteria causing food safety and spoilage risks in the manufacture of vacuum-packaged cooked sausages. *Appl. Environ. Microbiol.* 81, 7088–7097. <https://doi.org/10.1128/AEM.02228-15>
- Hung, C., Zhou, Y., Pinkner, J.S., Dodson, K.W., Crowley, J.R., Heuser, J., Chapman, M.R., Hadjifrangiskou, M., Henderson, J.P., Hultgren, S.J., 2013. *Escherichia coli* biofilms have an organized and complex extracellular matrix structure. *MBio* 4, 645–658. <https://doi.org/10.1128/mBio.00645-13>
- Illikoud, N., Gohier, R., Werner, D., Barrachina, C., Roche, D., Jaffrès, E., Zagorec, M., 2019. Transcriptome and Volatilome Analysis During Growth of *Brochothrix thermosphacta* in Food: Role of Food Substrate and Strain Specificity for the Expression of Spoilage Functions. *Front. Microbiol.* 10, 2527. <https://doi.org/10.3389/FMICB.2019.02527>
- Iulietto, M.F., Sechi, P., Borgogni, E., Cenci-Goga, B.T., 2015. Meat Spoilage: A critical review of a neglected alteration due to ropy slime producing bacteria. *Ital. J. Anim. Sci.* 14, 316–326. <https://doi.org/10.4081/IJAS.2015.4011>
- Jääskeläinen, E., Hultman, J., Parshintsev, J., Riekkola, M.L., Björkroth, J., 2016. Development of spoilage bacterial community and volatile compounds in chilled beef under vacuum or

- high oxygen atmospheres. *Int. J. Food Microbiol.* 223, 25–32.
<https://doi.org/10.1016/J.IJFOODMICRO.2016.01.022>
- Jacques, M., Malouin, F., 2022. One Health-One Biofilm. *Vet. Res.* 53, 51.
<https://doi.org/10.1186/S13567-022-01067-4>
- Jain, C., Rodriguez-R, L.M., Phillippy, A.M., Konstantinidis, K.T., Aluru, S., 2018. High throughput ANI analysis of 90K prokaryotic genomes reveals clear species boundaries. *Nat. Commun.* 9, 5114. <https://doi.org/10.1038/s41467-018-07641-9>
- Jain, N., Ådén, J., Nagamatsu, K., Evans, M.L., Li, X., McMichael, B., Ivanova, M.I., Almqvist, F., Buxbaum, J.N., Chapman, M.R., 2017. Inhibition of curli assembly and *Escherichia coli* biofilm formation by the human systemic amyloid precursor transthyretin. *Proc. Natl. Acad. Sci. U. S. A.* 114, 12184–12189. <https://doi.org/10.1073/PNAS.1708805114>
- Janet, R., Richard, W., Tim, S., Craig, H., 2018. How to Sustainably Feed 10 Billion People by 2050, in 21 Charts. *World Resour. Inst.*
- Jang, I.A., Kim, J., Park, W., 2016. Endogenous hydrogen peroxide increases biofilm formation by inducing exopolysaccharide production in *Acinetobacter oleivorans* DR1. *Sci. Rep.* 6, 21121-undefined. <https://doi.org/10.1038/srep21121>
- Javed, M., Matloob, A., Ettoumi, F., Sheikh, A.R., Zhang, R., Xu, Y., 2023. Novel nanobubble technology in food science: Application and mechanism. *Food Innov. Adv.* 2, 135–144.
<https://doi.org/10.48130/fia-2023-0014>
- Jeffries, J., Thongsomboon, W., Visser, J.A., Enriquez, K., Yager, D., Cegelski, L., 2021. Variation in the ratio of curli and phosphoethanolamine cellulose associated with biofilm architecture and properties. *Biopolymers* 112. <https://doi.org/10.1002/bip.23395>

- Jespersen, L., Huffman, R., 2014. Building food safety into the company culture: a look at Maple Leaf Foods. *Perspect. Public Health* 134, 200–205. <https://doi.org/10.1177/1757913914532620>
- Johansson, P., Jääskeläinen, E., Nieminen, T., Hultman, J., Auvinen, P., Björkroth, K.J., 2020. Microbiomes in the context of refrigerated raw meat spoilage. *Meat Muscle Biol.* 4, 12–13. <https://doi.org/10.22175/MMB.10369>
- Johansson, P., Jääskeläinen, E., Säde, E., Björkroth, J., 2023. *Vagococcus proximus* sp. nov. and *Vagococcus intermedius* sp. nov., originating from modified atmosphere packaged broiler meat. *Int. J. Syst. Evol. Microbiol.* 73, 005963. <https://doi.org/10.1099/ijsem.0.005963>
- Johnson, R., 2017. The U.S. - EU Beef Hormone Dispute.
- Joint, I., Mühlhling, M., Querellou, J., 2010. Culturing marine bacteria - An essential prerequisite for biodiscovery: Minireview. *Microb. Biotechnol.* 3, 564–575. <https://doi.org/10.1111/j.1751-7915.2010.00188.x>
- Kable, M.E., Srisengfa, Y., Laird, M., Zaragoza, J., McLeod, J., Heidenreich, J., Marco, M.L., 2016. The core and seasonal microbiota of raw bovine milk in tanker trucks and the impact of transfer to a milk processing facility. *MBio* 7. <https://doi.org/10.1128/MBIO.00836-16>
- Kalchayanand, N., Worlie, D., Wheeler, T., 2019. A Novel Aqueous Ozone Treatment as a Spray Chill Intervention against *Escherichia coli* O157:H7 on Surfaces of Fresh Beef. *J. Food Prot.* 82, 1874–1878. <https://doi.org/10.4315/0362-028X.JFP-19-093>
- Kamal, S.M., Rybtke, M.L., Nimitz, M., Sperlein, S., Giske, C., Trček, J., Deschamps, J., Briandet, R., Dini, L., Jänsch, L., Tolker-Nielsen, T., Lee, C., Römling, U., 2019. Two FtsH proteases contribute to fitness and adaptation of *Pseudomonas aeruginosa* Clone C strains. *Front.*

- Microbiol. 10, 1372. <https://doi.org/10.3389/fmicb.2019.01372>
- Kamal, S.M., Simpson, D.J., Wang, Z., Gänzle, M., Römling, U., 2021. Horizontal transmission of stress resistance genes shape the ecology of beta- and gamma-Proteobacteria. *Front. Microbiol.* 12, 696522. <https://doi.org/10.3389/fmicb.2021.696522>
- Kämpfer, P., 2014. *Acinetobacter*. *Encycl. Food Microbiol.* Second Ed. 11–17. <https://doi.org/10.1016/B978-0-12-384730-0.00002-1>
- Kandel, S.L., Joubert, P.M., Doty, S.L., 2017. Bacterial Endophyte Colonization and Distribution within Plants. *Microorganisms* 5. <https://doi.org/10.3390/MICROORGANISMS5040077>
- Katoh, K., Standley, D.M., 2013. MAFFT Multiple Sequence Alignment Software Version 7: Improvements in Performance and Usability. *Mol. Biol. Evol.* 30, 772–780. <https://doi.org/10.1093/molbev/mst010>
- Kennedy, K.M., de Goffau, M.C., Perez-Muñoz, M.E., Arrieta, M.C., Bäckhed, F., Bork, P., Braun, T., Bushman, F.D., Dore, J., de Vos, W.M., Earl, A.M., Eisen, J.A., Elovitz, M.A., Ganal-Vonarburg, S.C., Gänzle, M.G., Garrett, W.S., Hall, L.J., Hornef, M.W., Huttenhower, C., Konnikova, L., Lebeer, S., Macpherson, A.J., Massey, R.C., McHardy, A.C., Koren, O., Lawley, T.D., Ley, R.E., O’Mahony, L., O’Toole, P.W., Pamer, E.G., Parkhill, J., Raes, J., Rattei, T., Salonen, A., Segal, E., Segata, N., Shanahan, F., Sloboda, D.M., Smith, G.C.S., Sokol, H., Spector, T.D., Surette, M.G., Tannock, G.W., Walker, A.W., Yassour, M., Walter, J., 2023. Questioning the fetal microbiome illustrates pitfalls of low-biomass microbial studies. *Nature* 613, 639–649. <https://doi.org/10.1038/s41586-022-05546-8>
- Kergourlay, G., Taminiou, B., Daube, G., Champomier Vergès, M.C., 2015. Metagenomic insights into the dynamics of microbial communities in food. *Int. J. Food Microbiol.* 213, 31–39.

<https://doi.org/10.1016/J.IJFOODMICRO.2015.09.010>

Khambhati, K., Patel, J., Saxena, V., Parvathy, A., Jain, N., 2021. Gene regulation of biofilm-associated functional amyloids. *Pathogens* 10. <https://doi.org/10.3390/pathogens10040490>

Klaura, J., Breeman, G., Scherer, L., 2023. Animal lives embodied in food loss and waste. *Sustain. Prod. Consum.* 43, 308–318. <https://doi.org/10.1016/J.SPC.2023.11.004>

Klemm, P., Schembri, M., 2004. Type 1 fimbriae, curli, and antigen 43: adhesion, colonization, and biofilm formation. *EcoSal Plus* 1. <https://doi.org/10.1128/ecosalplus.8.3.2.6>

Kolmogorov, M., Yuan, J., Lin, Y., Pevzner, P.A., 2019. Assembly of long, error-prone reads using repeat graphs. *Nat. Biotechnol.* 37, 540–546. <https://doi.org/10.1038/s41587-019-0072-8>

Korany, A.M., Hua, Z., Green, T., Hanrahan, I., El-Shinawy, S.H., El-Kholy, A., Hassan, G., Zhu, M.J., 2018. Efficacy of ozonated water, chlorine, chlorine dioxide, quaternary ammonium compounds and peroxyacetic acid against *Listeria monocytogenes* biofilm on polystyrene surfaces. *Front. Microbiol.* 9, 411379. <https://doi.org/10.3389/FMICB.2018.02296/BIBTEX>

Koschorreck, M., Hentschel, I., Boehrer, B., 2017. Oxygen Ebullition From Lakes. *Geophys. Res. Lett.* 44, 9372–9378. <https://doi.org/10.1002/2017GL074591>

Kostaki, M., Chorianopoulos, N., Braxou, E., Nychas, G.J., Giaouris, E., 2012. Differential biofilm formation and chemical disinfection resistance of sessile cells of *Listeria monocytogenes* strains under monospecies and dual-species (with *Salmonella enterica*) conditions. *Appl. Environ. Microbiol.* 78, 2586–2595. <https://doi.org/10.1128/AEM.07099-11>

Kostakioti, M., Hadjifrangiskou, M., Hultgren, S.J., 2013. Bacterial biofilms: development, dispersal, and therapeutic strategies in the dawn of the postantibiotic era. *Cold Spring Harb.*

Perspect. Med. 3. <https://doi.org/10.1101/cshperspect.a010306>

Kostakioti, M., Hadjifrangiskou, M., Pinkner, J.S., Hultgren, S.J., 2009. QseC-mediated dephosphorylation of QseB is required for expression of genes associated with virulence in uropathogenic *Escherichia coli*. *Mol. Microbiol.* 73, 1020–1031. <https://doi.org/10.1111/J.1365-2958.2009.06826.X>

Koutsoumanis, K., Allende, A., Bolton, D., Bover-Cid, S., Chemaly, M., De Cesare, A., Herman, L., Hilbert, F., Lindqvist, R., Nauta, M., Nonno, R., Peixe, L., Ru, G., Simmons, M., Skandamis, P., Suffredini, E., Fox, E., Gosling, R., Gil, B.M., Møretrø, T., Stessl, B., da Silva Felício, M.T., Messens, W., Simon, A.C., Alvarez-Ordóñez, A., 2024. Persistence of microbiological hazards in food and feed production and processing environments. *EFSA J.* 22, e8521. <https://doi.org/10.2903/J.EFSA.2024.8521>

Koutsoumanis, K., Tsaloumi, S., Aspidou, Z., Tassou, C., Gougouli, M., 2021. Application of Quantitative Microbiological Risk Assessment (QMRA) to food spoilage: Principles and methodology. *Trends Food Sci. Technol.* 114, 189–197. <https://doi.org/10.1016/J.TIFS.2021.05.011>

Kozlov, A.M., Darriba, D., Flouri, T., Morel, B., Stamatakis, A., 2019. RAxML-NG: a fast, scalable and user-friendly tool for maximum likelihood phylogenetic inference. *Bioinformatics* 35, 4453–4455.

Kumar, S., Stecher, G., Li, M., Knyaz, C., Tamura, K., 2018. MEGA X: Molecular evolutionary genetics analysis across computing platforms. *Mol. Biol. Evol.* 35, 1547–1549. <https://doi.org/10.1093/molbev/msy096>

Kuo, C.H., Ochman, H., 2009. Inferring clocks when lacking rocks: The variable rates of

molecular evolution in bacteria. *Biol. Direct* 4, 35. <https://doi.org/10.1186/1745-6150-4-35/FIGURES/3>

Kwak, G.Y., Choi, O., Goo, E., Kang, Y., Kim, J., Hwang, I., 2020. Quorum sensing-independent cellulase-sensitive pellicle formation is critical for colonization of *Burkholderia glumae* in rice plants. *Front. Microbiol.* 10. <https://doi.org/10.3389/FMICB.2019.03090>

Lachmann, R., Halbedel, S., Adler, M., Becker, N., Allerberger, F., Holzer, A., Boone, I., Falkenhorst, G., Kleta, S., Al Dahouk, S., Stark, K., Luber, P., Flieger, A., Wilking, H., 2021. Nationwide outbreak of invasive listeriosis associated with consumption of meat products in health care facilities, Germany, 2014–2019. *Clin. Microbiol. Infect.* 27, 1035e1-1035e5. <https://doi.org/10.1016/j.cmi.2020.09.020>

Lambert, R.J.W., Johnston, M.D., 2001. The effect of interfering substances on the disinfection process: a mathematical model. *J. Appl. Microbiol.* 91, 548–555. <https://doi.org/10.1046/j.1365-2672.2001.01422.x>

Lambré, C., Barat Baviera, J.M., Bolognesi, C., Chesson, A., Coconcelli, P.S., Crebelli, R., Gott, D.M., Grob, K., Lampi, E., Riviere, G., Steffensen, I.L., Tlustos, C., Van Loveren, H., Vernis, L., Zorn, H., Bolton, D., Bover-Cid, S., de Knecht, J., Peixe, L., Skandamis, P., Martino, C., Messens, W., Tard, A., Mortensen, A., 2022. Evaluation of the safety and efficacy of lactic acid to reduce microbiological surface contamination on carcasses from kangaroos, wild pigs, goats and sheep. *EFSA J.* 20, e07265. <https://doi.org/10.2903/J.EFSA.2022.7265>

Langsrud, S., Moen, B., Møretro, T., Løype, M., Heir, E., 2016. Microbial dynamics in mixed culture biofilms of bacteria surviving sanitation of conveyor belts in salmon-processing plants. *J. Appl. Microbiol.* 120, 366–378. <https://doi.org/10.1111/JAM.13013>

- Lauritsen, C.V., Kjeldgaard, J., Ingmer, H., Bisgaard, M., Christensen, H., 2019. Microbiota encompassing putative spoilage bacteria in retail packaged broiler meat and commercial broiler abattoir. *Int. J. Food Microbiol.* 300, 14–21. <https://doi.org/10.1016/J.IJFOODMICRO.2019.04.003>
- Laursen, M.F., Dalgaard, M.D., Bahl, M.I., 2017. Genomic GC-content affects the accuracy of 16S rRNA gene sequencing based microbial profiling due to PCR bias. *Front. Microbiol.* 8, 287367. <https://doi.org/10.3389/fmicb.2017.01934>
- Laverty, G., Gorman, S.P., Gilmore, B.F., 2014. Biomolecular mechanisms of *Pseudomonas aeruginosa* and *Escherichia coli* biofilm formation. *Pathogens* 3, 596–632. <https://doi.org/10.3390/pathogens3030596>
- Law, J.W.F., Mutalib, N.S.A., Chan, K.G., Lee, L.H., 2014. Rapid methods for the detection of foodborne bacterial pathogens: principles, applications, advantages and limitations. *Front. Microbiol.* 5. <https://doi.org/10.3389/FMICB.2014.00770>
- Lee, C., Wigren, E., Trček, J., Peters, V., Kim, J., Hasni, M.S., Nimtz, M., Lindqvist, Y., Park, C., Curth, U., 2015. A novel protein quality control mechanism contributes to heat shock resistance of worldwide-distributed *Pseudomonas aeruginosa* clone C strains. *Environ. Microbiol.* 17, 4511–4526. <https://doi.org/10.1111/1462-2920.12915>
- Lee, J.H., Lee, J., 2010. Indole as an intercellular signal in microbial communities. *FEMS Microbiol. Rev.* 34, 426–444. <https://doi.org/10.1111/J.1574-6976.2009.00204.X>
- Leff, J.W., Fierer, N., 2013. Bacterial Communities Associated with the Surfaces of Fresh Fruits and Vegetables. *PLoS One* 8. <https://doi.org/10.1371/journal.pone.0059310>
- Leisner, J.J., Laursen, B.G., Prévost, H., Drider, D., Dalgaard, P., 2007. *Carnobacterium*: Positive

- and negative effects in the environment and in foods. *FEMS Microbiol. Rev.* 31, 592–613.
<https://doi.org/10.1111/j.1574-6976.2007.00080.x>
- Lelieveld, H.L.M., Mostert, M.A., Curiel, G.J., 2014. Hygienic design of food processing equipment. *Hyg. Food Process. Princ. Pract.* Second Ed. 91–141.
<https://doi.org/10.1533/9780857098634.2.91>
- Letunic, I., Bork, P., 2021. Interactive tree of life (iTOL) v5: an online tool for phylogenetic tree display and annotation. *Nucleic Acids Res.* 49, W293–W296.
<https://doi.org/10.1093/nar/gkab301>
- Li, H., Mercer, R., Behr, J., Heinzlmeir, S., McMullen, L.M., Vogel, R.F., Gänzle, M.G., 2020. Heat and pressure resistance in *Escherichia coli* relates to protein folding and aggregation. *Front. Microbiol.* 11, 111. <https://doi.org/10.3389/fmicb.2020.00111>
- Li, Z., Chen, J.H., Hao, Y., Nair, S.K., 2012. Structures of the PelD cyclic diguanylate effector involved in pellicle formation in *Pseudomonas aeruginosa* PAO1. *J. Biol. Chem.* 287, 30191–30204. <https://doi.org/10.1074/jbc.M112.378273>
- Liang, Y., Gao, H., Chen, J., Dong, Y., Wu, L., He, Z., Liu, X., Qiu, G., Zhou, J., 2010. Pellicle formation in *Shewanella oneidensis*. *BMC Microbiol.* 10, 1–11.
<https://doi.org/10.1186/1471-2180-10-291/TABLES/1>
- Lim, J.Y., May, J.M., Cegelski, L., 2012. Dimethyl sulfoxide and ethanol elicit increased amyloid biogenesis and amyloid-integrated biofilm formation in *Escherichia coli*. *Appl. Environ. Microbiol.* 78, 3369–3378. https://doi.org/10.1128/AEM.07743-11/SUPPL_FILE/AEM-AEM07743-11-S02.ZIP
- Liu, C., Sun, D., Zhu, J., Liu, J., Liu, W., 2020. The regulation of bacterial biofilm formation by

cAMP-CRP: A mini-review. *Front. Microbiol.* 11, 802.
<https://doi.org/10.3389/FMICB.2020.00802/BIBTEX>

Liu, N.T., Bauchan, G.R., Francoeur, C.B., Shelton, D.R., Lo, Y.M., Nou, X., 2016. *Ralstonia insidiosa* serves as bridges in biofilm formation by foodborne pathogens *Listeria monocytogenes*, *Salmonella enterica*, and Enterohemorrhagic *Escherichia coli*. *Food Control* 65, 14–20. <https://doi.org/10.1016/j.foodcont.2016.01.004>

Liu, N.T., Lefcourt, A.M., Nou, X., Shelton, D.R., Zhang, G., Lo, Y.M., 2013. Native microflora in fresh-cut produce processing plants and their potentials for biofilm formation. *J. Food Prot.* 76, 827–832. <https://doi.org/10.4315/0362-028X.JFP-12-433>

Lodewyckx, C., Vangronsveld, J., Porteous, F., Moore, E.R.B., Taghavi, S., Mezgeay, M., Van Der Lelie, D., 2002. Critical Reviews in Plant Sciences Endophytic Bacteria and Their Potential Applications Endophytic Bacteria and Their Potential Applications. CRC. *Crit. Rev. Plant Sci.* 21, 583–606. <https://doi.org/10.1080/0735-260291044377>

Louw, N.L., Lele, K., Ye, R., Edwards, C.B., Wolfe, B.E., 2023. Microbiome assembly in fermented foods. *Annu. Rev. Microbiol.* 77, 381–402. <https://doi.org/10.1146/ANNUREV-MICRO-032521-041956>

Machado, M.A.M., Castro, V.S., da Cunha-Neto, A., Vallim, D.C., Pereira, R. de C.L., dos Reis, J.O., de Almeida, P.V., Galvan, D., Conte-Junior, C.A., Figueiredo, E.E. de S., 2023. Heat-resistant and biofilm-forming *Escherichia coli* in pasteurized milk from Brazil. *Brazilian J. Microbiol.* 54, 1035. <https://doi.org/10.1007/S42770-023-00920-8>

Maes, S., Heyndrickx, M., Vackier, T., Steenackers, H., Verplaetse, A., Reu, K. De, 2019a. Identification and spoilage potential of the remaining dominant microbiota on food contact

surfaces after cleaning and disinfection in different food industries. *J. Food Prot.* 82, 262–275. <https://doi.org/10.4315/0362-028X.JFP-18-226>

Maes, S., Vackier, T., Nguyen Huu, S., Heyndrickx, M., Steenackers, H., Sampers, I., Raes, K., Verplaetse, A., De Reu, K., 2019b. Occurrence and characterisation of biofilms in drinking water systems of broiler houses. *BMC Microbiol.* 19, 1–15. <https://doi.org/10.1186/S12866-019-1451-5/TABLES/3>

Mai-Prochnow, A., Zhou, R., Zhang, T., Ostrikov, K. (Ken), Mugunthan, S., Rice, S.A., Cullen, P.J., 2021. Interactions of plasma-activated water with biofilms: inactivation, dispersal effects and mechanisms of action. *npj Biofilms Microbiomes* 2021 71 7, 1–12. <https://doi.org/10.1038/s41522-020-00180-6>

Maillet, A., Bouju-Albert, A., Roblin, S., Vaissié, P., Leuillet, S., Dousset, X., Jaffrès, E., Combrisson, J., Prévost, H., 2021. Impact of DNA extraction and sampling methods on bacterial communities monitored by 16S rDNA metabarcoding in cold-smoked salmon and processing plant surfaces. *Food Microbiol.* 95, 103705. <https://doi.org/10.1016/J.FM.2020.103705>

Mangalappalli-Illathu, A.K., Vidović, S., Korber, D.R., 2008. Differential adaptive response and survival of *Salmonella enterica* serovar Enteritidis planktonic and biofilm cells exposed to benzalkonium chloride. *Antimicrob. Agents Chemother.* 52, 3669–3680. <https://doi.org/10.1128/AAC.00073-08>

Marouani-Gadri, N., Augier, G., Carpentier, B., 2009. Characterization of bacterial strains isolated from a beef-processing plant following cleaning and disinfection — Influence of isolated strains on biofilm formation by Sakai and EDL 933 *E. coli* O157:H7. *Int. J. Food Microbiol.*

133, 62–67. <https://doi.org/10.1016/J.IJFOODMICRO.2009.04.028>

Marsha A. Echols, 1998. Food Safety Regulation in the European Union and the United States: Different Cultures, Different Laws. *Columbia J. Eur. Law*.

Marti, R., Muniesa, M., Schmid, M., Ahrens, C.H., Naskova, J., Hummerjohann, J., 2016. Short communication: Heat-resistant *Escherichia coli* as potential persistent reservoir of extended-spectrum β -lactamases and Shiga toxin-encoding phages in dairy. *J. Dairy Sci.* 99, 8622–8632. <https://doi.org/10.3168/jds.2016-11076>

Marti, R., Schmid, M., Kulli, S., Schneeberger, K., Naskova, J., Knöchel, S., Ahrens, C.H., Hummerjohann, J., 2017. Biofilm formation potential of heat-resistant *Escherichia coli* dairy isolates and the complete genome of multidrug-resistant, heat-resistant strain FAM21845. *Appl. Environ. Microbiol.* 83, e00628-17-undefined. <https://doi.org/10.1128/AEM.00628-17>

Marti, S., Chabane, Y.N., Alexandre, S., Coquet, L., Vila, J., Jouenne, T., Dé, E., 2011. Growth of *Acinetobacter baumannii* in pellicle enhanced the expression of potential virulence factors. *PLoS One* 6, e26030. <https://doi.org/10.1371/journal.pone.0026030>

Martin-Visscher, L.A., Van Belkum, M.J., Garneau-Tsodikova, S., Whittall, R.M., Zheng, J., McMullen, L.M., Vederas, J.C., 2008. Isolation and characterization of carnocyclin A, a novel circular bacteriocin produced by *Carnobacterium maltaromaticum* UAL307. *Appl. Environ. Microbiol.* 74, 4756–4763. <https://doi.org/10.1128/AEM.00817-08>

Martínez-Suárez, J. V., Ortiz, S., López-Alonso, V., 2016. Potential impact of the resistance to quaternary ammonium disinfectants on the persistence of *Listeria monocytogenes* in food processing environments. *Front. Microbiol.* 7, 196653. <https://doi.org/10.3389/FMICB.2016.00638/BIBTEX>

- Martiny, J.B.H., Bohannan, B.J.M., Brown, J.H., Colwell, R.K., Fuhrman, J.A., Green, J.L., Horner-Devine, M.C., Kane, M., Krumins, J.A., Kuske, C.R., Morin, P.J., Naeem, S., Øvreås, L., Reysenbach, A.L., Smith, V.H., Staley, J.T., 2006. Microbial biogeography: putting microorganisms on the map. *Nat. Rev. Microbiol.* 2006 42 4, 102–112. <https://doi.org/10.1038/nrmicro1341>
- Maury, M.M., Bracq-Dieye, H., Huang, L., Vales, G., Lavina, M., Thouvenot, P., Disson, O., Leclercq, A., Brisse, S., Lecuit, M., 2019. Hypervirulent *Listeria monocytogenes* clones' adaption to mammalian gut accounts for their association with dairy products. *Nat. Commun.* 10, 2488-undefined. <https://doi.org/10.1038/s41467-019-10380-0>
- Mcglynn, W., 2004. Guidelines for the Use of Chlorine Bleach as a Sanitizer in Food Processing Operations handling articles. *Food Technol. Fact Sheet* 2.
- McLauchlan, K.K., Higuera, P.E., Miesel, J., Rogers, B.M., Schweitzer, J., Shuman, J.K., Tepley, A.J., Varner, J.M., Veblen, T.T., Adalsteinsson, S.A., Balch, J.K., Baker, P., Batllori, E., Bigio, E., Brando, P., Cattau, M., Chipman, M.L., Coen, J., Crandall, R., Daniels, L., Enright, N., Gross, W.S., Harvey, B.J., Hatten, J.A., Hermann, S., Hewitt, R.E., Kobziar, L.N., Landesmann, J.B., Loranty, M.M., Maezumi, S.Y., Mearns, L., Moritz, M., Myers, J.A., Pausas, J.G., Pellegrini, A.F.A., Platt, W.J., Roozeboom, J., Safford, H., Santos, F., Scheller, R.M., Sherriff, R.L., Smith, K.G., Smith, M.D., Watts, A.C., 2020. Fire as a fundamental ecological process: Research advances and frontiers. *J. Ecol.* 108, 2047–2069. <https://doi.org/10.1111/1365-2745.13403>
- McLean, J.S., Pinchuk, G.E., Geydebekht, O. V., Bilskis, C.L., Zakrajsek, B.A., Hill, E.A., Saffarini, D.A., Romine, M.F., Gorby, Y.A., Fredrickson, J.K., Beliaev, A.S., 2008. Oxygen-dependent autoaggregation in *Shewanella oneidensis* MR-1. *Environ. Microbiol.* 10, 1861–

1876. <https://doi.org/10.1111/j.1462-2920.2008.01608.x>

Mercer, R.G., Quinlan, M., Rose, A.R., Noll, S., Beatty, J.T., Lang, A.S., 2012. Regulatory systems controlling motility and gene transfer agent production and release in *Rhodobacter capsulatus*. FEMS Microbiol. Lett. 331, 53–62. <https://doi.org/10.1111/J.1574-6968.2012.02553.X>

Mercer, R.G., Zheng, J., Garcia-Hernandez, R., Ruan, L., Gänzle, M.G., McMullen, L.M., 2015. Genetic determinants of heat resistance in *Escherichia coli*. Front. Microbiol. 6, 932. <https://doi.org/10.3389/fmicb.2015.00932>

Mertz, A.W., Koo, O.K., O'Bryan, C.A., Morawicki, R., Sirsat, S.A., Neal, J.A., Crandall, P.G., Ricke, S.C., 2014. Microbial ecology of meat slicers as determined by denaturing gradient gel electrophoresis. Food Control 42, 242–247. <https://doi.org/10.1016/J.FOODCONT.2014.02.027>

Mettler, E., Carpentier, B., 1998. Variations over time of microbial load and physicochemical properties of floor materials after cleaning in food industry premises. J. Food Prot. 61, 57–65. <https://doi.org/10.4315/0362-028X-61.1.57>

Miller, M.B., Bassler, B.L., 2001. Quorum sensing in bacteria. Annu. Rev. Microbiol. 55, 165–199. <https://doi.org/10.1146/ANNUREV.MICRO.55.1.165>

Møretro, T., Langsrud, S., 2017. Residential bacteria on surfaces in the food industry and their implications for food safety and quality. Compr. Rev. Food Sci. Food Saf. 16, 1022–1041. <https://doi.org/10.1111/1541-4337.12283>

Møretro, T., Langsrud, S., Heir, E., 2013. Bacteria on Meat Abattoir Process Surfaces after Sanitation: Characterisation of Survival Properties of *Listeria monocytogenes* and the

Commensal Bacterial Flora. Adv. Microbiol. 3, 255–264.
<https://doi.org/10.4236/aim.2013.33037>

Møretør, T., Moen, B., Heir, E., Hansen, A., Langsrud, S., 2016. Contamination of salmon fillets and processing plants with spoilage bacteria. *Int. J. Food Microbiol.* 237, 98–108.
<https://doi.org/10.1016/J.IJFOODMICRO.2016.08.016>

Møretør, T., Schirmer, B.C.T., Heir, E., Fagerlund, A., Hjemli, P., Langsrud, S., 2017. Tolerance to quaternary ammonium compound disinfectants may enhance growth of *Listeria monocytogenes* in the food industry. *Int. J. Food Microbiol.* 241, 215–224.
<https://doi.org/10.1016/J.IJFOODMICRO.2016.10.025>

Møretør, T., Vestby, L.K., Nesse, L.L., Storheim, S.E., Kotlarz, K., Langsrud, S., 2009. Evaluation of efficacy of disinfectants against *Salmonella* from the feed industry. *J. Appl. Microbiol.* 106, 1005–1012. <https://doi.org/10.1111/j.1365-2672.2008.04067.x>

Mukhopadhyay, S., Gorris, L.G.M., 2014. Hurdle Technology. *Encycl. Food Microbiol.* Second Ed. 221–227. <https://doi.org/10.1016/B978-0-12-384730-0.00166-X>

National Center for Biotechnology Information, 2024. PubChem compound summary for CID 6585, peracetic acid [WWW Document]. URL <https://pubchem.ncbi.nlm.nih.gov/compound/Peracetic-Acid> (accessed 7.3.24).

Nemergut, D.R., Schmidt, S.K., Fukami, T., O’Neill, S.P., Bilinski, T.M., Stanish, L.F., Knelman, J.E., Darcy, J.L., Lynch, R.C., Wickey, P., Ferrenberg, S., 2013. Patterns and processes of microbial community assembly. *Microbiol. Mol. Biol. Rev.* 77, 342–356.
<https://doi.org/10.1128/MMBR.00051-12>

Nguyen, L.-T., Schmidt, H.A., von Haeseler, A., Minh, B.Q., 2015. IQ-TREE: A fast and effective

- stochastic algorithm for estimating maximum-likelihood phylogenies. *Mol. Biol. Evol.* 32, 268–274. <https://doi.org/10.1093/molbev/msu300>
- Novak, J.S., Yuan, J.T.C., 2004. Increased inactivation of ozone-treated *Clostridium perfringens* Vegetative Cells and Spores on Fabricated Beef Surfaces Using Mild Heat. *J. Food Prot.* 67, 342–346.
- O’Leary, N.A., Cox, E., Holmes, J.B., Anderson, W.R., Falk, R., Hem, V., Tsuchiya, M.T.N., Schuler, G.D., Zhang, X., Torcivia, J., Ketter, A., Breen, L., Cothran, J., Bajwa, H., Tinne, J., Meric, P.A., Hlavina, W., Schneider, V.A., 2024. Exploring and retrieving sequence and metadata for species across the tree of life with NCBI Datasets. *Sci. Data* 11, 1–10. <https://doi.org/10.1038/s41597-024-03571-y>
- O’Toole, G., Kaplan, H.B., Kolter, R., 2000. Biofilm formation as microbial development. *Annu. Rev. Microbiol.* 54, 49–79. <https://doi.org/10.1146/annurev.micro.54.1.49>
- O’Toole, G.A., 2024. We have a community problem. *J. Bacteriol.* 206, e00073-24. <https://doi.org/10.1128/JB.00073-24>
- Oh, M.H., Han, K., 2020. AbaR is a LuxR type regulator essential for motility and the formation of biofilm and pellicle in *Acinetobacter baumannii*. *Genes and Genomics* 42, 1339–1346. <https://doi.org/10.1007/S13258-020-01005-8>
- Otter, J.A., Vickery, K., Walker, J.T., Delancey Pulcini, E., Stoodley, P., Goldenberg, S.D., Salkeld, J.A.G., Chewins, J., Yezli, S., Edgeworth, J.D., 2015. Surface-attached cells, biofilms and biocide susceptibility: implications for hospital cleaning and disinfection. *J. Hosp. Infect.* 89, 16–27. <https://doi.org/10.1016/j.jhin.2014.09.008>
- Pacheco, T., Gomes, A.É.I., Siqueira, N.M.G., Assoni, L., Darrieux, M., Venter, H., Ferraz, L.F.C.,

2021. SdiA, a quorum-sensing regulator, suppresses fimbriae expression, biofilm formation, and quorum-sensing signaling molecules production in *Klebsiella pneumoniae*. *Front. Microbiol.* 12, 1229. <https://doi.org/10.3389/FMICB.2021.597735/BIBTEX>
- Page, A.J., Cummins, C.A., Hunt, M., Wong, V.K., Reuter, S., Holden, M.T.G., Fookes, M., Falush, D., Keane, J.A., Parkhill, J., 2015. Roary: rapid large-scale prokaryote pan genome analysis. *Bioinformatics* 31, 3691–3693. <https://doi.org/10.1093/bioinformatics/btv421>
- Palaiodimou, L., Fanning, S., Fox, E.M., 2021. Genomic insights into persistence of *Listeria* species in the food processing environment. *J. Appl. Microbiol.* 131, 2082–2094. <https://doi.org/10.1111/jam.15089>
- Pampoukis, G., Lytjou, A.E., Argyri, A.A., Panagou, E.Z., Nychas, G.J.E., 2022. Recent Advances and Applications of Rapid Microbial Assessment from a Food Safety Perspective. *Sensors (Basel)*. 22. <https://doi.org/10.3390/S22072800>
- Papenfort, K., Bassler, B., 2016a. Quorum-sensing signal-response systems in gram-negative bacteria. *Nat. Rev. Microbiol.* 12, 576–588. <https://doi.org/10.1038/nrmicro.2016.89>. Quorum-Sensing
- Papenfort, K., Bassler, B.L., 2016b. Quorum sensing signal-response systems in Gram-negative bacteria. *Nat. Rev. Microbiol.* 14, 576–588. <https://doi.org/10.1038/NRMICRO.2016.89>
- Parks, D.H., Chuvochina, M., Rinke, C., Mussig, A.J., Chaumeil, P.-A., Hugenholtz, P., 2021. GTDB: an ongoing census of bacterial and archaeal diversity through a phylogenetically consistent, rank normalized and complete genome-based taxonomy. *Nucleic Acids Res.* <https://doi.org/10.1093/NAR/GKAB776>
- Passarelli-Araujo, H., Franco, G.R., Venancio, T.M., 2022. Network analysis of ten thousand

- genomes shed light on *Pseudomonas* diversity and classification. *Microbiol. Res.* 254, 126919. <https://doi.org/10.1016/J.MICRES.2021.126919>
- Paytubi, S., Cansado, C., Madrid, C., Balsalobre, C., 2017. Nutrient composition promotes switching between pellicle and bottom biofilm in *Salmonella*. *Front. Microbiol.* 8. <https://doi.org/10.3389/FMICB.2017.02160>
- Pelletier, F., Garant, D., Hendry, A.P., 2009. Eco-evolutionary dynamics. *Philos. Trans. R. Soc. B Biol. Sci.* 364, 1483. <https://doi.org/10.1098/RSTB.2009.0027>
- Peng, S., Hummerjohann, J., Stephan, R., Hammer, P., 2013. Short communication: heat resistance of *Escherichia coli* strains in raw milk at different subpasteurization conditions. *J. Dairy Sci.* 96, 3543–3546. <https://doi.org/10.3168/jds.2012-6174>
- Pightling, A.W., Pettengill, J.B., Luo, Y., Baugher, J.D., Rand, H., Strain, E., 2018. Interpreting whole-genome sequence analyses of foodborne bacteria for regulatory applications and outbreak investigations. *Front. Microbiol.* 9, 1482. <https://doi.org/10.3389/FMICB.2018.01482>
- Pinto, R.M., Soares, F.A., Reis, S., Nunes, C., Van Dijck, P., 2020. Innovative strategies toward the disassembly of the EPS matrix in bacterial biofilms. *Front. Microbiol.* 11, 952-. <https://doi.org/10.3389/fmicb.2020.00952>
- Podlesny, D., Arze, C., Dörner, E., Verma, S., Dutta, S., Walter, J., Fricke, W.F., 2022. Metagenomic strain detection with SameStr: identification of a persisting core gut microbiota transferable by fecal transplantation. *Microbiome* 10, 53. <https://doi.org/10.1186/S40168-022-01251-W>
- Pothakos, V., Snauwaert, C., De Vos, P., Huys, G., Devlieghere, F., 2014. Psychrotrophic

- members of *Leuconostoc gasicomitatum*, *Leuconostoc gelidum* and *Lactococcus piscium* dominate at the end of shelf-life in packaged and chilled-stored food products in Belgium. *Food Microbiol.* 39, 61–67. <https://doi.org/10.1016/j.fm.2013.11.005>
- Pothakos, V., Stellato, G., Ercolini, D., Devlieghere, F., 2015. Processing environment and ingredients are both sources of *Leuconostoc gelidum*, which emerges as a major spoiler in ready-to-eat meals. *Appl. Environ. Microbiol.* 81, 3529–3541. <https://doi.org/10.1128/AEM.03941-14>
- Qian, Chenhao, Liu, Y., Barnett-Neefs, C., Salgia, S., Serbetci, O., Adalja, A., Acharya, J., Zhao, Q., Ivanek, R., Wiedmann, M., 2023. A perspective on data sharing in digital food safety systems. *Crit. Rev. Food Sci. Nutr.* 63, 12513–12529. <https://doi.org/10.1080/10408398.2022.2103086>
- Qian, C., Murphy, S.I., Orsi, R.H., Wiedmann, M., 2023. How Can AI Help Improve Food Safety? *Annu. Rev. Food Sci. Technol.* 14, 517–538. <https://doi.org/10.1146/annurev-food-060721-013815>
- Quan, J., Wu, Z., Ye, Y., Peng, L., Wu, J., Ruan, D., Qiu, Y., Ding, R., Wang, X., Zheng, E., Cai, G., Huang, W., Yang, J., 2020. Metagenomic characterization of intestinal regions in pigs with contrasting feed efficiency. *Front. Microbiol.* 11, 32. <https://doi.org/10.3389/FMICB.2020.00032/BIBTEX>
- Quijada, N.M., Mann, E., Wagner, M., Rodríguez-Lázaro, D., Hernández, M., Schmitz-Esser, S., 2018. Autochthonous facility-specific microbiota dominates washed-rind Austrian hard cheese surfaces and its production environment. *Int. J. Food Microbiol.* 267, 54–61. <https://doi.org/10.1016/J.IJFOODMICRO.2017.12.025>

- R Core Team, 2015. R: a language and environment for statistical computing. R Found. Stat. Comput.
- Rafii, F., 2014. *Serratia*. *Encycl. Food Microbiol. Second Ed.* 371–375. <https://doi.org/10.1016/B978-0-12-384730-0.00304-9>
- Rahman, S., Khan, I., Oh, D.H., 2016. Electrolyzed Water as a Novel Sanitizer in the Food Industry: Current Trends and Future Perspectives. *Compr. Rev. Food Sci. Food Saf.* 15, 471–490. <https://doi.org/10.1111/1541-4337.12200>
- Ramachandran, G., Aheto, K., Shirtliff, M.E., Tennant, S.M., 2016. Poor biofilm-forming ability and long-term survival of invasive *Salmonella* Typhimurium ST313. *Pathog. Dis.* 74, 49. <https://doi.org/10.1093/femspd/ftw049>
- Rattray, J.B., Thomas, S.A., Wang, Y., Molotkova, E., Gurney, J., Varga, J.J., Brown, S.P., 2022. Bacterial quorum sensing allows graded and bimodal cellular responses to variations in population density. *MBio* 13. <https://doi.org/10.1128/mbio.00745-22>
- Ravash, N., Hesari, J., Feizollahi, E., Dhaliwal, H.K., Roopesh, M.S., 2023. Valorization of cold plasma technologies for eliminating biological and chemical food hazards. *Food Eng. Rev.* 2023 161 16, 22–58. <https://doi.org/10.1007/S12393-023-09348-0>
- Rice, R.G., Graham, D., Lowe, M.T., 2002. Recent ozone applications in food processing and sanitation [WWW Document]. *Food Saf. Mag.* URL <https://www.food-safety.com/articles/4369-recent-ozone-applications-in-food-processing-and-sanitation> (accessed 6.27.24).
- Røder, H.L., Raghupathi, P.K., Herschend, J., Brejnrod, A., Knøchel, S., Sørensen, S.J., Burmølle, M., 2015. Interspecies interactions result in enhanced biofilm formation by co-cultures of

- bacteria isolated from a food processing environment. *Food Microbiol.* 51, 18–24.
<https://doi.org/10.1016/J.FM.2015.04.008>
- Rodríguez-López, P., Saá-Ibusquiza, P., Mosquera-Fernández, M., López-Cabo, M., 2015. *Listeria monocytogenes*-carrying consortia in food industry. Composition, subtyping and numerical characterisation of mono-species biofilm dynamics on stainless steel. *Int. J. Food Microbiol.* 206, 84–95. <https://doi.org/10.1016/J.IJFOODMICRO.2015.05.003>
- Rodríguez-R, L.M., Conrad, R.E., Viver, T., Feistel, D.J., Lindner, B.G., Venter, S.N., Orellana, L.H., Amann, R., Rossello-Mora, R., Konstantinidis, K.T., 2024. An ANI gap within bacterial species that advances the definitionsdefinitionsof intra-species units. *MBio* 15, e02696. https://doi.org/10.1128/MBIO.02696-23/SUPPL_FILE/MBIO.02696-23-S0001.PDF
- Roller, B.R.K., Stoddard, S.F., Schmidt, T.M., 2016. Exploiting rRNA operon copy number to investigate bacterial reproductive strategies. *Nat. Microbiol.* 2016 111 1, 1–7. <https://doi.org/10.1038/nmicrobiol.2016.160>
- Rolon, M.L., Voloshchuk, O., Bartlett, K. V., LaBorde, L.F., Kovac, J., 2024. Multi-species biofilms of environmental microbiota isolated from fruit packing facilities promoted tolerance of *Listeria monocytogenes* to benzalkonium chloride. *Biofilm* 7, 100177. <https://doi.org/10.1016/J.BIOFLM.2024.100177>
- Roy, D., Lapointe, G., 2016. Introduction to the microbial ecology of foods. *Model. Microb. Ecol. Foods Quant. Microbiol. Food Process.* 1–15. <https://doi.org/10.1002/9781118823071.CH1>
- Ruan, H., Wu, Y., Zhang, N., Tao, Y., Wang, K., Yan, B., Zhao, J., Zhang, H., Gänzle, M.G., Chen, W., Fan, D., 2024. *Serratia marcescens* causes the brown discoloration of frozen steamed stuffed buns during resteamng. *J. Agric. Food Chem.* 72, 4991–5002.

https://doi.org/10.1021/ACS.JAFC.3C08467/ASSET/IMAGES/LARGE/JF3C08467_0008.JPEG

Ryan, R.P., Germaine, K., Franks, A., Ryan, D.J., Dowling, D.N., 2008. Bacterial endophytes: recent developments and applications. *FEMS Microbiol. Lett.* 278, 1–9. <https://doi.org/10.1111/J.1574-6968.2007.00918.X>

Sadiq, F.A., De Reu, K., Steenackers, H., Van de Walle, A., Burmølle, M., Heyndrickx, M., 2023. Dynamic social interactions and keystone species shape the diversity and stability of mixed-species biofilms – an example from dairy isolates. *ISME Commun.* 3, 118. <https://doi.org/10.1038/S43705-023-00328-3>

Saini, J.K., Marsden, J.L., Fung, D.Y.C., Crozier-Dodson, B.A., 2012. Evaluation of potential for translocation of *Listeria monocytogenes* from floor drains to food contact surfaces in the surrounding environment using *Listeria innocua* as a surrogate. *Adv. Microbiol.* 2, 565–570. <https://doi.org/10.4236/aim.2012.24073>

Sarron, E., Gadonna-Widehem, P., Aussenac, T., 2021. Ozone treatments for preserving fresh vegetables quality: A critical review. *Foods* 10. <https://doi.org/10.3390/FOODS10030605>

Schellhorn, H.E., 2020. Function, evolution, and composition of the RpoS regulon in *Escherichia coli*. *Front. Microbiol.* <https://doi.org/10.3389/fmicb.2020.560099>

Scher, K., Romling, U., Yaron, S., 2005. Effect of heat, acidification, and chlorination on *Salmonella enterica* serovar Typhimurium cells in a biofilm formed at the air-liquid interface. *Appl. Environ. Microbiol.* 71, 1163–1168. <https://doi.org/10.1128/AEM.71.3.1163-1168.2005>

Schön, K., Schornsteiner, E., Dzieciol, M., Wagner, M., Müller, M., Schmitz-Esser, S., 2016.

- Microbial communities in dairy processing environment floor-drains are dominated by product-associated bacteria and yeasts. *Food Control* 70, 210–215. <https://doi.org/10.1016/J.FOODCONT.2016.05.057>
- Schulz-Bohm, K., Martín-Sánchez, L., Garbeva, P., 2017. Microbial volatiles: Small molecules with an important role in intra- and inter-kingdom interactions. *Front. Microbiol.* 8, 2484. <https://doi.org/10.3389/FMICB.2017.02484>
- Seemann, T., 2014. Prokka: rapid prokaryotic genome annotation. *Bioinformatics* 30, 2068–2069. <https://doi.org/10.1093/bioinformatics/btu153>
- Sekhon, A.S., Unger, P., Singh, A., Yang, Y., Michael, M., 2022. Impact of gas ultrafine bubbles on the potency of chlorine solutions against *Listeria monocytogenes* biofilms. *J. Food Saf.* 42, e12954. <https://doi.org/10.1111/JFS.12954>
- Seridou, P., Kalogerakis, N., 2021. Disinfection applications of ozone micro- and nanobubbles. *Environ. Sci. Nano* 8, 3493–3510. <https://doi.org/10.1039/D1EN00700A>
- Shayanthan, A., Ordoñez, P.A.C., Oresnik, I.J., 2022. The role of synthetic microbial communities (SynCom) in sustainable agriculture. *Front. Agron.* 4, 896307. <https://doi.org/10.3389/fagro.2022.896307>
- Shi, J., Cai, H., Qin, Z., Li, X., Yuan, S., Yue, X., Sui, Y., Sun, A., Cui, J., Zuo, J., Wang, Q., 2023. Ozone micro-nano bubble water preserves the quality of postharvest parsley. *Food Res. Int.* 170, 113020. <https://doi.org/10.1016/J.FOODRES.2023.113020>
- Simões, M., Simões, L.C., Vieira, M.J., 2010. A review of current and emergent biofilm control strategies. *LWT - Food Sci. Technol.* 43, 573–583. <https://doi.org/10.1016/j.lwt.2009.12.008>
- Snyder, A.B., Martin, N., Wiedmann, M., 2024. Microbial food spoilage: impact, causative agents

- and control strategies. *Nat. Rev. Microbiol.* 2024 1–15. <https://doi.org/10.1038/s41579-024-01037-x>
- Soyluoglu, M., Kim, D., Karanfil, T., 2023. Characteristics and Stability of Ozone Nanobubbles in Freshwater Conditions. *Environ. Sci. Technol.* 57, 21898–21907. https://doi.org/10.1021/ACS.EST.3C07443/SUPPL_FILE/ES3C07443_SI_001.PDF
- Srey, S., Jahid, I.K., Ha, S. Do, 2013. Biofilm formation in food industries: a food safety concern. *Food Control* 31, 572–585. <https://doi.org/10.1016/j.foodcont.2012.12.001>
- Stellato, G., De Filippis, F., La Storia, A., Ercolini, D., 2015. Coexistence of lactic acid bacteria and potential spoilage microbiota in a dairy processing environment. *Appl. Environ. Microbiol.* 81, 7893–7904.
- Stellato, G., La Storia, A., De Filippis, F., Borriello, G., Villani, F., Ercolini, D., 2016. Overlap of Spoilage-Associated Microbiota between Meat and the Meat Processing Environment in Small-Scale and Large-Scale Retail Distributions. *Appl. Environ. Microbiol.* 82, 4045. <https://doi.org/10.1128/AEM.00793-16>
- Stoddard, S.F., Smith, B.J., Hein, R., Roller, B.R.K., Schmidt, T.M., 2015. *rrnDB*: improved tools for interpreting rRNA gene abundance in bacteria and archaea and a new foundation for future development. *Nucleic Acids Res.* 43, D593. <https://doi.org/10.1093/NAR/GKU1201>
- Stempel, N., Nusser, M., Neidig, A., Brenner-Weiss, G., Overhage, J., 2017. The oxidative stress agent hypochlorite stimulates c-di-GMP synthesis and biofilm formation in *Pseudomonas aeruginosa*. *Front. Microbiol.* 8, 2311. <https://doi.org/10.3389/fmicb.2017.02311>
- Takeuchi-Storm, N., Hansen, L.T., Nielsen, N.L., Andersen, J.K., 2023. Presence and persistence of *Listeria monocytogenes* in the Danish ready-to-eat food production environment. *Hygiene*

3, 18–32. <https://doi.org/10.3390/hygiene3010004>

Talagrand-Reboul, E., Jumas-Bilak, E., Lamy, B., 2017. The social life of *Aeromonas* through biofilm and quorum sensing systems. *Front. Microbiol.* 8. <https://doi.org/10.3389/FMICB.2017.00037>

Tan, X., Chung, T., Chen, Y., Macarisin, D., Laborde, L., Kovac, J., 2019. The occurrence of *Listeria monocytogenes* is associated with built environment microbiota in three tree fruit processing facilities. *Microbiome* 7. <https://doi.org/10.1186/s40168-019-0726-2>

Tassinari, E., Duffy, G., Bawn, M., Burgess, C.M., McCabe, E.M., Lawlor, P.G., Gardiner, G., Kingsley, R.A., 2019. Microevolution of antimicrobial resistance and biofilm formation of *Salmonella* Typhimurium during persistence on pig farms. *Sci. Rep.* 9, 1–12. <https://doi.org/10.1038/s41598-019-45216-w>

Taylor, T.M., Aiyegoro, O.A., 2024. Microbial contamination of fresh meat. *Encycl. Meat Sci.* 181–188. <https://doi.org/10.1016/B978-0-323-85125-1.00041-7>

The Pew Charitable Trusts, n.d. A Guide for Conducting a Food Safety Root Cause Analysis [WWW Document]. URL <https://www.pewtrusts.org/en/research-and-analysis/reports/2020/03/a-guide-for-conducting-a-food-safety-root-cause-analysis> (accessed 7.25.24).

Thi Phan, K.K., Truong, T., Wang, Y., Bhandari, B., 2020. Nanobubbles: Fundamental characteristics and applications in food processing. *Trends Food Sci. Technol.* 95, 118–130. <https://doi.org/10.1016/J.TIFS.2019.11.019>

Thomas D. Brock, 1999. Robert Koch: A life in medicine and bacteriology. *Am. Soc. Microbiol.* 64, 475–476. <https://doi.org/10.1086/416466>

- Tilocca, B., Cao, A., Migheli, Q., 2020. Scent of a Killer: Microbial Volatilome and Its Role in the Biological Control of Plant Pathogens. *Front. Microbiol.* 11, 509409. <https://doi.org/10.3389/FMICB.2020.00041/BIBTEX>
- Ude, S., Arnold, D.L., Moon, C.D., Timms-Wilson, T., Spiers, A.J., 2006. Biofilm formation and cellulose expression among diverse environmental *Pseudomonas* isolates. *Environ. Microbiol.* 8, 1997–2011. <https://doi.org/10.1111/J.1462-2920.2006.01080.X>
- Umbard, M., 2015. Beer microbiology – what is a pellicle? – a Ph.D. in beer – a study of beer and fermentation science [WWW Document]. URL <https://phdinbeer.com/2015/01/30/beer-microbiology-what-is-a-pellicle/> (accessed 8.18.22).
- Unger, P., Sekhon, A.S., Sharma, S., Lampien, A., Michael, M., 2023. Impact of gas ultrafine bubbles on the efficacy of antimicrobials for eliminating fresh and aged *Listeria monocytogenes* biofilms on dairy processing surfaces. *J. Food Saf.* 43, e13057. <https://doi.org/10.1111/JFS.13057>
- United Nations, 2023. Food loss and waste reduction | United Nations.
- United States of Food and Drug Administration, 2011. Raw Milk Misconceptions and the Danger of Raw Milk Consumption [WWW Document]. U.S. Dep. Heal. Hum. Serv. URL <http://www.fda.gov/food/foodborneillnesscontaminants/buystoreservesafefood/ucm247991.htm> (accessed 5.3.23).
- Upadhyay, A., 2021. Application of ultra-fine bubble technology to reduce *Listeria monocytogenes* contamination of fresh produce Principal Investigator. *Cent. Food Saf.*
- Valentino, V., Sequino, G., Cobo-Díaz, J.F., Álvarez-Ordóñez, A., De Filippis, F., Ercolini, D., 2022. Evidence of virulence and antibiotic resistance genes from the microbiome mapping in

- minimally processed vegetables producing facilities. *Food Res. Int.* 162, 112202.
<https://doi.org/10.1016/J.FOODRES.2022.112202>
- Van der Veen, S., Abee, T., 2011. Mixed species biofilms of *Listeria monocytogenes* and *Lactobacillus plantarum* show enhanced resistance to benzalkonium chloride and peracetic acid. *Int. J. Food Microbiol.* 144, 421–431. <https://doi.org/10.1016/j.ijfoodmicro.2010.10.029>
- Van Rossum, T., Ferretti, P., Maistrenko, O.M., Bork, P., 2020. Diversity within species: interpreting strains in microbiomes. *Nat. Rev. Microbiol.* 18, 491–506.
<https://doi.org/10.1038/s41579-020-0368-1>
- Vargas, D.A., Casas, D.E., Chávez-Velado, D.R., Jiménez, R.L., Betancourt-Barszcz, G.K., Randazzo, E., Lynn, D., Echeverry, A., Brashears, M.M., Sánchez-Plata, M.X., Miller, M.F., 2021. In-plant intervention validation of a novel ozone generation technology (Bio-Safe) compared to lactic acid in variety meats. *Foods* 2021, Vol. 10, Page 2106 10, 2106.
<https://doi.org/10.3390/FOODS10092106>
- Vellend, M., 2010. Conceptual synthesis in community ecology. *Q. Rev. Biol.* 85, 183–206.
<https://doi.org/10.1086/652373>
- Verbeke, F., De Craemer, S., Debunne, N., Janssens, Y., Wynendaele, E., Van de Wiele, C., De Spiegeleer, B., 2017. Peptides as quorum sensing molecules: Measurement techniques and obtained levels in vitro and in vivo. *Front. Neurosci.* 11, 255803.
<https://doi.org/10.3389/FNINS.2017.00183/BIBTEX>
- Verma, S., Kumar, M., Kumar, A., Das, S., Chakdar, H., Varma, A., Saxena, A.K., 2021. Diversity of Bacterial Endophytes of Maize (*Zea mays*) and Their Functional Potential for Micronutrient Biofortification. *Curr. Microbiol.* 79. <https://doi.org/10.1007/S00284-021->

- Vestby, L.K., Grønseth, T., Simm, R., Nesse, L.L., 2020. Bacterial Biofilm and its Role in the Pathogenesis of Disease. *Antibiot.* (Basel, Switzerland) 9. <https://doi.org/10.3390/ANTIBIOTICS9020059>
- Visvalingam, J., Ells, T.C., Yang, X., 2017. Impact of persistent and nonpersistent generic *Escherichia coli* and *Salmonella* sp. recovered from a beef packing plant on biofilm formation by *E. coli* O157. *J. Appl. Microbiol.* 123, 1512–1521. <https://doi.org/10.1111/jam.13591>
- Visvalingam, J., Wang, H., Ells, T.C., Yang, X., 2019. Facultative anaerobes shape multispecies biofilms composed of meat processing surface bacteria and *Escherichia coli* O157:H7 or *Salmonella enterica* serovar Typhimurium. *Appl. Environ. Microbiol.* 85, e01123-19-undefined. <https://doi.org/10.1128/AEM.01123-19>
- Visvalingam, J., Zhang, P., Ells, T.C., Yang, X., 2018. Dynamics of biofilm formation by *Salmonella* Typhimurium and beef processing plant bacteria in mono- and dual-species cultures. *Microb. Ecol.* 78, 375–387. <https://doi.org/10.1007/s00248-018-1304-z>
- Wagner, E.M., Fischel, K., Rammer, N., Beer, C., Palmetzhofer, A.L., Conrady, B., Roch, F.F., Hanson, B.T., Wagner, M., Rychli, K., 2021. Bacteria of eleven different species isolated from biofilms in a meat processing environment have diverse biofilm forming abilities. *Int. J. Food Microbiol.* 349, 109232. <https://doi.org/10.1016/J.IJFOODMICRO.2021.109232>
- Wagner, E.M., Pracser, N., Thalgueter, S., Fischel, K., Rammer, N., Pospíšilová, L., Alispahic, M., Wagner, M., Rychli, K., 2020. Identification of biofilm hotspots in a meat processing environment: detection of spoilage bacteria in multi-species biofilms. *Int. J. Food Microbiol.* 328, 108668. <https://doi.org/10.1016/j.ijfoodmicro.2020.108668>

- Wang, H., He, A., Yang, X., 2018. Dynamics of microflora on conveyor belts in a beef fabrication facility during sanitation. *Food Control* 85, 42–47.
<https://doi.org/10.1016/J.FOODCONT.2017.09.017>
- Wang, Q., Cole, J.R., 2024. Updated RDP taxonomy and RDP Classifier for more accurate taxonomic classification. *Microbiol. Resour. Announc.* 13, e01063-23.
<https://doi.org/10.1128/MRA.01063-23/ASSET/8BA7CA32-9BA0-4D05-AC5F-2807D026B349/ASSETS/IMAGES/LARGE/MRA.01063-23.F001.JPG>
- Wang, R., Bono, J.L., Kalchayanand, N., Shackelford, S., Harhay, D.M., 2012. Biofilm formation by Shiga toxin-producing *Escherichia coli* O157:H7 and non-O157 strains and their tolerance to sanitizers commonly used in the food processing environment. *J. Food Prot.* 75, 1418–1428. <https://doi.org/10.4315/0362-028X.JFP-11-427>
- Wang, R., Guragain, M., Chitlapilly Dass, S., Palanisamy, V., Bosilevac, J.M., 2024. Impact of intense sanitization on environmental biofilm communities and the survival of *Salmonella enterica* at a beef processing plant. *Front. Microbiol.* 15, 1338600.
<https://doi.org/10.3389/FMICB.2024.1338600/BIBTEX>
- Wang, R., Kalchayanand, N., King, D.A., Luedtke, B.E., Bosilevac, J.M., Arthur, T.M., 2014. Biofilm formation and sanitizer resistance of *Escherichia coli* O157:H7 strains isolated from “high event period” meat contamination. *J. Food Prot.* 77, 1982–1987.
<https://doi.org/10.4315/0362-028X.JFP-14-253>
- Wang, R., Kalchayanand, N., Schmidt, J.W., Harhay, D.M., 2013. Mixed biofilm formation by Shiga toxin-producing *Escherichia coli* and *Salmonella enterica* serovar Typhimurium enhanced bacterial resistance to sanitization due to extracellular polymeric substances. *J.*

- Food Prot. 76, 1513–1522. <https://doi.org/10.4315/0362-028X.JFP-13-077>
- Wang, R., Schmidt, J.W., Harhay, D.M., Bosilevac, J.M., King, D.A., Arthur, T.M., 2017. Biofilm formation, antimicrobial resistance, and sanitizer tolerance of *Salmonella enterica* strains isolated from beef trim. *Foodborne Pathog. Dis.* 14, 687–695. <https://doi.org/10.1089/fpd.2017.2319>
- Wang, Z., Fang, Y., Zhi, S., Simpson, D.J., Gill, A., McMullen, L.M., Neumann, N.F., Gänzle, M.G., 2020. The locus of heat resistance confers resistance to chlorine and other oxidizing chemicals in *Escherichia coli*. *Appl. Environ. Microbiol.* 86, e02123-19. <https://doi.org/10.1128/AEM.02123-19>
- Wang, Z., Hu, H., Zhu, T., Zheng, J., Gänzle, M.G., Simpson, D.J., 2021a. Ecology and function of the transmissible Locus of Stress Tolerance in *Escherichia coli* and plant-associated *Enterobacteriaceae*. *mSystems* e0037821. <https://doi.org/10.1128/mSystems.00378-21>
- Wang, Z., Zhu, T., Chen, Z., Meng, J., Simpson, D.J., Gänzle, M.G., 2021b. Genetic determinants of stress resistance in desiccated *Salmonella enterica*. *Appl. Environ. Microbiol.* 87. <https://doi.org/10.1128/AEM.01683-21>
- Waśkiewicz, A., Irzykowska, L., 2014. *Flavobacterium* spp. – Characteristics, Occurrence, and Toxicity. *Encycl. Food Microbiol. Second Ed.* 938–942. <https://doi.org/10.1016/B978-0-12-384730-0.00126-9>
- Waters, C.M., Bassler, B.L., 2005. Quorum sensing: Cell-to-cell communication in bacteria. *Annu. Rev. Cell Dev. Biol.* 21, 319–346. <https://doi.org/10.1146/annurev.cellbio.21.012704.131001>
- Waters, N.R., Abram, F., Brennan, F., Holmes, A., Pritchard, L., 2020. Easy phylotyping of *Escherichia coli* via the EzClermont web app and command-line tool. *Access Microbiol.* 2,

e000143. <https://doi.org/10.1099/ACMI.0.000143>

- Watnick, P., Kolter, R., 2000. Biofilm, city of microbes. *J. Bacteriol.* 182, 2675–2679.
- Weber, H., Pesavento, C., Possling, A., Tischendorf, G., Hengge, R., 2006. Cyclic-di-GMP-mediated signalling within the σS network of *Escherichia coli*. *Mol. Microbiol.* 62, 1014–1034. <https://doi.org/10.1111/j.1365-2958.2006.05440.x>
- Wei, Q., Wang, X., Sun, D.W., Pu, H., 2019. Rapid detection and control of psychrotrophic microorganisms in cold storage foods: A review. *Trends Food Sci. Technol.* 86, 453–464. <https://doi.org/10.1016/J.TIFS.2019.02.009>
- Weiss-Muszkat, M., Shakh, D., Zhou, Y., Pinto, R., Belausov, E., Chapman, M.R., Sela, S., 2010. Biofilm formation by and multicellular behavior of *Escherichia coli* O55:H7, an atypical enteropathogenic strain. *Appl. Environ. Microbiol.* 76, 1545–1554. <https://doi.org/10.1128/AEM.01395-09>
- Werum, V., Ehrmann, M., 2024. *Dellagليا* spp. an underestimated genus isolated from high-oxygen modified-atmosphere packaged meat. *Food Microbiol.* 117, 104398. <https://doi.org/10.1016/J.FM.2023.104398>
- Wevers, E., Moons, P., Van Houdt, R., Lurquin, I., Aertsen, A., Michiels, C.W., 2009. Quorum sensing and butanediol fermentation affect colonization and spoilage of carrot slices by *Serratia plymuthica*. *Int. J. Food Microbiol.* 134, 63–69. <https://doi.org/10.1016/J.IJFOODMICRO.2008.12.017>
- Wheeler, T.L., Kalchayanand, N., Bosilevac, J.M., 2014. Pre- and post-harvest interventions to reduce pathogen contamination in the U.S. beef industry. *Meat Sci.* 98, 372–382. <https://doi.org/10.1016/j.meatsci.2014.06.026>

- Wiernasz, N., Gigout, F., Cardinal, M., Cornet, J., Rohloff, J., Courcoux, P., Vigneau, E., Skírnisdóttir, S., Passerini, D., Pilet, M.F., Leroi, F., 2021. Effect of the manufacturing process on the microbiota, organoleptic properties and volatilome of three salmon-based products. *Foods* 10. <https://doi.org/10.3390/foods10112517>
- Wijman, J.G.E., De Leeuw, P.P.L.A., Moezelaar, R., Zwietering, M.H., Abee, T., 2007. Air-liquid interface biofilms of *Bacillus cereus*: formation, sporulation, and dispersion. *Appl. Environ. Microbiol.* 73, 1481–1488. <https://doi.org/10.1128/AEM.01781-06>
- Wolfe, B.E., Button, J.E., Santarelli, M., Dutton, R.J., 2014. Cheese rind communities provide tractable systems for in situ and in vitro studies of microbial diversity. *Cell* 158, 422–433. <https://doi.org/10.1016/j.cell.2014.05.041>
- Wood, T.K., Knabel, S.J., Kwan, B.W., 2013. Bacterial persister cell formation and dormancy. *Appl. Environ. Microbiol.* 79, 7116–7121. <https://doi.org/10.1128/AEM.02636-13>
- Wu, C., Lim, J.Y., Fuller, G.G., Cegelski, L., 2012. Quantitative analysis of amyloid-integrated biofilms formed by uropathogenic *Escherichia coli* at the air-liquid interface. *Biophys. J.* 103, 464–471. <https://doi.org/10.1016/j.bpj.2012.06.049>
- Wuyts, S., Van Beeck, W., Oerlemans, E.F.M., Wittouck, S., Claes, I.J.J., De Boeck, I., Weckx, S., Lievens, B., De Vuyst, L., Lebeer, S., 2018. Carrot juice fermentations as man-made microbial ecosystems dominated by lactic acid bacteria. *Appl. Environ. Microbiol.* 84, e00134-18. <https://doi.org/10.1128/AEM.00134-18>
- Xu, J.G., Huang, X.N., Meng, J., Chen, J.Y., Han, B.Z., 2022. Characterization and comparison of the bacterial community on environmental surfaces through a fresh-cut vegetables processing line in China. *Food Res. Int.* 155, 111075.

<https://doi.org/10.1016/J.FOODRES.2022.111075>

- Xu, J.G., Meng, J., Bao, W.J., Kang, J.M., Chen, J.Y., Han, B.Z., 2021. Occurrence of disinfectant-resistant bacteria in a fresh-cut vegetables processing facility and their role in protecting *Salmonella* Enteritidis. RSC Adv. 11, 10291–10299. <https://doi.org/10.1039/D0RA09325D>
- Xu, L., Zhang, Y., Read, N., Liu, S., Friman, V.P., 2017. *Devosia nitraria* sp. nov., a novel species isolated from the roots of *Nitraria sibirica* in China. Antonie Van Leeuwenhoek 110, 1475. <https://doi.org/10.1007/S10482-017-0901-Z>
- Xu, Z.S., Ju, T., Yang, X., Gänzle, M., 2023a. A meta-analysis of bacterial communities in food processing facilities: Driving forces for assembly of core and accessory microbiomes across different food commodities. Microorganisms 11, 1575. <https://doi.org/10.3390/MICROORGANISMS11061575>
- Xu, Z.S., Yang, X., Gänzle, M.G., 2021. Resistance of biofilm-and pellicle-embedded strains of *Escherichia coli* encoding the transmissible locus of stress tolerance (tLST) to oxidative sanitation chemicals. Int. J. Food Microbiol. 359, 109425. <https://doi.org/10.1016/j.ijfoodmicro.2021.109425>
- Xu, Z.S., Zhu, T., Wang, Z., Yang, X., Gänzle, M.G., 2023b. Socializing at the air-liquid interface: a functional genomic analysis on biofilm-related genes during pellicle formation by *Escherichia coli* and its interaction with *Aeromonas australiensis*. Appl. Environ. Microbiol. 89, e00456-23. <https://doi.org/10.1128/AEM.00456-23>
- Xue, T., Chen, X., Shang, F., 2014. Short communication: Effects of lactose and milk on the expression of biofilm-associated genes in *Staphylococcus aureus* strains isolated from a dairy cow with mastitis. J. Dairy Sci. 97, 6129–6134. <https://doi.org/10.3168/jds.2014-8344>

- Xue, W., Macleod, J., Blaxland, J., 2023. The Use of Ozone Technology to Control Microorganism Growth, Enhance Food Safety and Extend Shelf Life: A Promising Food Decontamination Technology. *Foods* 12. <https://doi.org/10.3390/FOODS12040814>
- Yam, K.C., Okamoto, S., Roberts, J.N., Eltis, L.D., 2011. Adventures in *Rhodococcus* - from steroids to explosives. *Can. J. Microbiol.* 57, 155–168. <https://doi.org/10.1139/W10-115>
- Yamamoto, K., Arai, H., Ishii, M., Igarashi, Y., 2011. Trade-off between oxygen and iron acquisition in bacterial cells at the air–liquid interface. *FEMS Microbiol. Ecol.* 77, 83–94. <https://doi.org/10.1111/J.1574-6941.2011.01087.X>
- Yang, X., 2016. Microbial ecology of beef carcasses and beef products. *Model. Microb. Ecol. Foods Quant. Microbiol. Food Process.* 442–462. <https://doi.org/10.1002/9781118823071.ch22>
- Yang, X., He, A., Badoni, M., Tran, F., Wang, H., 2017a. Mapping sources of contamination of *Escherichia coli* on beef in the fabrication facility of a commercial beef packing plant. *Food Control* 75, 153–159. <https://doi.org/10.1016/J.FOODCONT.2016.12.004>
- Yang, X., Narvaez-Bravo, C., Zhang, P., 2023a. Driving forces shaping the microbial ecology in meat packing plants. *Front. Microbiol.* 14, 1333696. <https://doi.org/10.3389/FMICB.2023.1333696/BIBTEX>
- Yang, X., Tran, F., Youssef, M.K., Gill, C.O., 2015. Determination of sources of *Escherichia coli* on beef by multiple-locus variable-number tandem repeat analysis. *J. Food Prot.* 78, 1296–1302. <https://doi.org/10.4315/0362-028X.JFP-15-014>
- Yang, X., Tran, F., Zhang, P., 2022. Comparative genomic analyses of *Escherichia coli* from meat processing environment in relation to their biofilm formation and persistence.

<https://doi.org/10.21203/rs.3.rs-2042635/v1>

- Yang, X., Wang, H., He, A., Tran, F., 2017b. Microbial efficacy and impact on the population of *Escherichia coli* of a routine sanitation process for the fabrication facility of a beef packing plant. *Food Control* 71, 353–357. <https://doi.org/10.1016/J.FOODCONT.2016.07.016>
- Yang, X., Wang, H., Hrycauk, S., Holman, D.B., Ells, T.C., 2023b. Microbial Dynamics in Mixed-Culture Biofilms of *Salmonella* Typhimurium and *Escherichia coli* O157:H7 and Bacteria Surviving Sanitation of Conveyor Belts of Meat Processing Plants. *Microorganisms* 11. <https://doi.org/10.3390/MICROORGANISMS11020421>
- Yang, X., Wang, H., Hrycauk, S., Klassen, M.D., 2021. Effects of peroxyacetic acid spray and storage temperature on the microbiota and sensory properties of vacuum-packed subprimal cuts of meat. *Appl. Environ. Microbiol.* 87, e03143-20. https://doi.org/10.1128/AEM.03143-20/SUPPL_FILE/AEM.03143-20-S0002.XLSX
- Yang, Y., Mikš-Krajnik, M., Zheng, Q., Lee, S.B., Lee, S.C., Yuk, H.G., 2016. Biofilm formation of *Salmonella* Enteritidis under food-related environmental stress conditions and its subsequent resistance to chlorine treatment. *Food Microbiol.* 54, 98–105. <https://doi.org/10.1016/j.fm.2015.10.010>
- Yano, T., Kubota, H., Hanai, J., Hitomi, J., Tokuda, H., 2013. Stress Tolerance of *Methylobacterium* Biofilms in Bathrooms. *Microbes Environ.* 28, 87. <https://doi.org/10.1264/JSME2.ME12146>
- Yuan, L., Hansen, M.F., Røder, H.L., Wang, N., Burmølle, M., He, G., 2019. Mixed-species biofilms in the food industry: current knowledge and novel control strategies. *Crit. Rev. Food Sci. Nutr.* 60, 2277–2293. <https://doi.org/10.1080/10408398.2019.1632790>

- Yun, J.H., Kim, J.H., Lee, J.E., 2019. Surface film formation in static-fermented rice vinegar: a case study. *Mycobiology* 47, 250–255. <https://doi.org/10.1080/12298093.2019.1575585>
- Zhang, H., Wang, J., Chang, Z., Liu, X., Chen, W., Yu, Y., Wang, X., Dong, Q., Ye, Y., Zhang, X., 2021. *Listeria monocytogenes* contamination characteristics in two ready-to-eat meat plants from 2019 to 2020 in Shanghai. *Front. Microbiol.* 12, 729114. <https://doi.org/10.3389/fmicb.2021.729114>
- Zhang, J., Liu, Y.X., Guo, X., Qin, Y., Garrido-Oter, R., Schulze-Lefert, P., Bai, Y., 2021. High-throughput cultivation and identification of bacteria from the plant root microbiota. *Nat. Protoc.* 16, 988–1012. <https://doi.org/10.1038/s41596-020-00444-7>
- Zhang, P., Essendoubi, S., Keenlside, J., Reuter, T., Stanford, K., King, R., Lu, P., Yang, X., 2021. Genomic analysis of Shiga toxin-producing *Escherichia coli* O157:H7 from cattle and pork-production related environments. *NPJ Sci. food* 5. <https://doi.org/10.1038/S41538-021-00097-0>
- Zhang, P., Gänzle, M., Yang, X., 2019. Complementary antibacterial effects of bacteriocins and organic acids as revealed by comparative analysis of *Carnobacterium* spp. from meat. *Appl. Environ. Microbiol.* 85. <https://doi.org/10.1128/AEM.01227-19>
- Zhang, P., Tran, F., Stanford, K., Yang, X., 2020. Are antimicrobial interventions associated with heat-resistant *Escherichia coli* on meat? *Appl. Environ. Microbiol.* 86, e00512-20. <https://doi.org/10.1128/AEM.00512-20>
- Zhang, P., Yang, X., 2022. Genetic Characteristics of the Transmissible Locus of Stress Tolerance (tLST) and tLST Harboring *Escherichia coli* as Revealed by Large-Scale Genomic Analysis. *Appl. Environ. Microbiol.* 88. <https://doi.org/10.1128/AEM.02185->

21/SUPPL_FILE/AEM.02185-21-S0002.XLSX

- Zhang, Y., Wei, J., Qiu, Y., Niu, C., Song, Z., Yuan, Y., Yue, T., 2019. Structure-Dependent Inhibition of *Stenotrophomonas maltophilia* by Polyphenol and Its Impact on Cell Membrane. *Front. Microbiol.* 10. <https://doi.org/10.3389/FMICB.2019.02646>
- Zhang, Z., Yang, L., He, Y., Luo, X., Zhao, S., Jia, X., 2021. Composition of fecal microbiota in grazing and feedlot angus beef cattle. *Animals* 11, 1–8. <https://doi.org/10.3390/ani11113167>
- Zheng, J., Wittouck, S., Salvetti, E., Franz, C.M.A.P., Harris, H.M.B., Mattarelli, P., O'toole, P.W., Pot, B., Vandamme, P., Walter, J., Watanabe, K., Wuyts, S., Felis, G.E., Gänzle, M.G., Lebeer, S., 2020. A taxonomic note on the genus *Lactobacillus*: Description of 23 novel genera, emended description of the genus *Lactobacillus* Beijerinck 1901, and union of *Lactobacillaceae* and *Leuconostocaceae*. *Int. J. Syst. Evol. Microbiol.* 70, 2782–2858. <https://doi.org/10.1099/ijsem.0.004107>
- Zheng, Z., Li, S., Su, J., Leung, A.W.S., Lam, T.W., Luo, R., 2022. Symphonizing pileup and full-alignment for deep learning-based long-read variant calling. *Nat. Comput. Sci.* 2, 797–803. <https://doi.org/10.1038/s43588-022-00387-x>
- Zhi, S., Banting, G., Li, Q., Edge, T.A., Topp, E., Sokurenko, M., Scott, C., Braithwaite, S., Ruecker, N.J., Yasui, Y., McAllister, T., Chui, L., Neumann, N.F., 2016. Evidence of naturalized stress-tolerant strains of *Escherichia coli* in municipal wastewater treatment plants. *Appl. Environ. Microbiol.* 82, 5505–5518. <https://doi.org/10.1128/AEM.00143-16>
- Zhu, Y., Wang, W., Li, M., Zhang, J., Ji, L., Zhao, Z., Zhang, R., Cai, D., Chen, L., 2022. Microbial diversity of meat products under spoilage and its controlling approaches. *Front. Nutr.* 9, 2976. <https://doi.org/10.3389/FNUT.2022.1078201/BIBTEX>

- Ziyaina, M., Rasco, B., 2021. Inactivation of microbes by ozone in the food industry: A review. *African J. Food Sci.* 15, 113–120. <https://doi.org/10.5897/AJFS2020.2074>
- Zou, Y., Xue, W., Luo, G., Deng, Z., Qin, P., Guo, R., Sun, H., Xia, Y., Liang, S., Dai, Y., Wan, D., Jiang, R., Su, L., Feng, Q., Jie, Z., Guo, T., Xia, Z., Liu, C., Yu, J., Lin, Y., Tang, S., Huo, G., Xu, X., Hou, Y., Liu, X., Wang, J., Yang, H., Kristiansen, K., Li, J., Jia, H., Xiao, L., 2019. 1,520 Reference Genomes From Cultivated Human Gut Bacteria Enable Functional Microbiome Analyses. *Nat. Biotechnol.* 37, 179–185. <https://doi.org/10.1038/s41587-018-0008-8>
- Zwirzitz, B., Wetzels, S.U., Dixon, E.D., Fleischmann, S., Selberherr, E., Thalgueter, S., Quijada, N.M., Dzieciol, M., Wagner, M., Stessl, B., 2021. Co-occurrence of *Listeria* spp. and spoilage associated microbiota during meat processing due to cross-contamination events. *Front. Microbiol.* 12, 632935. <https://doi.org/10.3389/FMICB.2021.632935/FULL>
- Zwirzitz, B., Wetzels, S.U., Dixon, E.D., Stessl, B., Zaiser, A., Rabanser, I., Thalgueter, S., Pinior, B., Roch, F.F., Strachan, C., Zanghellini, J., Dzieciol, M., Wagner, M., Selberherr, E., 2020. The sources and transmission routes of microbial populations throughout a meat processing facility. *npj Biofilms Microbiomes* 2020 6:1–12. <https://doi.org/10.1038/s41522-020-0136-z>

Appendix

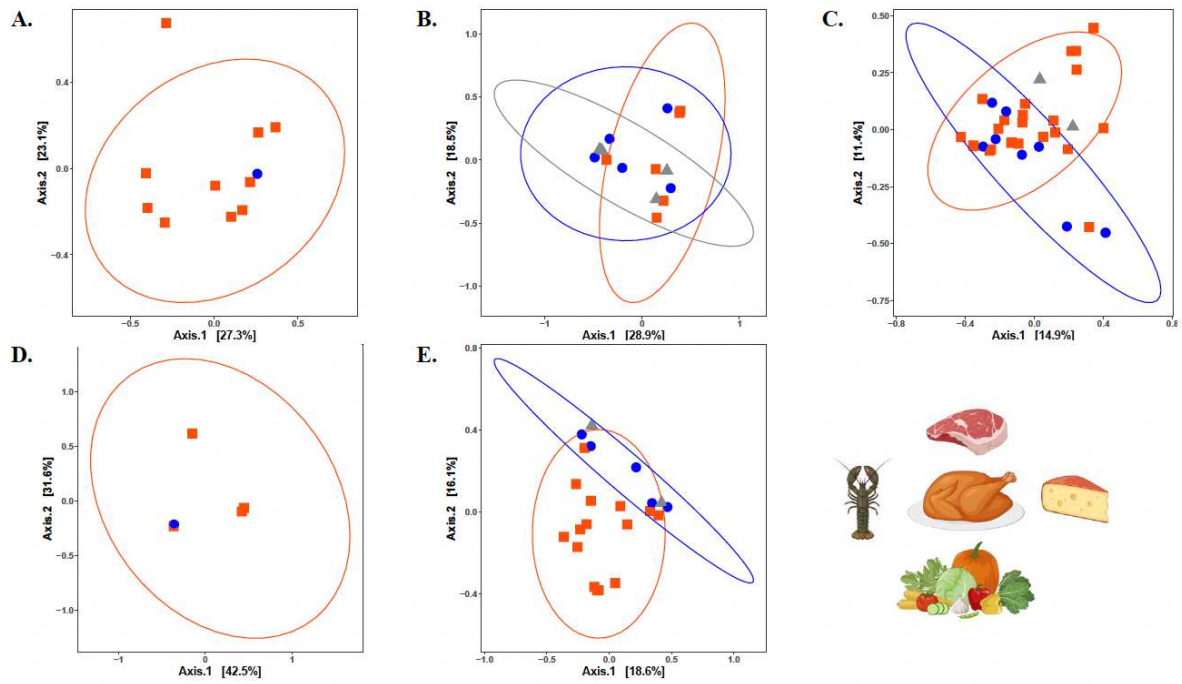


Figure S2.1. Principal coordinates analysis (PCoA) with Jaccard index for bacterial diversity based on nutrients intensity of environmental samples from food processing facilities.

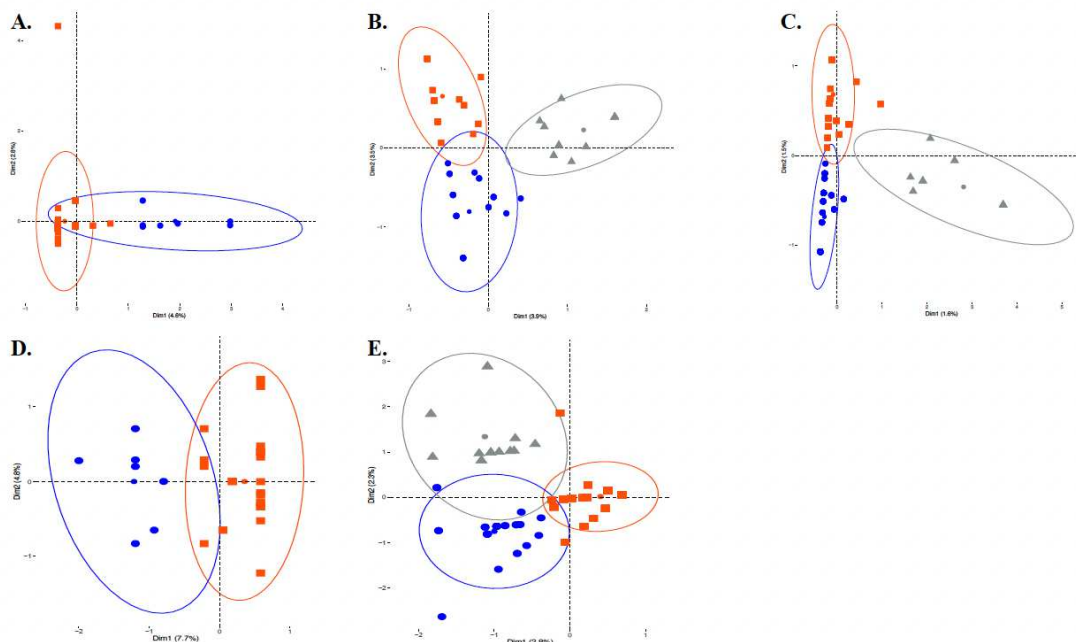


Figure S2.2. Multiple correspondence analysis (MCA) plots for bacterial diversity based on nutrients intensity of environmental samples from food processing facilities.

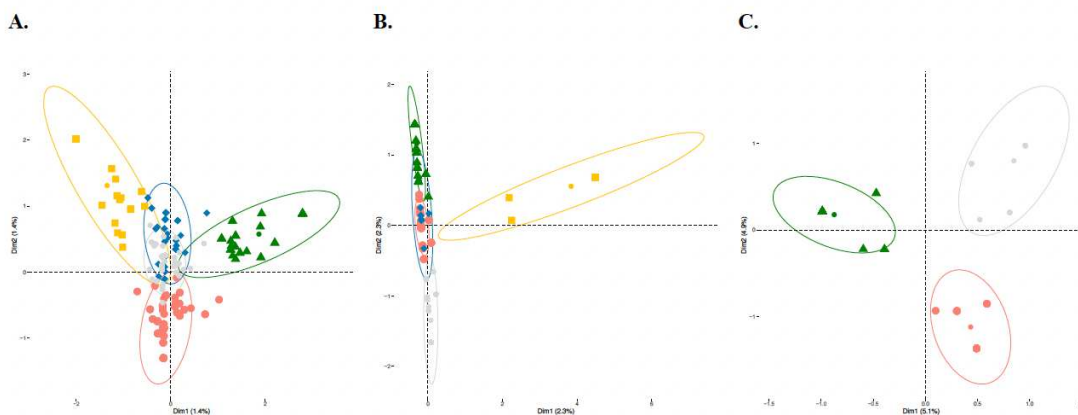


Figure S2.3. Multiple correspondence analysis (MCA) plots for bacterial diversity among different type of processing facilities associated with different nutrients level.

Table S2.1. List of publications and samples used in this study (provided as excel file, available from <https://doi.org/10.3390/microorganisms11061575>).

Table S2.2. Permutational MANOVA analysis on Jaccard distance matrix of all the samples from the 5 food commodities to test the association of community variance.

Comparison	P. value	P. adjusted sig
Ready to eat vs Meat processing facility	0.047	0.47
Ready to eat vs Seafood processing facility	0.016	0.16
Ready to eat vs Fresh produce facility	0.018	0.18
Ready to eat vs cheese processing facility	0.009	0.09
Meat processing facility vs Seafood processing facility	0.001	0.01*
Meat processing facility vs Fresh produce facility	0.001	0.01*
Meat processing facility vs cheese processing facility	0.001	0.01*
Seafood processing facility vs Fresh produce facility	0.001	0.01*
Seafood processing facility vs cheese processing facility	0.001	0.01*
Fresh produce facility vs cheese processing facility	0.001	0.01*

Table S2.3. Permutational MANOVA analysis on Jaccard distance matrix of all the samples from high-nutrient surfaces to test the association of community with different food commodity variables.

Comparison	P. value	P. adjusted sig
Ready to eat vs Meat processing facility	0.314	1.00
Ready to eat vs Seafood processing facility	0.184	1.00
Ready to eat vs Fresh produce facility	0.353	1.00
Ready to eat vs cheese processing facility	0.280	1.00
Meat processing facility vs Seafood processing facility	0.001	0.01*
Meat processing facility vs Fresh produce facility	0.025	0.25
Meat processing facility vs cheese processing facility	0.005	0.05*
Seafood processing facility vs Fresh produce facility	0.086	0.86

Seafood processing facility vs cheese processing facility	0.002	0.02*
Fresh produce facility vs cheese processing facility	0.024	0.24

Table S2.4. Permutational MANOVA analysis on Jaccard distance matrix of all the samples from low-nutrient surfaces to test the association of community with different food commodity variables.

Comparison	P. value	P. adjusted sig
Ready to eat vs Meat processing facility	0.133	1.00
Ready to eat vs Seafood processing facility	NA	NA
Ready to eat vs Fresh produce facility	0.33	1.00
Ready to eat vs cheese processing facility	0.167	1.00
Meat processing facility vs Seafood processing facility	0.819	1.00
Meat processing facility vs Fresh produce facility	0.012	0.108
Meat processing facility vs cheese processing facility	0.002	0.018*
Seafood processing facility vs Fresh produce facility	0.500	1.00
Seafood processing facility vs cheese processing facility	0.167	1.00
Fresh produce facility vs cheese processing facility	0.006	0.05*

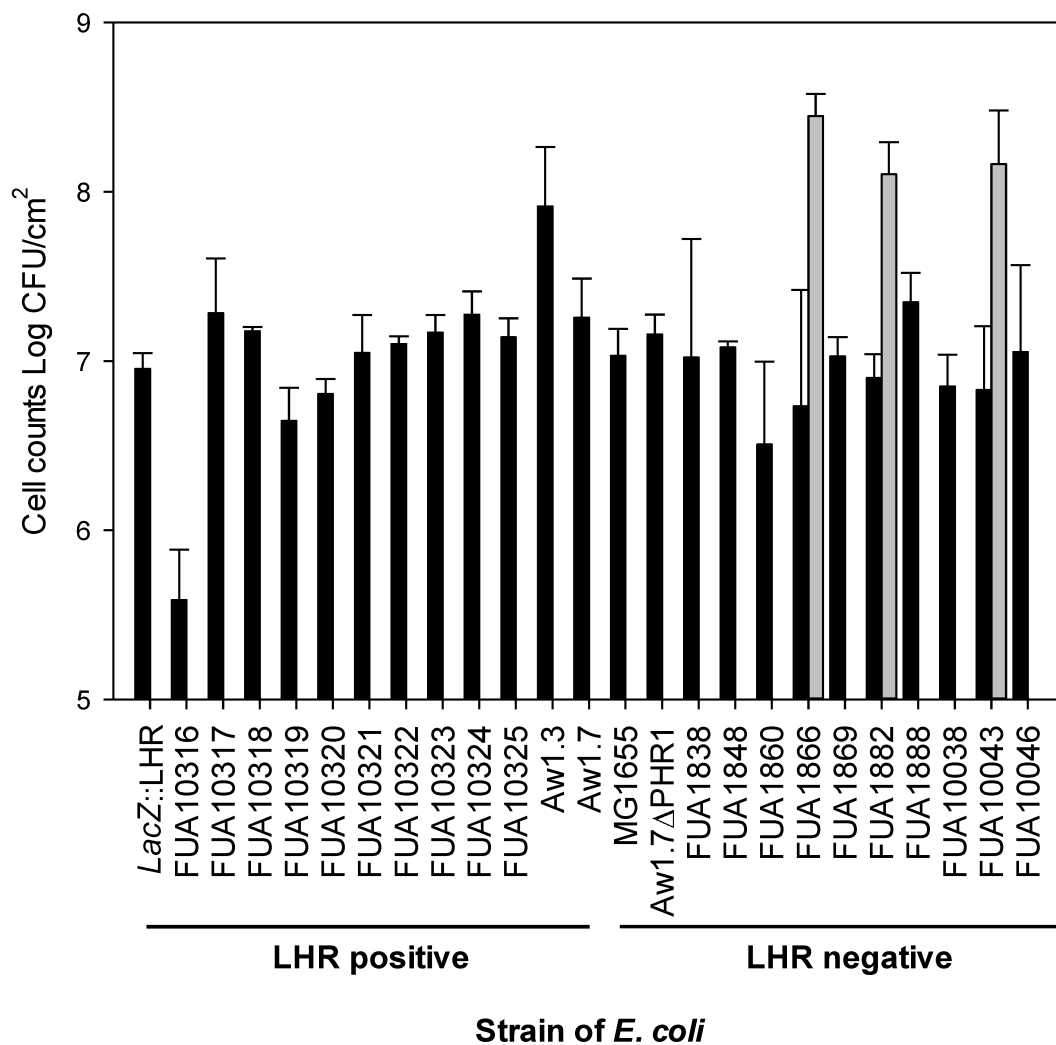


Figure S3.1. Biofilm formation of strains of *E. coli*.

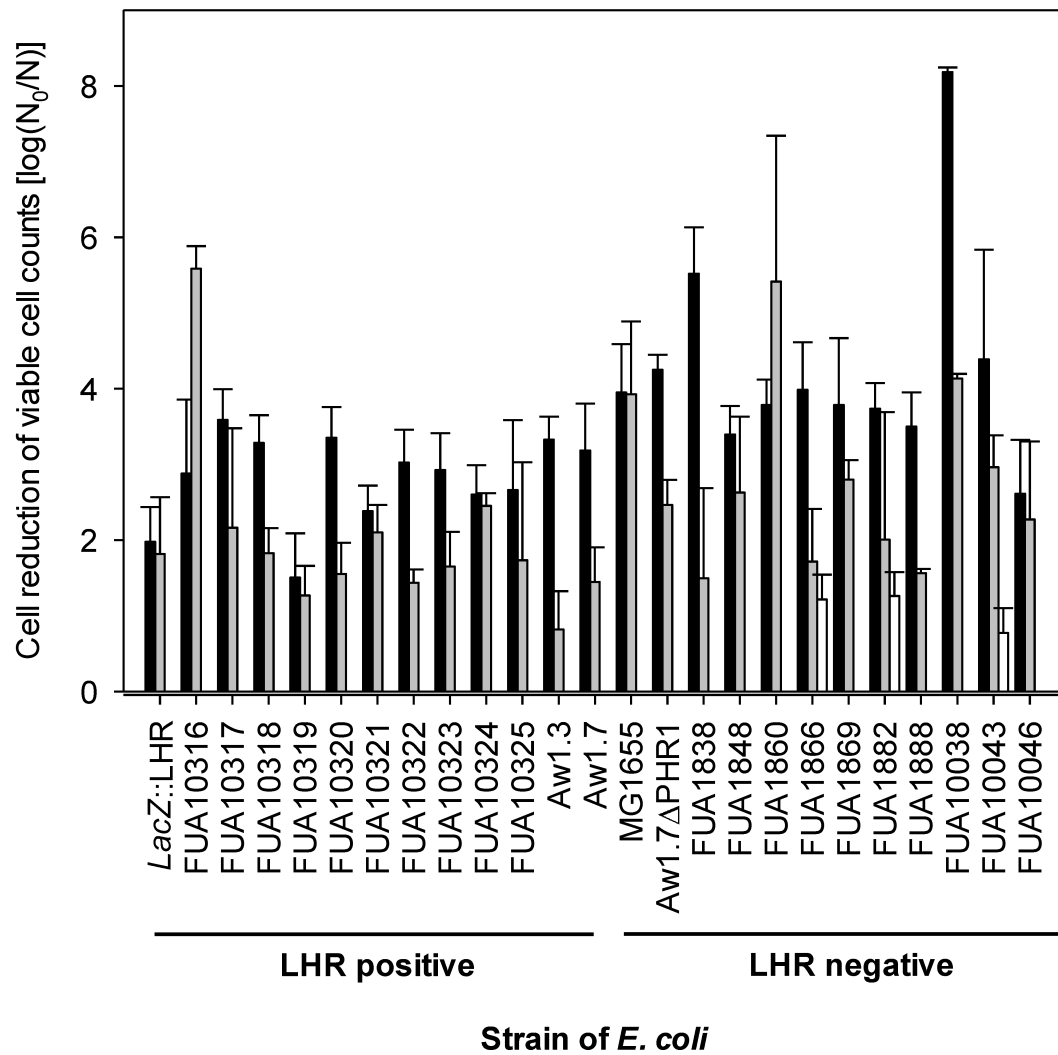


Figure S3.2. Chlorine resistance of *E. coli* in planktonic state (black bars), biofilm-embedded (grey bars) or pellicle-embedded (white bars).

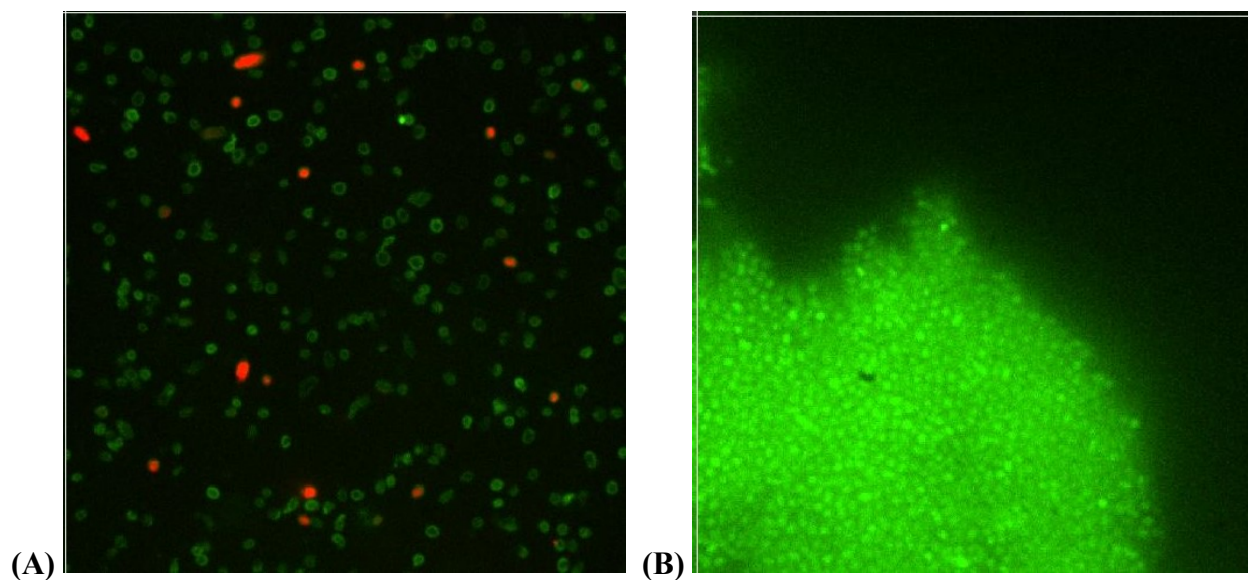


Figure S3.3. Confocal laser scanning microscopy of spatial distribution of bacterial biofilm cells. (A) Dual-strain biofilm-embedded cells composed of *A. australiensis* 03-09 and *E. coli* FUA10323 attached to stainless steel surface. (B) Dual-strain pellicle-embedded cells formed at air-liquid interface. All cells were cultured in LBNS broth at ambient temperature for 6 days before staining with propidium iodide and SYTO9.

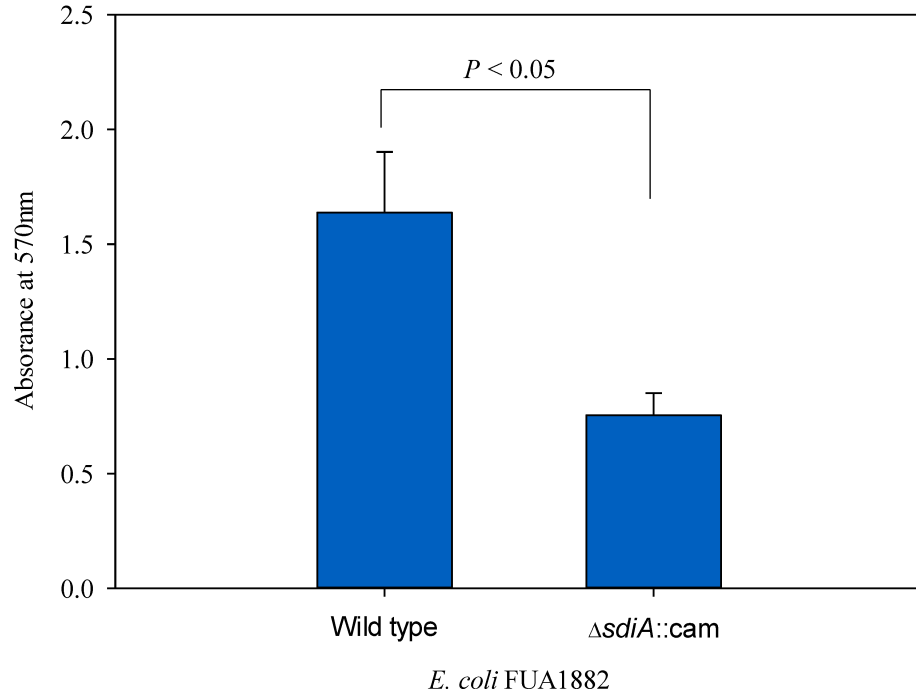


Figure S4.2. Biomass quantification of dual-species biofilms formed by *A. australiensis* with either wild type or *sdiA*-deficient *E. coli* FUA1882 by crystal violet staining. Biofilms were formed on stainless steel coupons in LBNS broth at 25°C after 6-day incubation. Data are shown as means \pm standard deviations for three independent experiments with technical replicates. T-test was used to analyze the difference between wild type and mutant strain. Significant difference is determined if *P* value is less than 0.05 ($P < 0.05$).

Table S5.2. Permutational multivariate analysis of variance on Bray-Curtis distance matrix of samples from March 2023 by culture-dependent and culture-independent approaches to test the association of community variance.

Method	Comparison	P. adjusted value
Culture-independent	FCS vs NFCS	0.516
	FCS vs Meat	0.096
	FCS vs Water	0.396
	NFCS vs Meat	0.072
	NFCS vs Water	0.252
	Meat vs Water	1.000
	zone1 vs zone3	0.405
	zone1 vs zone2	0.750
	zone1 vs zone4	0.525
	zone1 vs Meat	0.465
	zone1 vs water	0.915
	zone3 vs zone2	0.015
	zone3 vs zone4	1.000
	zone3 vs Meat	0.855
	zone3 vs water	1.000
	zone2 vs zone4	0.105
	zone2 vs Meat	0.165
	zone2 vs water	0.840
	zone4 vs Meat	1.000
	zone4 vs water	1.000
	Cutting vs Packaging	1.000
	Cutting vs Cooling	0.450
	Cutting vs Killing	1.000
	Cutting vs Shipping	1.000
	Cutting vs Meat	0.090
	Cutting vs Water	0.468
	Packaging vs Cooling	1.000
	Packaging vs Killing	1.000
	Packaging vs Shipping	1.000
	Packaging vs Meat	1.000
	Packaging vs Water	1.000
	Cooling vs Killing	1.000
	Cooling vs Shipping	1.000
	Cooling vs Meat	1.000
	Cooling vs Water	1.000
	Killing vs Shipping	NA
	Killing vs Meat	1.000
	Killing vs Water	NA
	Shipping vs Meat	1.000
	Shipping vs Water	NA
	Prior vs Post	0.066
	Prior vs Meat	0.336
Prior vs Water	1.000	
Post vs Meat	0.060	
Post vs Water	0.102	
Culture-dependent	FCS vs NFCS	0.660
	FCS vs Meat	0.042

FCS vs Water	0.150
NFCS vs Meat	0.048
NFCS vs Water	0.156
Meat vs Water	1.000
zone1 vs zone3	0.105
zone1 vs zone2	1.000
zone1 vs zone4	1.000
zone1 vs Meat	0.135
zone1 vs water	0.480
zone3 vs zone2	0.555
zone3 vs zone4	0.435
zone3 vs Meat	0.060
zone3 vs water	1.000
zone2 vs zone4	0.615
zone2 vs Meat	0.180
zone2 vs water	0.900
zone4 vs Meat	0.855
zone4 vs water	1.000
Cutting vs Packaging	0.198
Cutting vs Cooling	0.720
Cutting vs Killing	1.000
Cutting vs Shipping	1.000
Cutting vs Meat	0.108
Cutting vs Water	0.324
Packaging vs Cooling	1.000
Packaging vs Killing	1.000
Packaging vs Shipping	1.000
Packaging vs Meat	0.900
Packaging vs Water	1.000
Cooling vs Killing	1.000
Cooling vs Shipping	1.000
Cooling vs Meat	0.540
Cooling vs Water	1.000
Killing vs Shipping	NA
Killing vs Meat	1.000
Killing vs Water	NA
Shipping vs Meat	1.000
Shipping vs Water	NA
Prior vs Post	0.006
Prior vs Meat	0.036
Prior vs Water	1.000
Post vs Meat	0.012
Post vs Water	0.102

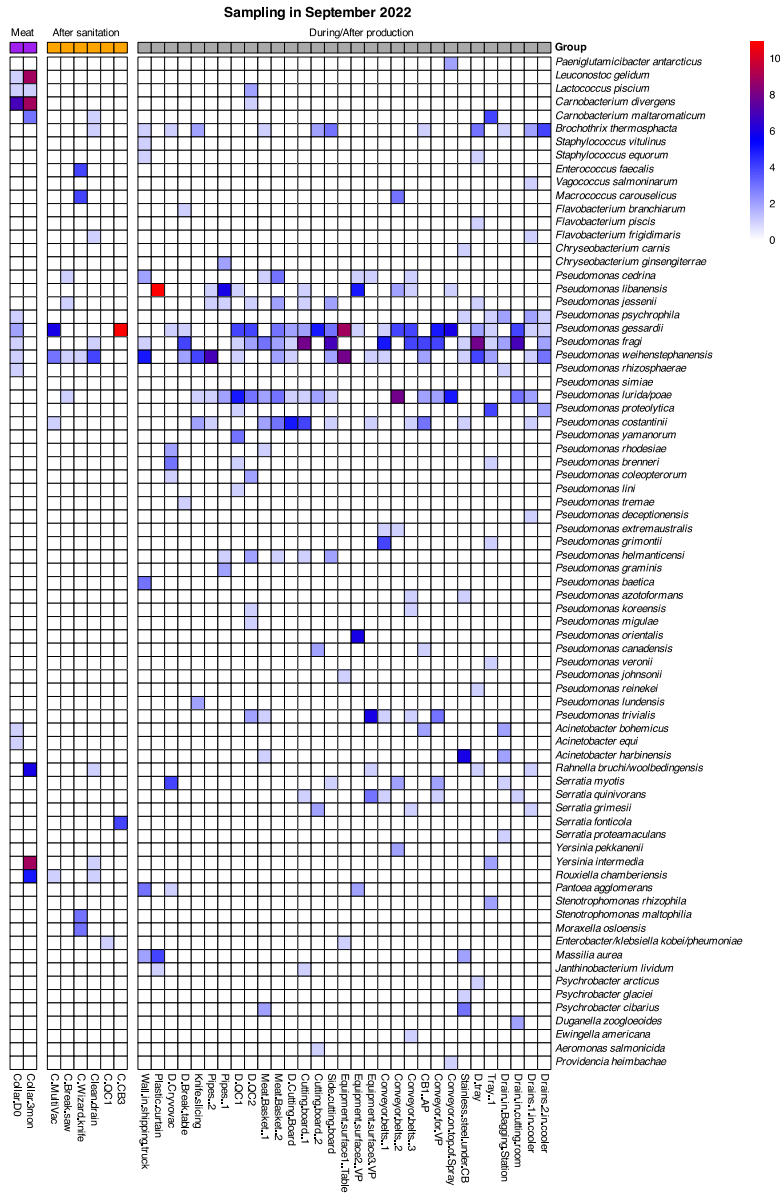


Figure S5.1. Heatmap of bacterial isolates collected from meat samples, environmental surface samples during the first time sampling, September 2022. Taxonomy classification was determined based on 16S rRNA gene and blasted against NCBI database.

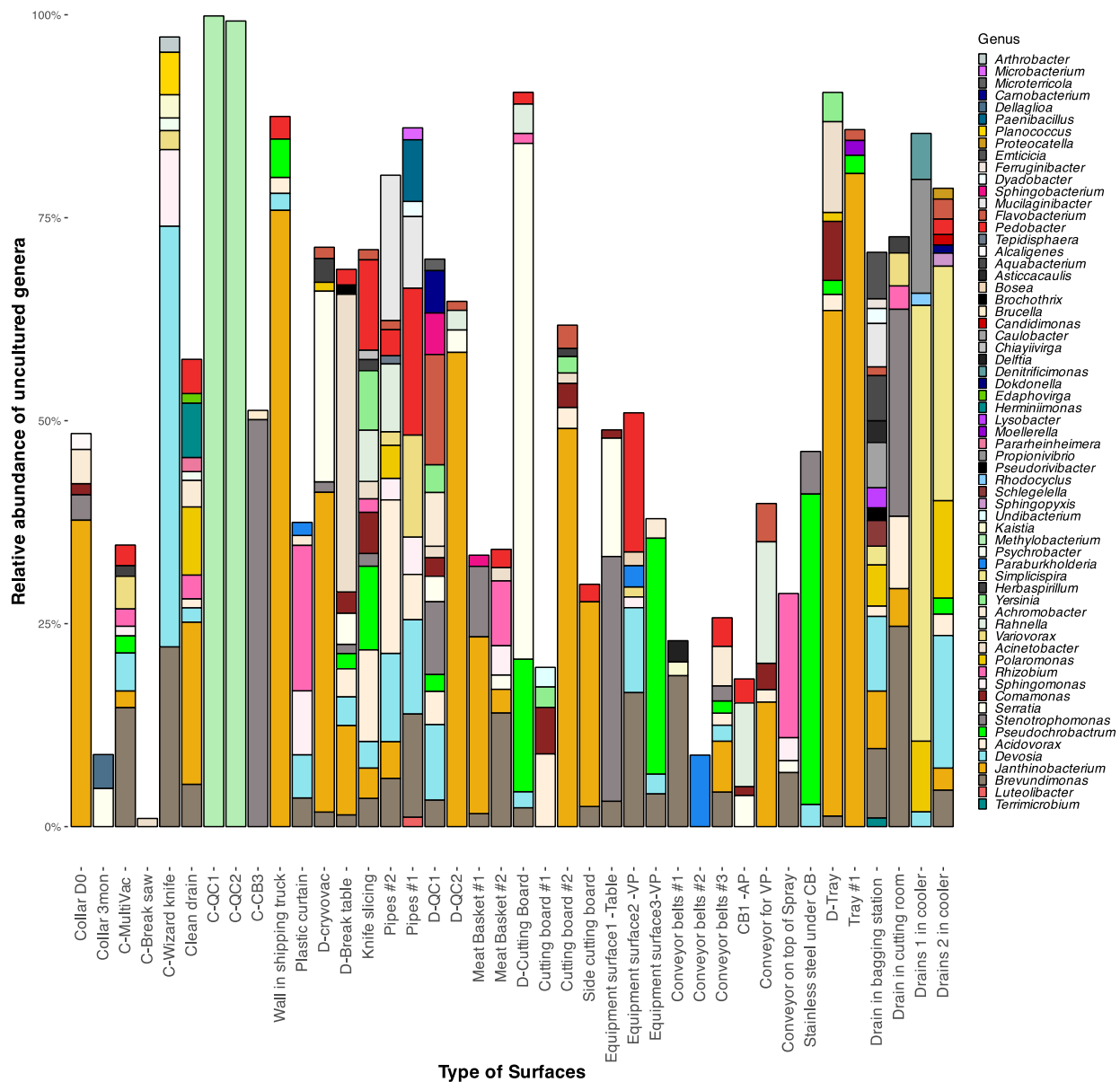


Figure S5.2. Relative abundance of genera that were only detected by 16S sequencing, among samples collected in the first sampling, September 2022. Only genera with no less than 1% relative abundance were plotted.

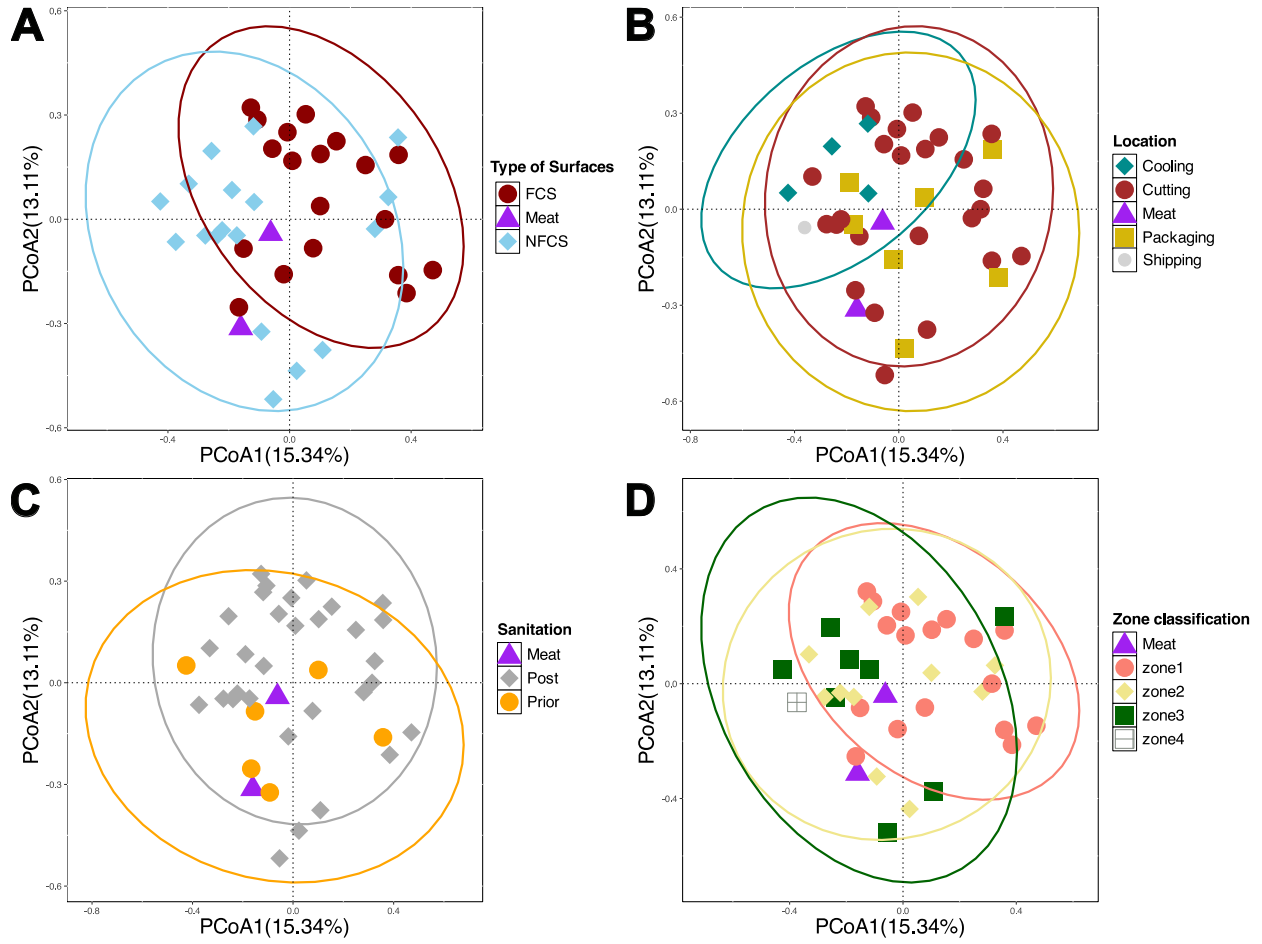


Figure S5.3. Principal coordinate analysis, using Bray-Curtis distance with 605 isolates classified at species level for 40 sampling sites, collected at the first sampling time, September 2022.

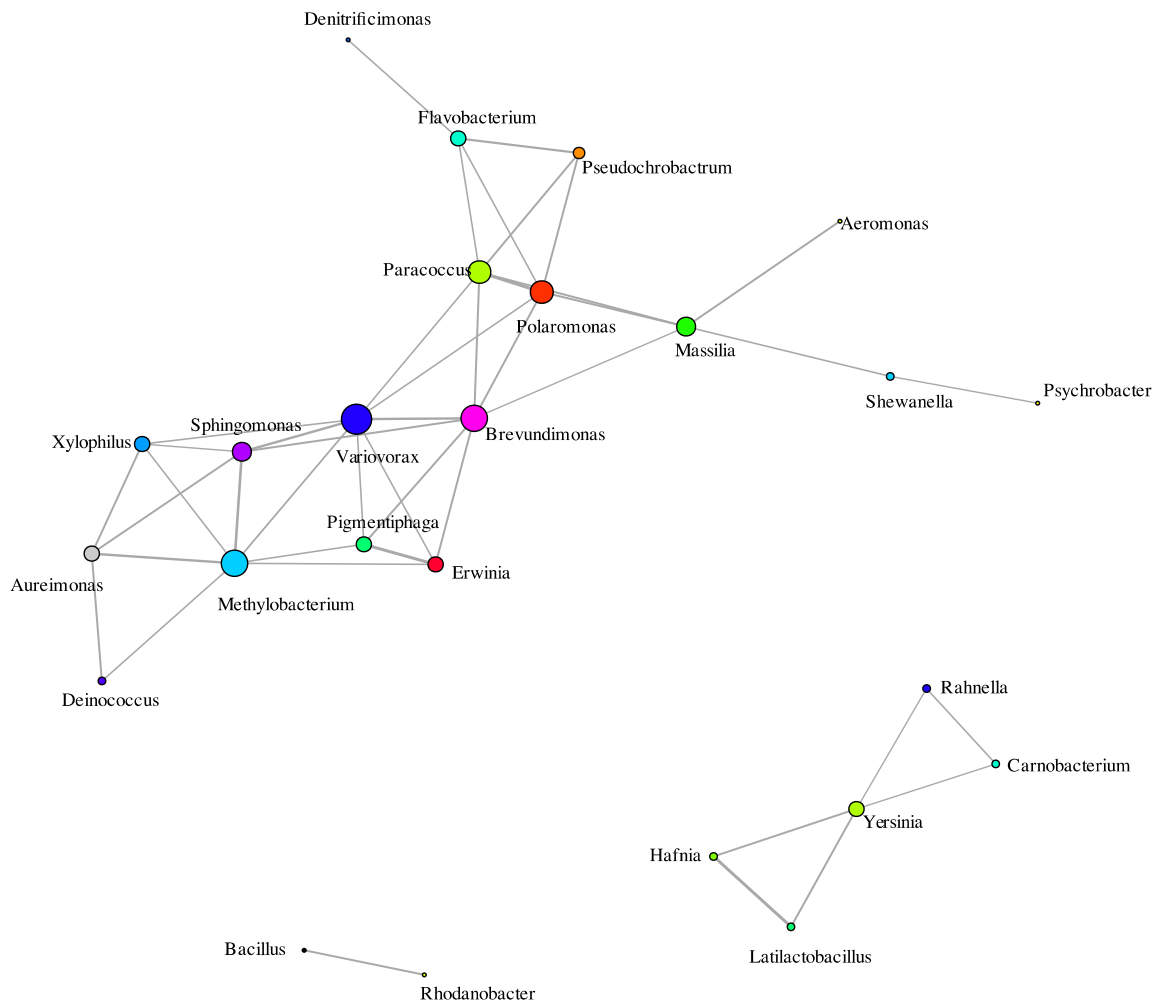


Figure S5.4. Bacterial coexistence network based on the microbial communities characterized by 16S rRNA gene sequencing. Nodes are colored at genus level. The network connections are determined using Spearman correlation test. Only correlations with a significance level of $P < 0.0001$ and a coefficient of ≥ 0.5 are included.

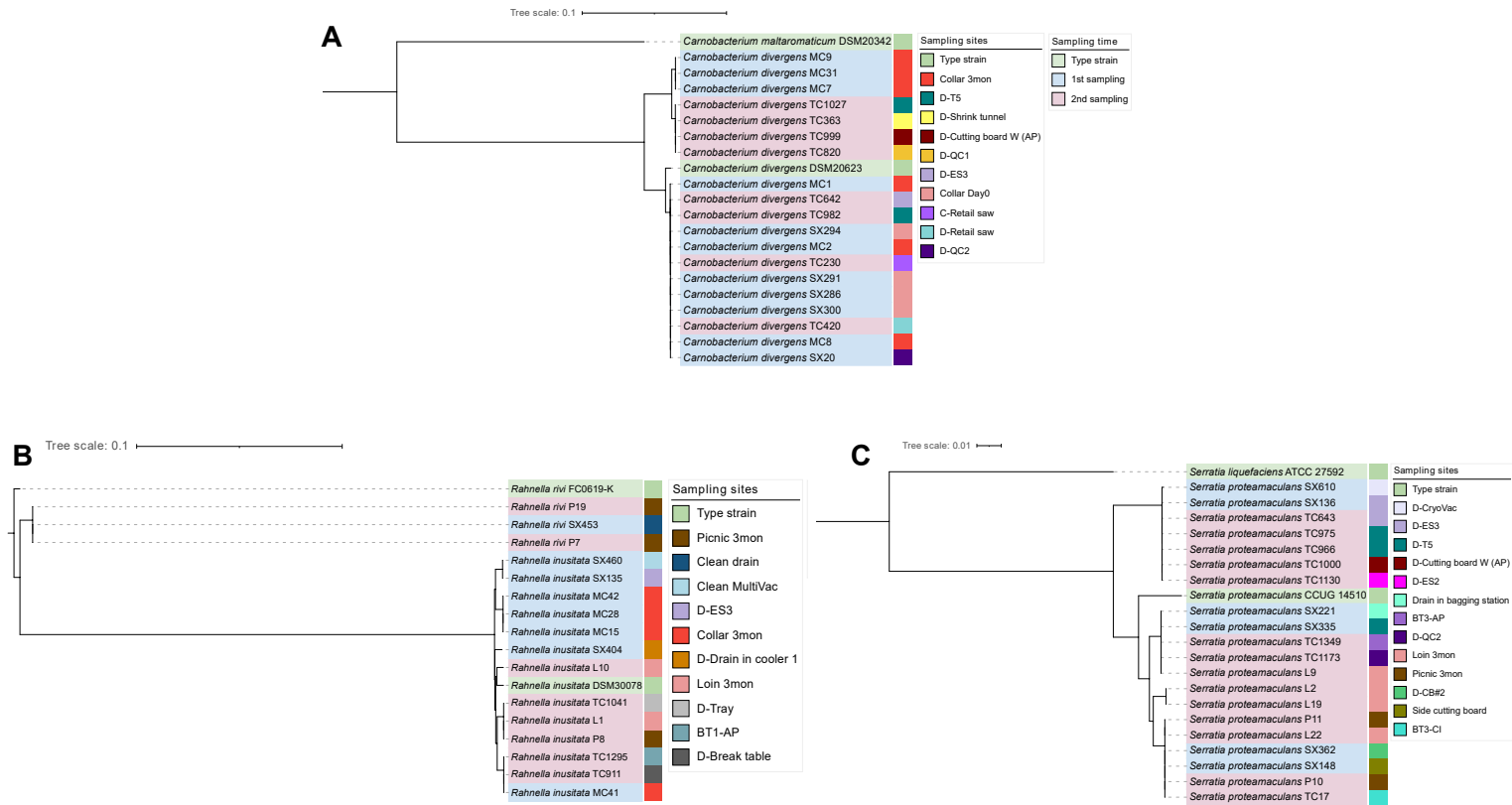


Figure S5.5. Phylogenetic tree of strains of *C. divergens* (A), *Rahnella* (B) and *S. proteamaculans* (C) isolated from a meat processing facility. The phylogeny was inferred based on core genome alignment, using the GTR+I+G4 model with 1000 bootstrap replicates. Strains are color coded based on sampling time (clades) and sampling sites (legend). Type strains of the target species and its closely related species as outgroups were included for tree visualization.